TRANSLATIONAL RESEARCH IN THYROID CANCER

EDITED BY: Vasyl Vasko, Electron Kebebew, Sheue-Yann Cheng and Kirk Ernest Jensen

PUBLISHED IN: Frontiers in Endocrinology

frontiers Research Topics

frontiers

ISSN 1664-8714
ISBN 978-2-88963-763-8
DOI 10.3389/978-2-88963-763-8

About Frontiers

Frontiers is more than just an open-access publisher of scholarly articles: it is a pioneering approach to the world of academia, radically improving the way scholarly research is managed. The grand vision of Frontiers is a world where all people have an equal opportunity to seek, share and generate knowledge. Frontiers provides immediate and permanent online open access to all its publications, but this alone is not enough to realize our grand goals.

Frontiers Journal Series

The Frontiers Journal Series is a multi-tier and interdisciplinary set of open-access, online journals, promising a paradigm shift from the current review, selection and dissemination processes in academic publishing. All Frontiers journals are driven by researchers for researchers; therefore, they constitute a service to the scholarly community. At the same time, the Frontiers Journal Series operates on a revolutionary invention, the tiered publishing system, initially addressing specific communities of scholars, and gradually climbing up to broader public understanding, thus serving the interests of the lay society, too.

Dedication to Quality

Each Frontiers article is a landmark of the highest quality, thanks to genuinely collaborative interactions between authors and review editors, who include some of the world's best academicians. Research must be certified by peers before entering a stream of knowledge that may eventually reach the public - and shape society; therefore, Frontiers only applies the most rigorous and unbiased reviews.
Frontiers revolutionizes research publishing by freely delivering the most outstanding research, evaluated with no bias from both the academic and social point of view. By applying the most advanced information technologies, Frontiers is catapulting scholarly publishing into a new generation.

What are Frontiers Research Topics?

Frontiers Research Topics are very popular trademarks of the Frontiers Journals Series: they are collections of at least ten articles, all centered on a particular subject. With their unique mix of varied contributions from Original Research to Review Articles, Frontiers Research Topics unify the most influential researchers, the latest key findings and historical advances in a hot research area! Find out more on how to host your own Frontiers Research Topic or contribute to one as an author by contacting the Frontiers Editorial Office: researchtopics@frontiersin.org

TRANSLATIONAL RESEARCH IN THYROID CANCER

Topic Editors:
Vasyl Vasko, Uniformed Services University of the Health Sciences, United States
Electron Kebebew, National Cancer Institute (NCI), United States
Sheue-Yann Cheng, National Cancer Institute at Frederick, United States
Kirk Ernest Jensen, Uniformed Services University of the Health Sciences, United States

Citation: Vasko, V., Kebebew, E., Cheng, S.-Y., Jensen, K. E., eds. (2020). Translational Research in Thyroid Cancer. Lausanne: Frontiers Media SA.
doi: 10.3389/978-2-88963-763-8

Table of Contents

frontiers in Endocrinology

EDITORIAL
published: 15 April 2020
doi: 10.3389/fendo.2020.00224

Editorial: Translational Research in Thyroid Cancer

Vasyl Vasko[1]*, *Electron Kebebew*[2], *Sheue-yann Cheng*[3] and *Kirk Ernest Jensen*[1]

[1] Department of Pediatrics, Uniformed Services University of the Health Sciences, Bethesda, MD, United States, [2] Department of Surgery, Stanford University, Stanford, CA, United States, [3] Laboratory of Molecular Biology, National Cancer Institute, Bethesda, MD, United States

Keywords: thyroid cancer, stem cells, cell signaling, FNA (fine needle aspiration), reactive oxygen species

Editorial on the Research Topic

Translational Research in Thyroid Cancer

Advances in high-throughput molecular technologies have improved our understanding of the molecular changes associated with thyroid cancer initiation and progression. The translation into clinical use, based on molecular profiling of thyroid tumors, has allowed a significant improvement in thyroid cancer diagnosis, patient risk stratification and in the identification of targets for precision therapy. This Research Topic, "Translational Research in Thyroid Cancer" contains a collection of studies that address emerging questions in thyroid cancer biology, and details approaches that leverage genomic-based algorithms to improve thyroid cancer diagnosis.

The evolution of cancer is not solely dictated by an individual tumor cell's irregular proliferation conferring gains in somatic mutations. A tumor's microenvironment, along with individual cancer cell genome instability, encourages clonal expansion, and heterogeneity. McGonagle and Nucera write a timely review discussing how novel experimental models will enhance our understanding of clonal and sub-clonal reconstruction and tumor evolution exposed to treatments during ultra-precision targeted therapies.

In keeping with this theme, the research article of Kim and Koo addresses the role of cancer stem cells in thyroid cancer. Cancer stem cells (CSCs) have important roles in cancer development, growth, recurrence, and metastasis owing to their potential to self-renew and differentiate into various cells lineages. This study highlights how the overexpression of CSC markers in thyroid cancer tissue is associated with shorter progression-free survival. It also demonstrates that staining of CSC markers may provide useful information for predicting patient outcomes.

Several studies in this collection examine associations between genomic abnormalities and cell signaling activation in thyroid cancer. Kari et al. explore molecular mechanisms implicated in development of follicular thyroid cancer (FTC). The authors have examined a mouse model for FTC caused by tissue-specific ablation of the Protein Kinase A (PKA) regulatory subunit, Prkar1a, either by itself or in combination with knockout of Pten. To understand the mechanism by which PKA activates mTOR, the authors examined intracellular kinases known to modulate mTOR function. Although AMP-activated kinase (AMPK) has been characterized as a negative regulator of mTOR activity, this tumor model exhibited activation of both AMPK and mTOR. Because the AMPK/LKB1 pathway has traditionally been considered a tumor suppressor, results of this study indicates that it may have a more complex role in the thyroid gland.

Reactive oxygen species (ROS), such as hydrogen peroxide (H_2O_2), are required for normal thyroid cell proliferation as well as for synthesis of the main hormones secreted by thyroid follicular cells. Thyroid follicular cells need to protect themselves against oxidative stress, and one

OPEN ACCESS

Edited and reviewed by:
Terry Francis Davies, Icahn School of Medicine at Mount Sinai, United States

***Correspondence:**
Vasyl Vasko
vasyl.vasko@gmail.com

Specialty section:
This article was submitted to Thyroid Endocrinology, a section of the journal Frontiers in Endocrinology

Received: *20 March 2020*
Accepted: *27 March 2020*
Published: *15 April 2020*

Citation:
Vasko V, Kebebew E, Cheng S and Jensen KE (2020) Editorial: Translational Research in Thyroid Cancer. Front. Endocrinol. 11:224. doi: 10.3389/fendo.2020.00224

such protective mechanism is the antioxidant response pathway centered on the nuclear factor erythroid 2-related transcription factor 2 (Nrf2). Renaud et al. contributed an article reviewing the involvement of Nrf2 signaling in thyroid physiology and particularly in thyroid cancer.

The review paper submitted by Ramírez-Moya and Santisteban focuses on understanding the functional significance of the most up- or down-regulated miRNAs in thyroid cancer on the main signaling pathways hyperactivated in this tumor type. Specifically, this study discusses the major miRNAs targeting proteins of the MAPK, PI3K, and TGFβ pathways in thyroid cancer. Given the importance of miRNAs in cancer as diagnostic, prognostic, and therapeutic candidates, a better understanding of this cross-talk might shed new light on the treatment of thyroid cancer.

Aberrant gene methylation plays an important role in human tumorigenesis, including thyroid tumorigenesis. Liu et al. performed an analysis of the methylation status of cellular retinoic acid binding protein 2 (CRABP2) and the expression patterns of methylation enzymes (DNMT1, DNMT3A, and DNMT3B). This study emphasizes that resveratrol, a non-toxic polyphenol compound, exerts demethylation in the same way as gemcitabine, and can be considered as an alternative demethylating drug for cancer prevention and treatment.

Though less frequent than the adult type, differentiated thyroid cancer (DTC) can also develop during childhood. The differences in the clinical and pathological features of pediatric vs. adult thyroid cancer could relate to a different genetic profile. In this Research Topic, Galuppini et al. characterize pediatric and adult thyroid cancers focusing on clinical features and outcomes; molecular profile, with particular reference to the study of point mutations of the *BRAF*, *RAS*, *TERT* genes, and *RET/PTC* translocations; and correlations between clinical and molecular findings. This study underscores how pediatric DTC is clinically more aggressive at diagnosis and more likely to recur than its adult counterpart. Unlike the adult disease, point mutations have not been demonstrated to have a key genetic role.

Fine needle aspiration (FNA) cytology, a diagnostic test central to thyroid nodule management, may yield indeterminate results in up to 30% of cases. In this Research Topic, two studies address the diagnostic utility of the Afirma genomic tests in the evaluation of thyroid nodules. Hao et al. examine the analytical robustness and reproducibility of the Afirma Genomic Sequencing Classifier test. The work of Angell et al. assesses the analytical and clinical validation of the Afirma Xpression Atlas (XA), which detects gene variants and fusions from a curated panel of 511 genes via dedicated FNA samples using whole-transcriptome RNA-sequencing. These studies show that genomic information provided by the Afirma test may inform clinical decision-making with precision medicine insights across a broad range of FNA sample types encountered in the care of patients with thyroid nodules and thyroid cancer.

This original series of articles details emerging approaches in thyroid cancer research and applications of molecular-based algorithms for diagnosis of thyroid cancer.

AUTHOR CONTRIBUTIONS

All authors listed have made a substantial, direct and intellectual contribution to the work, and approved it for publication.

Conflict of Interest: The authors declare that the research was conducted in the absence of any commercial or financial relationships that could be construed as a potential conflict of interest.

frontiers in Endocrinology

REVIEW
published: 02 July 2019
doi: 10.3389/fendo.2019.00430

miRNA-Directed Regulation of the Main Signaling Pathways in Thyroid Cancer

Julia Ramírez-Moya[1,2] *and Pilar Santisteban*[1,2]*

[1] *Instituto de Investigaciones Biomédicas "Alberto Sols", Consejo Superior Investigaciones Científicas and Universidad Autónoma de Madrid (CSIC-UAM), Madrid, Spain,* [2] *Centro de Investigación Biomédica en Red de Cáncer (CIBERONC), Instituto de Salud Carlos III (ISCIII), Madrid, Spain*

In the last two decades, great strides have been made in the study of microRNAs in development and in diseases such as cancer, as reflected in the exponential increase in the number of reviews on this topic including those on undifferentiated and well-differentiated thyroid cancer. Nevertheless, few reviews have focused on understanding the functional significance of the most up- or down-regulated miRNAs in thyroid cancer for the main signaling pathways hyperactivated in this tumor type. The aim of this review is to discuss the major miRNAs targeting proteins of the MAPK, PI3K, and TGFβ pathways, to define their mechanisms of action through the 3′UTR regions of their target genes, and to describe how they affect thyroid tumorigenesis through their actions on cell proliferation, migration, and invasion. Given the importance of miRNAs in cancer as diagnostic, prognostic and therapeutic candidates, a better understanding of this cross-talk might shed new light on the biomedical treatment of thyroid cancer.

Keywords: miRNAs, MAPK, PI3K, TGFβ, thyroid, cancer

OPEN ACCESS

Edited by:
Vasyl Vasko,
Uniformed Services University of the Health Sciences, United States

Reviewed by:
Jeffrey Knauf,
Memorial Sloan Kettering Cancer Center, United States
Shuai Zhang,
Tianjin University of Traditional Chinese Medicine, China

***Correspondence:**
Pilar Santisteban
psantisteban@iib.uam.es

Specialty section:
This article was submitted to Thyroid Endocrinology, a section of the journal Frontiers in Endocrinology

Received: *29 April 2019*
Accepted: *14 June 2019*
Published: *02 July 2019*

Citation:
Ramírez-Moya J and Santisteban P (2019) miRNA-Directed Regulation of the Main Signaling Pathways in Thyroid Cancer. Front. Endocrinol. 10:430. doi: 10.3389/fendo.2019.00430

INTRODUCTION

A wealth of studies over the last decade has highlighted the importance of microRNAs (miRNAs) in cancer development. This is likely due to the extreme versatility of these small molecules as key regulators of gene expression. miRNAs are defined as small non-coding RNAs of length 19–25 nucleotides that control gene expression at the posttranscriptional level by hybridizing to target mRNAs at the 3′ untranslated region (3′UTR), suppressing their translation or inducing their degradation.

The finding that one miRNA can target a large number of different mRNAs, and that one mRNA molecule can be targeted by numerous miRNAs, gives these molecules the potential to fine-tune gene expression levels in physiological and pathological processes such as cancer (1–3). Indeed, many miRNAs are known to target mRNAs involved in cancer including oncogenes and tumor suppressors, and therefore play essential roles in cancer initiation, progression and metastasis formation (4). Conversely, it is also recognized that oncogenes and tumor suppressors exert their actions by controlling the expression of specific miRNAs. These finding overall support the existence of feedback mechanisms between miRNAs and their targets in human cancers including thyroid cancer, which is the most commonly occurring endocrine malignancy and whose incidence has increased steadily over the last four decades (5, 6).

Thyroid cancer of epithelial/follicular origin comprises different histological subtypes. Carcinomas with the ability to maintain differentiation are termed well-differentiated thyroid

carcinomas (WDTC) and include two subtypes—papillary (PTC) and follicular (FTC) thyroid carcinoma. The other subtypes are poorly differentiated (PDTC) and (undifferentiated) anaplastic (ATC) thyroid carcinomas (7). PTCs are the most frequent differentiated thyroid carcinomas and represent 80–85% of all thyroid malignancies, whereas ATC is the less frequent malignancy but the most aggressive, and has an extremely poor prognosis (median survival of 6 months after diagnosis).

It is well-accepted that thyroid cancer fits a stepwise model of progression, which considers thyroid carcinomas as tumors accumulating mutations that drive tumorigenesis through a dedifferentiation process. Analysis of the genome sequence has recently revealed the genomic landscape of these tumors (8, 9), which has led to a redesign of the stepwise model of thyroid cancer progression. Depending on the key oncogenic drivers associated with PTC and FTC, tumors are grouped together into BRAF-like and RAS-like, as a function of their characteristic molecular features. Typically, PTCs are considered BRAF-like tumors, whereas FTCs are considered RAS-like. However, the follicular variants of PTC are considered RAS-like, and consequently more akin to FTC. Additional drivers are involved in the progression to PDTC and to ATC [reviewed in (10)].

The molecular classification of thyroid carcinomas is based on the mutations in the main known signaling pathways. In the case of PTC, it is accepted that it is a MAPK pathway-driven cancer with RAS and BRAF activating mutations being the main oncogenic players, which are found in an exclusive manner (11). The follicular variant of PTC, a RAS pathway-like tumor, shares characteristics with PTC and FTC and is associated with the activation of both MAPK and PI3K signaling (12). In the case of FTC, the main driver is RAS. While RAS proteins can activate both the MAPK and PI3K pathways, the oncogenic variants of RAS are likely more dependent on PI3K activation to initiate tumorigenesis (13). Finally, mutations activating both MAPK and PI3K have been detected in PDTC and ATC, which together with mutations in genes involved in aggressiveness increase the mutational burden in these tumors (13).

Considering thyroid cancer, one of the most important consequences of the new era of genomic studies is the possibility to differentiate between the two genetic types, particularly the manner in which BRAF and RAS signaling promotes tumor development and growth. BRAF-driven tumors have high MEK-ERK activity whereas RAS-driven tumors show the opposite and activate PI3K. BRAF-driven tumors are very heterogeneous in terms of gene expression, miRNA profiles, and epigenetic alterations. TGFβ signaling contributes to this heterogeneity, as BRAF induces the secretion of functional TGFβ, which together with MAPK signaling supports cell migration, invasion and epithelial-mesenchymal transition (EMT) (14). Accordingly, PTC tumors express high levels of TGFβ and other components of this pathway such as its receptor TβRII and phosphorylated SMAD2 protein (14–16). These data indicate that TGFβ/SMAD activity is associated with PTC invasion, nodal metastasis and BRAF status, and should be considered an important pathway in thyroid cancer.

Regarding miRNAs, which are the focus of this review, The Cancer Genome Atlas (TCGA) research network recently revealed that activation of the aforementioned oncogenes deregulates miRNA expression in thyroid cells (8), suggesting that miRNA expression patterns are relevant for pathogenesis in patients, as they contribute to loss of differentiation and induce tumor progression. The known mechanisms of miRNA deregulation in cancer include amplification, deletion, mutation, and epigenetic silencing (17, 18). As an illustration of the complexity of these regulatory networks, TCGA analysis revealed the presence of six miRNA clusters in PTC. Cluster 1 is associated with RAS-mutated tumors and the follicular variant and it is enriched with the miRNAs miR-181 and miR-182, whereas the BRAF tumors are defined by five miRNA clusters (Clusters 2–6). Cluster 5 (enriched with miR-146b and miR-375, and low levels of miR-204), together with Cluster 6 (with high levels of miR-21 and low levels of miR-204), are associated with the less-differentiated tumors and a higher risk of recurrence (10). Beyond these clinically relevant miRNA expression patterns, the role(s) of specific miRNAs in thyroid carcinogenesis is under intensive investigation.

Individual miRNAs regulate important processes of tumor biology and new examples of miRNAs that coordinately regulate cancer pathways are reported almost daily. In the context of thyroid cancer, miRNA regulation by the major signaling pathways has been reviewed in depth; however, to our knowledge, a comprehensive analysis of the most important miRNAs that control the main signaling pathways activated in thyroid cancer—MAPK, PI3K, and TGFβ–has received less attention. Thus, we will review here what we know about miRNA regulation of the main signaling pathways altered in thyroid cancer. To this end, we will focus on the most important miRNAs up- and down-regulated in thyroid cancer and how they target components of the signal transduction pathways involved in the MAPK, PI3K, and TGFβ pathways.

Our approach will be an analysis of the signaling pathways from the membrane to the nucleus, describing both up- and down-regulated miRNAs in thyroid cancer that regulate the main proteins involved in these pathways.

MAPK Signaling Pathway

This MAPK signaling pathway employs a series of protein kinases to transmit signals from the cell membrane to the nucleus, in order to control several cellular processes such as proliferation, differentiation, migration, invasion and apoptosis. MAPK hyperactivation has been implicated in many different pathologies including cancer (19).

Mechanistically, MAPK signaling functions through growth factor and mitogen binding to plasma membrane tyrosine kinase receptors, inducing receptor dimerization and autophosphorylation of specific residues that are recognized by the adaptor proteins SHC1 and GRB2. In turn, these adaptor proteins recruit GTPase exchange factors such as SOS to promote GDP–GTP exchange on RAS proteins. After their activation, RAS proteins recruit to the plasma membrane RAF (BRAF or RAF1), inducing the sequential activation of MEK and ERK. This process is enabled by scaffold proteins that modulate pathway activation, being its components translocate to various cellular compartments, particularly the nucleus where proteins

involved in proliferation such c-FOS, c-JUN, c-MYC, or ELK1 are activated (13).

Upregulated miRNAs Modulating the MAPK Pathway Activity in Thyroid Cancer

Few studies have described upregulated miRNAs targeting the MAPK pathway in thyroid tumors. Because MAPK signaling must be activated to induce tumorigenesis, miRNAs that are upregulated could inhibit antagonists of this pathway, which would maintain the hyperactivation observed in thyroid cancer. Indeed, it has been established that miR-21 targets inhibitors of the RAS-MAPK pathway (*SPRY1*, *SPRY2*, *BTG2*, and *PDCD4*), therefore activating this pathway in lung cancer (20). miR-21 is a key oncogenic miRNA upregulated in many cancers, including PTC, but further studies will confirm the role of inhibit these targets in thyroid tumors. Interestingly, mutated *BRAF* might regulate or interact with miRNAs in the pathogenesis and progression of PTC, as the expression levels of several important upregulated miRNAs such as miR-221, miRNA-222, miRNA-146b, and miRNA-181, were shown to be significantly higher in PTC patients with BRAF mutations (21, 22).

Downregulated miRNAs Modulating the MAPK Pathway in Thyroid Cancer

The lethal miRNA family let-7, which was first discovered in the worm (23), was also the first to be implicated in human disease through their regulation of the RAS-ERK/MAPK pathway (24). Indeed, the 3′ UTR of all three RAS genes (*HRAS*, *KRAS*, and *NRAS*) encloses multiple binding sites for let-7 family members, and enforced expression of let-7 in human cancer cells reduces RAS protein levels. Accordingly, the downregulation of let-7 expression reported in several human cancers could lead to RAS pathway activation. This mechanism has also been observed in thyroid cancer cells (25), where RAS activation and downregulation of some members of the let-7 family was noted. The sweeping importance of let-7 downregulation in cancer is supported by the finding that let-7 can suppress tumor growth in several cancers such as lung or colon cancer (26).

Regarding thyroid carcinomas, three independent studies have shown that let-7f is downregulated in PTC (27–29), although the analysis of TCGA data would indicate that it is not significantly downregulated. Let-7f has been linked to RAS protein levels in PTC (30). Moreover, stable transfection of let-7f in TPC-1 cells, a human PTC cell line that spontaneously harbors the *RET/PTC1* oncogene, inhibits MAPK activation, and leads to an obvious reduction in cell proliferation and the induction of thyroid differentiation markers (25).

Epidermal growth factor receptor (EGFR), a tyrosine kinase receptor that can shuttle from the membrane to the nucleus, is an oncogene overexpressed in a variety of human cancers including thyroid cancer (31–34), and mediates cell proliferation via ERK and AKT signaling. Basing their study on previous works showing a general downregulation of miR-137 in many different types of human cancer, Luo et al. (33) used real-time PCR to show that mean expression of miR-137 was lower in samples of fresh PTC tissue than in adjacent normal tissue ($n = 25$), although according to TCGA data miR-137 expression is not significantly different (8). Interestingly, the authors found that miR-137 directly targets EGFR and used loss- and gain-of-function studies to show that an miR-137 mimic significantly downregulated EGFR mRNA and protein, whereas an miR-137 inhibitor had the opposite effect. miR-137 was also found to downregulate cell proliferation, colony formation ability, and invasion, and negatively regulated ERK and AKT signaling. Interestingly, EGFR depletion abrogated the effect of miR-137 inhibition on ERK and AKT signaling, suggesting that the role of miR-137 on ERK and AKT signaling was EGFR dependent (33). The EGFR family member, ERBB2 (encoding the neuregulin receptor), is also considered an oncogene and is overexpressed in many cancers (35, 36). ERBB2 is associated with RAS-MAPK and PI3K-AKT signaling and its overexpression would likely reduce the sensitivity of cells to chemotherapy and radiotherapy (36, 37). ERBB2 was recently described to be targeted by miR-375 in PTC tissue (37). Interestingly, whereas miR-375 is significantly upregulated in PTC according to both TCGA data (8) and an independent miRNA deep sequencing study (38), Wang et al. (37) reported miR-375 as being downregulated in PTC tissues ($n = 60$, real-time PCR assay) and cell lines. The authors studied the biological effect of miR-375 on human PTC cell lines establishing that its overexpression inhibited proliferation and induced apoptosis *in vitro*, and decreased migration and invasion *in vivo*. Nevertheless, the precise mechanism of action miR-375 and whether it is associated with MAPK/ERK or PI3K/AKT pathways. was not addressed, and thus further studies are needed to better understand the mechanism of action of miR-375 in thyroid cancer.

Other studies have described several downregulated miRNAs that inhibit the MAPK/ERK pathway downstream of its receptors. For instance, Liu et al. identified miR-4728 as a significantly downregulated miRNA in 18 pairs of human PTC and non-cancerous normal tissue, as determined by real-time PCR analysis (39). However, no changes were observed in TCGA data (8). Functionally, miR-4728 inhibits PTC cell proliferation and decreases the mRNA and protein levels of the GTPase exchange factor SOS1, thereby inhibiting MAPK/ERK activity (39). Similarly, miR-20b has also been described to directly target *SOS1*, in addition to the extracellular signal-regulated kinase 2 (*ERK2*), consequently downregulating the signaling pathway (40). Depletion of *SOS1* or *ERK2* has similar effects to that observed from miR-20b overexpression, decreasing cell viability and invasion, and the rescue of these two genes partially reversed the effects of miR-20b in a PTC cell line. Finally, overexpression of miR-20b decreased tumor growth in a xenograft model, leading the authors to conclude that miR-20b has a tumor suppressor function *in vivo* (40). In contrast to TCGA data (8), which did not find this miRNA to be significantly differentially expressed, Hong et al. found miR-20b downregulated when analyzing 47 pairs of PTC and their matched adjacent normal tissue (40). This result was consistent with an earlier study demonstrating that miR-20b is significantly downregulated in PTC by using next-generation deep sequencing ($n = 14$) and microarray analysis ($n = 9$) (41).

The RAF kinase family comprises three serine/threonine-specific protein kinase isoforms: A-RAF, B-RAF, and RAF1. RAF1 is directly downstream of and can be activated by RAS. Once activated, cellular RAF1 guides the receptor signals from the cell membrane to the nucleus by phosphorylating and activating the dual specificity protein kinases MEK1 and MEK2, therefore activating the MAPK/ERK pathway and regulating cell cycle, proliferation, apoptosis, and migration. RAF1 is upregulated in thyroid cancer, which could be in part caused by the deregulation of miR-195 (42). This miRNA is downregulated in thyroid cancer (8, 42) and directly targets *RAF1* to block thyroid cancer cell proliferation. Another member of this kinase family, BRAF, is also an effector of RAS and a main component of the MAPK/ERK pathway. Mutations in *BRAF* induce uncontrolled and persistent activation of this kinase-signaling pathway, causing over-proliferation of cancer cells. BRAF expression is controlled by miR-9, which is downregulated in PTC according to both TCGA data and to a study by Guo et al. (8, 43). These authors found that miR-9 directly targets the BRAF 3′UTR. Furthermore, miR-9 suppress the viability of PTC cells by inducing apoptosis, therefore acting as a tumor suppressor miRNA (43). A summary of miRNAs and their targets in the MAPK pathway is shown in **Table 1** and is schematically represented in **Figure 1**.

TABLE 1 | Summary of miRNAs affecting the main signaling pathways in thyroid cancer.

miRNA	Target/s	Pathway affected
UPREGULATED miRNAs		
miR-146b	PTEN	PI3K
	ST8SIA4	PI3K
	SMAD4	TGFβ
miR-21	PTEN	PI3K
miR-146a	ST8SIA4	PI3K
miR-34a	GAS1	PI3K
miR-221	$p27^{Kip1}$	PI3K
miR-222	$p27^{Kip1}$	PI3K
miR-29b	SMAD3	TGFβ
miR-23b	SMAD3	TGFβ
DOWNREGULATED miRNAs		
Let-7	RAS	MAPK
		PI3K
miR-137	EGFR	MAPK
		PI3K
miR-375	ERBB2	MAPK
		PI3K
miR-4728	SOS1	MAPK
miR-20b	SOS1	MAPK
	ERK2	MAPK
miR-195	RAF1	MAPK
miR-9	BRAF	MAPK
miR-126	PIK3R2	PI3K
miR-451a	MIF	PI3K
	AKT1	PI3K
	c-MYC	PI3K
miR-145	AKT3	PI3K
miR-99a	mTOR	PI3K
miR-663	TGFβ1	TGFβ
miR-7	TGFβRII	TGFβ
miR-144	TGFβRII	TGFβ
miR-200	TGFβRI	TGFβ
	SMAD2	TGFβ
miR-30	SMAD2	TGFβ

PI3K Signaling Pathway

The phosphoinositide 3-kinase–protein kinase B/AKT (PI3K-PKB/AKT) pathway a critical molecular signaling pathways involved in key cellular processes. Protein kinase B (also known as AKT) is the main downstream effector of PI3K, and its activation regulates several cellular processes, such as proliferation, growth, apoptosis, cell survival and angiogenesis in several cell systems, including thyroid cells. Constitutive or enhanced signaling of this pathway is common in thyroid cancer (44, 45), and elevated AKT activity has been associated with tumor size and invasion in both FTC and PTC, with the exception of tumors with BRAF activating mutations (44). Mutations in different components of the PI3K pathway are rare in WDTC, but have a significant prevalence in PDTC and ATC, suggesting a role for PI3K activation in the progression to undifferentiated carcinomas (13).

Upregulated miRNAs Modulating the PI3K Pathway Activity in Thyroid Cancer

The tumor suppressor PTEN is the main negative regulator of the PI3K pathway. PTEN antagonizes the PI3K pathway via its lipid phosphate activity, which diminishes the cytosolic localization of AKT and its subsequent activation. Some upregulated miRNAs have been shown to inhibit PTEN expression, thereby increasing PI3K pathway activity. For example, it was recently shown that miR-146b is the most upregulated miRNA in thyroid cancer (8, 38) and PTEN is one of its main targets. In a thyroid cell system, miR-146b expression decreased the expression of PTEN, which was accompanied by PI3K/AKT hyperactivation, leading to the nuclear exclusion of two main downstream effectors, FOXO1 and $p27^{Kip1}$ and a corresponding increase in cellular proliferation. Moreover, miR-146b-induced repression of PTEN protected cells from apoptosis and increased migration and invasion, chiefly by regulating genes implicated in EMT (46). Interestingly, intratumor administration of a miR-146b inhibitor (antagomiR-146b) blocked tumor growth *in vivo* in a xenograft mouse model (46), and a similar result was obtained in a thyroid orthotopic tumor model after systemic administration of the antagomiR (47). Importantly, this inhibition increased the protein levels of the miR-146b target PTEN (46). In addition to miR-146b, miR-21 is a highly relevant tumor-associated miRNA and is the most frequent upregulated oncomiR in solid tumors, including PTC. miR-21 is regulated by the oncoprotein RAS through activator protein-1 (AP-1) (48). PTEN has also been identified as a target of miR-21 (49), and this was subsequently experimentally validated in a thyroid cell system

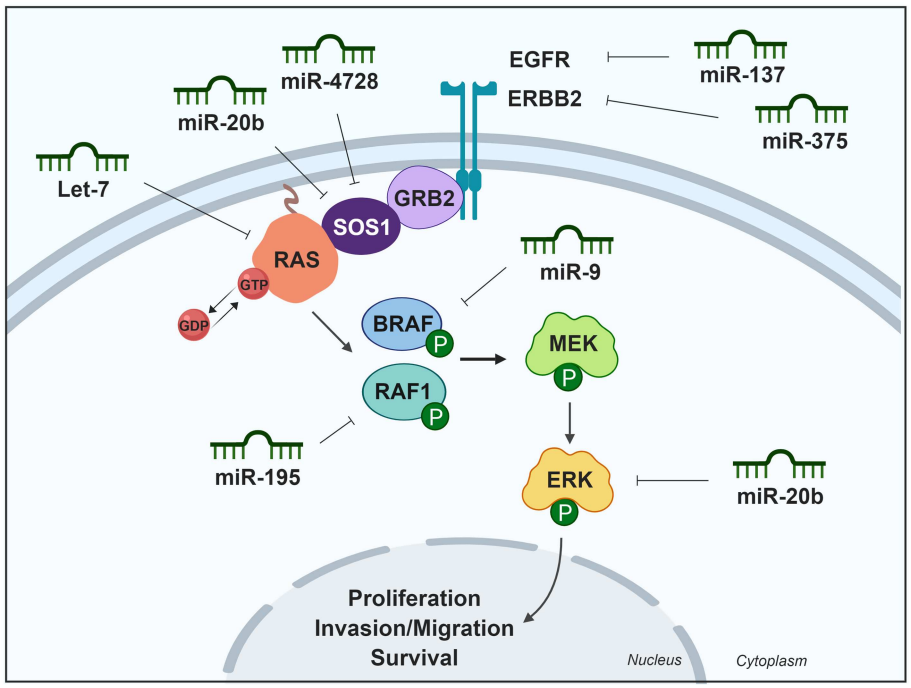

FIGURE 1 | Differentially expressed miRNAs in thyroid cancer tissues modulating the MAPK pathway. Green miRNAs represent downregulated miRNAs when comparing tumoral vs. control tissue. Created with BioRender.

(48). Consequently, PTEN expression is repressed by AP-1 in response to RAS signaling, which is mediated by miR-21. Further, the same group described that the induction of miR-21 requires the activation of at least two RAS downstream pathways, MAPK and PI3K itself (50).

The PI3K/AKT signaling pathway has been reported to be under regulation by the sialyltransferase family in cancer (51). miR-146a is also upregulated in thyroid carcinoma (8, 38) and bioinformatic analyses showed that miR-146a, together with miR-146b, target the sialyltransferase family member ST8SIA4. *In vitro* analysis showed that ST8SIA4 transfection decreased the invasiveness of an miR-146a/b-overexpressing FTC cell line, whereas ST8SIA4 silencing inverted the effects of miR-146a/b inhibition. PI3K p110α, phosphorylated AKT and phosphorylated mTOR were all increased in miR-146a/b-overexpressing cells and their expression was partially reduced after ST8SIA4 restoration. Overall, these results suggest that miR-146a/b activates the PI3K-AKT-mTOR signaling pathway, which is suppressed by ST8SIA4 (52).

Other upregulated miRNAs have been found to play activating roles in the PI3K/AKT signaling pathway. miR-34a, which is upregulated in thyroid cancer (8, 38, 53), promotes cell proliferation and colony formation and inhibits apoptosis. Silencing of *GAS1* had similar effects, in terms of cell growth, as the overexpression of miR-34a. Furthermore, PI3K is activated in PTC cells that overexpress the miR-34a, and depletion of AKT reversed the cell growth, and the anti-apoptotic effects of miR-34a. Thus, miR-34a is thought to function via activation of the PI3K pathway, likely by repressing *GAS1* expression and thereby activating RET and downstream PI3K pathways (53). By contrast, Liu et al. (54) described miR-34a as a downregulated tumor-suppressor miRNA in thyroid cancer tissue and cell lines. They showed that miR-34a decreases the phosphorylation of AKT via MET inhibition. MET acts as a receptor tyrosine kinase and plays key roles in promoting cell growth and proliferation by transducing extracellular stimuli to intracellular signaling circuits including the PI3K pathway.

Activated AKT phosphorylates several targets, such as $p27^{Kip1}$, a kinase inhibitor protein that regulates the cell cycle by preventing the transition from G1 to S phase. Phosphorylation of $p27^{Kip1}$ impairs its nuclear import and leads to cytoplasmic accumulation and cell resistance to G1 arrest (55). Some upregulated miRNAs have been shown to target this effector directly, including miR-221 and miR-222, which negatively regulated $p27^{Kip1}$ expression through two target sites in its 3′UTR region. Consistently, enforced expression of miR-221 and miR-222 induced a PTC cell line to progress to the S phase of the cell cycle (28). Moreover, an inverse correlation was found between miR-221 and miR-222 up-regulation and down-regulation of $p27^{Kip1}$ protein levels in human thyroid papillary carcinoma (28).

Downregulated miRNAs Modulating the PI3K Pathway in Thyroid Cancer

The PI3K pathway can also be regulated by miRNAs that are under-expressed in thyroid cancer, usually by inhibiting genes and regulators of this pathway and thereby decreasing pathway activity. As mentioned previously, inhibition of the EGFR and ERBB2 receptors by miR-137 and miR-375, respectively, does

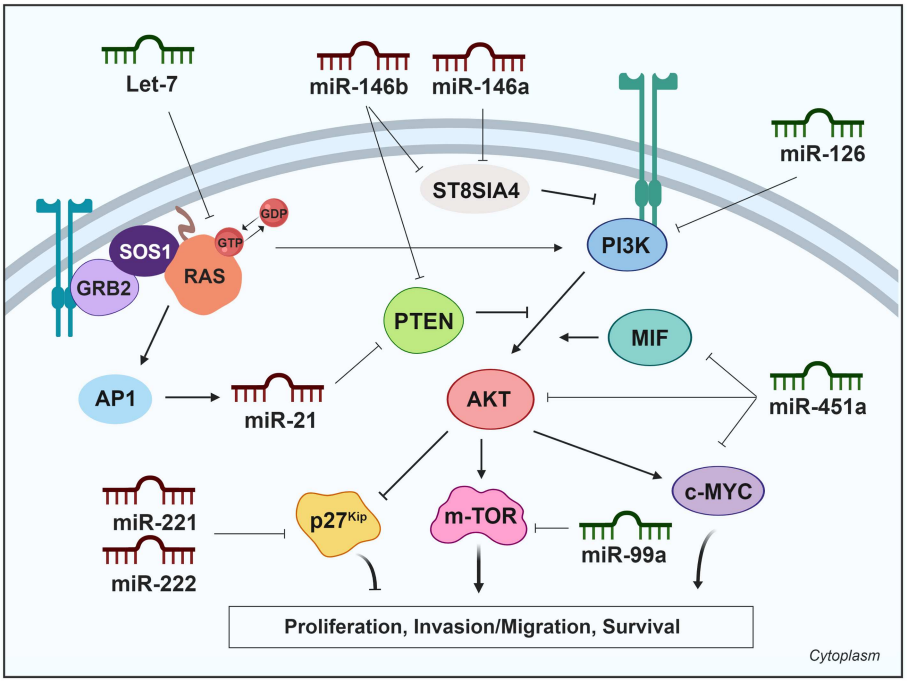

FIGURE 2 | Differentially expressed miRNAs in thyroid cancer tissues modulating the PI3K pathway. Green miRNAs represent downregulated miRNAs when comparing tumoral vs. control tissue and red miRNAs represent the upregulated. Created with BioRender.

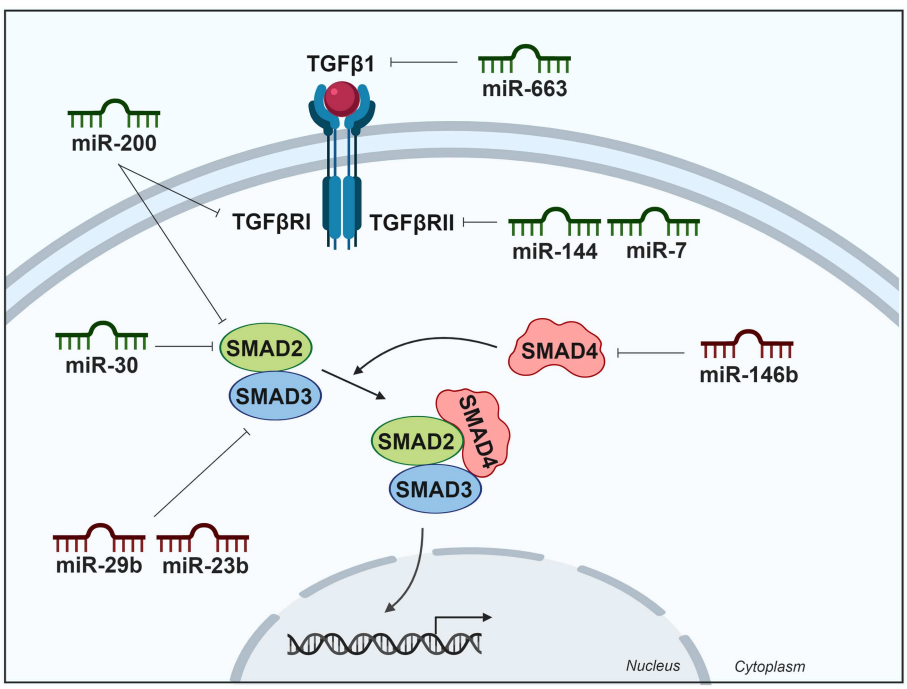

FIGURE 3 | Differentially expressed miRNAs in thyroid cancer tissues modulating the TGFβ pathway. Green miRNAs represent downregulated miRNAs when comparing tumoral vs. control tissue and red miRNAs represent the upregulated. Created with BioRender.

not only affect the MAPK pathway, but also the PI3K pathway. Class I PI3Ks are heterodimeric molecules composed of a p110 catalytic subunit and a p85 regulatory subunit (45). miR-126 was found to act as a proliferation suppressor in BRAF-mutated undifferentiated thyroid cancer cell lines by targeting *PIK3R2* encoding subunit p85β, and reducing protein translation, as

demonstrated by miR-126 mimic transfection and reduction of p85β and pAKT protein levels (56).

miR-451a is one of the most downregulated miRNAs in thyroid cancer, and reduces the protein levels of its recognized targets *MIF*, *AKT1*, and *c-MYC* in PTC cell lines, attenuating AKT pathway activation (57). The pro-inflamatory cytokine MIF (Macrophage migration inhibitory factor) is overexpressed in various tumors, where it promotes tumor growth by the stimulation of multiple signaling cascades, including the AKT pathway (58). Finally, c-MYC is a well-studied oncogenic transcription factor that integrates signals from multiple pathways, including the AKT pathway. c-MYC regulates gene expression and induces cell proliferation, differentiation, and transformation (57, 59). Overall, it seems that miR-451a displays tumor suppressor functions by targeting multiple elements of the PI3K/AKT pathway in PTC.

miR-145 is also downregulated in thyroid cancer (8, 60), and directly targets *AKT3*, reducing AKT levels and inhibiting the PI3K pathway (60). Overexpression of miR-145 in thyroid cancer cell lines resulted in decreased cell proliferation, migration, invasion, VEGF secretion and E-cadherin expression, and decreased tumor growth and metastasis in a xenograft mouse model. Therefore, miR-145 mediates its effects through the PI3K/AKT pathway, and could be an important regulator of thyroid cancer growth.

A major response of the PI3K pathway is the activation of mTOR, which is enhanced by AKT. mTOR is a serine/threonine protein kinase in the PI3K signaling cascade (61). mTOR phosphorylates and activates p70 S6 kinase, and also inhibits eukaryotic translation initiation factor 4E binding protein, resulting in enhanced protein synthesis and cell proliferation. Yang et al. were the first to describe that miR-99a directly targets the mTOR signaling pathway in breast cancer side population cells (62). Subsequently, miR-99a was identified as a downregulated miRNA in PTC (8) and ATC (63) samples. It was experimentally confirmed that miR-99a reduces tumorigenicity in anaplastic thyroid cells *in vitro* and *in vivo* by targeting and reducing mTOR levels, and decreasing downstream phosphorylated proteins eukaryotic translation initiation factor 4E binding protein and p70 S6 kinase (63). A summary of miRNAs and their targets in the PI3K pathway is shown in **Table 1** and is schematically represented in **Figure 2**.

TGFβ Signaling Pathway

The consequence of activated TGFβ signaling is context-dependent and this factor can be classified both as a tumor suppressor and a tumor promoter. Thyroid cancer is an example of this paradox; however, the mechanism underlying this switch of TGFβ action is not well-understood. In thyroid tumors, TGFβ commonly acts as a tumor suppressor at early stages but as a tumor promoter at later stages. The important role of TGFβ activation in BRAF-mutated papillary thyroid tumors has been well-described (14). In early stages of tumorigenesis, the TGFβ pathway is a negative regulator of thyroid follicular cell growth, but the mechanism by which thyroid cancer cells evade its inhibitory signal remains unclear. Some upregulated miRNAs target components of this pathway to inhibit the anti-proliferative signals. By contrast, at later states, the TGFβ pathway induces EMT, migration and invasion, cooperating with BRAF (14).

TGFβ1 is a member of a family of cytokines involved in cell growth (64), differentiation, and apoptosis. This cytokine binds to the type II TGFβ receptor (TGFβRII), recruiting type I TGFβ receptor (TGFβRI) phosphorylating it, initiating signal transduction mediated by downstream SMAD proteins (65, 66). The activated receptor phosphorylates the cytoplasmic transcription factors SMAD2 and SMAD3 (SMAD2/3), allowing them to translocate to the nucleus. SMAD4 acts as a partner with SMAD2/3 to facilitate this process. This translocated heteromeric complex then controls the gene expression contributing to thyroid cancer.

Upregulated miRNA Modulating the TGFβ Pathway Activity in Thyroid Cancer

Several miRNAs are linked to the TGFβ signaling pathway by targeting some of its components. For example, miR-23b and miR-29b are upregulated in PTC according to TCGA data (8) and it has been described that they are regulated by TSH, and their upregulation is required for thyroid cell growth (67). Both miRNAs target SMAD3, inhibiting the TGFβ pathway and promoting thyroid cell growth. Interestingly, an increased expression of these miRNAs was also detected in experimental and human goiter—an enlargement of the thyroid gland (67). In addition, miR-146b is, as previously mentioned, the most upregulated miRNA in PTC and is regarded as an important diagnostic marker. miR-146b binds directly to the 3′UTR of SMAD4. The inhibition of miR-146b was found to increase SMAD4 levels in PTC cell lines, consequently increasing the cellular response to the TGFβ anti-proliferative signals and therefore decreasing cell proliferation (68).

Downregulated miRNA Modulating the TGFβ Pathway Activity in Thyroid Cancer

Although not downregulated in PTC samples according to TCGA (8), the downregulation miR-663 has been reported in PTC tumors when compared with normal adjacent tissues by real-time PCR ($n = 91$) (69). The same authors showed that miR-663 expression was reduced in extrathyroidal invasion PTC tissues compared with non-extrathyroidal invasion PTCs by microarray analysis. A subsequent analysis showed that miR-663 directly targets TGFβ1, thereby regulating the expression of EMT markers and matrix metalloproteinases to suppress PTC cell invasion and migration (70).

miR-7 and miR-144 have been described as downregulated in FTC as compared with follicular thyroid adenoma tissues, and both are reported to target TGFβRII (71). Both miRNAs are also downregulated in PTC (8, 72, 73), and they have been described to functionally act as tumor suppressor miRNAs by reducing cell aggressiveness.

The miR-30 and miR-200 families, which are downregulated in ATC (29, 74), have been involved in the inhibition of TGFβ signaling. The expression of these microRNAs in ATC cells reduced their invasive potential and induced mesenchymal-epithelial transition by regulating the expression of the marker

proteins of this process. The miR-200 family targets TGFβRI and SMAD2, which are upregulated in most primary ATC. Moreover, miR-30 family members also target and decrease SMAD2 expression levels (29). A summary of miRNAs and their targets in the TGFβ pathway is shown in **Table 1** and is schematically represented in **Figure 3**.

CONCLUDING REMARKS

It is currently well-accepted that in human carcinogenesis one of the mechanisms involved is the deregulation of miRNAs through several mechanisms such as epigenetic changes, impaired transcription, amplification or deletion of miRNA genes and defects in the miRNA biogenesis machinery. In the context of thyroid cancer, several dysregulated miRNAs have been shown to affect the hallmarks of these tumors including proliferative signaling and growth suppressor evasion, or affecting invasion and metastasis.

In this review, we have described the up- and down-regulated miRNAs that target the components of the three main signaling pathways activated in thyroid cancer—MAPK, PI3K, and TGFβ. After an exhaustive review of the bibliography, we observed that both up- and down-regulated miRNAs play important roles in these pathways; specifically, that the upregulated miRNAs target factors that suppress pathway activation, whereas the downregulated miRNAs target factors activating the pathways. In this balanced fashion, the three pathways remain activated in cancer with miRNAs functioning as crucial modulators of pathway activity. Given their important roles across thyroid tumorigenesis, miRNAs can be considered as therapeutic targets, since the fine-tuning of their expression can modulate the activity of fundamental pathways hyperactivated in cancer.

AUTHOR CONTRIBUTIONS

JR-M performed an exhaustive revision of the bibliography. JR-M and PS wrote the manuscript.

FUNDING

We acknowledge the support of grants SAF2016-75531-R (MINECO/FEDER, UE); Asociación Española Contra el Cancer (AECC; GCB141423113); CIBERONC from the Instituto de Salud Carlos III (ISCIII) and B2017/BMD-3724 Tironet2 (Comunidad de Madrid). JR-M, holds a FPU fellowship from Spanish Ministry of Education.

ACKNOWLEDGMENTS

We are grateful to Dr. Kenneth McCreath for helpful comments on the manuscript.

REFERENCES

1. Lu J, Getz G, Miska EA, Alvarez-Saavedra E, Lamb J, Peck D, et al. MicroRNA expression profiles classify human cancers. *Nature.* (2005) 435:834–8. doi: 10.1038/nature03702
2. Volinia S, Calin GA, Liu CG, Ambs S, Cimmino A, Petrocca F, et al. A microRNA expression signature of human solid tumors defines cancer gene targets. *Proc Natl Acad Sci USA.* (2006) 103:2257–61. doi: 10.1073/pnas.0510565103
3. Peng Y, Croce CM. The role of microRNAs in human cancer. *Signal Transduct Target Ther.* (2016) 1:15004. doi: 10.1038/sigtrans.2015.4
4. Zhang B, Pan X, Cobb GP, Anderson TA. microRNAs as oncogenes and tumor suppressors. *Dev Biol.* (2007) 302:1–12. doi: 10.1016/j.ydbio.2006.08.028
5. Davies L, Welch HG. Increasing incidence of thyroid cancer in the United States, 1973–2002. *JAMA.* (2006) 295:2164–7. doi: 10.1001/jama.295.18.2164
6. Lim H, Devesa SS, Sosa JA, Check D, Kitahara CM. Trends in thyroid cancer incidence and mortality in the United States, 1974–2013. *JAMA.* (2017) 317:1338–48. doi: 10.1001/jama.2017.2719
7. Nikiforov YE, Nikiforova MN. Molecular genetics and diagnosis of thyroid cancer. *Nat Rev Endocrinol.* (2011) 7:569–80. doi: 10.1038/nrendo.2011.142
8. Cancer Genome Atlas Research N. Integrated genomic characterization of papillary thyroid carcinoma. *Cell.* (2014) 159:676–90. doi: 10.1016/j.cell.2014.09.050
9. Landa I, Ibrahimpasic T, Boucai L, Sinha R, Knauf JA, Shah RH, et al. Genomic and transcriptomic hallmarks of poorly differentiated and anaplastic thyroid cancers. *J Clin Invest.* (2016) 126:1052–66. doi: 10.1172/JCI85271
10. Riesco-Eizaguirre G, Santisteban P. Endocrine tumours: advances in the molecular pathogenesis of thyroid cancer: lessons from the cancer genome. *Eur J Endocrinol.* (2016) 175:R203–17. doi: 10.1530/EJE-16-0202
11. Kimura ET, Nikiforova MN, Zhu Z, Knauf JA, Nikiforov YE, Fagin JA. High prevalence of BRAF mutations in thyroid cancer: genetic evidence for constitutive activation of the RET/PTC-RAS-BRAF signaling pathway in papillary thyroid carcinoma. *Cancer Res.* (2003) 63:1454–7.
12. Santarpia L, Myers JN, Sherman SI, Trimarchi F, Clayman GL, El-Naggar AK. Genetic alterations in the RAS/RAF/mitogen-activated protein kinase and phosphatidylinositol 3-kinase/Akt signaling pathways in the follicular variant of papillary thyroid carcinoma. *Cancer.* (2010) 116:2974–83. doi: 10.1002/cncr.25061
13. Zaballos MA, Santisteban P. Key signaling pathways in thyroid cancer. *J Endocrinol.* (2017) 235:R43–61. doi: 10.1530/JOE-17-0266
14. Riesco-Eizaguirre G, Rodriguez I, De la Vieja A, Costamagna E, Carrasco N, Nistal M, et al. The BRAFV600E oncogene induces transforming growth factor beta secretion leading to sodium iodide symporter repression and increased malignancy in thyroid cancer. *Cancer Res.* (2009) 69:8317–25. doi: 10.1158/0008-5472.CAN-09-1248
15. Kimura ET, Kopp P, Zbaeren J, Asmis LM, Ruchti C, Maciel RM, et al. Expression of transforming growth factor beta1, beta2, and beta3 in multinodular goiters and differentiated thyroid carcinomas: a comparative study. *Thyroid.* (1999) 9:119–25. doi: 10.1089/thy.1999.9.119
16. Vasko V, Espinosa AV, Scouten W, He H, Auer H, Liyanarachchi S, et al. Gene expression and functional evidence of epithelial-to-mesenchymal transition in papillary thyroid carcinoma invasion. *Proc Natl Acad Sci USA.* (2007) 104:2803–8. doi: 10.1073/pnas.0610733104
17. Morales S, Monzo M, Navarro A. Epigenetic regulation mechanisms of microRNA expression. *Biomol Concepts.* (2017) 8:203–12. doi: 10.1515/bmc-2017-0024
18. Moutinho C, Esteller M. MicroRNAs and Epigenetics. *Adv Cancer Res.* (2017) 135:189–220. doi: 10.1016/bs.acr.2017.06.003
19. Krishna M, Narang H. The complexity of mitogen-activated protein kinases (MAPKs) made simple. *Cell Mol Life Sci.* (2008) 65:3525–44. doi: 10.1007/s00018-008-8170-7

20. Hatley ME, Patrick DM, Garcia MR, Richardson JA, Bassel-Duby R, van Rooij E, et al. Modulation of K-Ras-dependent lung tumorigenesis by microRNA-21. *Cancer Cell.* (2010) 18:282–93. doi: 10.1016/j.ccr.2010.08.013
21. Chou CK, Chen RF, Chou FF, Chang HW, Chen YJ, Lee YF, et al. miR-146b is highly expressed in adult papillary thyroid carcinomas with high risk features including extrathyroidal invasion and the BRAF(V600E) mutation. *Thyroid.* (2010) 20:489–94. doi: 10.1089/thy.2009.0027
22. Sun Y, Yu S, Liu Y, Wang F, Liu Y, Xiao H. Expression of miRNAs in papillary thyroid carcinomas is associated with BRAF mutation and clinicopathological features in Chinese patients. *Int J Endocrinol.* (2013) 2013:128735. doi: 10.1155/2013/128735
23. Reinhart BJ, Slack FJ, Basson M, Pasquinelli AE, Bettinger JC, Rougvie AE, et al. The 21-nucleotide let-7 RNA regulates developmental timing in *Caenorhabditis elegans*. *Nature.* (2000) 403:901–6. doi: 10.1038/35002607
24. Johnson SM, Grosshans H, Shingara J, Byrom M, Jarvis R, Cheng A, et al. RAS is regulated by the let-7 microRNA family. *Cell.* (2005) 120:635–47. doi: 10.1016/j.cell.2005.01.014
25. Ricarte-Filho JC, Fuziwara CS, Yamashita AS, Rezende E, da-Silva MJ, Kimura ET. Effects of let-7 microRNA on cell growth and differentiation of papillary thyroid cancer. *Transl Oncol.* (2009) 2:236–41. doi: 10.1593/tlo.09151
26. Negrini M, Ferracin M, Sabbioni S, Croce CM. MicroRNAs in human cancer: from research to therapy. *J Cell Sci.* (2007) 120 (Pt 11):1833–40. doi: 10.1242/jcs.03450
27. Pallante P, Visone R, Ferracin M, Ferraro A, Berlingieri MT, Troncone G, et al. MicroRNA deregulation in human thyroid papillary carcinomas. *Endocr Relat Cancer.* (2006) 13:497–508. doi: 10.1677/erc.1.01209
28. Visone R, Pallante P, Vecchione A, Cirombella R, Ferracin M, Ferraro A, et al. Specific microRNAs are downregulated in human thyroid anaplastic carcinomas. *Oncogene.* (2007) 26:7590–5. doi: 10.1038/sj.onc.1210564
29. Braun J, Hoang-Vu C, Dralle H, Huttelmaier S. Downregulation of microRNAs directs the EMT and invasive potential of anaplastic thyroid carcinomas. *Oncogene.* (2010) 29:4237–44. doi: 10.1038/onc.2010.169
30. Perdas E, Stawski R, Nowak D, Zubrzycka M. The role of miRNA in papillary thyroid cancer in the context of miRNA Let-7 family. *Int J Mol Sci.* (2016) 17:909. doi: 10.3390/ijms17060909
31. Schiff BA, McMurphy AB, Jasser SA, Younes MN, Doan D, Yigitbasi OG, et al. Epidermal growth factor receptor (EGFR) is overexpressed in anaplastic thyroid cancer, and the EGFR inhibitor gefitinib inhibits the growth of anaplastic thyroid cancer. *Clin Cancer Res.* (2004) 10:8594–602. doi: 10.1158/1078-0432.CCR-04-0690
32. Gule MK, Chen Y, Sano D, Frederick MJ, Zhou G, Zhao M, et al. Targeted therapy of VEGFR2 and EGFR significantly inhibits growth of anaplastic thyroid cancer in an orthotopic murine model. *Clin Cancer Res.* (2011) 17:2281–91. doi: 10.1158/1078-0432.CCR-10-2762
33. Luo Y, Li X, Dong J, Sun W. microRNA-137 is downregulated in thyroid cancer and inhibits proliferation and invasion by targeting EGFR. *Tumour Biol.* (2016) 37:7749–55. doi: 10.1007/s13277-015-4611-8
34. Seebacher NA, Stacy AE, Porter GM, Merlot AM. Clinical development of targeted and immune based anti-cancer therapies. *J Exp Clin Cancer Res.* (2019) 38:156. doi: 10.1186/s13046-019-1094-2
35. Muthuswamy SK, Li D, Lelievre S, Bissell MJ, Brugge JS. ErbB2, but not ErbB1, reinitiates proliferation and induces luminal repopulation in epithelial acini. *Nat Cell Biol.* (2001) 3:785–92. doi: 10.1038/ncb0901-785
36. Bang YJ. Advances in the management of HER2-positive advanced gastric and gastroesophageal junction cancer. *J Clin Gastroenterol.* (2012) 46:637–48. doi: 10.1097/MCG.0b013e3182557307
37. Wang XZ, Hang YK, Liu JB, Hou YQ, Wang N, Wang MJ. Over-expression of microRNA-375 inhibits papillary thyroid carcinoma cell proliferation and induces cell apoptosis by targeting ERBB2. *J Pharmacol Sci.* (2016) 130:78–84. doi: 10.1016/j.jphs.2015.12.001
38. Riesco-Eizaguirre G, Wert-Lamas L, Perales-Paton J, Sastre-Perona A, Fernandez LP, Santisteban P. The miR-146b-3p/PAX8/NIS regulatory circuit modulates the differentiation phenotype and function of thyroid cells during carcinogenesis. *Cancer Res.* (2015) 75:4119–30. doi: 10.1158/0008-5472.CAN-14-3547
39. Liu Z, Zhang J, Gao J, Li Y. MicroRNA-4728 mediated regulation of MAPK oncogenic signaling in papillary thyroid carcinoma. *Saudi J Biol Sci.* (2018) 25:986–90. doi: 10.1016/j.sjbs.2018.05.014
40. Hong S, Yu S, Li J, Yin Y, Liu Y, Zhang Q, et al. MiR-20b displays tumor-suppressor functions in papillary thyroid carcinoma by regulating the MAPK/ERK signaling pathway. *Thyroid.* (2016) 26:1733–43. doi: 10.1089/thy.2015.0578
41. Swierniak M, Wojcicka A, Czetwertynska M, Stachlewska E, Maciag M, Wiechno W, et al. In-depth characterization of the microRNA transcriptome in normal thyroid and papillary thyroid carcinoma. *J Clin Endocrinol Metab.* (2013) 98:E1401–9. doi: 10.1210/jc.2013-1214
42. Wang F, Jiang C, Sun Q, Yan F, Wang L, Fu Z, et al. miR-195 is a key regulator of Raf1 in thyroid cancer. *Onco Targets Ther.* (2015) 8:3021–8. doi: 10.2147/OTT.S90710
43. Guo F, Hou X, Sun Q. MicroRNA-9-5p functions as a tumor suppressor in papillary thyroid cancer via targeting BRAF. *Oncol Lett.* (2018) 16:6815–21. doi: 10.3892/ol.2018.9423
44. Shinohara M, Chung YJ, Saji M, Ringel MD. AKT in thyroid tumorigenesis and progression. *Endocrinology.* (2007) 148:942–7. doi: 10.1210/en.2006-0937
45. Nozhat Z, Hedayati M. PI3K/AKT pathway and its mediators in thyroid carcinomas. *Mol Diagn Ther.* (2016) 20:13–26. doi: 10.1007/s40291-015-0175-y
46. Ramirez-Moya J, Wert-Lamas L, Santisteban P. MicroRNA-146b promotes PI3K/AKT pathway hyperactivation and thyroid cancer progression by targeting PTEN. *Oncogene.* (2018) 37:3369–83. doi: 10.1038/s41388-017-0088-9
47. Ramirez-Moya J, Wert-Lamas L, Riesco-Eizaguirre G, Santisteban P. Impaired microRNA processing by DICER1 downregulation endows thyroid cancer with increased aggressiveness. *Oncogene.* (2019). doi: 10.1038/s41388-019-0804-8. [Epub ahead of print].
48. Talotta F, Cimmino A, Matarazzo MR, Casalino L, De Vita G, D'Esposito M, et al. An autoregulatory loop mediated by miR-21 and PDCD4 controls the AP-1 activity in RAS transformation. *Oncogene.* (2009) 28:73–84. doi: 10.1038/onc.2008.370
49. Meng F, Henson R, Wehbe-Janek H, Ghoshal K, Jacob ST, Patel T. MicroRNA-21 regulates expression of the PTEN tumor suppressor gene in human hepatocellular cancer. *Gastroenterology.* (2007) 133:647–58. doi: 10.1053/j.gastro.2007.05.022
50. Frezzetti D, De Menna M, Zoppoli P, Guerra C, Ferraro A, Bello AM, et al. Upregulation of miR-21 by Ras *in vivo* and its role in tumor growth. *Oncogene.* (2011) 30:275–86. doi: 10.1038/onc.2010.416
51. Ma H, Zhou H, Song X, Shi S, Zhang J, Jia L. Modification of sialylation is associated with multidrug resistance in human acute myeloid leukemia. *Oncogene.* (2015) 34:726–40. doi: 10.1038/onc.2014.7
52. Ma W, Zhao X, Liang L, Wang G, Li Y, Miao X, et al. miR-146a and miR-146b promote proliferation, migration and invasion of follicular thyroid carcinoma via inhibition of ST8SIA4. *Oncotarget.* (2017) 8:28028–41. doi: 10.18632/oncotarget.15885
53. Ma Y, Qin H, Cui Y. MiR-34a targets GAS1 to promote cell proliferation and inhibit apoptosis in papillary thyroid carcinoma via PI3K/Akt/Bad pathway. *Biochem Biophys Res Commun.* (2013) 441:958–63. doi: 10.1016/j.bbrc.2013.11.010
54. Liu H, Deng H, Zhao Y, Li C, Liang Y. LncRNA XIST/miR-34a axis modulates the cell proliferation and tumor growth of thyroid cancer through MET-PI3K-AKT signaling. *J Exp Clin Cancer Res.* (2018) 37:279. doi: 10.1186/s13046-018-0950-9
55. Liang J, Zubovitz J, Petrocelli T, Kotchetkov R, Connor MK, Han K, et al. PKB/Akt phosphorylates p27, impairs nuclear import of p27 and opposes p27-mediated G1 arrest. *Nat Med.* (2002) 8:1153–60. doi: 10.1038/nm761
56. Rahman MA, Salajegheh A, Smith RA, Lam AK. MicroRNA-126 suppresses proliferation of undifferentiated (BRAF(V600E) and BRAF(WT)) thyroid carcinoma through targeting PIK3R2 gene and repressing PI3K-AKT proliferation-survival signalling pathway. *Exp Cell Res.* (2015) 339:342–50. doi: 10.1016/j.yexcr.2015.09.010
57. Minna E, Romeo P, Dugo M, De Cecco L, Todoerti K, Pilotti S, et al. miR-451a is underexpressed and targets AKT/mTOR pathway in papillary thyroid carcinoma. *Oncotarget.* (2016) 7:12731–47. doi: 10.18632/oncotarget.7262
58. Lue H, Thiele M, Franz J, Dahl E, Speckgens S, Leng L, et al. Macrophage migration inhibitory factor (MIF) promotes cell survival by activation of the Akt pathway and role for CSN5/JAB1 in the control of autocrine MIF activity. *Oncogene.* (2007) 26:5046–59. doi: 10.1038/sj.onc.1210318

59. Tu WB, Helander S, Pilstal R, Hickman KA, Lourenco C, Jurisica I, et al. Myc and its interactors take shape. *Biochim Biophys Acta.* (2015) 1849:469–83. doi: 10.1016/j.bbagrm.2014.06.002
60. Boufraqech M, Zhang L, Jain M, Patel D, Ellis R, Xiong Y, et al. miR-145 suppresses thyroid cancer growth and metastasis and targets AKT3. *Endocr Relat Cancer.* (2014) 21:517–31. doi: 10.1530/ERC-14-0077
61. Saji M, Ringel MD. The PI3K-Akt-mTOR pathway in initiation and progression of thyroid tumors. *Mol Cell Endocrinol.* (2010) 321:20–8. doi: 10.1016/j.mce.2009.10.016
62. Yang Z, Han Y, Cheng K, Zhang G, Wang X. miR-99a directly targets the mTOR signalling pathway in breast cancer side population cells. *Cell Prolif.* (2014) 47:587–95. doi: 10.1111/cpr.12146
63. Huang HG, Luo X, Wu S, Jian B. MiR-99a inhibits cell proliferation and tumorigenesis through targeting mTOR in human anaplastic thyroid cancer. *Asian Pac J Cancer Prev.* (2015) 16:4937–44. doi: 10.7314/apjcp.2015.16.12.4937
64. Carneiro C, Alvarez CV, Zalvide J, Vidal A, Dominguez F. TGF-beta1 actions on FRTL-5 cells provide a model for the physiological regulation of thyroid growth. *Oncogene.* (1998) 16:1455–65. doi: 10.1038/sj.onc.1201662
65. Massague J. TGFbeta signaling: receptors, transducers, and Mad proteins. *Cell.* (1996) 85:947–50.
66. Pardali K, Moustakas A. Actions of TGF-beta as tumor suppressor and pro-metastatic factor in human cancer. *Biochim Biophys Acta.* (2007) 1775:21–62. doi: 10.1016/j.bbcan.2006.06.004
67. Leone V, D'Angelo D, Pallante P, Croce CM, Fusco A. Thyrotropin regulates thyroid cell proliferation by up-regulating miR-23b and miR-29b that target SMAD3. *J Clin Endocrinol Metab.* (2012) 97:3292–301. doi: 10.1210/jc.2012-1349
68. Geraldo MV, Yamashita AS, Kimura ET. MicroRNA miR-146b-5p regulates signal transduction of TGF-beta by repressing SMAD4 in thyroid cancer. *Oncogene.* (2012) 31:1910–22. doi: 10.1038/onc.2011.381
69. Wang Z, Zhang H, He L, Dong W, Li J, Shan Z, et al. Association between the expression of four upregulated miRNAs and extrathyroidal invasion in papillary thyroid carcinoma. *Onco Targets Ther.* (2013) 6:281–7. doi: 10.2147/OTT.S43014
70. Wang Z, Zhang H, Zhang P, Dong W, He L. MicroRNA-663 suppresses cell invasion and migration by targeting transforming growth factor beta 1 in papillary thyroid carcinoma. *Tumour Biol.* (2016) 37:7633–44. doi: 10.1007/s13277-015-4653-y
71. Chi J, Zheng X, Gao M, Zhao J, Li D, Li J, et al. Integrated microRNA-mRNA analyses of distinct expression profiles in follicular thyroid tumors. *Oncol Lett.* (2017) 14:7153–60. doi: 10.3892/ol.2017.7146
72. Guan H, Liang W, Xie Z, Li H, Liu J, Liu L, et al. Down-regulation of miR-144 promotes thyroid cancer cell invasion by targeting ZEB1 and ZEB2. *Endocrine.* (2015) 48:566–74. doi: 10.1007/s12020-014-0326-7
73. Yue K, Wang X, Wu Y, Zhou X, He Q, Duan Y. microRNA-7 regulates cell growth, migration and invasion via direct targeting of PAK1 in thyroid cancer. *Mol Med Rep.* (2016) 14:2127–34. doi: 10.3892/mmr.2016.5477
74. Zhu G, Xie L, Miller D. Expression of microRNAs in thyroid carcinoma. *Methods Mol Biol.* (2017) 1617:261–80. doi: 10.1007/978-1-4939-7046-9_19

Conflict of Interest Statement: The authors declare that the research was conducted in the absence of any commercial or financial relationships that could be construed as a potential conflict of interest.

frontiers in Endocrinology

ORIGINAL RESEARCH
published: 04 July 2019
doi: 10.3389/fendo.2019.00438

Analytical Verification Performance of Afirma Genomic Sequencing Classifier in the Diagnosis of Cytologically Indeterminate Thyroid Nodules

*Yangyang Hao[1], Yoonha Choi[1], Joshua E. Babiarz[1], Richard T. Kloos[2], Giulia C. Kennedy[1,2,3], Jing Huang[1] and P. Sean Walsh[1]**

[1] Research and Development, Veracyte, South San Francisco, CA, United States, [2] Medical Affairs, Veracyte, South San Francisco, CA, United States, [3] Department of Clinical Affairs, Veracyte, South San Francisco, CA, United States

OPEN ACCESS

Edited by:
Vasyl Vasko, Uniformed Services University of the Health Sciences, United States

Reviewed by:
Giampaolo Papi, Local Health Unit of Modena, Italy
Miloš Žarković, Faculty of Medicine, University of Belgrade, Serbia

***Correspondence:**
P. Sean Walsh
sean@veracyte.com

Specialty section:
This article was submitted to Thyroid Endocrinology, a section of the journal Frontiers in Endocrinology

Received: *30 April 2019*
Accepted: *18 June 2019*
Published: *04 July 2019*

Citation:
Hao Y, Choi Y, Babiarz JE, Kloos RT, Kennedy GC, Huang J and Walsh PS (2019) Analytical Verification Performance of Afirma Genomic Sequencing Classifier in the Diagnosis of Cytologically Indeterminate Thyroid Nodules. Front. Endocrinol. 10:438. doi: 10.3389/fendo.2019.00438

Background: Fine needle aspiration (FNA) cytology, a diagnostic test central to thyroid nodule management, may yield indeterminate results in up to 30% of cases. The Afirma® Genomic Sequencing Classifier (GSC) was developed and clinically validated to utilize genomic material obtained during the FNA to accurately identify benign nodules among those deemed cytologically indeterminate so that diagnostic surgery can be avoided. A key question for diagnostic tests is their robustness under different perturbations that may occur in the lab. Herein, we describe the analytical performance of the Afirma GSC.

Results: We examined the analytical sensitivity of the Afirma GSC to varied input RNA amounts and the limit of detection of malignant signals with heterogenous samples mixed with adjacent normal or benign tissues. We also evaluated the analytical specificity from potential interfering substances such as blood and genomic DNA. Further, the inter-laboratory, intra-run, and inter-run reproducibility of the assay were examined. Analytical sensitivity analysis showed that Afirma GSC calls are tolerant to variation in RNA input amount (5–30 ng), and up to 75% dilution of malignant FNA material. Analytical specificity studies demonstrated Afirma GSC remains accurate in presence of up to 75% blood or 30% genomic DNA. The Afirma GSC results are highly reproducible across different operators, runs, reagent lots, and laboratories.

Conclusion: The analytical robustness and reproducibility of the Afirma GSC test support its routine clinical use among thyroid nodules with indeterminant FNA cytology.

Keywords: thyroid cancer, RNA-Seq, genomics, analytical verification, molecular diagnostics, lab developed test, clinical robustness, Afirma GSC

INTRODUCTION

The pre-operative testing of thyroid nodules to differentiate benignity from malignancy is primarily based on fine needle aspiration (FNA) biopsy followed by cytological examination of the collected specimen. While several cytological reporting systems exist and share broad similarities, perhaps the most common is The Bethesda System for Reporting Thyroid Cytopathology (1). About 20–30% of sufficient FNA biopsies are considered neither benign nor malignant and collectively are labeled as cytologically indeterminate (2). Given the possibility of thyroid cancer, patients with an indeterminate FNA are often advised to undergo an invasive surgical procedure to remove part, or all, of the thyroid gland. However, about three-quarters of cytologically indeterminate nodules are found to be benign upon surgical pathology evaluation. Several studies have documented the significant impact of unnecessary diagnostic surgery including direct and indirect medical costs, surgical complications, and impaired patient quality of life (3). Thus, we have developed a molecular test that utilizes genomic information from the thyroid nodule, coupled with machine-learned algorithms, to safely avoid unnecessary diagnostic surgery among patients with indeterminate FNA cytology.

Previously, a microarray-based gene expression classifier (GEC) was developed to classify FNAs with indeterminate FNA cytology, for the goal of achieving a high sensitivity and high negative predictive value performance (4, 5). GEC utilized FNA specimens and reduced unnecessary surgeries (6). More recently, the Afirma GSC was developed using next-generation RNA-sequencing data with improved specificity while maintaining both high test sensitivity and negative predictive values (7). The Afirma platform migration provided broader genomic content for assay improvement compared to the GEC: (1) the measurement of RNA expression via RNA sequencing rather than microarray enabled enhanced detection of transcript levels of nuclear/mitochondrial RNAs and changes in genomic copy number, including loss of heterozygosity; (2) the benign vs. malignant (BM) classifier now consists of an ensemble of machine learning classifiers leveraging global expression patterns of a large number of genes and includes Hürthle and Neoplasm cassettes to improve specificity among Hürthle-containing samples (8); (3) In addition to the BM classifier, the Afirma GSC suite includes three other genomic classifiers: a parathyroid (PTA) classifier, a medullary thyroid cancer (MTC) classifier, and a *BRAF* V600E classifier. Finally, the presence of *RET/PTC1* and *RET/PTC3* fusions, which are highly associated with malignancy, are reported when detected. Each of the components is integrated into the GSC diagnostic flow to provide a GSC benign vs. suspicious result (7). These technical improvements result in substantially improved specificity while maintaining >90% sensitivity (7). The improved test specificity of Afirma GSC results in substantially more patients receiving a benign genomic result which facilitates further reductions in unnecessary surgery (9, 10). The improved specificity also increased the GSC positive predictive value which leads to greater confidence in the need for surgery among those with GSC suspicious results (9, 10).

Here we evaluate the analytical validity of the Afirma GSC suite to demonstrate its robustness to various potential technical variables and interferents arising from sample or laboratory processing. It is critical that clinical tests be robust to real-world conditions so that patients receive consistent, accurate results. Because the Afirma GSC was developed as a rule-out test with a high negative predictive value (NPV) and the intent to avoid unnecessary diagnostic surgeries, many of the analytical validity studies were designed to evaluate the potential of conditions that might introduce a false negative result. In this study, we performed analytical sensitivity analyses to evaluate variable total RNA input amounts on classification results, and the impact of mixing benign or adjacent normal samples into malignant samples via limit of detection (LOD) studies. We also performed analytical specificity analyses to evaluate the impact of mixing blood with the FNA specimen, and the impact of mixing genomic DNA content into the FNA specimen due to incomplete separation of DNA from RNA. We evaluated the reproducibility of Afirma GSC result across different laboratories. Finally, we assessed the reproducibility of Afirma GSC results for replicates within runs, between runs, across multiple reagent lots, and performance by multiple operators on different days. We conclude that the Afirma GSC suite shows robust performance across the tested conditions.

MATERIALS AND METHODS

Specimens

Ethics committee approval—This research was approved by the Copernicus Group Independent Review Board (Cary, North Carolina). A waiver of written informed consent was granted regarding de-identified biological materials from the CLIA laboratory. IRB approval and written Informed consent in accordance with the Declaration of Helsinki was provided by all patients whose samples were previously used for training and validation of the Afirma GSC as previously described (7).

Prospective FNA clinical samples were acquired and shipped under controlled temperature and stored at −80°C until extraction. See Walsh et al. (11) for a description of normal adjacent tissue and blood samples used in this study.

RNA Extraction, Library Preparation and RNA Sequencing

The RNA library for clinical FNA specimens was purified, prepared, and sequenced as previously described (7). Briefly, total RNA was extracted using the AllPrep Micro Kit (QIAGEN). RNA yield was quantified with the QuantiFluor RNA System (Promega, Madison, WI), and the RNA Integrity Number (RIN) was evaluated using the Bioanalyzer 2100 (Agilent Technology, Santa Clara, CA).

Control samples, including Universal Human Reference (UHR; Agilent, Santa Clara, CA), were included with replicates. Fifteen nanogram of samples and controls were transferred to 96 well-plates and sequencing libraries were prepared with the TruSeq RNA Exome Library Preparation Kit (Illumina, San Diego, CA) automated on the Microlab STAR robotics platform (Hamilton, Reno, NV). Briefly, RNA specimens were fragmented,

reversed transcribed, end-repaired, A-tailed, and ligated with adapters, followed by PCR, two rounds of exome capture, and a final PCR amplification according to the manufacturer's recommendation. RNA libraries were then sequenced on NextSeq 500 sequencers (Illumina, San Diego, CA). Sequencing runs with >75% of bases ≥Q30 and <1% phiX error rate were accepted.

Sequencing Data Processing and Afirma GSC Result Generation

RNA-sequencing data were processed through the bioinformatics pipeline as depicted in the workflow shown in **Figure 1**. Briefly, raw sequencing data in FASTQ format was mapped to the human reference genome assembly 37 using the STAR RNA-seq aligner (12). Samples passing the quality metrics from RNA-SeQC (13) were analyzed further. Reads data were counted using HTSeq (14). The read count matrix was then normalized using DESeq2 (15) for stabilizing highly variable genes and variation in sequencing depth. Gene fusions were detected using STAR-Fusion (16). The expression level data and fusion-calling results were passed to the Afirma GSC genomic classifier suite and scores and binary calls were generated by each classifier.

BRAF V600E Status

As a reference method, Competitive Allele-Specific Taqman PCR (castPCR™) for *BRAF* c.1799T>A (Thermo Fisher, Waltham, MA) was performed as previously described (7, 17, 18). Samples with a variant allele frequency (VAF) <5% were considered *BRAF* V600 wild type, while VAF ≥5% were considered *BRAF* V600E positive.

Analytical Verification Study Design

The analytical verification study includes 3 key components: analytical sensitivity, analytical specificity and reproducibility. These components test whether the RNA-sequencing based Afirma GSC genomic classifier suite can maintain the same critical clinical validity and classifier performance of sensitivity ≥90% and NPV ≥90% under conditions of technical variability and interferents potentially encountered in a real-life setting. Afirma GSC BM, *BRAF* V600E, MTC and PTA are all evaluated in a similar fashion.

Analytical Sensitivity

- Variability in total RNA input quantity study tests the classifier robustness at five RNA input values: 5, 10, 15, 20, and 30 ng. Both classifier positive and negative samples were sequenced in triplicate for evaluation.
- Dilution of malignant FNA content (limit of detection) tests the dilution effect of malignant (classifier positive) signal by adjacent normal or benign tissue. The dilution levels increase in increments of 20% or 25% for BM, *BRAF* V600E, MTC, and PTA classifiers, and in increments of 5% for RET/PTC fusion detection module.

Analytical Specificity

- In a real-life clinical setting, blood is a potential interferent in FNA biopsies. Selected benign, malignant, *BRAF* V600E, MTC and PTA positive samples were mixed with blood proportionally *in vitro* at 0, 25, 50, 75, and 100% to evaluate their impact on the Afirma GSC performance.
- Genomic DNA is another potential interferent and was tested for its possibility to skew the expression level estimations. Both classifier positive and negative samples were mixed with 0% or 30% genomic DNA and sequenced in triplicate for evaluation.

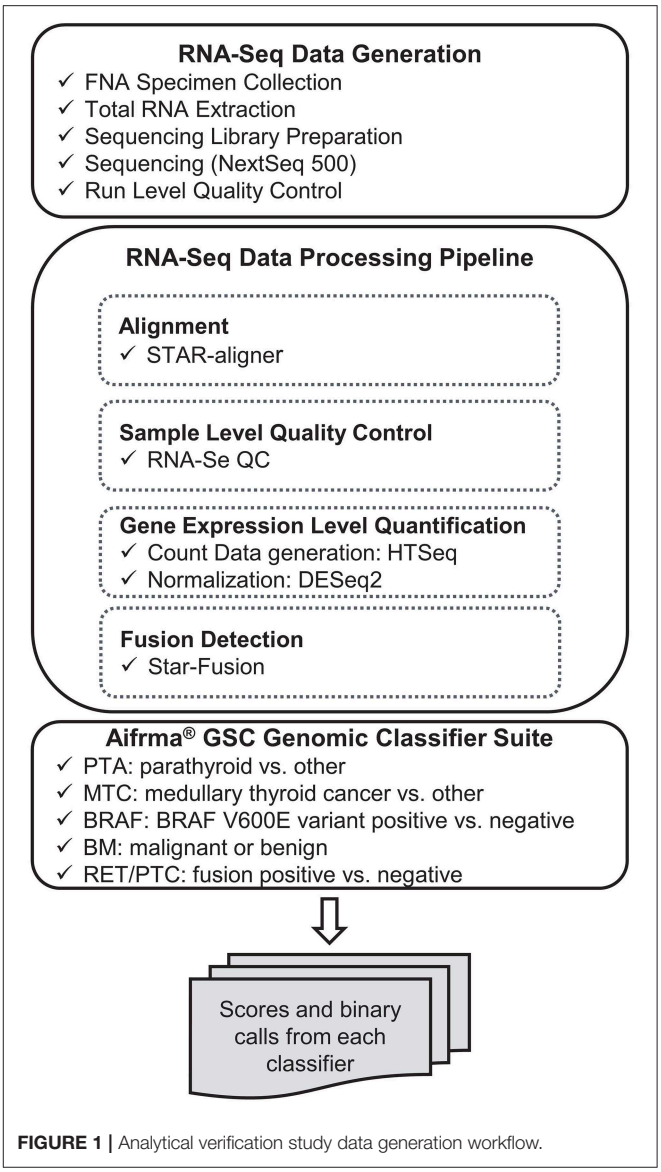

FIGURE 1 | Analytical verification study data generation workflow.

Reproducibility

- Inter-laboratory reproducibility tests the concordance of classifier as well as the stability of classifier scores. Samples covering the classifier score range were selected and sequenced in both R&D and CLIA laboratories.
- Assay reproducibility tests the assay stability of classifier calls and scores when samples are run by different operators, on different days and instruments, and across multiple lots

of reagents. Selected samples covering each classifier score range were tested in triplicate across three independent experimental runs.

Analytical Verification Data Analysis

Analytical Verification Statistical Analysis

The effects of RNA input amount variation (analytical sensitivity) and genomic DNA interference (analytical specificity) were evaluated using a linear mixed effect model (Equation 1) on the classifier scores (S_{ijk}). Specifically, μ_i indicates the sample effect and is fitted as a random effect. b_j is the experimental effect and is modeled as a fixed effect. For the input amount variation study, b_j is the input amount (5, 10, 15, 20, or 30 ng); while for the genomic DNA interference study, b_j is the percentage of genomic DNA (0% or 30%). ε_{ijk} is the residual, and k indicates the technical replicate. Analysis of variance (ANOVA) analysis tests whether the experimental effect is significant (significance level = 0.05).

$$S_{ijk} = \mu_i + b_j + \varepsilon_{ijk} \quad (1)$$

The dilution of malignant FNA (analytical sensitivity) is designed to quantify the impact of interfering classifier negative signals commonly encountered in a real-life clinical setting. To infer the trend of classifier scores at mixture points not tested experimentally (*in vitro*), an *in silico* mixing is performed for each experiment. For each gene g, the number of read counts C_{gj} at mixture percentage p_j ($p_j = 0,\ 0.01,\ 0.02,\ \ldots 1$) is calculated by Equation 2, where C_1 denotes the classifier positive sample and C_2 denotes the classifier negative sample. Then, C_{gj} is normalized using DESeq2 similarly as other RNA-Seq derived count data.

$$C_{gj} = p_j * C_{1g} + (1 - p_j)^* C_{2g} \quad (2)$$

For inter-laboratory reproducibility, the correlation coefficients of samples were computed using Pearson's correlation. The lab effect on classifier scores were estimated by a linear mixed effect model as specified in Equation 1, where b_j indicates the specific laboratory (RD or CLIA). For assay reproducibility, the classifier scores are modeled as:

$$S_{ijk} = \mu_i + r_j + \mu_i : r_j + \ \varepsilon_{ijk} \quad (3)$$

where μ_i is the fixed sample effect, and r_j is the run effect, which is modeled as a random effect. $\mu_i : r_j$ is the interaction effect between sample i and run j, which is modeled as a random effect as well. All 95% confidence intervals for standard deviation (SD) were estimated by bootstrapping.

Reproducibility Acceptance Specification Determination

A 3-step simulation study was performed for each classifier to define the tolerable variability level, beyond which, the performance is severely affected.

- (1) Random noise ϵ is generated from the normal distribution $\epsilon \sim N(0,\ \sigma^2)$, where standard deviation σ spans between 0.36 and 2.10 with an increment of 0.02. Such simulated noise is added to the original classifier scores to create the simulated scores mimicking the classifier being impacted by different levels of noise.
- (2) Performance metrics (for example: sensitivity, specificity, PPA, NPA, etc.) are computed on the simulated scores.
- (3) Steps (1) and (2) are repeated 1,000 times for each noise setting and the median performance metrics are computed.

The maximum score variability tolerated for each classifier is determined with median clinical performance metrics higher or equal to the pre-specified product requirements.

RESULTS

Analytical Sensitivity—Total RNA Input Quantity

The standard input quantity of total RNA to the Afirma® GSC assay is 15 ng. However, the quantity of input material may vary in the lab due to quantitation and pipetting variance. We analyzed the Afirma GSC performance over a range of input amounts wider than expected to occur in the lab to determine the robustness of the test for both classifier positive and negative samples. The titration levels of input mass were evaluated in triplicate at 5, 10, 15, 20, and 30 ng (**Figure 2A** and **Figure S1**). There was no significant difference in the GSC BM scores across different input amount when evaluated with a linear mixed effect model (BM classifier: p-value = 0.97, **Figure 2A**). The *BRAF* V600E, MTC, and PTA classifiers were also evaluated (**Table S1**), and no significant difference in their scores were observed. Finally, a *RET/PTC1* fusion positive sample was tested across the same input amounts and all input amounts tested resulted in *RET/PTC1* true positive calls (**Figure S1D**). This study showed highly robust analytical sensitivity of the Afirma GSC genomic test to variability in RNA input quantity.

Analytical Sensitivity—Dilution of Malignant FNA Content (Limit of Detection)

During routine FNA procedures, Adjacent Normal Tissue (ANT) may also be sampled in varying quantities. We sought to define the limit of detection of a classifier positive nodule in the background of adjacent normal tissue or benign tissue. The tolerance of a classifier positive signal to dilution as evaluated using *in vitro* total RNA mixtures from a malignant FNA sample. The limit of detection for classifier positive signals was evaluated at 0, 40, 60, 80, and 100% of adjacent normal tissue or benign tissue as diluted by total RNA mass. The pure adjacent normal tissue was classified as benign by the GSC, whereas all pure malignant FNA samples and different degree of mixtures resulted in malignant GSC calls (**Table 1** and **Table S2**). MTC, PTA and RET-PTC fusions were evaluated in a similar way. Overall, each GSC component could tolerate dilution by more than 75% RNA derived from benign or adjacent normal tissue and still make the correct prediction (**Table 1** and **Table S2**). To understand if the classifier can distinguish the malignant signal in a higher benign background, an *in silico* mixing approach was explored (see Methods). The *in silico* modeling shows that the BM classifier can differentiate a 5% malignant signal in a background of 95% benign RNA (**Table 1**), suggesting that the presence of malignant signals plays a persistent and dominant role in classification.

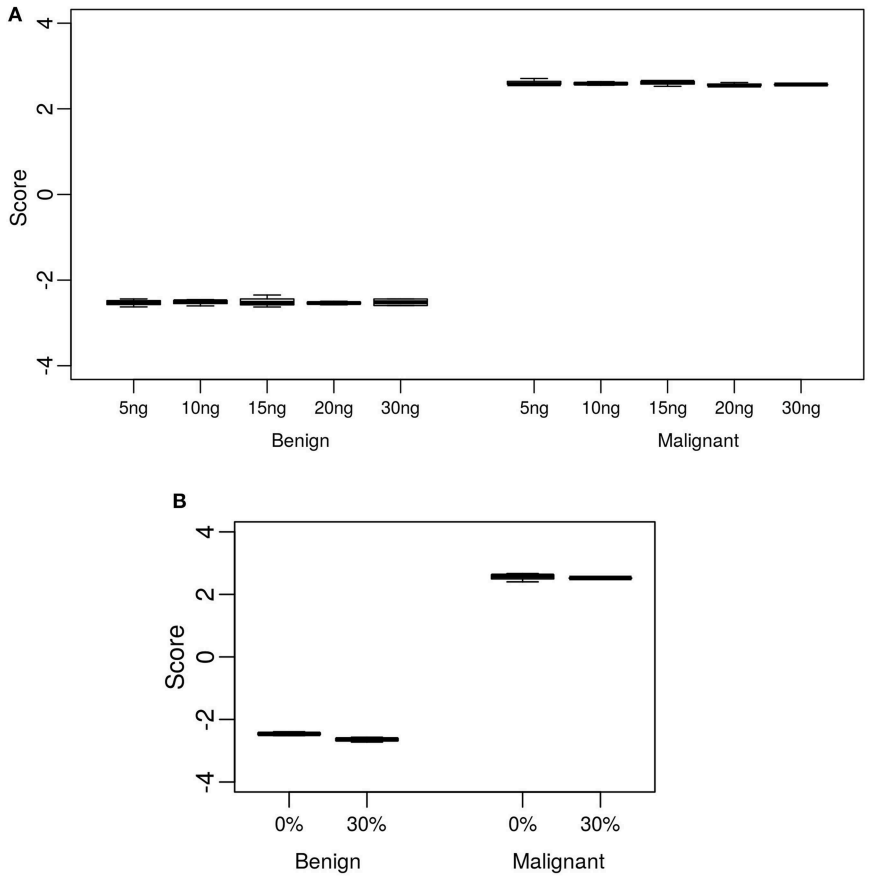

FIGURE 2 | Analytical sensitivity and specificity of the Afirma GSC BM classifier. The y-axis spans the observed score range of the classifier being tested. **(A)** Effect of input mass variation on Afirma GSC scores. Each box represents classifier scores of technical triplicates for either one benign sample or malignant sample. The x-axis shows the total input mass. Overall, GSC scores for each sample did not differ significantly with RNA input amount (p-value = 0.97). **(B)** Analytical specificity of the Afirma GSC BM classifier against genomic DNA (gDNA). The x-axis shows the percentage of gDNA spiked into 15 ng of total RNA samples before library preparation. Each box represents classifier scores of all technical replicates for either one benign or malignant sample. Overall, the Afirma GSC BM classifier scores of the same samples with 30% gDNA spike-in are not significantly different from the scores of the corresponding pure RNA samples (p-value = 0.064).

TABLE 1 | LOD in malignant FNA mixed with benign or adjacent normal tissue.

Classifier/module	RNA mixture	LOD in classifier positive FNA	
		In vitro	*In silico*
BM	ANT + Malignant	20%	5%
BM	Benign + Malignant	20%	5%
MTC	Benign + MTC	25%	20%
PTA	Benign + PTA	25%	15%
RET-PTC	Benign + RET-PTC	10%	

ANT, Adjacent Normal Tissue.

Additional *in silico* modeling on the PTA and MTC classifiers also revealed robust classification in the background of benign cells, at 15 and 20%, respectively (**Table 1**). This suggests that when representing a true positive signal, the genomic classifiers are very robust to high level of contamination from true negative content.

The limit of detection for the *BRAF* V600E classifier was determined by comparing the classifier call to the *BRAF* V600E variant status derived by castPCR. 264 total samples were evaluated; 62 had a *BRAF* V600E VAF $\geq$5% and 202 had a *BRAF* V600E 0% $\leq$ VAF $<$ 5%. The classifier had 100% positive percent agreement (PPA) with *BRAF* V600E castPCR positive samples and a 99% negative percent agreement (NPA) with *BRAF* V600E castPCR negative samples (see **Table S3**). Therefore, the *BRAF* V600E classifier limit of detection is 5% VAF.

Analytical Specificity—Blood

Blood may be inadvertently sampled during FNA procedures, with varying amounts of this unintended contaminant observed. To evaluate the tolerance of the GSC classifier to the impact of blood interference, RNA from FNA samples was mixed with RNA derived from a fresh, whole blood sample to create an *in vitro* mixture. The percentages of blood-derived RNA mixtures tested, while holding the total RNA input constant at 15 ng, are 0, 25, 50, 75, and 100%. A fitted sigmoid curve of the GSC

TABLE 2 | Blood interference in Afirma GSC prediction.

Classifier	RNA mixture	Maximum interference level of blood
		In vitro
BM	Benign + Blood	100%
BM	Malignant + Blood	75%
BRAF V600E	*BRAF* V600E + Blood	75%
MTC	MTC + Blood	75%
PTA	PTA + Blood	75%

BM classifier scores suggested that the malignant sample can be correctly classified with substantially less than the experimentally assessed 25% of the original malignant FNA content (**Table 2** and **Table S4**). The benign sample mixed with blood was correctly classified for all titration points (**Table 2** and **Table S4**). *BRAF* V600E, MTC, and PTA classifiers were evaluated in a similar way. Overall, all classifiers could tolerate presence of >75% blood content in the sample mixture and still make the correct prediction (**Table 2** and **Table S4**). This suggests the genomic classifier is robust to blood contamination.

Analytical Specificity—Genomic DNA

Genomic DNA (gDNA) is removed from samples during RNA extraction, however the removal may not be complete in all samples tested. To test the impact of gDNA contamination, we spiked high amounts of gDNA into purified RNA. Testing pure gDNA in the Afirma GSC assay did not produce any sequencing library, and thus the potential for interference in such setting is minimal. To test the impact of gDNA contamination in a sample that produces sequence-able libraries, we evaluated 30% gDNA added to RNA. This level of gDNA contamination can be observed during RIN evaluation in the bioanalyzer traces of RNA (**Figure S2A**). We reasoned that if such a high level of gDNA contamination were observed in a QC step, but did not interfere with the assay, then lesser amounts of contamination would not affect performance. To experimentally assess the extent of gDNA interference on the Afirma GSC BM results, *in vitro* mixtures were created with one malignant and one benign sample each with 30% gDNA spiked in, while maintaining the total RNA input constant at 15 ng. Afirma GSC scores of the BM classifier for each sample did not differ significantly between samples with and without 30% genomic DNA spiked in (p-value = 0.064). As shown in **Figure 2B**, the observed score differences are very small when shown in the score range of BM classifier. These observations support that the Afirma GSC test is robust against genomic DNA interference. The *BRAF* V600E, MTC classifiers and RET/PTC fusion detection module were evaluated and no significant difference was observed (**Table S5** and **Figure S2**). The PTA classifier had a statistically significant difference ($p = 0.005$), but this observation was due to the extremely reproducible scores and a small shift in the PTA score at 30% gDNA (**Table S5** and **Figure S2**). This score shift represents <1% of the total score space of the PTA classifier and will not have an impact on PTA classification performance.

Reproducibility—Acceptance Specification

To understand the threshold of variation the Afirma GSC can tolerate, an *in-silico* simulation with increasing levels of random variation was performed. The GSC BM classifier score indicated that the classifier can tolerate a total variation of scores SD $\leq$ 0.44 from all technical sources without substantially impacting sensitivity and specificity (**Table 3**). The *BRAF* V600E, MTC, and PTA classifiers were also evaluated in a similar fashion, and the maximum tolerable variation level are summarized in **Table 3** column "SD Specification." As with the GSC BM classifier, these specification values serve as the acceptance thresholds to be compared against the technical variation levels estimated from reproducibility studies.

Reproducibility—Inter-laboratory

The Afirma GSC was developed in the Veracyte R&D laboratory and transferred to the CLIA laboratory for clinical use. To confirm that the two labs achieve the same GSC BM results, a total of 40 unique patients spanning the entire GSC BM score range were used to evaluate the inter-laboratory reproducibility. The Afirma GSC BM classifier call results from the two laboratories were 100% concordant (40 of 40). Additionally, the Afirma GSC BM scores of the 40 samples between the two laboratories were highly correlated ($R^2 = 0.99$) and demonstrated strong inter-laboratory reproducibility of the Afirma GSC BM classifier. The inter-laboratory pooled SD of Afirma GSC BM scores was estimated to be 0.130 (95% CI: [0.114, 0.144]), which is substantially below the pre-determined acceptance threshold of SD $\leq$ 0.44 from *in-silico* simulation (**Figure 3**). Other classifiers were evaluated in the same fashion and rendered similar results (**Table 3** and **Figure S3**).

Reproducibility—Assay Inter-run and Intra-run

In a CLIA lab production environment, samples are processed continually by different operators, on different machines, and across different lots of reagents. It is therefore critical to ensure performance stability across these variables to ensure that patients tested over the lifetime of the product receive consistent results. We performed reproducibility studies that examined identical samples run by different operators, on different days and instruments, across multiple lots of reagents.

To evaluate the tolerance of the Afirma GSC BM to experimental variation due to equipment, operator, reagent lot, and days, 15 malignant and benign FNA samples spanning the entire score range were tested in triplicate across three independent experimental runs. The intra- and inter-run reproducibility of the Afirma GSC BM were evaluated using total RNA from 134 assays that passed QC, tested in 3 experimental runs.

The pooled intra-run SD of Afirma GSC BM scores, quantifying variability from technical replication, was estimated to be 0.069 (95% CI: [0.053, 0.073]). The pooled inter-run SD of GSC scores, measuring the total experimental variability other than sample-specific effects, was estimated to be 0.274 (95% CI: [0.228, 0.310]) across all samples in this study. In comparison, the total SD of inter-class scores

TABLE 3 | Afirma GSC classifier suite reproducibility result summary.

Classifier	Score range	Biological variation		SD specification	Technical variation					
		Inter-class			Inter-lab		Inter-run		Intra-run	
		N	SD (95% CI)		N	SD (95% CI)	N	SD (95% CI)	N	SD (95% CI)
BM	8	191	1.452 (1.306–1.634)	0.440	80	0.130 (0.114 −0.144)	134	0.274 (0.228–0.310)	134	0.069 (0.053–0.073)
BRAF V600E	13	264	3.417 (3.189–3.698)	0.640	42	0.298 (0.249–0.344)	134	0.186 (0.169–0.202)	134	0.133 (0.115–0.153)
MTC	12	211	2.912 (2.424–3.499)	2.000	50	0.174 (0.088–0.253)	53	0.189 (0.114–0.257)	53	0.189 (0.081–0.214)
PTA	10.5	195	1.242 (0.735–1.845)	1.210	50	0.104 (0.090–0.117)	36	0.105 (0.082–0.124)	36	0.078 (0.040–0.079)

"SD Specification" was derived by in-silico simulation on the training set scores for each classifier. "N" is the sample size for each study. 95% confidence interval is included for all SD estimates.

between benign and malignant samples, reflecting biological difference, was estimated to be 1.452 (95% CI: [1.306, 1.634]) (**Figure 3**). Observed technical variation of the BM and other classifiers were all below the pre-determined specs from the *in-silico* simulation (**Table 3**, **Figure 3** and **Figure S3**). RET/PTC fusion positive samples were all called positive in all replicates across all batches. Thus, the Afirma GSC genomic test is highly robust to routinely encountered sequencing operational variations.

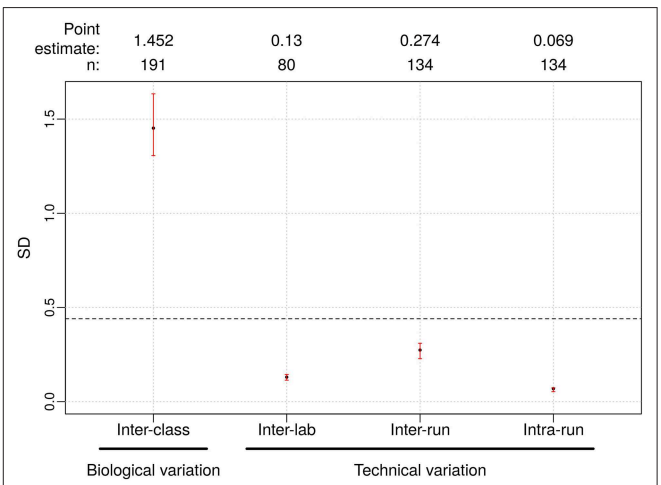

FIGURE 3 | Reproducibility results for Afirma GSC BM classifier. The left most is the biological variation calculated as the inter-class score SD between benign and malignant samples and was computed from all samples passing quality control criteria in the clinical validation study. On the right side, technical variability from different sources were listed. Dashed line: the maximum tolerable level of technical variation in GSC scores derived from simulation (0.44). Black dots: observed values. Vertical red lines: 95% CI. The sample size used to calculate the point estimate and the 95% CI is shown at the top.

DISCUSSION

The Afirma GSC classifier is a novel genomic diagnostic test that leverages whole transcriptome RNA-sequencing and machine learning methods to accurately predict benign vs. malignant thyroid nodules. It is an enhanced version of its predecessor, the Afirma GEC classifier (5). The clinical validity of the GSC has been established (7). Equally important to clinical validation is the establishment of analytical validation, as outlined by the Evaluation of Genomic Applications in Practice and Prevention (EGAPP) Working Group and the Centers for Disease Control's ACCE (Analytic and Clinical validity, Clinical utility and associated Ethical) Project (19, 20). All analytical validation studies were performed in a prospective manner, whereby the acceptance criteria for each study were determined (1) based on previously approved design requirements and (2) prior to the study being performed in the laboratory. Here we report the analytical validation of the GSC and demonstrate its robustness to various technical variations along the entire pipeline process of plating, library generation, sequencing, and algorithm analysis. More specifically, we show the tolerance of the classifier to the impact of variation in RNA input amount, and heterogenous sample inputs resulting from admixture with blood, genomic DNA, and adjacent normal tissues. Sample collection, storage, and shipping were unchanged from the Afirma GEC and their analytical validity was previously established (11).

Our studies demonstrated that the Afirma GSC classifier is robust to technical variability encountered in routine clinical sample processing. Analytical sensitivity studies showed that classifier calls are not impacted by variation in RNA input deviating from the standard amount (15 ng); it can tolerate variance up to −10 ng to +15 ng (range, 5–30 ng). Clinical sample collection procedures may yield an impure nodule sample due to the needle passing through other tissues on its way to the thyroid nodule of interest. Limit of detection studies here demonstrated that the BM classifier is robust to dilution of malignant FNA content by adjacent normal (80%) and benign FNA content (80%) and *in silico* modeling shows that the BM classifier can tolerate even higher dilution (95%). All other components of the GSC test system also demonstrated significant resistance to the effects of dilution.

Potential interferents such as blood and genomic DNA may also be mixed in the samples due to variability in sample collection, preparation, or biological heterogeneity. Analytical specificity analyses showed that malignant signals remained sufficiently detectable with up to 75% of blood mixed into a malignant sample. Also, no changes in classifier calls were found with up to 30% of genomic DNA in the sample mixture. These

results suggest that the Afirma GSC test is robust to heterogenous sample content.

We selected both positive and negative control samples and FNA samples that cover the entire score range to evaluate the reproducibility of GSC test results according to regulatory requirements of genomic applications. We showed that the Afirma GSC scores and calls are reproducible for samples replicated across different reagents, operators, equipment and runs. The accuracy of the test performed at the CLIA-certified laboratory was established by an inter-laboratory comparison study, showing that the test results generated from the CLIA-certified commercial laboratory are consistent with those generated in the R&D laboratory where the test was developed. Combined with the clinical validation study previously published (7), the GSC successfully fulfills the analytic criteria of EGAPP level I.

CONCLUSION

The Afirma GSC demonstrates robust reproducibility and analytical performance against technical variability that may arise from clinical sample collection and laboratory processing. These findings support its clinical use among cytologically indeterminant thyroid nodules to inform patient care.

DATA AVAILABILITY

Restrictions apply to the datasets: The datasets for this manuscript are not publicly available because: the dataset and the research methodologies are proprietary. Requests to access the datasets should be directed to GK, Ph.D.; Giulia@veracyte.com.

ETHICS STATEMENT

This research was approved by the Copernicus Group Independent Review Board (Cary, North Carolina). A waiver of written informed consent was granted regarding de-identified biological materials from the CLIA laboratory. IRB approval and written Informed consent in accordance with the Declaration of Helsinki was provided by all patients whose samples were previously used for training and validation of the Afirma GSC as previously described (7).

AUTHOR CONTRIBUTIONS

YH, YC, JB, RK, GK, JH, and PW designed, performed, analyzed, and interpreted the study. YH, JC, JB, RK, GK, JH, and PW implemented the analysis, prepared figures, and drafted the manuscript. YH, JB, RK, GK, JH, and PW edited and revised the manuscript. All authors have read and approved the final manuscript.

FUNDING

Funding for the publication of this article was provided by Veracyte, Inc.

ACKNOWLEDGMENTS

We'd like to thank Zhanzhi Hu, Ying Shen, and Ting Liu for their contributions to laboratory studies and data analysis.

SUPPLEMENTARY MATERIAL

The Supplementary Material for this article can be found online at: https://www.frontiersin.org/articles/10.3389/fendo.2019.00438/full#supplementary-material

REFERENCES

1. Cibas ES, Ali SZ. The 2017 bethesda system for reporting *Thyroid* Cytopathology. *Thyroid*. (2017) 27:1341–6. doi: 10.1089/thy.2017.0500
2. Keutgen XM, Filicori F, and Fahey TJ 3rd. Molecular diagnosis for indeterminate thyroid nodules on fine needle aspiration: advances and limitations. *Expert Rev Mol Diagn*. (2013) 13:613–23. doi: 10.1586/14737159.2013.811893
3. Li H, Robinson KA, Anton B, Saldanha IJ, Ladenson PW. Cost-effectiveness of a novel molecular test for cytologically indeterminate thyroid nodules. *J Clin Endocrinol Metab*. (2011) 96:E1719–26. doi: 10.1210/jc.2011-0459
4. Chudova D, Wilde JI, Wang ET, Wang H, Rabbee N, Egidio CM, et al. Molecular classification of thyroid nodules using high-dimensionality genomic data. *J Clin Endocrinol Metab*. (2010) 95:5296–304. doi: 10.1210/jc.2010-1087
5. Alexander EK, Kennedy GC, Baloch ZW, Cibas ES, Chudova D, Diggans J, et al. Preoperative diagnosis of benign thyroid nodules with indeterminate cytology. *N Engl J Med*. (2012) 367:705–15. doi: 10.1056/NEJMoa1203208
6. Kloos RT. Molecular profiling of thyroid nodules: current role for the afirma gene expression classifier on clinical decision making. *Mol Imaging Radionucl Ther*. (2017) 26:36–49. doi: 10.4274/2017.26.suppl.05
7. Patel KN, Angell TE, Babiarz J, Barth NM, Blevins T, Duh QY, et al. Performance of a genomic sequencing classifier for the preoperative diagnosis of cytologically indeterminate thyroid nodules. *JAMA Surg*. (2018) 153:817–24. doi: 10.1001/jamasurg.2018.1153
8. Hao Y, Duh QY, Kloos RT, Babiarz J, Harrell RM, Traweek ST, et al. Identification of Hurthle cell cancers: solving a clinical challenge with genomic sequencing and a trio of machine learning algorithms. *BMC Syst Biol*. (2019) 13:27. doi: 10.1186/s12918-019-0693-z
9. Angell TE, Heller HT, Cibas ES, Barletta JA, Kim MI, Krane JF, et al. Independent comparison of the afirma genomic sequencing classifier and gene expression classifier for cytologically indeterminate *Thyroid* nodules. *Thyroid*. (2019) 29:650–6. doi: 10.1089/thy.2018.0726
10. Harrell RM, Eyerly-Webb SA, Golding AC, Edwards CM, Bimston DN. Statistical comparison of afirma gsc and afirma gec outcomes in a community endocrine surgical practice: early findings. *Endocr Pract*. (2019) 25:161–4. doi: 10.4158/EP-2018-0395
11. Walsh PS, Wilde JI, Tom EY, Reynolds JD, Chen DC, Chudova DI, et al. Analytical performance verification of a molecular diagnostic for cytology-indeterminate thyroid nodules. *J Clin Endocrinol Metab*. (2012) 97:E2297–306. doi: 10.1210/jc.2012-1923
12. Dobin A, Davis CA, Schlesinger F, Drenkow J, Zaleski C, Jha S, et al. STAR: ultrafast universal RNA-seq aligner. *Bioinformatics*. (2013) 29:15–21. doi: 10.1093/bioinformatics/bts635
13. DeLuca DS, Levin JZ, Sivachenko A, Fennell T, Nazaire MD, Williams C, et al. RNA-SeQC: RNA-seq metrics for quality control and process optimization. *Bioinformatics*. (2012) 28:1530–2. doi: 10.1093/bioinformatics/bts196

14. Anders S, Pyl PT, Huber W. HTSeq–a Python framework to work with high-throughput sequencing data. *Bioinformatics*. (2015) 31:166–9. doi: 10.1093/bioinformatics/btu638
15. Love MI, Huber W, Anders S. Moderated estimation of fold change and dispersion for RNA-seq data with DESeq2. *Genome Biol*. (2014) 15:550. doi: 10.1186/s13059-014-0550-8
16. Haas B, Dobin A, Stransky N, Li B, Yang X, Tickle T, et al. STAR-Fusion: fast and accurate fusion transcript detection from RNA-Seq. *bioRxiv*. (2017). doi: 10.1101/120295
17. Kloos RT, Reynolds JD, Walsh PS, Wilde JI, Tom EY, Pagan M, et al. Does addition of BRAF V600E mutation testing modify sensitivity or specificity of the Afirma Gene Expression Classifier in cytologically indeterminate thyroid nodules? *J Clin Endocrinol Metab*. (2013) 98:E761–8. doi: 10.1210/jc.2012-3762
18. Diggans J, Kim SY, Hu Z, Pankratz D, Wong M, Reynolds J, et al. Machine learning from concept to clinic: reliable detection of BRAF V600E DNA mutations in thyroid nodules using high-dimensional RNA expression data. *Pac Symp Biocomput*. (2015) 371–82. doi: 10.1142/9789814644730_0036
19. Teutsch SM, Bradley LA, Palomaki GE, Haddow JE, Piper M, Calonge N, et al. The Evaluation of Genomic Applications in Practice and Prevention (EGAPP) Initiative: methods of the EGAPP Working Group. *Genet Med*. (2009) 11:3–14. doi: 10.1097/GIM.0b013e318184137c
20. Sun F, Bruening W, Uhl S, Ballard R, Tipton R, Schoelles K. *Quality Regulation and Clinical Utility of Laboratory-Developed Molecular Tests*. AHRQ Technology Assessment Program, USA Department of Health and Human Services, (2010).

Conflict of Interest Statement: All authors are Veracyte Inc. employees and equity owners.

frontiers in Endocrinology

PERSPECTIVE
published: 18 July 2019
doi: 10.3389/fendo.2019.00468

Clonal Reconstruction of Thyroid Cancer: An Essential Strategy for Preventing Resistance to Ultra-Precision Therapy

Elizabeth R. McGonagle[1] *and Carmelo Nucera*[1,2]*

[1] *Division of Experimental Biology, Laboratory of Human Thyroid Cancers Preclinical and Translational Research, Department of Pathology, Cancer Research Institute (CRI), Center for Vascular Biology Research (CVBR), Beth Israel Deaconess Medical Center, Harvard Medical School, Boston, MA, United States,* [2] *Broad Institute of Harvard and MIT, Cambridge, MA, United States*

OPEN ACCESS

Edited by:
Yuji Nagayama, Nagasaki University, Japan

Reviewed by:
Rosa Marina Melillo, University of Naples Federico II, Italy
Vasyl Vasko, Uniformed Services University of the Health Sciences, United States

***Correspondence:**
Carmelo Nucera
cnucera@bidmc.harvard.edu

Specialty section:
This article was submitted to Thyroid Endocrinology, a section of the journal Frontiers in Endocrinology

Received: *18 January 2019*
Accepted: *27 June 2019*
Published: *18 July 2019*

Citation:
McGonagle ER and Nucera C (2019) Clonal Reconstruction of Thyroid Cancer: An Essential Strategy for Preventing Resistance to Ultra-Precision Therapy. Front. Endocrinol. 10:468. doi: 10.3389/fendo.2019.00468

The introduction of ultra-precision targeted therapy has become a significant advancement in cancer therapeutics by creating treatments with less off target effects. Specifically with papillary thyroid carcinoma (PTC), the cancer's hallmark genetic mutation $BRAF^{V600E}$ can be targeted with selective inhibitors, such as vemurafenib. Despite initial positive tumor responses of regression and decreased viability, both single agent or combination agent drug treatments provide a selective pressure for drug resistant evolving clones within the overall heterogeneous tumor. Also, there are evidences suggesting that sequential monotherapy is ineffective and selects for resistant and ultimately lethal tumor clones. Reconstructing both clonal and subclonal thyroid tumor heterogeneous cell clusters for somatic mutations and epigenetic profile, copy number variation, cytogenetic alterations, and non-coding RNA expression becomes increasingly critical as different clonal enrichments implicate how the tumor may respond to drug treatment and dictate its invasive, metastatic, and progressive abilities, and predict prognosis. Therefore, development of novel preclinical and clinical empirical models supported by mathematical assessment will be the tools required for estimating the parameters of clonal and subclonal evolution, and unraveling the dormant vs. non-dormant state of thyroid cancer. In sum, novel experimental models performing the reconstruction both pre- and post-drug treatment of the thyroid tumor will enhance our understanding of clonal and sub-clonal reconstruction and tumor evolution exposed to treatments during ultra-precision targeted therapies. This approach will improve drug development strategies in thyroid oncology and identification of disease-specific biomarkers.

Keywords: ultra-precision therapy, $BRAF^{V600E}$, microenvironment, vemurafenib, CDK4/6, palbociclib, copy number variations, clonal evolution

NEXT STEP TO ULTRA-PRECISION TARGETED THERAPIES IN THYROID CARCINOMA

Papillary thyroid carcinoma (PTC) is the most frequent type of thyroid cancer, accounting for almost 80% of thyroid cancer cases. The genetic hallmark of human PTC is the somatic $BRAF^{V600E}$ mutation. Constitutive activation of the BRAF proto-oncogene (e.g., valine to glutamic acid substitution, V600E) leads to activation of ERK1/2 pathway and other intracellular pathways associated with abnormal cell proliferation and growth (1–3).

$BRAF^{V600E}$ can be targeted with selective inhibitors such as vemurafenib, the first FDA approved orally administered inhibitor (4). Inhibition of the $BRAF^{V600E}$ oncogene has shown promising results for the suppression of the BRAF-ERK1/2 pathways and an overall regression in tumor growth (5). Concurrently, vemurafenib has also been shown to aid in cancer cell redifferentiation for increased iodide incorporation in RAIR, $BRAF^{V600E}$ patients (6). However, despite early clinical success with vemurafenib treatment, this drug therapy can generate positive selection for drug resistant cancer clones (7), and disease progression is observed in the clinic (8–10). Studies consistently show that $BRAF^{V600E}$-cancer cells go into cell cycle arrest upon vemu treatment, but with continued exposure exhibit a rebound of pERK1/2 and resume proliferation (7, 11–14).

Given cancer's hallmark of "enabling replicative immortality," unregulated replication creates greater possibility for mutations to arise and succeed in the cell population, since most cancer cells dedifferentiate and require activation of angiogenic, invasive, and metastatic genes (15). Each tumor is comprised of a diverse number of cells, each with a unique genetic profile. The unique genetic profile of each cancer cell means within any given tumor there is a diverse range of tumor clones with diverse cell clusters each containing different mutations.

Cancer is considered a "disease of the genome," whereby a variety of genetic mutations leads to individual cells that proliferate and divide without regard to their internal regulatory mechanisms (16). Cancer's deregulation of proliferation allows for a greater possibility for genetic mutations to occur during mitotic division, as well as the greater chance that gene mutations will not trigger cellular death pathways. Mutations that do not induce apoptosis be they somatic copy number mutations, insertions, deletions, or whole chromosome amplifications, create a heterogeneous population of tumor cells. Over an entire tumor, each individual cell is undergoing its own dysfunctional replication and acquiring its own unique mutations. It is throughout a tumor's progression that some populations of cells with mutations, that increase the tumor's fitness to its environment, are selected. Indeed, an important characteristic of cancer is its "evolutionary character," which in many ways should be considered an additional hallmark of the disease (17). Tumor cells are composed of an uniform clonal composition for driver mutations. Driver mutations, mostly acquired somatically, confer a growth advantage to the tumor, enabling outgrowth of neoplastic clones and contributing to tumor progression (18).

Throughout a tumor cell's evolution, the cell has to evolve many different mechanisms to prevent induction of cell death (e.g., apoptosis) and suppression of growth signals. Part of a cell's evolution to evade these signals involves genetic mutations, which predisposes the cells to being able to survive with mutations that would otherwise not survive in non-cancerous or malignant cells. Tumorigenesis requires increased mutability in order for tumor cells to bypass regulatory and apoptotic pathways and signals. Increased mutability of cells is achieved through down regulation of genomic maintenance mechanisms, including P53 gene inactivation (19). The down regulation of genomic maintenance creates a foundation for cancer cells to acquire new genetic mutations and be susceptible to mutagens.

Cancer's evolution is not solely dictated by individual tumor cell's irregular proliferation conferring gains in somatic mutations. A tumor's microenvironment, along with individual cancer cell genome instability, encourages clonal expansion and heterogeneity (20). While each cancer cell could contain a hallmark driver mutation, such as $BRAF^{V600E}$ in PTC (21), these PTC cells are likewise able to diversify through different subclonal genetic alterations. The driver or classical genetic biomarker would be a mutation at the clonal level which leads to the progression of those cells to become cancerous. Nonetheless, these cells are still dividing and proliferating, albeit irregularly, and are able to gain somatic mutations. So in addition to their driver mutation, tumor cells are evolving multiple subclonal mutations that can be positively selected for just as their primary driver mutation was initially and might impact prognosis and clinical outcome (22).

The microenvironment is able to exert selective pressures on the tumor, allowing for positive selection of those clones with underlying subclonal mutations which are better suited to the changing microenvironment. Normal cells exhibit a behavior referred to as "fitness sensing" whereby cells compete with neighboring cells, and those cells that are less fit compared to their neighbors die (23). In the case of a tumor with subclonal heterogeneity, intercellular competition between cells could aid in the positive selection of resistant clones driven by interaction in the tumor's microenvironment. Genetically diverse cells may not be competing with each other but also interacting with each other (24, 25). Consequently tumors could be increasing their genetic complexity and heterogeneity by allowing multiple tumor subclones to survive within the overall tumor environment and to interact and influence one another.

Within a recurring tumor repopulated maybe by cells containing vemurafenib (FDA-approved, selective inhibitor of $BRAF^{V600E}$) resistant subclones (8), intercellular competition could occur between different subclones, making those selected cells "super competitor cells." This type of subclonal intercellular competition could potentially select subclones that confer the greatest possible resistance, invasive, and metastatic abilities to the tumor.

While cancer cells undergo a form of gradualism in terms of their clonal expansion, targeted drug therapy can be understood as creating a punctuated equilibrium event within the life of a tumor (26). For example, in patients with $BRAF^{V600E}$ positive melanoma upon treatment with vemurafenib therapy

(an example of ultra-precision therapy), some tumor cells will respond to the treatment and die (27). However, those cells containing advantageous subclonal mutations, in addition to $BRAF^{V600E}$, will be able to overcome inhibition of $BRAF^{V600E}$ and subsequently of the ERK1/2 intracellular signaling, and will continue to survive and proliferate. Subclones that are able to survive drug therapy are aided by a process called "competitive release," where not only do passenger mutations allow individual cells to survive treatment, but any potential competing cells have been killed through drug therapy (28). In this way, tumor undergoes a punctuated equilibrium event, facilitated by targeted drug therapy, where those cells with selectively advantageous subclonal mutations rapidly become the majority of the cells composing the tumor.

While all of the cells of a single tumor may contain a genetic biomarker mutation, such as $BRAF^{V600E}$ in PTC, the individual tumor clones may contain additional genetic alterations as subclonal genetic event. Treatment of a tumor with vemurafenib will suppress the $BRAF^{V600E}$ mutation, eliciting cytostatic effects on tumor growth inhibition (7, 12, 29), but cell populations within any tumor that have subclonal genetic alterations could bypass the inhibition of oncogenic pathways by targeted therapy and still allow the tumor cell to grow (30). These tumor subclones, under the exacerbated selective pressure of targeted therapy will evoke in the tumor drug resistance, will survive and could eventually lead to tumor progression (31).

Specifically in PTC-derived cells harboring the heterozygous $BRAF^{V600E}$ mutation and with loss of the CDKN2A (P16) gene, targeted drug treatment therapy positively selected for a number of drug resistant clones and drove tumor clonal evolution (**Figure 1**) (7). In this study, PTC-derived cells harboring the $BRAF^{V600E}$ mutation were treated with both vemurafenib and palbociclib. Palbociclib is an FDA approved CDK4/6 inhibitor typically used to treat patients with advanced stage HER2 negative breast cancer (32). Single treatment therapy with vemurafenib on $BRAF^{V600E}$ and $P16^{-/-}$ thyroid tumor cells lead to a clonal expansion of treatment resistant clones, showing chromosome 5 amplifications and RBM (RNA-binding motif) gene family mutations (7). Importantly, combined therapy with vemurafenib and palbociclib was able to ameliorate either primary or secondary drug resistance in these tumor cells by inducing cell death and inhibiting the adaptive subclonal evolution (7).

Combination therapy is seen as the best treatment option for overcoming resistance to single agent targeted therapy (**Table 1**). However, combination therapy also has the potential to drive tumor recurrence by selecting subclones that are resistant to both agents used in the dual therapy treatment (40). Statistical models highlight that tumor cells are much more likely to become resistant to dual therapy through the occurrence of one gene mutation conferring resistance to both drugs simultaneously than through sequential mutations conferring resistance to each drug separately (41).

Not only does targeted drug therapy have the potential to positively select cancer cells with resistant subclonal mutations, but could also enrich the population of cells carrying

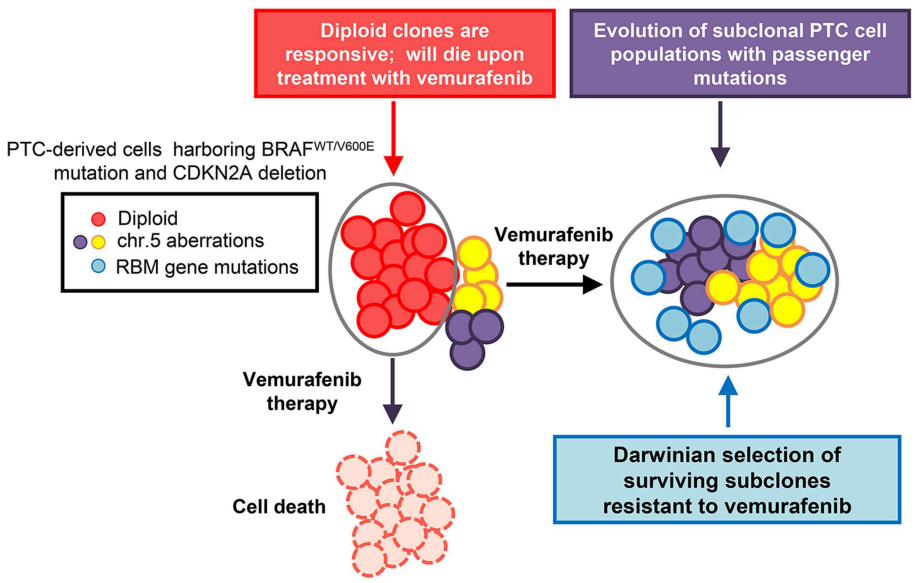

FIGURE 1 | Model of thyroid carcinoma clonal evolution. PTC-derived KTC1 cells clonally harbor the hallmark heterozygous $BRAF^{WT/V600E}$ mutation and show loss of the CDKN2A (P16) gene. The diploid clones compose the majority of the tumor cells genetic landscape; with there being other subclonal populations present within the overall tumor. Upon treatment with targeted therapy, in this case using the selective $BRAF^{V600E}$ inhibitor, vemurafenib, diploid KTC1 clones will respond positively to the drug treatment and die. However, those clones containing additional subclonal mutations, such as mutations in RBMX and RBM10 genes, or chromosome 5p amplifications, are able to overcome drug induced suppression of the $BRAF^{V600E}$ pathway. Through the course of vemurafenib treatment, subclones with passenger mutations, such as RBM gene family somatic mutations, can be positively selected. This tumor geography will then become enriched with populations of drug resistant mutant clones. This tumor composed primarily of vemurafenib-resistant clones, might be effectively untreatable and has the potential to lead to tumor progression.

advantageous and potentially cancerous passenger mutations. One study showed that somatic mutations in the thyroglobulin (Tg) gene were associated with poorer clinical prognosis (42). Additionally, the study found that PTC samples with Tg mutations showed more distant metastasis compared with PTC samples that did not contain somatic Tg mutations. Given that most of the Tg mutated PTC samples also contained MAPK pathway mutations, such as $BRAF^{V600E}$, Tg mutations were more likely passenger mutations that are advantageous in the malignant evolution of PTC as opposed to the actual drivers of PTC. Since Tg mutations are associated with mutations in genes encoding components of the MAPK signaling pathway, it is possible that some subclones harboring both driver and maybe passenger mutations, such as RBM gene family mutations (e.g., RBM10, RBMX) (7), could survive to vemurafenib treatment and allow for a recurring tumor that is more invasive and drug resistant (7).

Another experimental model focusing on tumor heterogeneity in breast cancers identified a subclonal genetic marker associated with CD44+ breast cancer stem cells. Previous studies had demonstrated that CD44+ cells displayed increased tumorigenesis compared to CD44− cells (43). Given this knowledge, researches began genetically profiling CD44+ breast cancer tumor cells and identified a CD44+ cell-specific gene, Protein C receptor (PROCR) (44). PROCR is a transmembrane protein commonly expressed in endothelial cells, and has been shown to have anticoagulation as well as anti-inflammatory functions (45). Importantly for this breast cancer model, PROCR has been previously noted to also be a marker for mammary epithelial stem cells (46). While not necessarily a passenger mutation, the discovery of the PROCR gene being specific to CD44+ breast cancer cells creates a better understanding of the cellular mechanisms and pathways activated in breast cancer. Understanding the relationship between the CD44 and PROCR genes allows for a better clonal reconstruction of the overall heterogeneous tumor and for the identification of ultra-precision therapy.

In the PTC experimental model, an understanding of the subclonal construction of the tumor having chromosome 5 amplifications and RBM gene family mutations, revealed potential pathways for secondary resistance. This knowledge of both the clonal and subclonal configuration of the tumor, allowed for a more effective solution to treating $BRAF^{V600E}$ and $CDKN2A^{-/-}$ mutant PTC's and for overcoming both innate/primary and secondary tumor resistance mechanisms.

Beyond elucidating better understandings of potential cellular pathways and genes involved in drug therapy resistance, clonal and subclonal reconstructions of tumors can also reveal biomarkers for early detection of aggressive thyroid cancer that could dictate future tumor behavior. With regard to thyroid cancers, PTC is classified as a differentiated thyroid cancer, and other types of thyroid carcinomas, such as anaplastic thyroid carcinoma (ATC), are classified as undifferentiated thyroid cancer. The transition from PTC to undifferentiated thyroid carcinoma is still poorly understood and furthermore effective treatments of ATC represent a large unmet clinical need. Clonal and subclonal reconstructions of both heterogeneous PTC (**Figure 2**) and ATC will strongly help to better understand the genes and cellular players involved in this malignant transition, and in the metastatic process. Given ATC's poor prognosis and limited treatment options, increased knowledge of subclonal reconstruction might allow for the development of better treatments and even potential targeted drug therapies.

Importantly, ATC show increased mutational burden compared to PTC. In one study examining the genetic profile of 196 ATC samples, only 41% (81 tumors) harbored BRAF mutations (47). If ATC arise from the high risk aggressive PTC, then they increase tumor mutational burden (47), suggesting

TABLE 1 | Targeted therapies in thyroid carcinoma.

Therapeutic	Target(s) (Inhibitory effects)	Median progression free survival
Vemurafenib	$BRAF^{V600E}$	50% of patients with progression-free survival of ~18 months (33)
Dabrafenib	$BRAF^{V600E}$	50% of patients with progression-free survival of ~11.3 months (34)
Sorafenib	Multi-kinase (including $BRAF^{WT}$ and $BRAF^{V600E}$)	~17.9 months (35)
Lenvatinib	VEGFR1-3, FGFR1-4, PDGFRα, PDGFRβ, KIT, RET (36–38)	~18.3 months (39)

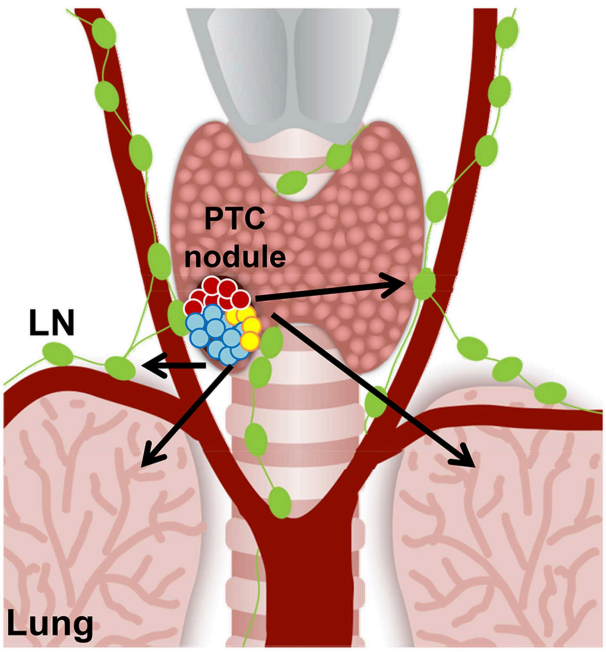

FIGURE 2 | Hypothetical cell composition of a $BRAF^{WT/V600E}$ papillary thyroid carcinoma (PTC) nodule. $BRAF^{WT/V600E}$ positive malignant thyroid nodule with heterogeneous tumor cell clusters that might have the potential for metastasis (arrows) to the neck lymph nodes (LN) and lungs/pleura. Red circles: diploid PTC cells; aqua and yellow circles: PTC cells with aneuploidy.

that additional mutations may trigger tumor resistance and overcome any potential single agent ultra-precision targeted therapy. Intriguingly, increased tumor mutational burden has been correlated with a positive outcome using immunotherapy (48). Subclonal reconstruction could also help to solidify understanding of which biomarkers and mutations indicate responsiveness to immunotherapy as well as targeted therapy. An additional area of unmet clinical need is in understanding and treating metastatic thyroid tumors; distant metastases may occur early and remain dormant in the metastatic niche (49). Tumor dormancy refers to the phenomenon where a small cluster of cells, derived from the primary tumor itself, metastasize and are able to survive in a quiescent state for an extended period of time without growth (50). Since some tumor cells are in a quiescent state, these cells can survive without growing or developing a tumor for years; until the dormant cells are then activated by some mechanism, in which case invasive tumors may arise from these dormant cells. The importance in considering dormant metastatic tumors is in considering their potential subclonality. If these cells are early evolved subclones, they could potentially harbor secondary mutations, which either facilitated their quiescent state or that eventually allows them to overcome single agent targeted therapy. Progression of metastatic tumors aligns with the parallel progression theory of thyroid tumorigenesis, and the metastatic thyroid tumors may arise from the dormant cell populations. Additionally, thyroid carcinoma metastases exhibit tissue specificity; with PTC primarily metastasizing to the neck lymph nodes (and lesser in the lungs) and medullary thyroid carcinomas (MTC) migrating to the liver and bone (49). A clonal reconstruction of the dormant thyroid tumor cells may also broaden the understanding of why certain cells become metastatic and why certain metastases can be tissue specific. Dormancy is thought to be prompted by a lack (or impairment) of angiogenesis, so comprehensive clonal examination could likewise illuminate genes and markers of the angiogenic balance (51).

In sum, some bioinformatics models have been designed and are being used to reconstruct the clonal and subclonal heterogeneity of tumors. However, we need novel experimental models performing the clonal and subclonal reconstruction both pre- and post-drug treatment(s) of the thyroid tumor for somatic mutational and epigenetic profile, copy number variation, cytogenetic alterations, and non-coding RNA expression. Clonal and subclonal evolution of tumor cell clusters is also driven by the selective pressure of targeted drug therapy, therefore the pre-treatment reconstruction and the post-treatment reconstruction would identify all clones and subclones that drug treatments positively select, those that are responsive to drug treatments and die, and clones containing passenger genetic alterations conferring secondary tumor resistance.

AUTHOR CONTRIBUTIONS

CN: design. CN and EM: editing.

ACKNOWLEDGMENTS

CN [Principal Investigator, Human Thyroid Cancers Preclinical and Translational Research at the Beth Israel Deaconess Medical Center (BIDMC)/Harvard Medical School] was awarded grants by the National Cancer Institute/National Institutes of Health (1R21CA165039-01A1 and 1R01CA181183-01A1), the American Thyroid Association (ATA) and ThyCa:Thyroid Cancer Survivors Association Inc. for Thyroid Cancer Research. CN has been a consultant for Loxo Oncology. CN was also a recipient of the Guido Berlucchi Young Investigator research award 2013 (Brescia, Italy) and BIDMC/CAO Grant (Boston, MA).

REFERENCES

1. Valvo V, Nucera C. Coding molecular determinants of thyroid cancer development and progression. *Endocrinol Metab Clin North Am*. (2019) 48:37–59. doi: 10.1016/j.ecl.2018.10.003
2. Fagin JA, Wells SA Jr. Biologic and clinical perspectives on thyroid cancer. *N Engl J Med*. (2016) 375:1054–67. doi: 10.1056/NEJMra1501993
3. Xing M, Alzahrani AS, Carson KA, Shong YK, Kim TY, Viola D, et al. Association between BRAF^{V600E} mutation and recurrence of papillary thyroid cancer. *J Clin Oncol*. (2015) 33:42–50. doi: 10.1200/JCO.2014.56.8253
4. Bollag G, Hirth P, Tsai J, Zhang J, Ibrahim PN, Cho H, et al. Clinical efficacy of a RAF inhibitor needs broad target blockade in BRAF-mutant melanoma. *Nature*. (2010) 467:596–9. doi: 10.1038/nature09454
5. Sosman JA, Kim KB, Schuchter L, Gonzalez R, Pavlick AC, Weber JS, et al. Survival in BRAF ^{V600}-mutant advanced melanoma treated with vemurafenib. *N Engl J Med*. (2012) 366:707–14. doi: 10.1056/NEJMoa1112302
6. Dunn LA, Sherman EJ, Baxi SS, Tchekmedyian V, Grewal RK, Larson SM, et al. Vemurafenib redifferentiation of BRAF mutant, RAI-refractory thyroid cancers. *J Clin Endocrinol Metab*. (2019) 104:1417–28. doi: 10.1210/jc.2018-01478
7. Antonello ZA, Hsu N, Bhasin M, Roti G, Joshi M, Van Hummelen P, et al. Vemurafenib-resistance via *de novo* RBM genes mutations and chromosome 5 aberrations is overcome by combined therapy with palbociclib in thyroid carcinoma with BRAF^{V600E}. *Oncotarget*. (2017) 8:84743–60. doi: 10.18632/oncotarget.21262
8. Wagle N, Emery C, Berger MF, Davis MJ, Sawyer A, Pochanard P, et al. Dissecting therapeutic resistance to RAF inhibition in melanoma by tumor genomic profiling. *J Clin Oncol*. (2011) 29:3085–96. doi: 10.1200/JCO.2010.33.2312
9. Trunzer K, Pavlick AC, Schuchter L, Gonzalez R, McArthur GA, Hutson TE, et al. Pharmacodynamic effects and mechanisms of resistance to vemurafenib in patients with metastatic melanoma. *J Clin Oncol*. (2013) 31:1767–74. doi: 10.1200/JCO.2012.44.7888
10. Solit DB, Rosen N. Resistance to BRAF inhibition in melanomas. *N Engl J Med*. (2011) 364:772–4. doi: 10.1056/NEJMcibr1013704
11. Montero-Conde C, Ruiz-Llorente S, Dominguez JM, Knauf JA, Viale A, Sherman EJ, et al. Relief of feedback inhibition of HER3 transcription by RAF and MEK inhibitors attenuates their antitumor effects in BRAF-mutant thyroid carcinomas. *Cancer Discov*. (2013) 3:520–33. doi: 10.1158/2159-8290.CD-12-0531
12. Danysh BP, Rieger EY, Sinha DK, Evers CV, Cote GJ, Cabanillas ME, et al. Long-Term vemurafenib treatment drives inhibitor resistance through a spontaneous KRAS G12D mutation in a BRAF^{V600E} papillary thyroid carcinoma model. *Oncotarget*. (2016) 7:30907–23. doi: 10.18632/oncotarget.9023

13. Poulikakos PI, Zhang C, Bollag G, Shokat KM, Rosen N. RAF inhibitors transactivate RAF dimers and ERK signalling in cells with wild-type BRA. *Nature*. (2010) 464:427–430. doi: 10.1038/nature08902
14. Sun C, Wang L, Huang S, Heynen GJ, Prahallad A, Robert C, et al. Reversible and adaptive resistance to $BRAF^{V600E}$ inhibition in melanoma. *Nature*. (2014) 508:118–22. doi: 10.1038/nature13121
15. Hanahan D, Weinberg RA. Hallmarks of cancer: the next generation. *Cell*. (2011) 144:646–74. doi: 10.1016/j.cell.2011.02.013
16. Yates LR, Campbell PJ. Evolution of the cancer genome. *Nat Rev Genet*. (2012) 13:795–806. doi: 10.1038/nrg3317
17. Goymer P. Natural selection: the evolution of cancer. *Nature*. (2008) 454:1046–8. doi: 10.1038/4541046a
18. Hutchinson L. Genetics: defining driver mutations in the genomic landscape of breast cancer. *Nat Rev Clin Oncol*. (2016) 13:327. doi: 10.1038/nrclinonc.2016.75
19. Morris SM. A role for p53 in the frequency and mechanism of mutation. *Mutat Res*. (2002) 511:45–62. doi: 10.1016/S1383-5742(01)00075-8
20. Marusyk A, Polyak K. Tumor heterogeneity: causes and consequences. *Biochim Biophys Acta*. (2010) 1805:105–17. doi: 10.1016/j.bbcan.2009.11.002
21. Cancer Genome Atlas Research Network. Integrated genomic characterization of papillary thyroid carcinoma. *Cell*. (2014) 159:676–90. doi: 10.1016/j.cell.2014.09.050
22. Landau DA, Carter SL, Stojanov P, McKenna A, Stevenson K, Lawrence MS, et al. Evolution and impact of subclonal mutations in chronic lymphocytic leukemia. *Cell*. (2013) 152:714–26. doi: 10.1016/j.cell.2013.01.019
23. Di Gregorio A, Bowling S, Rodriguez TA. Cell competition and its role in the regulation of cell fitness from development to cancer. *Dev Cell*. (2016) 38:621–34. doi: 10.1016/j.devcel.2016.08.012
24. Snuderl M, Fazlollahi L, Le LP, Nitta M, Zhelyazkova BH, Davidson CJ, et al. Mosaic amplification of multiple receptor tyrosine kinase genes in glioblastoma. *Cancer Cell*. (2011) 20:810–7. doi: 10.1016/j.ccr.2011.11.005
25. Bach LA, Bentzen SM, Alsner J, Christiansen FB. An evolutionary-game model of tumour-cell interactions: possible relevance to gene therapy. *Eur J Cancer*. (2001) 37:2116–20. doi: 10.1016/S0959-8049(01)00246-5
26. Cross WCH, Graham TA, Wright NA. New paradigms in clonal evolution: punctuated equilibrium in cancer. *J Pathol*. (2016) 240:126–36. doi: 10.1002/path.4757
27. Burrell RA, Swanton C. Tumour heterogeneity and the evolution of polyclonal drug resistance. *Mol Oncol*. (2014) 8:1095–111. doi: 10.1016/j.molonc.2014.06.005
28. Fischer A, Vázquez-García I, Illingworth CJR, Mustonen V. High-definition reconstruction of clonal composition in cancer. *Cell Rep*. (2014) 7:1740–52. doi: 10.1016/j.celrep.2014.04.055
29. Prete A, Lo AS, Sadow PM, Bhasin SS, Antonello ZA, Vodopivec DM, et al. Pericytes elicit resistance to vemurafenib and sorafenib therapy in thyroid carcinoma via the TSP-1/TGFbeta1 axis. *Clin Cancer Res*. (2018) 24:6078–97. doi: 10.1158/1078-0432.CCR-18-0693
30. Navin N, Krasnitz A, Rodgers L, Cook K, Meth J, Kendall J, et al. Inferring tumor progression from genomic heterogeneity. *Genome Res*. (2010) 20:68–80. doi: 10.1101/gr.099622.109
31. Xue Y, Martelotto L, Baslan T, Vides A, Solomon M, Mai TT, et al. An approach to suppress the evolution of resistance in $BRAF^{V600E}$-mutant cancer. *Nat Med*. (2017) 23:929–37. doi: 10.1038/nm.4369
32. Lu J. Palbociclib: a first-in-class CDK4/CDK6 inhibitor for the treatment of hormone-receptor positive advanced breast cancer. *J Hematol Oncol*. (2015) 8:98. doi: 10.1186/s13045-015-0194-5
33. Brose MS, Cabanillas ME, Cohen EE, Wirth LJ, Riehl T, Yue H, et al. Vemurafenib in patients with $BRAF^{V600E}$-positive metastatic or unresectable papillary thyroid cancer refractory to radioactive iodine: a non-randomised, multicentre, open-label, phase 2 trial. *Lancet Oncol*. (2016) 17:1272–82. doi: 10.1016/S1470-2045(16)30166-8
34. Falchook GS, Millward M, Hong D, Naing A, Piha-Paul S, Waguespack SG, et al. BRAF inhibitor dabrafenib in patients with metastatic BRAF-mutant thyroid cancer. *Thyroid*. (2015) 25:71–7. doi: 10.1089/thy.2014.0123
35. Lam ET, Ringel MD, Kloos RT, Prior TW, Knopp MV, Liang J, et al. Phase II clinical trial of sorafenib in metastatic medullary thyroid cancer. *J Clin Oncol*. (2010) 28:2323–30. doi: 10.1200/JCO.2009.25.0068
36. Tohyama O, Matsui J, Kodama K, Hata-Sugi N, Kimura T, Okamoto K, et al. Antitumor activity of lenvatinib (e7080): an angiogenesis inhibitor that targets multiple receptor tyrosine kinases in preclinical human thyroid cancer models. *J Thyroid Res*. (2014) 2014:638747. doi: 10.1155/2014/638747
37. Glen H, Mason S, Patel H, Macleod K, Brunton VG. E7080, a multi-targeted tyrosine kinase inhibitor suppresses tumor cell migration and invasion. *BMC Cancer*. (2011) 11:309. doi: 10.1186/1471-2407-11-309.
38. Matsui J, Yamamoto Y, Funahashi Y, Tsuruoka A, Watanabe T, Wakabayashi T, et al. E7080, a novel inhibitor that targets multiple kinases, has potent antitumor activities against stem cell factor producing human small cell lung cancer H146, based on angiogenesis inhibition. *Int J Cancer*. (2008) 122:664–71. doi: 10.1002/ijc.23131
39. Schlumberger M, Tahara M, Wirth LJ, Robinson B, Brose MS, Elisei R, et al. Lenvatinib versus placebo in radioiodine-refractory thyroid cancer. *N Engl J Med*. (2015) 372:621–30. doi: 10.1056/NEJMoa1406470
40. Groenendijk FH, Bernards R. Drug resistance to targeted therapies: deja vu all over again. *Mol Oncol*. (2014) 8:1067–83. doi: 10.1016/j.molonc.2014.05.004
41. Bozic I, Reiter JG, Allen B, Antal T, Chatterjee K, Shah P, et al. Evolutionary dynamics of cancer in response to targeted combination therapy. *Elife*. (2013) 2:e00747. doi: 10.7554/eLife.00747
42. Siraj AK, Masoodi T, Bu R, Beg S, Al-Sobhi SS, Al-Dayel F, et al. Genomic profiling of thyroid cancer reveals a role for thyroglobulin in metastasis. *Am J Hum Genet*. (2016) 98:1170–80. doi: 10.1016/j.ajhg.2016.04.014
43. Al-Hajj M, Wicha MS, Benito-Hernandez A, Morrison SJ, Clarke MF. Prospective identification of tumorigenic breast cancer cells. *Proc Natl Acad Sci USA*. (2003) 100:3983–8. doi: 10.1073/pnas.0530291100
44. Shipitsin M, Campbell LL, Argani P, Weremowicz S, Bloushtain-Qimron N, Yao J, et al. Molecular definition of breast tumor heterogeneity. *Cancer Cell*. (2007) 11:259–73. doi: 10.1016/j.ccr.2007.01.013
45. Yu QC, Song W, Wang D, Zeng YA. Identification of blood vascular endothelial stem cells by the expression of protein C receptor. *Cell Res*. (2016) 26:1079–98. doi: 10.1038/cr.2016.85
46. Wang D, Cai C, Dong X, Yu QC, Zhang XO, Yang L, et al. Identification of multipotent mammary stem cells by protein C receptor expression. *Nature*. (2015) 517:81–4. doi: 10.1038/nature13851
47. Pozdeyev N, Gay LM, Sokol ES, Hartmaier R, Deaver KE, Davis S, et al. Genetic analysis of 779 advanced differentiated and anaplastic thyroid cancers. *Clin Cancer Res*. (2018) 24:3059–68. doi: 10.1158/1078-0432.CCR-18-0373
48. Meléndez B, Van Campenhout C, Rorive S, Remmelink M, Salmon I, D'Haene N. Methods of measurement for tumor mutational burden in tumor tissue. *Transl Lung Cancer Res*. (2018) 7:661–7. doi: 10.21037/tlcr.2018.08.02
49. Ringel MD. Metastatic dormancy and progression in thyroid cancer: targeting cells in the metastatic frontier. *Thyroid*. (2011) 21:487–92. doi: 10.1089/thy.2011.2121
50. Phay JE, Ringel MD. Metastatic mechanisms in follicular cell-derived thyroid cancer. *Endocr Relat Cancer*. (2013) 20:R307–19. doi: 10.1530/ERC-13-0187
51. Naumov GN, Akslen LA, Folkman J. Role of angiogenesis in human tumor dormancy: animal models of the angiogenic switch. *Cell Cycle*. (2006) 5:1779–87. doi: 10.4161/cc.5.16.3018

Conflict of Interest Statement: The authors declare that the research was conducted in the absence of any commercial or financial relationships that could be construed as a potential conflict of interest.

frontiers in Endocrinology

ORIGINAL RESEARCH
published: 02 August 2019
doi: 10.3389/fendo.2019.00523

Immunohistochemical Analysis of Cancer Stem Cell Marker Expression in Papillary Thyroid Cancer

*Hye Min Kim and Ja Seung Koo**

Department of Pathology, Yonsei University College of Medicine, Seoul, South Korea

Cancer stem cell (CSC) markers have prognostic significance in various cancers, but their clinical significance in papillary thyroid carcinoma (PTC) has not been demonstrated. In this study, CSC markers expressed in PTC and their relationships with prognosis were evaluated. We constructed tissue microarrays for 386 PTC cases, divided it into 42 low risk cases and 344 intermediate risk cases according to the American Thyroid Association 2009 Risk Stratification System. Immunohistochemical staining of CSC markers (CD15, CD24, CD44, CD166, and ALDH1A1) was performed, and the proportion of stained cells and immunostaining intensity were evaluated to determine positive marker expression. The relationships between CSC marker expression and other clinicopathological parameters or survival were analyzed. CD15 expression was higher in PTC with intermediate risk than in PTC with low risk (29.4 vs. 11.9%, $p = 0.017$). According to a multivariate analysis, CD15, CD44, CD166, and ALDH1A1 positivity were independently associated with a shorter progression-free survival (PFS) (odds ratio [OR]: 1.929, 2.960, 7.485, and 3.736; $p = 0.016$, $p = 0.026$, $p < 0.001$, and $p = 0.006$, respectively). Higher N and cancer stage were the only other clinical factors associated with a shorter PFS (OR: 2.953 and 1.898, $p = 0.011$ and $p = 0.034$). Overexpression of CSC markers in PTC was associated with shorter PFS during follow-up. Immunohistochemical staining of CSC markers may provide useful information for predicting patient outcomes.

Keywords: cancer stem cell, papillary thyroid cancer, prognosis, CD15, thyroid gland

OPEN ACCESS

Edited by:
Sheue-yann Cheng,
National Cancer Institute at Frederick, United States

Reviewed by:
Enke Baldini,
Sapienza University of Rome, Italy
Ilaria Ruffilli,
University of Pisa, Italy

***Correspondence:**
Ja Seung Koo
kjs1976@yuhs.ac

Specialty section:
This article was submitted to Thyroid Endocrinology, a section of the journal Frontiers in Endocrinology

Received: *28 December 2018*
Accepted: *16 July 2019*
Published: *02 August 2019*

Citation:
Kim HM and Koo JS (2019) Immunohistochemical Analysis of Cancer Stem Cell Marker Expression in Papillary Thyroid Cancer. Front. Endocrinol. 10:523. doi: 10.3389/fendo.2019.00523

INTRODUCTION

Thyroid cancer is the most common type of endocrine-related cancer, affecting 3.2 million people worldwide in 2015 (1). Among thyroid cancers, papillary thyroid cancer (PTC) accounts for 80–85% of cases. In general, the prognosis of PTC is favorable because of its low biological aggressiveness (2–4). However, in cases of disease recurrence or metastasis owing to a poor response or resistance to the standard treatment of thyroidectomy and radioactive iodine-131 therapy, patient death may occur and alternative treatment options should be sought. Therefore, numerous efforts have been made to identify markers of aggressive cancer behaviors. While the cause of aggressiveness in certain patients with PTC is unclear, several lines of evidence suggest an association with a rare subpopulation of tumor cells with stem cell-like features, also known as cancer stem cells (CSCs) (5, 6). CSCs have important roles in cancer development, growth, recurrence, and metastasis owing to their potential to self-renew and differentiate into various cells

lineages. These characteristics may result in the formation of heterogenous tumor cell masses and the acquisition of resistance to chemotherapy and radiotherapy (7–10).

The role of CSCs in malignancy was first demonstrated in a leukemia model. While tumorigenesis is not provoked in immunodeficient non-obese diabetic/severe combined immunodeficiency mice upon transplantation of most tumor cells, the transplantation of certain tumor cells induces tumorigenesis (11). Subsequent studies have further evaluated the role of CSCs in various solid and hematological malignancies. For example, CSCs were found to be related to resistance to therapy and poor prognosis in patients with esophageal and breast cancer (12–15). In line with these findings, CSC marker expression is correlated with poor prognosis in colorectal carcinoma, suggesting that the expression of CSC markers is associated with patient prognosis in various cancers (16, 17).

Several surrogate marker of CSCs have been previously described. For example, CD24, CD44, and ALDHA1 have been suggested to be CSC markers in breast cancer (13), and CD166 has been implicated in colon cancer (17). In a thyroid cancer cell line, CD15, CD44, CD166, and ALDHA1 are markers of thyroid epithelial cell stemness (18). Moreover, Xu et al. have shown that SSEA-1 (CD15) immunoreactivity is associated with an aggressive subtype of thyroid carcinoma (19). However, the relationship between CSC marker expression and patient prognosis in PTC remains unclear. Therefore, the objective of this study was to investigate the expression of CSC markers in PTC and evaluate its clinical significance.

MATERIALS AND METHODS

Cancer Stem Cell Marker Selection

To select candidate markers for CSCs, an *in silico* analysis and literature review were performed and the most extensively studied candidate markers were chosen (20, 21). CD44 expression was higher in thyroid cancer tissues than in normal thyroid tissues according to the Gene Expression across Normal and Tumor Tissue (GENT) web-accessible database (http://medical-genome.kribb.re.kr/GENT). The web-accessible database cBioPortal (http://www.cbioportal.org) was used to evaluate CSC marker abnormalities in thyroid cancer tissues (**Supplementary Figure S1**). As a result, CD15, CD24, CD44, CD166, and ALDH1A1 were selected as markers of CSCs in this study.

Patient Selection

A total of 386 patients pathologically diagnosed with PTC at Severance Hospital who underwent the surgical removal of cancer and for whom paraffin blocks were available were recruited. Patients were divided into two groups, low risk ($n = 42$) and intermediate risk ($n = 344$), according to the American Thyroid Association 2009 Risk Stratification System (22). All cases were retrospectively reviewed by a thyroid pathologist (JSK), and histological evaluation was performed after hematoxylin and eosin staining. Clinicopathological data were obtained from medical records and included age at diagnosis, sex, disease recurrence/metastasis, and all-cause mortality. The T, N, and cancer stage (23), margin (expanding or infiltrative), extent (confined to the thyroid parenchyma or with extrathyroidal spread), and presence of *BRAF* V600E mutations were also noted after reviewing the slides and surgical pathology reports. This study was approved by the Institutional Review Board of Severance Hospital and conducted in accordance with the principles set forth in the Declaration of Helsinki. The requirement to obtain informed consent was waived from the Institutional Review Board of Severance Hospital because this was a retrospective study.

Tissue Microarray

Representative areas were selected on hematoxylin and eosin-stained slides, and a corresponding spot was marked on the surface of the matching paraffin block. Tissue microarrays (TMAs) were constructed from representative tissue columns for the 386 PTC cases. Three-millimeter tissue cores were extracted from the selected areas using a manual tissue arrayer and placed into a 6×5 recipient block. Two tissue cores were extracted from each sample to minimize extraction bias. Each tissue core was assigned a unique TMA location number, which was linked to a database containing other clinicopathological data.

Immunohistochemistry

Antibodies used for immunohistochemistry are listed in **Supplementary Table S1**. All immunohistochemical analyses were performed with formalin-fixed, paraffin-embedded tissue sections using an automatic immunohistochemistry staining device (Benchmark XT; Ventana Medical System, Tucson, AZ, USA). Briefly, 5-μm-thick formaldehyde-fixed, paraffin-embedded tissue sections were transferred to adhesive slides and dried at 62°C for 30 min. Standard heat epitope retrieval was performed for 30 min in ethylene diamine tetraacetic acid, pH 8.0, in an autostainer. The samples were then incubated with primary antibodies. Afterwards, the sections were incubated with biotinylated anti-mouse immunoglobulins, peroxidase-labeled streptavidin (LSAB Kit, DakoCytomation, Agilent, Santa Clara, CA, USA), and 3,3′-diaminobenzidine. Negative control samples were processed without the primary antibody. Positive control tissues were used per the manufacturer's recommendation. Slides were counterstained with Harris hematoxylin. Optimal primary antibody incubation times and concentrations were determined by serial dilutions using a tissue block fixed and embedded exactly as performed for the samples.

Interpretation of Immunohistochemical Staining

Immunohistochemical markers were assessed by light microscopy. The stained slides were semi-quantitatively evaluated as described previously (24). Staining was evaluated by calculating the proportion of stained cells and immunostaining intensity. The immunostaining intensity was defined as follows: 0, negative; 1, weak; 2, moderate; and 3, strong. The scores for the proportion of stained cells and immunostaining intensity were multiplied, and staining was defined as positive when the final score was >10. *BRAF* V600E mutation status was evaluated using immunohistochemical staining, and was considered positive when >20% of tumor cells were positive (25).

TABLE 1 | Clinicopathological features of patients with papillary thyroid carcinoma according to the American Thyroid Association 2009 Risk Stratification System.

	Total $N = 386$ (%)	ATA low risk group $n = 42$ (%)	ATA intermediate risk group $n = 344$ (%)	*p*-value
Age (years)				0.370
<45	168 (43.5)	21 (50.0)	147 (42.7)	
≥45	218 (56.5)	21 (50.0)	197 (57.3)	
Sex				0.634
Male	81 (21.0)	10 (23.8)	71 (20.6)	
Female	305 (79.0)	32 (76.2)	273 (79.4)	
T stage				0.260
T1	279 (72.3)	33 (78.6)	246 (71.5)	
T2	100 (25.9)	9 (21.4)	91 (26.5)	
T3	7 (1.8)	0 (0.0)	7 (2.0)	
N stage				**<0.001**
N0	144 (37.3)	28 (66.7)	116 (33.7)	
N1	242 (62.7)	14 (33.3)	228 (66.3)	
Cancer stage				**0.006**
I	268 (69.4)	37 (88.1)	231 (67.2)	
II	118 (30.6)	5 (11.9)	113 (32.8)	
Expanding margin				**<0.001**
No	328 (85.0)	19 (45.2)	309 (89.8)	
Yes	58 (15.0)	23 (54.8)	35 (10.2)	
Tumor extension				**<0.001**
Intrathyroidal	110 (28.5)	42 (100.0)	68 (19.8)	
Extrathyroidal	276 (71.5)	0 (0.0)	276 (80.2)	
BRAF V600E mutation ($n = 320$)*				**<0.001**
No	95 (29.7)	30 (100.0)	65 (22.4)	
Yes	225 (70.3)	0 (0.0)	225 (77.6)	
Recurrence/metastasis				0.792
No	327 (84.7)	35 (83.3)	292 (84.9)	
Yes	59 (15.3)	7 (16.7)	52 (15.1)	
Mortality				0.246
No	367 (95.1)	42 (100.0)	325 (94.5)	
Yes	19 (4.9)	0 (0.0)	19 (5.5)	

**Cases that were not tested for the BRAF V600E mutation were excluded. ATA, American thyroid association. Bold values indicate statistically significant ($p < 0.05$).*

TABLE 2 | Expression of cancer stem cell markers according to the American Thyroid Association 2009 Risk Stratification System.

	Total $N = 386$ (%)	ATA low risk group $n = 42$ (%)	ATA intermediate risk group $n = 344$ (%)	*p*-value
CD15				**0.017**
Negative	280 (72.5)	37 (88.1)	243 (70.6)	
Positive	106 (27.5)	5 (11.9)	101 (29.4)	
CD24				0.999
Negative	384 (99.5)	42 (100.0)	342 (94.4)	
Positive	2 (0.5)	0 (0.0)	2 (0.6)	
CD44				0.052
Negative	76 (19.7)	13 (31.0)	63 (18.3)	
Positive	310 (80.3)	29 (69.0)	281 (81.7)	
CD166				0.347
Negative	339 (87.8)	35 (83.3)	304 (88.4)	
Positive	47 (12.2)	7 (16.7)	40 (11.6)	
ALDH1A1				0.212
Negative	378 (97.9)	40 (95.2)	338 (98.3)	
Positive	8 (2.1)	2 (4.8)	6 (1.7)	

ATA, American thyroid association. Bold value indicates statistically significant ($p < 0.05$).

Statistical Analysis

All data are presented as frequencies and percentages. Data were compared using the Chi-squared test or Fisher's exact test, as appropriate. Associations between the proportion of CSC marker-stained cells and *BRAF* V600E mutation status were analyzed using Spearman's rho. Univariate and multivariate Cox proportional hazard analyses were used to evaluate prognostic factors for progression-free survival (PFS) and overall survival (OS). For all statistical analyses, a two-tailed p-value of < 0.05 was considered statistically significant. Data analyses were performed using IBM SPSS Statistics for Windows, Version 21.0 (Released 2012; IBM Corp., Armonk, NY, USA).

RESULTS

Baseline Characteristics of Patients

The clinicopathological features of patients included in this study are presented in **Table 1**. Among the patients, 305 (79.0%) were female, and the mean age was 47.0 years (range: 20–82 years). The N and cancer stages were higher in patients in the intermediate risk group than in those in the low risk group. Moreover, infiltrative margins, extrathyroidal extension, and *BRAF* V600E mutation were more frequently observed in PTC with intermediate risk than in the low risk group. No significant differences were found with respect to age, gender, T stage, recurrence/metastasis, and mortality between the two groups.

Expression of CSC Markers in the Low and Intermediate Risk Groups

Among the CSC markers, CD44 positivity was most frequent, followed by CD166 positivity and CD15 positivity. The expression of CD15 was significantly higher in the intermediate risk group than in the low risk group (29.4 vs. 11.9%, $p = 0.017$; **Table 2**). CD24 positivity was found in only 2 (0.5%) cases, and there was no statistical difference in the expression of CD24 between the two groups. A heat map of CSC marker expression and representative images of immunohistochemical staining of CSC markers in PTC with low risk and intermediate risk are shown in **Figures 1**, **2**.

Correlations Between CSC Marker Expression and Clinicopathological Factors in PTC

We investigated the correlations between the expression of CSC markers and clinicopathological factors in PTC. CD15 positivity was associated with older age (≥45 years; $p = 0.036$), infiltrative margins ($p = 0.002$), *BRAF* V600E mutation ($p < 0.001$), and recurrence/metastasis ($p = 0.014$; **Figure 3**). Similarly, CD44 positivity was associated with a higher N stage ($p = 0.022$), infiltrative margins ($p < 0.001$), extrathyroidal involvement ($p = 0.038$), and recurrence/metastasis ($p = 0.019$).

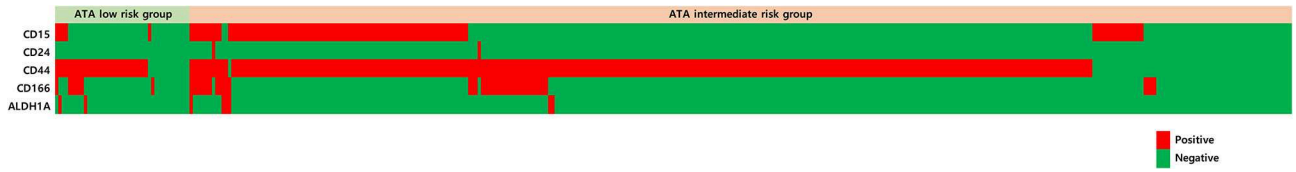

FIGURE 1 | Heat map of cancer stem cell markers expressed in papillary thyroid carcinoma with ATA low risk and ATA intermediate risk.

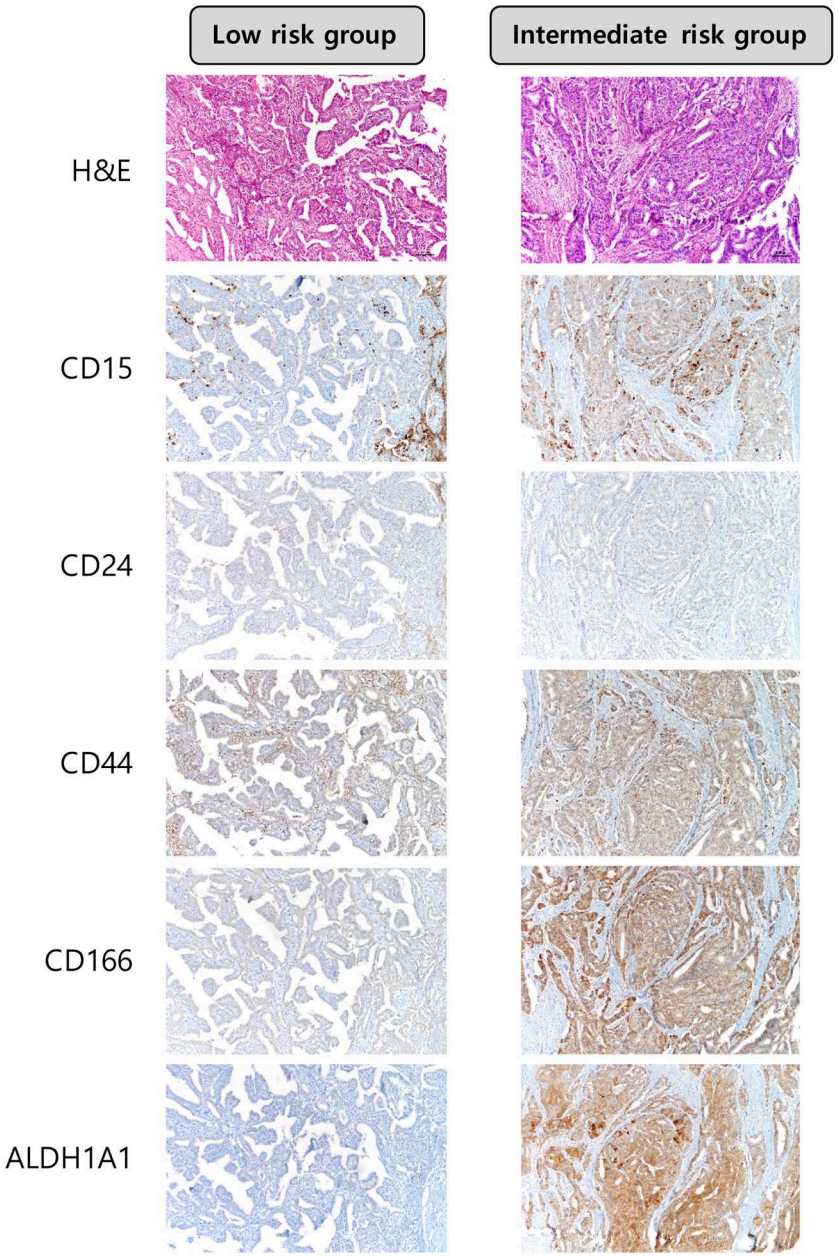

FIGURE 2 | Expression of cancer stem cell markers in papillary thyroid carcinoma with ATA low risk and ATA intermediate risk. The expression of CD15 was higher in PTCs with ATA intermediate risk ×100.

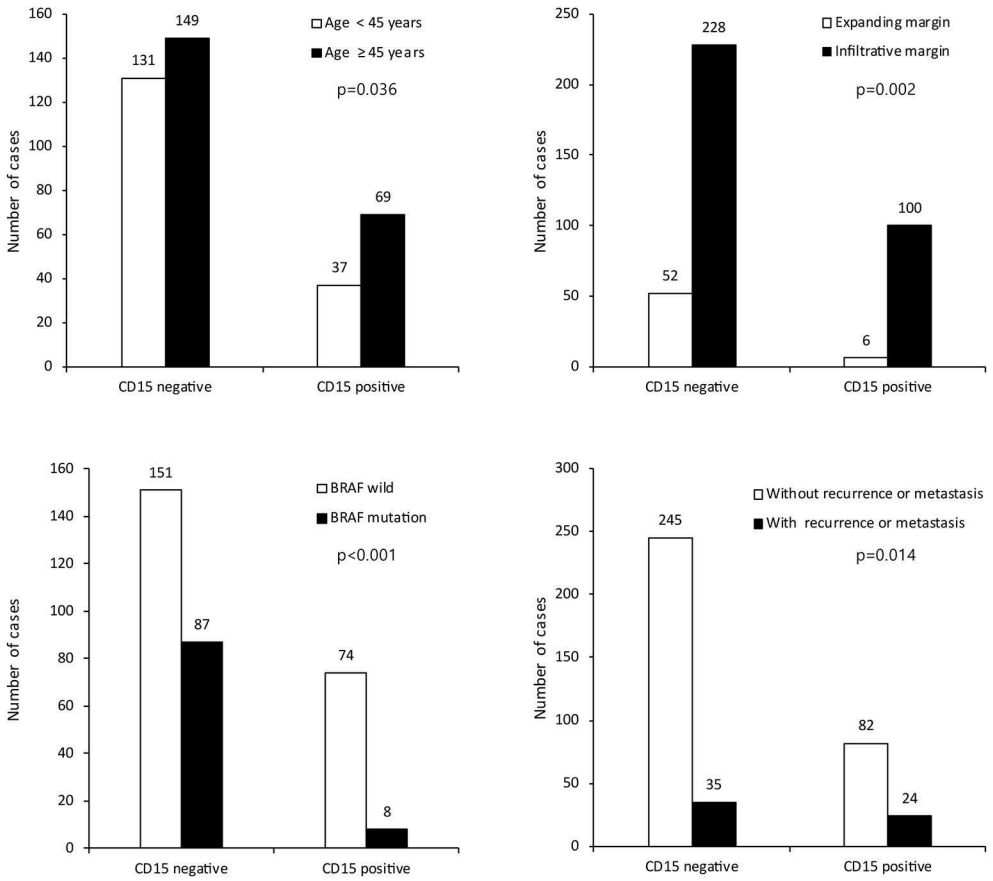

FIGURE 3 | Expression of cancer stem cell marker CD15 and its association with clinicopathologic factors.

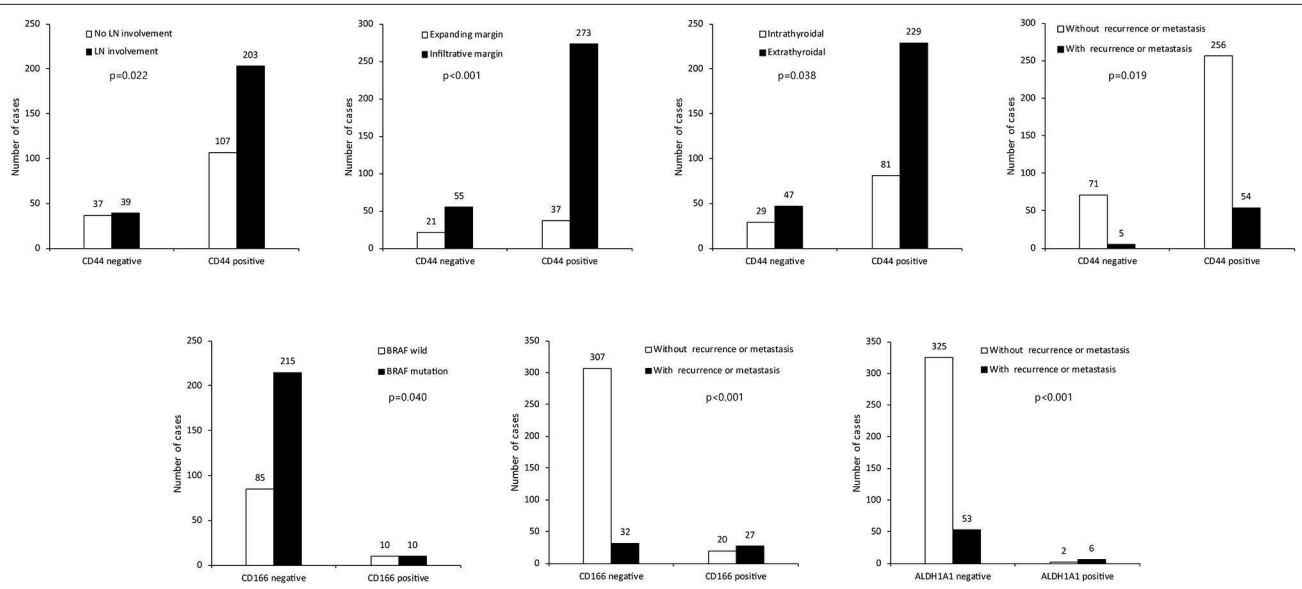

FIGURE 4 | Expression of cancer stem cell markers CD44, CD166, ALDH1A1, and clinicopathological factors. LN, lymph node.

TABLE 3 | Correlations between cancer stem cell marker expression and *BRAF* V600E mutation status.

Parameters	Total ($n = 320$)		PTC with lymph node metastasis ($n = 188$)	
	Correlation coefficient	*p*-value	Correlation coefficient	*p*-value
CD15	0.393	**<0.001**	0.367	**<0.001**
CD24	0.124	**0.026**	0.111	0.130
CD44	−0.050	0.369	−0.050	0.497
CD166	−0.045	0.427	−0.095	0.194
ALDH1A1	−0.024	0.668	−0.052	0.481

PTC, papillary thyroid carcinoma. Bold values indicate statistically significant ($p < 0.05$).

CD166 positivity was associated with *BRAF* V600E mutation and recurrence/metastasis ($p = 0.040$ and $p < 0.001$, respectively), and ALDH1A1 positivity was associated with recurrence/metastasis ($p < 0.001$; **Figure 4**).

Correlations Between CSC Markers and *BRAF* V600E Mutation Status

The *BRAF* V600E mutation status was evaluated by immunohistochemistry in 320 cases of PTC. In total, 225 of the cases (70.3%) exhibited the *BRAF* V600E mutation. The proportions of CD15- and CD24-stained cells were correlated with the *BRAF* V600E mutation status ($r = 0.393$, $p < 0.001$ and $r = 0.124$, $p = 0.026$; **Table 3**). An association between CD15-stained cells and *BRAF* V600E mutation status was also observed in PTC cases with lymph node metastasis ($r = 0.367$, $p < 0.001$). However, no significant correlations were observed between the frequencies of the remaining CSC markers and the *BRAF* V600E mutation status.

CSC Marker Expression Is Associated With Disease Recurrence or Metastasis in PTC

We investigated the impact of clinical parameters and CSC marker expression on the clinical outcomes of patients with PTC using a Cox proportional hazard analysis. The mean follow-up period was 79.1 months, with 59 patients (15.3%) suffering recurrence or metastasis and 19 patients (4.9%) dying during the follow-up period. According to a univariate analysis, higher N and cancer stages, extrathyroidal involvement, and CD15, CD44, CD166, and ALDH1A1 positivity were related to a shorter PFS. A multivariate analysis revealed that a higher N stage [odds ratio (OR): 2.953, 95% confidence interval (CI): 1.286–6.783, $p = 0.011$], higher cancer stage (OR: 1.898, 95% CI: 1.050–3.430, $p = 0.034$), CD15 positivity (OR: 1.929, 95% CI: 1.132–3.288, $p = 0.016$), CD44 positivity (OR: 2.960, 95% CI: 1.137–7.704, $p = 0.026$), CD166 positivity (OR: 7.485, 95% CI: 4.333–12.930, $p < 0.001$), and ALDH1A1 positivity (OR: 3.736, 95% CI: 1.467–9.515, $p = 0.006$) were independently associated with a shorter PFS. However, only a higher cancer stage (OR: 6.839, 95% CI: 2.462–19.000, $p < 0.010$) was associated with a shorter OS according to univariate and multivariate analyses (**Table 4**).

TABLE 4 | Cox proportional hazard analysis of progression-free survival and overall survival in papillary thyroid carcinoma.

	Progression free survival						Overall survival					
	Univariate analysis			Multivariate analysis			Univariate analysis			Multivariate analysis		
	Odds ratio	95% CI	*p*-value	Odds ratio	95% CI	*p*-value	Odds ratio	95% CI	*p*-value	Odds ratio	95% CI	*p*-value
Age ≥ 45 years	1.358	0.801–2.302	0.256				14.244	1.901–106.704	**0.010**			
Male sex	1.690	0.971–2.942	0.064				0.678	0.197–2.326	0.536			
Diameter ≥ 2.0 cm	1.567	0.925–2.656	0.095				2.299	0.934–5.659	0.070			
T stage	1.317	0.828–2.096	0.245				1.752	0.824–3.723	0.145			
N stage	4.253	2.018–8.967	**<0.001**	2.953	1.286–6.783	**0.011**	1.786	0.643–4.966	0.266			
Cancer stage	2.487	1.492–4.146	**<0.001**	1.898	1.050–3.430	**0.034**	6.839	2.462–19.000	**<0.001**	6.839	2.462–19.000	**<0.001**
Infiltrative margin	1.678	0.721–3.904	0.230				3.416	0.456–25.607	0.232			
Extrathyroidal involvement	2.025	1.026–3.998	**0.042**				0.860	0.327–2.262	0.759			
CD15 positivity	1.943	1.155–3.267	**0.012**	1.929	1.132–3.288	**0.016**	1.616	0.636–4.109	0.313			
CD24 positivity	n/a	n/a	n/a				n/a	n/a	n/a			
CD44 positivity	2.917	1.167–7.294	**0.022**	2.960	1.137–7.704	**0.026**	0.999	0.331–3.016	0.999			
CD166 positivity	8.056	4.810–13.494	**<0.0001**	7.485	4.333–12.930	**<0.001**	0.428	0.057–3.212	0.410			
ALDH1A1 positivity	7.236	3.105–16.861	**<0.001**	3.736	1.467–9.515	**0.006**	n/a	n/a	n/a			

CI, Confidence interval; n/a, not applicable. Bold values indicate statistically significant ($p < 0.05$).

DISCUSSION

In this study, we evaluated the expression of CSC markers in PTC and their correlations with clinicopathological parameters and prognosis. We found that in PTC with intermediate risk, the expression of the CSC marker CD15 was significantly elevated. Furthermore, the CSC markers CD15, CD44, CD166, and ALDH1A1 were associated with an aggressive phenotype and were each independently associated with a shorter PFS. The findings of our study are consistent with those of previous studies demonstrating that CSC marker expression is associated with aggressive biological features in various cancers (26–28). Collectively, our findings suggest that CSC markers are potential biological markers for PTC.

In a previous study, CD15 positivity was associated with poor survival in anaplastic thyroid cancer (19). Furthermore, Han et al. have demonstrated that CD24 and CD44 are associated with aggressive clinicopathological features in PTC (29). Together, these findings suggest that the expression of CSC markers may be associated with prognosis. In this study, among the five CSC markers analyzed, we found that CD15, CD44, CD166, and ALDH1A1 expression were independently associated with a shorter PFS. These results provide the first evidence that the expression of CSC markers is associated with patient prognosis in PTC. However, in a Cox proportional hazard analysis, only a higher cancer stage, but not CSC marker expression, was related to patient OS. This may be explained by the nature of PTC, which is relatively indolent compared to other malignancies (3, 4).

Several cellular pathways may mediate the link between CSCs and the pathogenesis of PTC, namely the Notch, Hedgehog (Hh), and Wnt/β-catenin pathways. The Notch pathway is known to facilitate the self-renewal of CSCs in various cancers and is involved in the interaction between the tumor stroma and the endothelium of the CSC microenvironment (30, 31). The Hh pathway is reportedly related to the maintenance of CSCs (32), and the activation of this pathway in cancers is associated with the development of resistance to chemotherapy or radiotherapy (33). The Wnt/β-catenin pathway has also been suggested to play an important role in CSC maintenance (34). Interestingly, a previous study has demonstrated that in PTC, the activation of molecules related to the β-catenin pathway in isolated CSCs promoted cancer migration and metastasis (34). Furthermore, loss-of-function mutations in adenomatosus polyposis coli is associated with CSC activation via β-catenin activation and enhancement of KRAS mutation in colorectal cancer tumorigenesis (35). Because RAS mutation has also been identified in PTC as well as BRAF mutation, these findings altogether suggest an association between CSC and PTC (36).

In a correlation analysis, the expression of the CSC markers CD15 and CD24 was significantly correlated with the *BRAF* V600E mutation status. In PTC, the *BRAF* V600E mutation is reportedly associated with extrathyroidal extension, multifocality, advanced cancer stage, lymph node metastasis, and recurrence (37). A possible explanation for the association between the *BRAF* V600E mutation status and the expression of CSC markers may involve c-MYC and HIF-1α, which are downstream molecules of the mitogen-activated protein kinase pathway. In human ovarian cancer cells, HIF-1α promotes CSC-like properties by upregulating SIRT1 expression (38). In addition, c-MYC overexpression leads to a significant increase in CSCs in breast cancer cell lines (39). Interestingly, Han et al. (29) recently showed that the *BRAF* V600E mutation is associated with CD44 expression in PTC with lymph node metastasis. However, in our study, a significant relationship between CD44 expression and the *BRAF* V600E mutation status was not observed. This difference among studies can likely be attributed to the difference in antibodies used for immunohistochemistry and differences in patient clinical characteristics; further studies are required to evaluate the association between the *BRAF* V600E mutation and the expression of CSC markers.

Our study has several important clinical implications. First, our findings suggest that CSC markers may have prognostic value in PTC. Lymph node involvement, infiltrative margins, and lymphovascular invasion are pathological factors traditionally associated with disease recurrence or metastasis in PTC (40). However, other biological markers reflecting disease recurrence or metastasis are largely unclear. Although a majority of PTCs are indolent in nature, the prognosis for PTC with recurrence or metastasis could be unfavorable (41, 42). Accordingly, it is necessary to identify markers for the identification of patients with high risk of disease recurrence or metastasis. Currently, the American Thyroid Association 2009 Risk Stratification System is the most widely accepted recommendation regarding the initial management of thyroid cancer, which includes cancer screening, staging and risk assessment, and treatment (22). Of note, in the present study, the expression of CD15 was significantly higher in the ATA intermediate risk group than in the low risk group. Moreover, CD15, CD44, CD166, and ALDH1A1 positivity were each independently associated with a shorter PFS, independently of higher N and cancer stage as well as other clinicopathological factors. These findings suggest that CSC markers are ancillary biological markers for evaluating patient prognosis in PTC. Second, CSCs may be potential therapeutic targets for the treatment of PTC. The role of CSCs in PTC tumorigenesis remains uncertain. However, owing to their important functions in tumor initiation and the development of treatment resistance, targeting CSCs may be useful for preventing cancer recurrence or metastasis (43, 44). Currently, the first-line therapy for PTC mainly consists of thyroidectomy and radioactive iodine-131 therapy, which targets mature tumor cells; however, in iodine treatment-refractory cases with disease recurrence or metastasis, chemotherapy using tyrosine kinase inhibitors is recommended (45). Nevertheless, considering the aggressive nature and the difficulty in controlling PTC with recurrence or metastasis (41), there is a need for additional therapeutic options. Targeting CSCs in PTC is a promising strategy for preventing tumor growth, invasion, and metastasis; however, this should be confirmed in clinical trials.

There are several limitations of this study. First, we used immunohistochemistry to evaluate the expression of CSC markers; the quantification of results is therefore difficult and there is the potential for inter-observer bias. Second, as a TMA was used rather than whole sections for histological examination,

samples may have been influenced by extraction bias during TMA construction. Third, we were not able to evaluate molecular changes or the mechanisms underlying CSC marker expression in thyroid cancer tissues, as we focused on expression at the protein level. Fourth, the study was retrospective and selection bias is possible. Further experiments are therefore necessary to elucidate the expression of CSC markers at the gene level and their contributions to the pathogenesis of the disease.

In conclusion, we found that the expression of the CSC marker CD15 was higher in the ATA intermediate risk group than in the low risk group and that the expression of CSC markers is associated with more aggressive tumor characteristics and poor prognosis, thus providing a rationale to evaluate CSC markers in PTC.

ETHICS STATEMENT

This study was approved by the Institutional Review Board of Severance Hospital and conducted in accordance with the principles set forth in the Declaration of Helsinki. The requirement to obtain informed consent was waived from Institutional Review Board of Severance Hospital because this study was performed retrospectively.

AUTHOR CONTRIBUTIONS

JK and HK analyzed the data, conceived of and designed the experiments. HK performed the experiments. JK contributed reagents, materials, analysis tools. HK wrote the paper. Every author has taken care to ensure the integrity of this work, and the final manuscript has been seen and approved by all authors before submission.

FUNDING

This study was supported by a grant from the National R&D Program for Cancer Control, Ministry of Health & Welfare, and Republic of Korea (1420080). This research was supported by Basic Science Research Program through the National Research Foundation of Korea (NRF) funded by the Ministry of Science, ICT, and Future Planning (2015R1A1A1A05001209).

SUPPLEMENTARY MATERIAL

The Supplementary Material for this article can be found online at: https://www.frontiersin.org/articles/10.3389/fendo.2019.00523/full#supplementary-material

REFERENCES

1. GBD 2015 Disease and Injury Incidence and Prevalence Collaborators. Global, regional, and national incidence, prevalence, and years lived with disability for 310 diseases and injuries, 1990-2015: a systematic analysis for the Global Burden of Disease Study 2015. *Lancet.* (2016) 388:1545–602. doi: 10.1016/S0140-6736(16)31678-6
2. Biersack H-J, Grünwald F. *Thyroid Cancer*. Berlin: Springer Science & Business Media (2005). doi: 10.1007/3-540-27845-1
3. Albores-Saavedra J, Henson DE, Glazer E, Schwartz AM. Changing patterns in the incidence and survival of thyroid cancer with follicular phenotype–papillary, follicular, and anaplastic: a morphological and epidemiological study. *Endocr Pathol.* (2007) 18:1–7. doi: 10.1007/s12022-007-0002-z
4. O'Neill CJ, Oucharek J, Learoyd D, Sidhu SB. Standard and emerging therapies for metastatic differentiated thyroid cancer. *Oncologist.* (2010) 15:146–56. doi: 10.1634/theoncologist.2009-0190
5. Campbell LL, Polyak K. Breast tumor heterogeneity: cancer stem cells or clonal evolution? *Cell Cycle.* (2007) 6:2332–8. doi: 10.4161/cc.6.19.4914
6. Shackleton M, Quintana E, Fearon ER, Morrison SJ. Heterogeneity in cancer: cancer stem cells versus clonal evolution. *Cell.* (2009) 138:822–9. doi: 10.1016/j.cell.2009.08.017
7. Clarke MF, Fuller M. Stem cells and cancer: two faces of eve. *Cell.* (2006) 124:1111–5. doi: 10.1016/j.cell.2006.03.011
8. Visvader JE, Lindeman GJ. Cancer stem cells in solid tumours: accumulating evidence and unresolved questions. *Nat Rev Cancer.* (2008) 8:755–68. doi: 10.1038/nrc2499
9. Derwahl M. Linking stem cells to thyroid cancer. *J Clin Endocrinol Metab.* (2011) 96:610–3. doi: 10.1210/jc.2010-2826
10. Monteiro J, Fodde R. Cancer stemness and metastasis: therapeutic consequences and perspectives. *Eur J Cancer.* (2010) 46:1198–203. doi: 10.1016/j.ejca.2010.02.030
11. Lapidot T, Sirard C, Vormoor J, Murdoch B, Hoang T, Caceres-Cortes J, et al. A cell initiating human acute myeloid leukaemia after transplantation into SCID mice. *Nature.* (1994) 367:645–8. doi: 10.1038/367645a0
12. Cabuk D, Yetimoglu E, Simsek T, Gacar G, Subasi C, Canturk Z, et al. The distribution of CD44+/CD24 - cancer stem cells in breast cancer and its relationship with prognostic factors. *J Buon.* (2016) 21:1121–8.
13. Park SY, Lee HE, Li H, Shipitsin M, Gelman R, Polyak K. Heterogeneity for stem cell-related markers according to tumor subtype and histologic stage in breast cancer. *Clin Cancer Res.* (2010) 16:876–87. doi: 10.1158/1078-0432.CCR-09-1532
14. Oliveira LR, Jeffrey SS, Ribeiro-Silva A. Stem cells in human breast cancer. *Histol Histopathol.* (2010) 25:371–85. doi: 10.14670/hh-25.371
15. Islam F, Gopalan V, Wahab R, Smith RA, Lam AK. Cancer stem cells in oesophageal squamous cell carcinoma: identification, prognostic and treatment perspectives. *Crit Rev Oncol Hematol.* (2015) 96:9–19. doi: 10.1016/j.critrevonc.2015.04.007
16. Mohamed SY, Kaf RM, Ahmed MM, Elwan A, Ashour HR, Ibrahim A. The prognostic value of cancer stem cell markers (Notch1, ALDH1, and CD44) in primary colorectal carcinoma. *J Gastrointest Cancer.* (2018). doi: 10.1007/s12029-018-0156-6. [Epub ahead of print].
17. Sim SH, Kang MH, Kim YJ, Lee KW, Kim DW, Kang SB, et al. P21 and CD166 as predictive markers of poor response and outcome after fluorouracil-based chemoradiotherapy for the patients with rectal cancer. *BMC Cancer.* (2014) 14:241. doi: 10.1186/1471-2407-14-241
18. Shimamura M, Nagayama Y, Matsuse M, Yamashita S, Mitsutake N. Analysis of multiple markers for cancer stem-like cells in human thyroid carcinoma cell lines. *Endocr J.* (2014) 61:481–90. doi: 10.1507/endocrj.EJ13-0526
19. Xu J, Hardin H, Zhang R, Sundling K, Buehler D, Lloyd RV. Stage-specific embryonic antigen-1 (SSEA-1) expression in thyroid tissues. *Endocr Pathol.* (2016) 27:271–5. doi: 10.1007/s12022-016-9448-1
20. Zheng X, Cui D, Xu S, Brabant G, Derwahl M. Doxorubicin fails to eradicate cancer stem cells derived from anaplastic thyroid carcinoma cells: characterization of resistant cells. *Int J Oncol.* (2010) 37:307–15. doi: 10.3892/ijo_00000679
21. Chiacchio S, Lorenzoni A, Boni G, Rubello D, Elisei R, Mariani G. Anaplastic thyroid cancer: prevalence, diagnosis and treatment. *Minerva Endocrinol.* (2008) 33:341–57.
22. Haugen BR, Alexander EK, Bible KC, Doherty GM, Mandel SJ, Nikiforov YE, et al. 2015 American thyroid association management guidelines for adult patients with thyroid nodules and differentiated thyroid cancer: the american thyroid association guidelines task force on thyroid nodules and differentiated thyroid cancer. *Thyroid.* (2016) 26:1–133. doi: 10.1089/thy.2015.0020

23. American Joint Committee on C, Amin MB. *AJCC Cancer Staging Manual*. New York, NY: Springer (2017).
24. Henry LR, Lee HO, Lee JS, Klein-Szanto A, Watts P, Ross EA, et al. Clinical implications of fibroblast activation protein in patients with colon cancer. *Clin Cancer Res.* (2007) 13:1736–41. doi: 10.1158/1078-0432.ccr-06-1746
25. Bullock M, O'Neill C, Chou A, Clarkson A, Dodds T, Toon C, et al. Utilization of a MAB for BRAF(V600E) detection in papillary thyroid carcinoma. *Endocr Relat Cancer.* (2012) 19:779–84. doi: 10.1530/ERC-12-0239
26. Jung CW, Han KH, Seol H, Park S, Koh JS, Lee SS, et al. Expression of cancer stem cell markers and epithelial-mesenchymal transition-related factors in anaplastic thyroid carcinoma. *Int J Clin Exp Pathol.* (2015) 8:560–8.
27. Guo Z, Hardin H, Lloyd RV. Cancer stem-like cells and thyroid cancer. *Endocr Relat Cancer.* (2014) 21:T285–300. doi: 10.1530/ERC-14-0002
28. Malaguarnera R, Morcavallo A, Giuliano S, Belfiore A. Thyroid cancer development and progression: emerging role of cancer stem cells. *Minerva Endocrinol.* (2012) 37:103–15.
29. Han SA, Jang JH, Won KY, Lim SJ, Song JY. Prognostic value of putative cancer stem cell markers (CD24, CD44, CD133, and ALDH1) in human papillary thyroid carcinoma. *Pathol Res Pract.* (2017) 213:956–63. doi: 10.1016/j.prp.2017.05.002
30. Pannuti A, Foreman K, Rizzo P, Osipo C, Golde T, Osborne B, et al. Targeting Notch to target cancer stem cells. *Clin Cancer Res.* (2010) 16:3141–52. doi: 10.1158/1078–0432.CCR-09-2823
31. Sosa Iglesias V, Giuranno L, Dubois LJ, Theys J, Vooijs M. Drug resistance in non-small cell lung cancer: a potential for NOTCH targeting? *Front Oncol.* (2018) 8:267. doi: 10.3389/fonc.2018.00267
32. Merchant AA, Matsui W. Targeting Hedgehog–a cancer stem cell pathway. *Clin Cancer Res.* (2010) 16:3130–40. doi: 10.1158/1078–0432.CCR-09-2846
33. Sims-Mourtada J, Izzo JG, Apisarnthanarax S, Wu TT, Malhotra U, Luthra R, et al. Hedgehog: an attribute to tumor regrowth after chemoradiotherapy and a target to improve radiation response. *Clin Cancer Res.* (2006) 12:6565–72. doi: 10.1158/1078–0432.CCR-06-0176
34. Todaro M, Iovino F, Eterno V, Cammareri P, Gambara G, Espina V, et al. Tumorigenic and metastatic activity of human thyroid cancer stem cells. *Cancer Res.* (2010) 70:8874–85. doi: 10.1158/0008–5472.CAN-10-1994
35. Moon BS, Jeong WJ, Park J, Kim TI, Min do S, Choi KY. Role of oncogenic K-Ras in cancer stem cell activation by aberrant Wnt/beta-catenin signaling. *J Natl Cancer Inst.* (2014) 106:djt373. doi: 10.1093/jnci/djt373
36. Ferrari SM, Fallahi P, Ruffilli I, Elia G, Ragusa F, Paparo SR, et al. Molecular testing in the diagnosis of differentiated thyroid carcinomas. *Gland Surg.* (2018) 7(Suppl. 1):S19–s29. doi: 10.21037/gs.2017.11.07
37. Liu X, Yan K, Lin X, Zhao L, An W, Wang C, et al. The association between BRAF (V600E) mutation and pathological features in PTC. *Eur Arch Otorhinolaryngol.* (2014) 271:3041–52. doi: 10.1007/s00405-013-2872-7
38. Qin J, Liu Y, Lu Y, Liu M, Li M, Li J, et al. Hypoxia-inducible factor 1 alpha promotes cancer stem cells-like properties in human ovarian cancer cells by upregulating SIRT1 expression. *Sci Rep.* (2017) 7:10592. doi: 10.1038/s41598-017-09244-8
39. Yin S, Cheryan VT, Xu L, Rishi AK, Reddy KB. Myc mediates cancer stem-like cells and EMT changes in triple negative breast cancers cells. *PLoS ONE.* (2017) 12:e0183578. doi: 10.1371/journal.pone.0183578
40. Bates MF, Lamas MR, Randle RW, Long KL, Pitt SC, Schneider DF, et al. Back so soon? Is early recurrence of papillary thyroid cancer really just persistent disease? *Surgery.* (2018) 163:118–23. doi: 10.1016/j.surg.2017.05.028
41. Ito Y, Kudo T, Kobayashi K, Miya A, Ichihara K, Miyauchi A. Prognostic factors for recurrence of papillary thyroid carcinoma in the lymph nodes, lung, and bone: analysis of 5,768 patients with average 10-year follow-up. *World J Surg.* (2012) 36:1274–8. doi: 10.1007/s00268-012-1423-5
42. Voutilainen PE, Multanen MM, Leppaniemi AK, Haglund CH, Haapiainen RK, Franssila KO. Prognosis after lymph node recurrence in papillary thyroid carcinoma depends on age. *Thyroid.* (2001) 11:953–7. doi: 10.1089/105072501753211028
43. Hombach-Klonisch S, Natarajan S, Thanasupawat T, Medapati M, Pathak A, Ghavami S, et al. Mechanisms of therapeutic resistance in cancer (stem) cells with emphasis on thyroid cancer cells. *Front Endocrinol.* (2014) 5:37. doi: 10.3389/fendo.2014.00037
44. Ke CC, Liu RS, Yang AH, Liu CS, Chi CW, Tseng LM, et al. CD133-expressing thyroid cancer cells are undifferentiated, radioresistant and survive radioiodide therapy. *Eur J Nucl Med Mol Imaging.* (2013) 40:61–71. doi: 10.1007/s00259-012-2242-5
45. National Comprehensive Cancer Network. *Thyroid Carcinoma (Version 2.2013).* Available online at: https://www.nccn.org/store/login/login.aspx?ReturnURL=https://www.nccn.org/professionals/physician_gls/pdf/thyroid.pdf (accessed August 30, 2018).

Conflict of Interest Statement: The authors declare that the research was conducted in the absence of any commercial or financial relationships that could be construed as a potential conflict of interest.

frontiers in Endocrinology

REVIEW
published: 02 August 2019
doi: 10.3389/fendo.2019.00510

Keap1/Nrf2 Signaling: A New Player in Thyroid Pathophysiology and Thyroid Cancer

Cedric O. Renaud[1], *Panos G. Ziros*[1], *Dionysios V. Chartoumpekis*[1,2], *Massimo Bongiovanni*[3] *and Gerasimos P. Sykiotis*[1]*

[1] *Service of Endocrinology, Diabetology and Metabolism, Lausanne University Hospital and University of Lausanne, Lausanne, Switzerland,* [2] *Division of Endocrinology, Department of Internal Medicine, School of Medicine, University of Patras, Patras, Greece,* [3] *Service of Clinical Pathology, Institute of Pathology, Lausanne University Hospital and University of Lausanne, Lausanne, Switzerland*

The Keap1/Nrf2 pathway is a key mediator of general redox and tissue-specific homeostasis. It also exerts a dual role in cancer, by preventing cell transformation of normal cells but promoting aggressiveness, and drug resistance of malignant ones. Although Nrf2 is well-studied in other tissues, its roles in the thyroid gland are only recently emerging. This review focuses on the involvement of Keap1/Nrf2 signaling in thyroid physiology, and pathophysiology in general, and particularly in thyroid cancer. Studies in mice and cultured follicular cells have shown that, under physiological conditions, Nrf2 coordinates antioxidant defenses, directly increases thyroglobulin production and inhibits its iodination. Increased Nrf2 pathway activation has been reported in two independent families with multinodular goiters due to germline loss-of-function mutations in *KEAP1*. Nrf2 pathway activation has also been documented in papillary thyroid carcinoma (PTC), due to somatic mutations, or epigenetic modifications in *KEAP1,* or other pathway components. In PTC, such Nrf2-activating *KEAP1* mutations have been associated with tumor aggressiveness. Furthermore, polymorphisms in the prototypical Nrf2 target genes *NQO1* and *NQO2* have been associated with extra-thyroidal extension and metastasis. More recently, mutations in the Nrf2 pathway have also been found in Hürthle-cell (oncocytic) thyroid carcinoma. Finally, in *in vitro,* and *in vivo* models of poorly-differentiated, and undifferentiated (anaplastic) thyroid carcinoma, Nrf2 activation has been associated with resistance to experimental molecularly-targeted therapy. Thus, Keap1/Nrf2 signaling is involved in both benign and malignant thyroid conditions, where it might serve as a prognostic marker or therapeutic target.

Keywords: thyroid, Nrf2 (nuclear factor erythroid 2-related factor 2), Keap1 (Kelch-like ECH-associated protein 1), thyroglobulin, oxidative stress, goiter, antioxidant

OPEN ACCESS

Edited by:
Vasyl Vasko,
Uniformed Services University of the Health Sciences, United States

Reviewed by:
Lucia Anna Muscarella,
Casa Sollievo della Sofferenza (IRCCS), Italy
Akira Hishinuma,
Dokkyo Medical University, Japan

***Correspondence:**
Gerasimos P. Sykiotis
gerasimos.sykiotis@chuv.ch

Specialty section:
This article was submitted to Thyroid Endocrinology, a section of the journal Frontiers in Endocrinology

Received: *29 April 2019*
Accepted: *12 July 2019*
Published: *02 August 2019*

Citation:
Renaud CO, Ziros PG, Chartoumpekis DV, Bongiovanni M and Sykiotis GP (2019) Keap1/Nrf2 Signaling: A New Player in Thyroid Pathophysiology and Thyroid Cancer. Front. Endocrinol. 10:510. doi: 10.3389/fendo.2019.00510

INTRODUCTION

Reactive oxygen species (ROS), such as hydrogen peroxide (H_2O_2), are required for normal thyroid cell proliferation as well as for synthesis of the main hormones secreted by thyroid follicular cells, triiodothyronine (T3), and thyroxine (T4) (1–3). However, an unchecked excess of ROS can cause oxidative stress (OS), a factor involved in the pathogenesis of a broad spectrum of diseases, including inflammation, and cancer (4). Thus, thyroid follicular cells need to protect themselves

against OS, and recent research has shown that one such protective mechanism is the antioxidant response pathway centered on the nuclear factor erythroid 2-related transcription factor 2 (Nrf2). Nrf2 is a conserved leucine zipper protein that plays a central role in tissue proteostasis by upregulating the transcription of a battery of antioxidant defense genes, and downregulating the transcription of proinflammatory cytokines (5–7). In basal conditions, Nrf2 is bound to its cytoplasmic inhibitory complex formed by Kelch-like ECH-associated protein 1 (Keap1) and Cullin 3 (Cul3), wherein Keap1 targets Nrf2 for polyubiquitination by Cul3 leading to subsequent degradation via the proteasome. Under conditions of OS, specific redox-reactive cysteines of Keap1 become oxidized, thereby abolishing its ability to target Nrf2 for polyubiquitination, and degradation (8–10). Nrf2 is thus stabilized and accumulates in the nucleus, where it binds to DNA sequences called Antioxidant Response Element (AREs) that are located in the promoters, and enhancers of its numerous target genes (11). A model illustrating the pathway, its activation mode, and some of its main target genes is shown in **Figure 1**. The major importance of Nrf2 in health preservation has been convincingly demonstrated via studies in Nrf2 knockout (KO) mice. Tissues of these mice show decreased expression levels of antioxidant and cytoprotective genes, and proteins like NAD(P)H quinone oxidoreductase 1 (Nqo1, a prototypical Nrf2 target gene), glutathione peroxidase 2 (Gpx2), and thioredoxin reductase 1 (Txnrd1). Conversely, oxidative damage to various tissues is increased (12). Nrf2 KO mice are viable, and fertile (13), but they are highly sensitive to challenges with various factors that trigger OS or other related cellular stresses; as a result of such exposures, Nrf2 KO mice develop respective pathologies, and thus serve as experimental models for the corresponding diseases (12, 14). This multiple-organ protection effect is likely due to the fact that Nrf2 not only regulates a wide range of ubiquitous cell-protective genes, but it also regulates the expression of tissue-specific genes involved in the specialized functional, and homeostatic mechanisms of each respective tissue (15). Nrf2 is ubiquitously expressed and it has been well-studied in several tissues; however, its roles in the thyroid gland are only recently starting to be addressed, with emerging evidence that supports indeed the existence of both general antioxidant as well as thyroid-specific physiological functions (16). This review summarizes the recent work on Keap1/Nrf2 signaling in thyroid physiology, and pathophysiology in general and in thyroid cancer in particular.

PHYSIOLOGY

Recent studies have shown that Nrf2 is a key antioxidant player in the thyroid gland. *In vivo* work using mice and rats demonstrated that Nrf2 promotes the transcription and protein synthesis of antioxidant and cytoptotective molecules such as Nqo1, Gpx2 and Txnrd1 in the thyroid gland (16, 17); of note, the latter two were long known to have roles that are necessary for the proper functioning of thyroid follicular cells (18, 19). *In vitro* studies in thyroid follicular cells indicate that these regulations take place in a cell-autonomous manner (16). These effects are present in basal conditions (16), and they are much more prominent in conditions of iodine overload (16, 17). Indeed, pharmacological doses of iodine induce the production of oxidative substances in thyroid follicular cells (16, 17). Given the fact that iodine is a fundamental component of thyroid hormones, this potentially reflects an exacerbation of a physiological phenomenon, whereby a certain oxidative state is necessary to facilitate normal thyroid hormone synthesis (2). In wild-type mice, despite an increased oxidative burden in response to iodine overload, oxidized protein and lipid levels do not increase (16); this indicates that endogenous antioxidant defenses are mobilized to prevent OS. Importantly, this protection is lost in Nrf2 KO mice, whose thyroid tissue shows increased levels of oxidized proteins, and lipids in response to pharmacological doses of iodine (16). Indeed, such exposures induce the transcription of genes encoding antioxidant and cytoprotective proteins like Nqo1, and Gpx2 (16, 17); this induction occurs in a Nrf2-dependant manner, because it is abolished in Nrf2 KO mice (16). Thus, it appears that Nrf2 plays a fundamental role in the protection of thyroid follicular cells against the constant oxidative conditions induced by iodine.

Interestingly, activation of Nrf2 by iodine, with subsequent upregulation of its target genes, has also been documented in human skin (20). This suggests that there may exist at least two mechanisms whereby iodine activates Nrf2: one that is specific to the thyroid and is related to the physiological oxidation reactions involving iodine as part of the process of thyroid hormone synthesis; and another that is either specific to the skin or shared among tissues.

In addition to its antioxidant defense effects, Nrf2 also plays a specific role in thyroidal functions. Studies in mice and cultured follicular cells have shown that Nrf2 has a dramatic impact on both the basal and the thyroid-stimulating hormone (TSH)-induced intra-thyroidal abundance of thyroglobulin (Tg) (16), which is the main protein produced by the gland, and the precursor molecule of T3 and T4. Nrf2 positively regulates the transcription of the gene encoding Tg via direct binding to two AREs in a conserved upstream enhancer (16). In Nrf2 KO mice, Tg production is effectively reduced; the same is true in cultured follicular thyroid cells, both in basal conditions, and in response to TSH stimulation (16). Another striking effect of Nrf2 is that it decreases Tg iodination, which is an essential step in thyroid hormone synthesis; in Nrf2 KO mice, the thyroidal levels of iodinated Tg are thus highly increased, especially in response to excess iodine (16). The mechanisms involved in this latter phenomenon warrant further elucidation; one proposed hypothesis is that Nrf2 activation reduces the levels of oxidative species, thereby reducing the efficiency of the oxidative reactions involved in Tg iodination. The various effects of Nrf2 on thyroid physiology are summarized in **Figure 2**.

In summary, Nrf2 emerges as an important regulator of thyroid follicle physiology: it increases the levels of Tg needed for hormone synthesis, prevents its excessive iodination, and protects against intrathyroidal oxidative damage, especially under conditions of iodine overload.

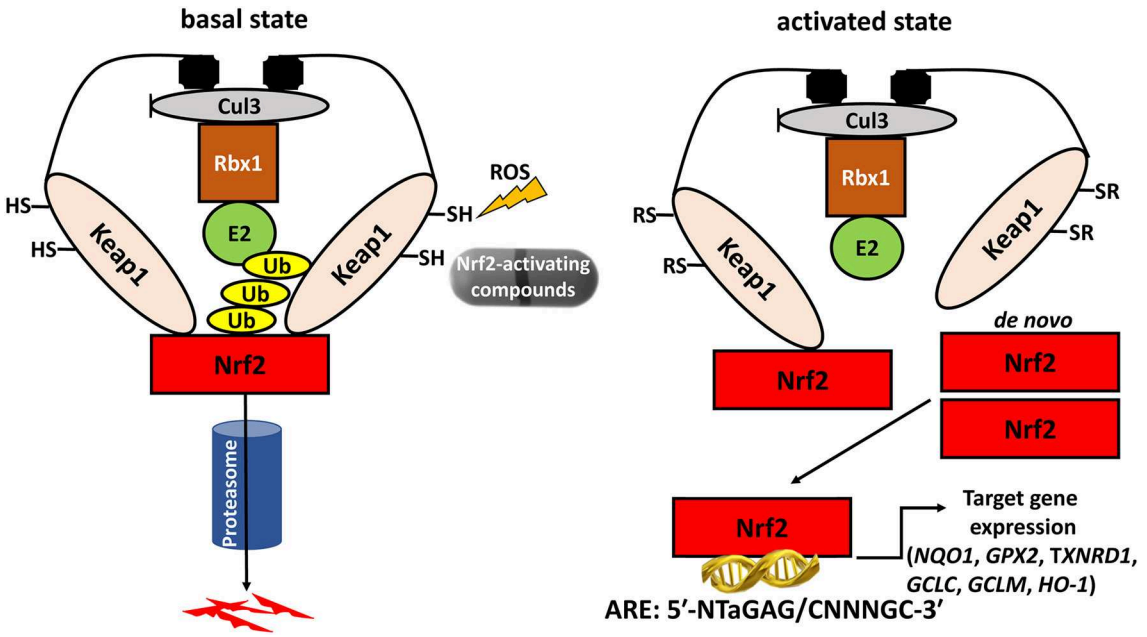

FIGURE 1 | The Keap1/Nrf2 system. Under basal conditions, Nrf2 is bound to its cytoplasmic inhibitory complex formed by Keap1 and Cul3 that targets Nrf2 for polyubiquitination and subsequent degradation by the proteasome. When oxidative stress occurs, the interaction between Nrf2 and the inhibitory complex is abrogated, leading to accumulation of *de novo* synthesized Nrf2 in the nucleus. Nrf2 then promotes the transcription of antioxidant and cytoprotective genes via binding to Antioxidant Response Elements (AREs) located in the genes' regulatory regions. Cul3: Cullin3; Rbx1: RING-box protein 1; E2: ubiquitin-conjugating enzyme 2; Ub: Ubiquitin; Keap1: Kelch-like ECH-associated protein 1; Nrf2: nuclear factor erythroid 2-related transcription factor 2; *NQO1*: NAD(P)H quinone dehydrogenase 1; *GPX2*: glutathione peroxidase 2; *TXNRD1*: thioredoxin reductase 1; *GCLC*: glutamate-cysteine ligase, catalytic subunit; *GCLM*: glutamate-cysteine ligase, modifier subunit; *HO-1*: heme oxygenase 1.

GOITER

Two independent case reports have described patients with hereditary multinodular goiters who harbored respective germline loss-of function mutations of *KEAP1*, leading to increased Nrf2 activation (21, 22). The first mutation was found in a 5-generation Japanese family presenting familial non-toxic goiter inherited in an autosomal dominant pattern (21). Genetic analysis revealed a heterozygous mutation in exon 3 of *KEAP1*, resulting in a single base-pair (bp) deletion and frameshift mutation (c.879_880delinsA, p.Asp294Thr, fs*23). This mutation affects the IVR (intervening region) domain of Keap1, which is responsible for its dimerization and its interaction with Cul3, as shown in **Figure 3**. In affected individuals, no Keap1 protein was generated by the mutant allele in the thyroid, and thus the total wild-type Keap1 protein levels in the thyroid were decreased. The mRNA levels of the gene encoding Nrf2 (*NFE2L2*, for NFE2-like 2) were unchanged, but the mRNA levels of *GSTA4* (Glutathione S-transferase A4), and *GCLC* (glutamate cysteine ligase, catalytic subunit) were increased (21). Since both these genes are known to be transcriptionally activated by Nrf2 in other tissues (23, 24), the data indicate that the heterozygous *KEAP1* loss-of-function mutation leads to activation of Nrf2.

The second germline mutation was described in a middle-aged Japanese woman with coexisting non-toxic multinodular goiter and Graves' disease, whose family history was also notable for goiter in her father, and two paternal aunts (22). Genetic analysis identified a heterozygous single point mutation (c.1448G>A, p.R483H) in *KEAP1*, affecting the Keap1 protein's DC (DGR and CTR, double-glycine repeat and C-terminal region) domain, responsible for Nrf2 binding, as shown in **Figure 3** (22). Histological analysis of the patient's thyroid nodules after total thyroidectomy showed increased Nrf2 nuclear accumulation, indicating altered Keap1/Nrf2 interaction (22). Interestingly, this same mutation had been previously described as a somatic event in non-small cell lung carcinoma tissue samples, where it was also accompanied by increased Nrf2 nuclear accumulation and by increased mRNA levels of *NFE2L2*, which is itself a target gene of Nrf2 (25), as well as by increased mRNA levels of the Nrf2 target genes *NQO1,* and *MRP2* (multidrug resistance protein 2) (26).

These two independent examples (21, 22) show that loss-of-function mutations in *KEAP1* can be a driver event in some rare forms of hereditary non-toxic multinodular goiter, and suggest that the genetic activation of Nrf2 is a likely goitrogenic mechanism in such cases. The relevance of these observations for the pathogenesis of more common forms of sporadic nodules, and goiters remains to be addressed. However, regardless of any broader relevance for the pathogenesis of goiter, these cases are important because they suggest that there

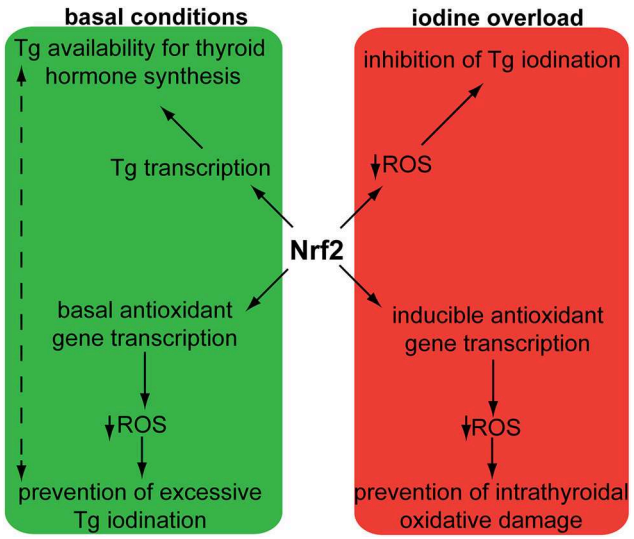

FIGURE 2 | Schematic representation of demonstrated and proposed pleiotropic functions of Nrf2 in follicular thyroid cells under basal conditions and in response to iodine overload. The solid arrows indicate mechanisms that have been sufficiently demonstrated experimentally. Nrf2: nuclear factor erythroid 2-related transcription factor 2; ROS: Reactive Oxygen Species; Tg: thyroglobulin. The dotted arrows indicate putative mechanisms that require further investigation. Originally published in Ziros et al. (16); used here with permission from Mary Ann Liebert Inc.

may be some particularities regarding Keap1/Nrf2 signaling in the thyroid as compared to other tissues: It can be reasonably assumed that in the patients harboring germline *KEAP1* loss-of-function mutations, Nrf2 was activated in all tissues. Yet, only the thyroid showed a prominent clinical phenotype leading to the diagnosis, and no extra-thyroidal diseases were reported in the same patients (21, 22). It is thus possible in theory that *KEAP1* haploinsufficiency may lead to more potent Nrf2 activation in the thyroid as compared to other tissues, or that the thyroid may be more sensitive than other tissues to similar increases in the activation status of the Nrf2 pathway (or both). Systematic surveillance, and extended phenotyping of the affected individuals in these families, as well as of any others that may be identified in the future, could help address this very intriguing question.

Another question raised by these observations concerns the thyroidal safety of compounds that activate Nrf2. One such compound, dimethyl fumarate (DMF) is already approved for the treatment of two different diseases (multiple sclerosis and psoriasis), and several others are being tested in clinical trials for other indications (27). Such indications include both the treatment of specific diseases, as well as the prevention of various pathologies associated with OS and/or environmental exposures to toxicants or pollutants, the so-called "chemoprevention" of disease (27). The cases of patients with *KEAP1* loss-of-function mutations described above suggest that the constitutive and life-long genetic activation of Nrf2 can lead to goiter (21, 22). This raises the question of whether the pharmacological activation of Nrf2 in children or adults (potentially lasting from weeks to decades, depending on the disease and the treatment), may have similar effects. It therefore appears prudent to monitor both thyroid function and thyroid volume (at least by palpation) in patients treated with Nrf2-activating compounds on a therapeutic or experimental basis. In that sense, consumption of a broccoli sprout beverage (yielding pharmacologically active amounts of the Nrf2-activating compound sulforaphane) has been recently shown to be safe for thyroid hormonal, and autoimmune status during a 12-week randomized trial (28). Other Nrf2-activating regimens should also be tested on an individual basis, to ensure their safety for the thyroid gland. Priority should be given to antioxidant compounds, known or suspected to affect thyroid function from *in vitro*, and preclinical studies, as summarized in a recent review (29).

THYROID CARCINOMAS

Pathogenesis and Prognosis

Despite the low rate of proliferation of thyroid follicular cells (30), thyroid tumors (benign or malignant) are quite frequent in the general population. Indeed, even though human thyroid cells divide only about five times during adulthood (30), the spontaneous mutation rate is much higher in the thyroid than in other tissues (31). This might account, at least in part, for the relatively high incidence of thyroid malignancies. About 1.3% of men and women will be diagnosed with thyroid cancer in their lifetime, and this incidence is growing in the last decades (32). Regarding the types of mutations found in thyroid carcinomas, genetic analyses indicate that single-base modifications (but not strand breaks or abasic sites) are more frequent than in cancers of other organs (31). Given that OS preferentially induces single-base mutations (33), these data suggest that mutations found in thyroid carcinomas are mainly due to OS-related DNA damage. In that context, the oxidant H_2O_2, a prerequisite for iodine oxidation and Tg iodination, could be causally implicated in the high mutagenesis rate of the thyroid (34), further supporting the importance of antioxidant mechanisms to ensure redox homeostasis. Furthermore, cells of established tumors also try to protect themselves against excessive OS in order to prevent apoptosis (35). These considerations suggest that the Keap1/Nrf2 pathway, as a key regulator of antioxidant defenses, may play important roles in the pathophysiology of thyroid carcinomas. In that sense, it is also noteworthy that Nrf2 has been described to participate in the regulation of DNA repair signaling after induction of DNA damage by ionizing radiation to colonic cells (36). Given that ionizing radiation to the neck before adulthood is a well-known risk factor for thyroid cancer (37), Nrf2 activation could potentially be a means of prevention against carcinogenesis in this case. More generally, based on studies of carcinomas arising in various other tissues, Nrf2 is known to exert a dual role in cancer, by preventing cell transformation of normal cells but promoting aggressiveness, and drug resistance of malignant ones (38–41). The various studies discussed below demonstrate that these concepts extend also to thyroid carcinomas, and they highlight some particularities of the involvement of Keap1/Nrf2 signaling in these specific tumors.

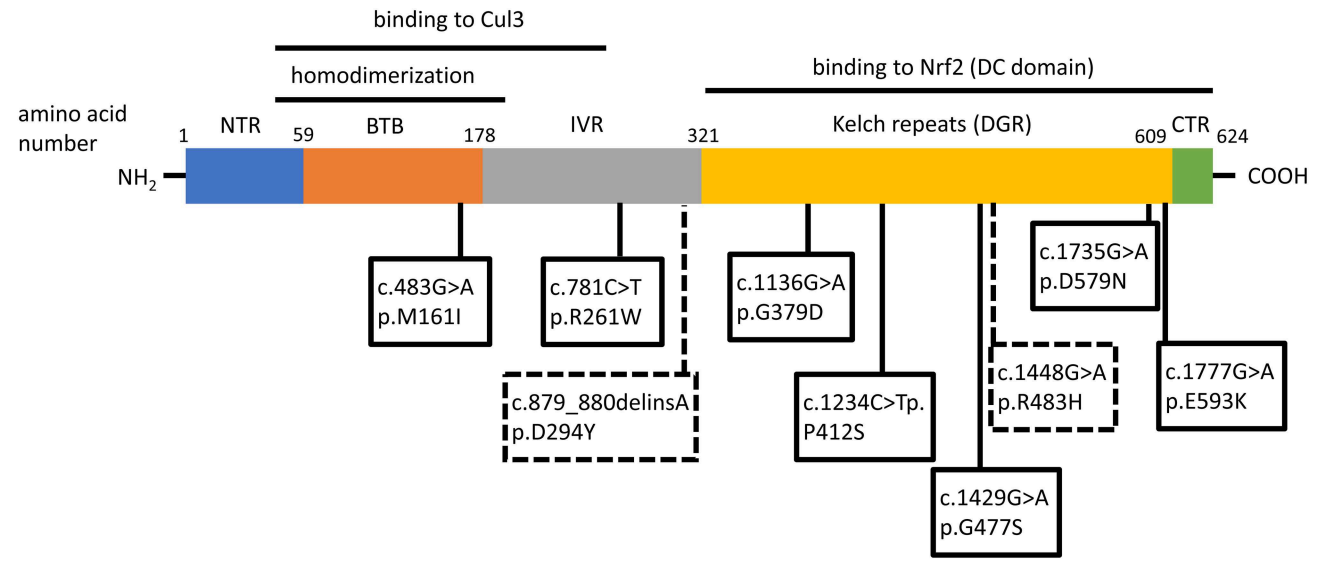

FIGURE 3 | Schematic structure of the Keap1 protein and mutations involved in thyroid gland disorders. Functional regions are indicated with corresponding amino acid number. Dotted lines and rectangles represent germline mutations involved in hereditary multinodular goiter. Solid lines and rectangles represent somatic mutations involved in thyroid cancers. Cul3: Cullin 3; NTR: netrin-like domain; BTB: Broad-Complex, Tramtrack and Bric-a-Brac; IVR: Intervening Region; DRG: Double-Glycine Repeat; DC: DGR and CTR, double-glycine repeat and C-terminal region; CTR: C-terminal Region; NTR: N-terminal Region; NH_2: amino-terminal end; COOH: carboxy-terminal end.

In papillary thyroid carcinoma (PTC), the most common thyroidal malignancy, immunohistochemical analysis showed that the protein levels of Nrf2 and Nqo1 were higher in carcinoma tissues compared to benign follicular adenomas and hyperplastic nodules; both proteins were undetectable in normal thyroid parenchyma adjacent to the PTC samples (42). The oxidized lipid 4-hydroxynonenal (4-HNE) was more abundant in PTC than in adjacent normal tissue, indicating the presence of OS in the cancer, and suggesting that antioxidant defense in PTC is somehow impaired, and/or insufficient to prevent oxidative damage (42). Interestingly, there was no correlation between the protein levels of Nrf2 and Nqo1 in PTC samples, neither between the protein levels of Nrf2 and Keap1; these observations argue against Keap1 downregulation as the principal mechanism of Nrf2 overexpression in PTC, and further suggest that the Nrf2 pathway is not only activated but also at least partially perturbed in PTC (42). In the same study, *in vitro* work with cell lines representing normal human thyrocytes and PTC cells showed that Nrf2 pathway activation promoted the viability of the PTC cell lines but not of normal cells, suggesting that inhibition of Nrf2 may be a potential therapeutic strategy in PTC (42).

In order to characterize the molecular mechanisms leading to Nrf2 activation in thyroid carcinoma, mutations in the Keap1/Nrf2 pathway were sought (42–44). *KEAP1,* and *NFE2L2* somatic mutations have been identified and characterized in various human cancers, including lung, liver, renal, and squamous cell cancers, leukemia, and others (40). Sequencing of PTC samples did not reveal any mutations in *NFE2L2* (and particularly in its known mutational hotspot in exon 2 that encodes one of the domains responsible for the binding to Keap1) (42–44); however, several different mutations were identified in *KEAP1*, albeit at a very low overall frequency (43, 44). The different somatic mutations identified in *KEAP1* in thyroid tumors are shown in **Figure 3**, **Table 1**. This is consistent with data showing that, in thyroid tumors overexpressing Nrf2, *NFE2L2* mRNA levels are not increased and may even be decreased, indicating that increased Nrf2 expression is due to post-transcriptional alterations rather than direct transcriptional upregulation (44). In carcinomas harboring a *KEAP1* mutation, immunohistochemical analysis showed increased expression of Nrf2 in comparison with normal parenchyma, suggesting a decreased inhibitory effect of Keap1 on Nrf2 (43).

In addition to mutations in the genes encoding the core components of the pathway (*KEAP1* and *NFE2L2*), modifications of their promoter sequences and of genes encoding other regulators of the pathway were also considered (44). Indeed, alterations of genes encoding the regulators comprising the Keap1/Cul3/Rbx1 E3-ubiquitin ligase complex that targets Nrf2 for proteasomal degradation, appear to be extremely frequent in PTC, because more than 80% of samples harbored a DNA alteration in at least one component of this complex (44). In contrast with DNA mutations, which were rare, copy number loss and promoter hypermethylation were often present; for example, these were the most common alterations affecting *RBX1,* and *KEAP1*, respectively. Hypermethylation in the promoter region of genes can cause gene silencing and this phenomenon can contribute to carcinogenesis (48). Silencing of *KEAP1* gene by hypermethylation has been described in several cancers (49). Specifically, *KEAP1* gene hypermethylation is associated with stabilized Nrf2 and increased expression of Nrf2 target genes in lung (45), colorectal (50), and prostate cancer (51). In cancers harboring such epigenetic alterations, prognosis is generally worse because cancer evolution is often more rapid (49).

TABLE 1 | List of *KEAP1* mutations involved in benign and malignant thyroid diseases.

Mutation	Inheritance	Localization	Biological effect	Associated disease
c.879_880delinsA, p.D294Y, fs*23	Germline	IVR domain	Increased Nrf2 pathway activity	familial non-toxic multinodular goiter (NTMG) (21) [also found in somatic form in lung adenocarcinoma (45)]
c.1448G>A, p.R483H	Germline	DC domain	Nrf2 nuclear accumulation	familial NTMG (22) [also found in somatic form in lung squamous-cell carcinoma (26)]
c.483G>A, p.M161I	Somatic	BTB domain	Nrf2 protein overexpression	PTC, tall-cell variant (43)
c.781C>T, p.R261W	Somatic	IVR domain	Nrf2 protein overexpression	PTC, classical variant (43)
c.1136G>A, p.G379D	Somatic	DC domain (Kelch 2)	Reduced Keap1-Nrf2 interaction Nrf2 protein overexpression	PTC, classical variant (43) [also found in somatic form in gallbladder adenocarcinoma (46)]
c.1234C>T, p.P412S	Somatic	DC domain (Kelch 3)	Nrf2 protein overexpression Nrf2 nuclear accumulation	PTC, classical variant (43) [also found in somatic form in ovarian carcinoma (47)]
c.1429G>A, p.G477S	Somatic	DC domain (Kelch 4)	Not tested	PTC, unspecified variant (44)
c.1735G>A, p.D579N	Somatic	DC domain (Kelch 6)	Nrf2 protein overexpression	PTC, follicular variant (43)
c.1777G>A, p.E593K	Somatic	DC domain (Kelch 6)	Nrf2 protein overexpression	PTC, classical variant (43)

IVR: Intervening Region; DC: DGR and CTR, double-glycine repeat and C-terminal region; BTB: Broad-Complex, Tramtrack and Bric-a-Brac; Nrf2, nuclear factor erythroid 2-related transcription factor 2; PTC, papillary thyroid carcinoma.

In PTC samples harboring such genetic alterations, despite reduced levels of *NFE2L2* mRNA, the mRNA levels of Nrf2 target genes were increased, consistent with Nrf2 pathway activation (44). Indeed, genes overexpressed in PTC were enriched in binding sites for the transcription factors c-Jun or Bach1/Bach 2 (44), which are positive and negative regulators, respectively, of Nrf2 signaling (52–55). Taken together, these data indicate that the Nrf2 transcriptional program is activated in PTC due to frequent concerted genetic mechanisms that disrupt multiple components of the Nrf2 inhibitory complex (44).

Mutations in *NFE2L2* itself are very rare in PTC, with only one copy number gain in a single sample reported to date (44). Occasional *NFE2L2* and *KEAP1* mutations were recently identified as part of whole-exome sequencing analysis of patient cohorts with Hürthle-cell (oncocytic) thyroid carcinoma (HCC) (56, 57), a type of differentiated thyroid carcinoma characterized by cells with abundant but dysfunctional mitochondria.

To further characterize Nrf2 pathway activation in thyroid carcinoma, some studies focused on specific upstream regulatory proteins. One such candidate was BRAF, because it is frequently activated by somatic mutation in PTC, and because it is a component of the mitogen-activated protein kinase (MAPK) pathway that is known to activate Nrf2 signaling in various contexts. Among PTC samples with strong expression of Nrf2, the *BRAF* V600E mutation was not more frequent compared to a general PTC cohort, suggesting that Nrf2 activation is not exclusively associated with *BRAF* mutation (42). Another study focused on neuregulin 1 (NRG1), a member of the epidermal growth factor-like family, which was found to be overexpressed in PTC (58, 59). NRG1 positively impacts Nrf2 protein levels in PTC and stimulates the upregulation of its target genes, including *NQO1*, *GCLC,* and *GCLM* (glutamate cysteine ligase, modulatory subunit) (58). The latter genes improve redox balance, as reflected in a higher ratio of reduced to oxidized glutathione (GSH/GSSG, GSH being the most abundant intracellular antioxidant), and this additional protection against ROS confers a survival advantage to the tumor cells (58). Similar to experimental knock-down of Nrf2 (42), knock-down of NRG1 abolished the survival advantage of PTC cells, suggesting that NRG1 may be a potential therapeutic target (58).

In PTC, some studies have associated the activation of the Keap1/Nrf2 pathway with more aggressive disease. In one such study, patients with the classical variant or tall-cell (more aggressive) variant of PTC whose tumors harbored somatic mutations in *KEAP1*, showed more frequent extra-thyroidal extension, and lymph node metastases (two thirds of cases), and distant metastasis (one third of cases) (43). Moreover, these patients were all classified as being at intermediate or high risk for recurrence according to the criteria established by the American Thyroid Association (60). Of note, *KEAP1* mutations were identified in only a small percentage of patients ($<$5%) (43). These findings suggest that the identification of somatic *KEAP1* mutations in thyroid carcinomas might serve as an additional prognostic factor. This concept has been previously established in patients with non-small cell lung carcinoma (a tumor with a much higher rate of *KEAP1* somatic mutations), where the presence of such mutations is associated with decreased disease-free survival and decreased overall survival (26).

Papillary thyroid microcarcinoma (PTMC, i.e., PTC of $\leq$1 cm), is often an indolent disease that does not always warrant surgery but may be eligible for active surveillance (61). However, occasional cases of PTMC show more aggressive behavior, and can even give local or, more rarely, distant metastases. It would thus be very useful to identify factors that could predict aggressive behavior in PTMC, as such patients would not be good candidates for active surveillance. In that sense, germline genetic polymorphisms in *NQO2*, a target gene of Nrf2 (62), were associated with more aggressive behavior of PTMC (63). Specifically, *NQO2* is known to harbor a tri-allelic polymorphism that consists of a 29 bp insertion (I29), a 29 bp deletion

(D), and a 16 bp insertion (I16). Patients with PTMC who were homozygous for the *NQO2* I29 allele were more likely to have lymph node metastasis at diagnosis compared with PTMC patients bearing the D allele (63). The association between *NQO2* I29 homozygosity and lymph node metastasis in PTMC was confirmed in multivariate analysis. Of note, the prevalence of the different polymorphisms was similar in patients with PTMC, and patients with benign hyperplastic nodules (63); this indicates that the polymorphism is not implicated in the initiation of PTMC but rather in its progression.

The same study (63) also evaluated a polymorphism in *NQO1*, the C609T missense variant, called *NQO1*2*. Previously, this polymorphism had been associated with higher cancer risk and worse prognosis in breast cancer (64–67), as well as with higher risk for occupational benzene poisoning, which is a risk factor for leukemia (68). In PTMC, the *NQO1*2* allele was associated with extra-thyroidal extension, but without statistical significance in multivariate analysis (63). It thus does not appear to have the same prognostic value as the *NQO2* I29 allele (63). Regarding Nqo1, in another study there was no correlation between the protein levels of Nqo1 (or Nrf2) with either PTC variants associated with more aggressive behavior (tall-cell, solid/trabecular, diffuse sclerosing, and oncocytic PTC variants) or with lymph node metastasis (42). Even though Nrf2 protein levels were increased in *KEAP1*-mutated tumors (43), current evidence does not support a prognostic role for Nrf2 or Nqo1 levels *per se*. In contrast, expression of heme oxygenase-1 (HO-1), another target gene of Nrf2 (69), was found to correlate with thyroid cancer aggressiveness (stage and risk of recurrence, plus a near-significant trend for extra-thyroidal invasion), but not with tumor size or lymph node metastasis (70). NRG1 overexpression was described as a positive prognostic factor for lymph node metastasis in PTC (58).

Treatment

As mentioned above, Nrf2 is generally known to exert a dual role in cancer: on the one hand, it prevents cell transformation of normal cells, and on the other hand, it promotes aggressiveness, and drug resistance of malignant ones (38–41). The latter, so-called "dark side" of Nrf2 (71), has been well-studied in other cancer types, where Nrf2 has been shown to promote resistance against chemotherapy and radiotherapy (40, 41). Although better described in lung, and liver carcinomas, such drug resistance mechanisms and their implications have more recently begun to be characterized in various models of thyroid carcinoma. It is thus interesting to discuss various pharmaceutical approaches that directly or indirectly target the Nrf2 pathway as a strategy for thyroid cancer treatment.

Proteasome inhibitors are targeted anti-cancer agents that are in clinical use in other types of cancer. They have also been used experimentally in patients with thyroid carcinomas without established alternative treatments, such as metastatic thyroid carcinomas that are radioiodine-refractory (72). Regarding their mechanisms of action, as elucidated in other cancer types, inhibition of the proteasome leads to accumulation of misfolded proteins, inducing endoplasmic reticulum (ER) stress, and subsequent apoptosis (73). Apoptosis is induced in part via induction of CCAAT/enhancer-binding protein homologous protein (CHOP), activation of the apoptosis signal-regulating kinase 1 (ASK1)/c-Jun N-terminal kinase (JNK) pathway, and cleavage of ER-resident caspase-12 (74). Because Nrf2 is degraded in a proteasome-dependent manner, proteasome inhibition also generally leads to Nrf2 activation. Thus, a series of studies have evaluated the involvement of Nrf2 in the sensitivity of thyroid carcinoma cells lines to proteasome inhibitors. Their results and conclusions are discussed below and summarized in **Figure 4**.

In vitro experiments in poorly differentiated thyroid carcinoma (PTDC) and undifferentiated (anaplastic) thyroid carcinoma (UTC/ATC) showed that the apoptotic response to proteasome inhibitor treatment can be predicted by the induction of CHOP. Cell lines that displayed higher CHOP protein induction were more sensitive to proteasome inhibitor treatment, while experimental knock-down of CHOP partially decreased the effects of the proteasome inhibitor (75). The expression of the gene encoding CHOP is regulated by several transcription factors, including oxygen-regulated protein 150 (ORP150), an inducible ER chaperone that suppresses *CHOP* expression (76); and Activating Transcription Factor 4 (ATF4), a transcription factor induced in response to proteasome inhibition that promotes *CHOP* expression (77). Both of these transcription factors can be, at least partially, regulated by Nrf2 (78). Nrf2 increases *ORP150* gene transcription both directly, by binding to the *ORP150* gene promoter, as well as indirectly, by promoting ATF4 recruitment to the *ORP150* gene, which also upregulates its expression (78). At the same time, Nrf2 antagonizes the recruitment of ATF4 on an ARE in the *CHOP* promoter, thereby preventing ATF4-mediated *CHOP* transcription (77). Overall, Nrf2 decreases *CHOP* gene expression, hence exerting an anti-apoptotic effect in response to proteasome inhibitor treatment, and thereby favoring drug resistance. Consistent with the aforementioned mechanisms, cell lines with low sensitivity to proteasome inhibitor treatment show increased expression levels of Nrf2, and ORP150 proteins (78). Experimental knock-down of ORP150 increased the sensitivity of tumor cell lines that were less responsive to proteasome inhibitor treatment. These lines also expressed higher *CHOP* mRNA levels (76). Similarly, experimental knock-down of Nrf2 inhibited the induction of *ORP150* mRNA and protein and significantly decreased the binding of ATF4 to the *ORP150* promoter (78). These findings suggest that pharmacological inhibition of Nrf2 could be a plausible strategy to increase the sensitivity of PDTC and UTC to proteasome inhibitors.

Generation of ROS is considered to be a crucial early event (79) during the initiation of apoptosis induced by the proteasome inhibitor bortezomib in some types of cancer. Indeed, UTC cell lines that are less sensitive to bortezomib do not show an early increase in ROS (80). Additionally, those less sensitive cell lines show higher levels of GSH, which is associated with higher expression levels and activity of the Nrf2 target gene *GCLC* (80). Moreover, Nrf2 is overexpressed in these cell lines, suggesting that bortezomib resistance can be due to Nrf2-mediated synthesis of GSH (80). Other research work using UTC and PDTC models indicates that p38 MAPK, an important anti-apoptotic factor activated in response to proteasome inhibition,

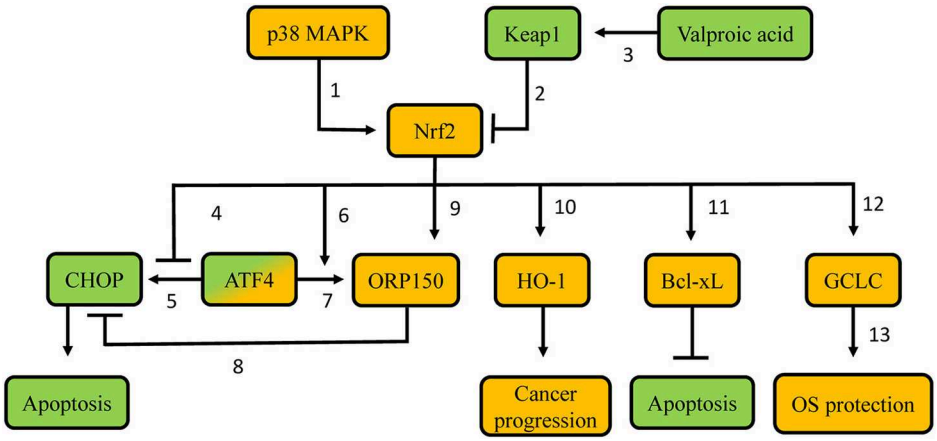

FIGURE 4 | Proposed molecular mechanisms involved in resistance of thyroid carcinoma cells to proteasome inhibitors. Green-labeled molecules promote sensitivity to proteasome inhibitors, orange-labeled molecules promote resistance to proteasome inhibitors. 1. p38 MAPK phosphorylates Nrf2, thus leading to Nrf2 nuclear accumulation; 2. Keap1 targets Nrf2 for poly-ubiquitination and proteasomal degradation; 3. Valproic acid demethylates the *KEAP1* promoter, thus favoring *KEAP1* gene transcription; 4. Nrf2 precludes recruitment of ATF4 to the *CHOP* promoter, thus decreasing *CHOP* transcription; 5. ATF4 promotes *CHOP* transcription via binding to its promoter; 6. Nrf2 promotes ATF4 recruitment on the *ORP150* promoter, thus increasing *ORP150* transcription; 7. ATF4 promotes *ORP150* transcription via binding to its promoter; 8. Potential competition between ORP150 and CHOP; 9. Nrf2 promotes *ORP150* transcription; 10. Nrf2 promotes *HO-1* transcription; 11. Potentially decreased Keap1-mediated Bcl-XL poly-ubiquitination; 12. Nrf2 promotes *GCLC* transcription; 13. Gclc protein favors GSH synthesis. MAPK: Mitogen-activated protein kinase; Keap1: Kelch-like ECH-associated protein 1; Nrf2: nuclear factor erythroid 2-related transcription factor 2; CHOP: CCAAT/enhancer-binding protein homologous protein; ATF4: Activating Transcription Factor 4; ORP150: oxygen-regulated protein 150; HO-1: heme-oxygenase 1; Bcl-xL: B-cell lymphoma-extra large; GCLC: glutamate-cystein ligase, catalytic subunit; OS: oxidative stress.

phosphorylates Nrf2, and promotes its accumulation in the nucleus, thereby inducing the transcription of *GCLC* (81). Pharmacological inhibition of p38 MAPK suppresses the nuclear translocation of Nrf2, thereby enhancing bortezomib-induced apoptosis, especially in bortezomib-resistant cell lines (81). These data indicate that the mechanisms by which Nrf2 promotes resistance to proteasome inhibitors in thyroid cancer are not limited to interactions with regulators of apoptosis (ATF4, ORP150, and CHOP), but also include the direct modulation of the cells' redox status.

Furthermore, overexpression of Nrf2 in PTC cells confers resistance to TRAIL (TNF-related apoptosis inducing ligand) (82). TRAIL is a molecule with growing interest in oncology, as it specifically triggers cell death (83). In TRAIL-resistant PTC, combination of the histone deacetylase inhibitor valproic acid with a TRAIL regimen leads to increased sensitivity both *in vitro,* and *in vivo* (orthotopic mouse model of PTC) (82). Interestingly, in a different epithelial cell model (human lens), valproic acid is also known to promote demethylation of the *KEAP1* promoter, leading to upregulation of *KEAP1* expression, and subsequent decreased Nrf2 protein abundance (84). Consistent with this, in TRAIL-resistant PTC, combination therapy with valproic acid and TRAIL decreases the nuclear levels, and activity of Nrf2, leading to downregulation of Bcl-xL, an anti-apoptotic molecule of the Bcl-2 family (85). Experimental knock-down of Nrf2 also decreases Bcl-xL protein levels, thereby promoting apoptosis in cancer cells (82). Interestingly, Keap1 has been shown to negatively regulate the activity of Bcl-xL by targeting it for poly-ubiquitination (86). These data indicate that Nrf2 promotes resistance not only to proteasome inhibitors, but also to other experimental therapies, and it could thus be considered as a candidate target to increase sensitivity to such treatments when they are tested in clinic trials. However, although this approach to treat/prevent PTC appears mechanistically appealing, it may have unexpected adverse effects. Indeed, human lens epithelial cells treated with 5-aza-2′deoxycytidine (a compound known to promote demethylation of CpG islands in the *KEAP1* promoter) displayed increased Keap1 protein levels, decreased Nrf2 stabilization, enhanced ROS, and increased cell death. These alterations resulted in a diabetic cataract lens phenotype (87), which is consistent with the fact that demethylation of the *KEAP1* promoter is also associated with enhanced age-related cataract in humans (88).

Finally, inhibitors of HO-1 have been shown to decrease proliferation, migration, and invasion of follicular thyroid carcinoma (FTC) and UTC cell lines, and to reduce FTC tumor growth in a xenograft model (89). This study demonstrates that desirable effects on thyroid carcinoma might be achieved not only by targeting Nrf2 directly, but also potentially by targeting other components of the Keap1/Nrf2 pathway and its downstream signaling.

CONCLUSION

In summary, Keap1/Nrf2 signaling is involved in both benign and malignant thyroid conditions, where it might serve as a prognosis marker, or therapeutic target. Ongoing research, including cell culture studies with normal and transformed thyroid follicular cells, thyroidal phenotyping of animal models, analysis of human thyroid tissue samples, and monitoring of thyroid function and volume in clinical studies, is expected to yield a better understanding of the involvement of Nrf2 in thyroid physiology, and pathophysiology. Such work is

important in order to ensure the thyroidal safety of Nrf2-activating compounds that are being developed for use in other indications, and it might also facilitate the development of new drugs for the prevention and the treatment of both benign thyroid diseases, and thyroid carcinomas.

AUTHOR CONTRIBUTIONS

CR drafted and edited the manuscript and the figures. PZ and MB edited the manuscript. DC prepared figures, edited the manuscript, and contributed to the discussion. GS conceived and edited the manuscript.

FUNDING

This work was supported by Swiss National Science Fund SNF-COST project IZCOZ0-177070; Swiss National Science Fund project 31003A_182105; and a Leenaards Foundation 2016 Fellowship for Academic Promotion in Clinical Medicine (all to GS); two Short Term Scientific Missions by European Cooperation in Science and Technology Action CA16112 NutRedOx–Personalized nutrition in aging society: redox control of major age-related diseases (to DC and GS); and a 3E-Exchange in Endocrinology Expertise fellowship by Section/Board of Endocrinology of the UEMS (to DC).

REFERENCES

1. Colin IM, Denef JF, Lengele B, Many MC, Gerard AC. Recent insights into the cell biology of thyroid angiofollicular units. *Endocr Rev*. (2013) 34:209–38. doi: 10.1210/er.2012-1015
2. Poncin S, Colin IM, Gerard AC. Minimal oxidative load: a prerequisite for thyroid cell function. *J Endocrinol*. (2009) 201:161–7. doi: 10.1677/JOE-08-0470
3. Poncin S, Van Eeckoudt S, Humblet K, Colin IM, Gerard AC. Oxidative stress: a required condition for thyroid cell proliferation. *Am J Pathol*. (2010) 176:1355–63. doi: 10.2353/ajpath.2010.090682
4. Pizzino G, Irrera N, Cucinotta M, Pallio G, Mannino F, Arcoraci V, et al. Oxidative stress: harms and benefits for human health. *Oxid Med Cell Longev*. (2017) 2017:8416763. doi: 10.1155/2017/8416763
5. Sykiotis GP, Bohmann D. Stress-activated cap'n'collar transcription factors in aging and human disease. *Sci Signal*. (2010) 3:re3. doi: 10.1126/scisignal.3112re3
6. Kobayashi EH, Suzuki T, Funayama R, Nagashima T, Hayashi M, Sekine H, et al. Nrf2 suppresses macrophage inflammatory response by blocking proinflammatory cytokine transcription. *Nat Commun*. (2016) 7:11624. doi: 10.1038/ncomms11624
7. Ahmed SM, Luo L, Namani A, Wang XJ, Tang X. Nrf2 signaling pathway: pivotal roles in inflammation. *Biochim Biophys Acta Mol Basis Dis*. (2017) 1863:585–97. doi: 10.1016/j.bbadis.2016.11.005
8. Motohashi H, Yamamoto M. Nrf2-Keap1 defines a physiologically important stress response mechanism. *Trends Mol Med*. (2004) 10:549–57. doi: 10.1016/j.molmed.2004.09.003
9. Kang MI, Kobayashi A, Wakabayashi N, Kim SG, Yamamoto M. Scaffolding of Keap1 to the actin cytoskeleton controls the function of Nrf2 as key regulator of cytoprotective phase 2 genes. *Proc Natl Acad Sci USA*. (2004) 101:2046–51. doi: 10.1073/pnas.0308347100
10. Itoh K, Wakabayashi N, Katoh Y, Ishii T, Igarashi K, Engel JD, et al. Keap1 represses nuclear activation of antioxidant responsive elements by Nrf2 through binding to the amino-terminal Neh2 domain. *Genes Dev*. (1999) 13:76–86. doi: 10.1101/gad.13.1.76
11. Nguyen T, Nioi P, Pickett CB. The Nrf2-antioxidant response element signaling pathway and its activation by oxidative stress. *J Biol Chem*. (2009) 284:13291–5. doi: 10.1074/jbc.R900010200
12. Li J, Stein TD, Johnson JA. Genetic dissection of systemic autoimmune disease in Nrf2-deficient mice. *Physiol Genomics*. (2004) 18:261–72. doi: 10.1152/physiolgenomics.00209.2003
13. Itoh K, Chiba T, Takahashi S, Ishii T, Igarashi K, Katoh Y, et al. An Nrf2/small Maf heterodimer mediates the induction of phase II detoxifying enzyme genes through antioxidant response elements. *Biochem Biophys Res Commun*. (1997) 236:313–22. doi: 10.1006/bbrc.1997.6943
14. Yamamoto M, Kensler TW, Motohashi H. The KEAP1-NRF2 system: a thiol-based sensor-effector apparatus for maintaining redox homeostasis. *Physiol Rev*. (2018) 98:1169–203. doi: 10.1152/physrev.00023.2017
15. Lee JM, Li J, Johnson DA, Stein TD, Kraft AD, Calkins MJ, et al. Nrf2, a multi-organ protector? *FASEB J*. (2005) 19:1061–6. doi: 10.1096/fj.04-2591hyp
16. Ziros PG, Habeos IG, Chartoumpekis DV, Ntalampyra E, Somm E, Renaud CO, et al. NFE2-Related transcription factor 2 coordinates antioxidant defense with thyroglobulin production and iodination in the thyroid gland. *Thyroid*. (2018) 28:780–98. doi: 10.1089/thy.2018.0018
17. Wang T, Liang X, Abeysekera IR, Iqbal U, Duan Q, Naha G, et al. activation of the Nrf2-keap 1 pathway in short-term iodide excess in thyroid in rats. *Oxid Med Cell Longev*. (2017) 2017:4383652. doi: 10.1155/2017/4383652
18. Ekholm R, Bjorkman U. Glutathione peroxidase degrades intracellular hydrogen peroxide and thereby inhibits intracellular protein iodination in thyroid epithelium. *Endocrinology*. (1997) 138:2871–8. doi: 10.1210/en.138.7.2871
19. Howie AF, Arthur JR, Nicol F, Walker SW, Beech SG, Beckett GJ. Identification of a 57-kilodalton selenoprotein in human thyrocytes as thioredoxin reductase and evidence that its expression is regulated through the calcium-phosphoinositol signaling pathway. *J Clin Endocrinol Metab*. (1998) 83:2052–8. doi: 10.1210/jcem.83.6.4875
20. Ben-Yehuda Greenwald M, Frusic-Zlotkin M, Soroka Y, Ben-Sasson S, Bianco-Peled H, Kohen R. A novel role of topical iodine in skin: activation of the Nrf2 pathway. *Free Radic Biol Med*. (2017) 104:238–48. doi: 10.1016/j.freeradbiomed.2017.01.011
21. Teshiba R, Tajiri T, Sumitomo K, Masumoto K, Taguchi T, Yamamoto K. Identification of a KEAP1 germline mutation in a family with multinodular goitre. *PLoS ONE*. (2013) 8:e65141. doi: 10.1371/journal.pone.0065141
22. Nishihara E, Hishinuma A, Kogai T, Takada N, Hirokawa M, Fukata S, et al. A novel germline mutation of KEAP1 (R483H) associated with a non-toxic multinodular goiter. *Front Endocrinol (Lausanne)*. (2016) 7:131. doi: 10.3389/fendo.2016.00131
23. Yang Y, Huycke MM, Herman TS, Wang X. Glutathione S-transferase alpha 4 induction by activator protein 1 in colorectal cancer. *Oncogene*. (2016) 35:5795–806. doi: 10.1038/onc.2016.113
24. Li M, Chiu JF, Kelsen A, Lu SC, Fukagawa NK. Identification and characterization of an Nrf2-mediated ARE upstream of the rat glutamate cysteine ligase catalytic subunit gene (GCLC). *J Cell Biochem*. (2009) 107:944–54. doi: 10.1002/jcb.22197
25. Kwak MK, Itoh K, Yamamoto M, Kensler TW. Enhanced expression of the transcription factor Nrf2 by cancer chemopreventive agents: role of antioxidant response element-like sequences in the nrf2 promoter. *Mol Cell Biol*. (2002) 22:2883–92. doi: 10.1128/MCB.22.9.2883-2892.2002
26. Takahashi T, Sonobe M, Menju T, Nakayama E, Mino N, Iwakiri S, et al. Mutations in keap1 are a potential prognostic factor in resected non-small cell lung cancer. *J Surg Oncol*. (2010) 101:500–6. doi: 10.1002/jso.21520
27. Cuadrado A, Rojo AI, Wells G, Hayes JD, Cousin SP, Rumsey WL, et al. Therapeutic targeting of the NRF2 and KEAP1 partnership in chronic diseases. *Nat Rev Drug Discov*. (2019) 18:295–317. doi: 10.1038/s41573-018-0008-x
28. Chartoumpekis DV, Ziros PG, Chen JG, Groopman JD, Kensler TW, Sykiotis GP. Broccoli sprout beverage is safe for thyroid hormonal and autoimmune status: results of a 12-week randomized trial. *Food Chem Toxicol*. (2019) 126:1–6. doi: 10.1016/j.fct.2019.02.004

29. Paunkov A, Chartoumpekis DV, Ziros PG, Chondrogianni N, Kensler TW, Sykiotis GP. Impact of antioxidant natural compounds on the thyroid gland and implication of the keap1/Nrf2 signaling pathway. *Curr Pharm Des.* (2019). doi: 10.2174/1381612825666190701165821. [Epub ahead of print].
30. Coclet J, Foureau F, Ketelbant P, Galand P, Dumont JE. Cell population kinetics in dog and human adult thyroid. *Clin Endocrinol (Oxf).* (1989) 31:655–65. doi: 10.1111/j.1365-2265.1989.tb01290.x
31. Maier J, van Steeg H, van Oostrom C, Karger S, Paschke R, Krohn K. Deoxyribonucleic acid damage and spontaneous mutagenesis in the thyroid gland of rats and mice. *Endocrinology.* (2006) 147:3391–7. doi: 10.1210/en.2005-1669
32. Mao Y, Xing M. Recent incidences and differential trends of thyroid cancer in the USA. *Endocr Relat Cancer.* (2016) 23:313–22. doi: 10.1530/ERC-15-0445
33. Valko M, Izakovic M, Mazur M, Rhodes CJ, Telser J. Role of oxygen radicals in DNA damage and cancer incidence. *Mol Cell Biochem.* (2004) 266:37–56. doi: 10.1023/B:MCBI.0000049134.69131.89
34. Krohn K, Maier J, Paschke R. Mechanisms of disease: hydrogen peroxide, DNA damage and mutagenesis in the development of thyroid tumors. *Nat Clin Pract Endocrinol Metab.* (2007) 3:713–20. doi: 10.1038/ncpendmet0621
35. Kumari S, Badana AK, Mohan GM, G S, Malla R. Reactive oxygen species: a key constituent in cancer survival. *Biomark Insights.* (2018) 13:1177271918755391. doi: 10.1177/1177271918755391
36. Kim SB, Pandita RK, Eskiocak U, Ly P, Kaisani A, Kumar R, et al. Targeting of Nrf2 induces DNA damage signaling and protects colonic epithelial cells from ionizing radiation. *Proc Natl Acad Sci USA.* (2012) 109:E2949–55. doi: 10.1073/pnas.1207718109
37. Lubin JH, Adams MJ, Shore R, Holmberg E, Schneider AB, Hawkins MM, et al. Thyroid cancer following childhood low-dose radiation exposure: a pooled analysis of nine cohorts. *J Clin Endocrinol Metab.* (2017) 102:2575–83. doi: 10.1210/jc.2016-3529
38. Zhang Y, Gordon GB. A strategy for cancer prevention: stimulation of the Nrf2-ARE signaling pathway. *Mol Cancer Ther.* (2004) 3:885–93.
39. Hayes JD, McMahon M, Chowdhry S, Dinkova-Kostova AT. Cancer chemoprevention mechanisms mediated through the Keap1-Nrf2 pathway. *Antioxid Redox Signal.* (2010) 13:1713–48. doi: 10.1089/ars.2010.3221
40. Menegon S, Columbano A, Giordano S. The dual roles of NRF2 in cancer. *Trends Mol Med.* (2016) 22:578–93. doi: 10.1016/j.molmed.2016.05.002
41. Lau A, Villeneuve NF, Sun Z, Wong PK, Zhang DD. Dual roles of Nrf2 in cancer. *Pharmacol Res.* (2008) 58:262–70. doi: 10.1016/j.phrs.2008.09.003
42. Ziros PG, Manolakou SD, Habeos IG, Lilis I, Chartoumpekis DV, Koika V, et al. Nrf2 is commonly activated in papillary thyroid carcinoma, and it controls antioxidant transcriptional responses and viability of cancer cells. *J Clin Endocrinol Metab.* (2013) 98:E1422–7. doi: 10.1210/jc.2013-1510
43. Danilovic DLS, de Mello ES, Frazzato EST, Wakamatsu A, de Lima Jorge AA, Hoff AO, et al. Oncogenic mutations in KEAP1 disturbing inhibitory Nrf2-Keap1 interaction: activation of antioxidative pathway in papillary thyroid carcinoma. *Head Neck.* (2018) 40:1271–8. doi: 10.1002/hed.25105
44. Martinez VD, Vucic EA, Pikor LA, Thu KL, Hubaux R, Lam WL. Frequent concerted genetic mechanisms disrupt multiple components of the NRF2 inhibitor KEAP1/CUL3/RBX1 E3-ubiquitin ligase complex in thyroid cancer. *Mol Cancer.* (2013) 12:124. doi: 10.1186/1476-4598-12-124
45. Muscarella LA, Parrella P, D'Alessandro V, la Torre A, Barbano R, Fontana A, et al. Frequent epigenetics inactivation of KEAP1 gene in non-small cell lung cancer. *Epigenetics.* (2011) 6:710–9. doi: 10.4161/epi.6.6.15773
46. Shibata T, Kokubu A, Gotoh M, Ojima H, Ohta T, Yamamoto M, et al. Genetic alteration of Keap1 confers constitutive Nrf2 activation and resistance to chemotherapy in gallbladder cancer. *Gastroenterology.* (2008) 135:1358–68, 1368.e1–4. doi: 10.1053/j.gastro.2008.06.082
47. Konstantinopoulos PA, Spentzos D, Fountzilas E, Francoeur N, Sanisetty S, Grammatikos AP, et al. Keap1 mutations and Nrf2 pathway activation in epithelial ovarian cancer. *Cancer Res.* (2011) 71:5081–9. doi: 10.1158/0008-5472.CAN-10-4668
48. Franco R, Schoneveld O, Georgakilas AG, Panayiotidis MI. Oxidative stress, DNA methylation and carcinogenesis. *Cancer Lett.* (2008) 266:6–11. doi: 10.1016/j.canlet.2008.02.026
49. Guo Y, Yu S, Zhang C, Kong AN. Epigenetic regulation of Keap1-Nrf2 signaling. *Free Radic Biol Med.* (2015) 88(Pt B):337–49. doi: 10.1016/j.freeradbiomed.2015.06.013
50. Hanada N, Takahata T, Zhou Q, Ye X, Sun R, Itoh J, et al. Methylation of the KEAP1 gene promoter region in human colorectal cancer. *BMC Cancer.* (2012) 12:66. doi: 10.1186/1471-2407-12-66
51. Zhang P, Singh A, Yegnasubramanian S, Esopi D, Kombairaju P, Bodas M, et al. Loss of kelch-like ECH-associated protein 1 function in prostate cancer cells causes chemoresistance and radioresistance and promotes tumor growth. *Mol Cancer Ther.* (2010) 9:336–46. doi: 10.1158/1535-7163.MCT-09-0589
52. Venugopal R, Jaiswal AK. Nrf2 and Nrf1 in association with Jun proteins regulate antioxidant response element-mediated expression and coordinated induction of genes encoding detoxifying enzymes. *Oncogene.* (1998) 17:3145–56. doi: 10.1038/sj.onc.1202237
53. Liu D, Duan X, Dong D, Bai C, Li X, Sun G, et al. Activation of the Nrf2 pathway by inorganic arsenic in human hepatocytes and the role of transcriptional repressor bach1. *Oxid Med Cell Longev.* (2013) 2013:984546. doi: 10.1155/2013/984546
54. Dhakshinamoorthy S, Jain AK, Bloom DA, Jaiswal AK. Bach1 competes with Nrf2 leading to negative regulation of the antioxidant response element (ARE)-mediated NAD(P)H:quinone oxidoreductase 1 gene expression and induction in response to antioxidants. *J Biol Chem.* (2005) 280:16891–900. doi: 10.1074/jbc.M500166200
55. Sun J, Hoshino H, Takaku K, Nakajima O, Muto A, Suzuki H, et al. Hemoprotein bach1 regulates enhancer availability of heme oxygenase-1 gene. *EMBO J.* (2002) 21:5216–24. doi: 10.1093/emboj/cdf516
56. Gopal RK, Kubler K, Calvo SE, Polak P, Livitz D, Rosebrock D, et al. Widespread chromosomal losses and mitochondrial DNA alterations as genetic drivers in hurthle cell carcinoma. *Cancer Cell.* (2018) 34:242–55 e5. doi: 10.1016/j.ccell.2018.06.013
57. Ganly I, Makarov V, Deraje S, Dong Y, Reznik E, Seshan V, et al. Integrated genomic analysis of hurthle cell cancer reveals oncogenic drivers, recurrent mitochondrial mutations, and unique chromosomal landscapes. *Cancer Cell.* (2018) 34:256–70 e5. doi: 10.1016/j.ccell.2018.07.002
58. Zhang TT, Qu N, Sun GH, Zhang L, Wang YJ, Mu XM, et al. NRG1 regulates redox homeostasis via NRF2 in papillary thyroid cancer. *Int J Oncol.* (2018) 53:685–93. doi: 10.3892/ijo.2018.4426
59. He H, Li W, Liyanarachchi S, Wang Y, Yu L, Genutis LK, et al. The role of NRG1 in the predisposition to papillary thyroid carcinoma. *J Clin Endocrinol Metab.* (2018) 103:1369–79. doi: 10.1210/jc.2017-01798
60. Haugen BR, Alexander EK, Bible KC, Doherty GM, Mandel SJ, Nikiforov YE, et al. 2015 american thyroid association management guidelines for adult patients with thyroid nodules and differentiated thyroid cancer: the american thyroid association guidelines task force on thyroid nodules and differentiated thyroid cancer. *Thyroid.* (2016) 26:1–133. doi: 10.1089/thy.2015.0020
61. Tuttle RM, Zhang L, Shaha A. A clinical framework to facilitate selection of patients with differentiated thyroid cancer for active surveillance or less aggressive initial surgical management. *Expert Rev Endocrinol Metab.* (2018) 13:77–85. doi: 10.1080/17446651.2018.1449641
62. Wang W, Jaiswal AK. Nuclear factor Nrf2 and antioxidant response element regulate NRH:quinone oxidoreductase 2 (NQO2) gene expression and antioxidant induction. *Free Radic Biol Med.* (2006) 40:1119–30. doi: 10.1016/j.freeradbiomed.2005.10.063
63. Lee J, Kim KS, Lee MH, Kim YS, Lee MH, Lee SE, et al. NAD(P)H: quinone oxidoreductase 1 and NRH:quinone oxidoreductase 2 polymorphisms in papillary thyroid microcarcinoma: correlation with phenotype. *Yonsei Med J.* (2013) 54:1158–67. doi: 10.3349/ymj.2013.54.5.1158
64. Fowke JH, Shu XO, Dai Q, Jin F, Cai Q, Gao YT, et al. Oral contraceptive use and breast cancer risk: modification by NAD(P)H:quinone oxoreductase (NQO1) genetic polymorphisms. *Cancer Epidemiol Biomarkers Prev.* (2004) 13:1308–15.
65. Menzel HJ, Sarmanova J, Soucek P, Berberich R, Grunewald K, Haun M, et al. Association of NQO1 polymorphism with spontaneous breast cancer in two independent populations. *Br J Cancer.* (2004) 90:1989–94. doi: 10.1038/sj.bjc.6601779

66. Sarmanova J, Susova S, Gut I, Mrhalova M, Kodet R, Adamek J, et al. Breast cancer: role of polymorphisms in biotransformation enzymes. *Eur J Hum Genet.* (2004) 12:848–54. doi: 10.1038/sj.ejhg.5201249
67. Fagerholm R, Hofstetter B, Tommiska J, Aaltonen K, Vrtel R, Syrjakoski K, et al. NAD(P)H:quinone oxidoreductase 1 NQO1*2 genotype (P187S) is a strong prognostic and predictive factor in breast cancer. *Nat Genet.* (2008) 40:844–53. doi: 10.1038/ng.155
68. Rothman N, Smith MT, Hayes RB, Traver RD, Hoener B, Campleman S, et al. Benzene poisoning, a risk factor for hematological malignancy, is associated with the NQO1 609C–>T mutation and rapid fractional excretion of chlorzoxazone. *Cancer Res.* (1997) 57:2839–42.
69. Feng XE, Liang TG, Gao J, Kong P, Ge R, Li QS. Heme oxygenase-1, a key enzyme for the cytoprotective actions of halophenols by upregulating Nrf2 expression via activating Erk1/2 and PI3K/Akt in EA.hy926 Cells. *Oxid Med Cell Longev.* (2017) 2017:7028478. doi: 10.1155/2017/7028478
70. Wang TY, Liu CL, Chen MJ, Lee JJ, Pun PC, Cheng SP. Expression of haem oxygenase-1 correlates with tumour aggressiveness and BRAF V600E expression in thyroid cancer. *Histopathology.* (2015) 66:447–56. doi: 10.1111/his.12562
71. Wang XJ, Sun Z, Villeneuve NF, Zhang S, Zhao F, Li Y, et al. Nrf2 enhances resistance of cancer cells to chemotherapeutic drugs, the dark side of Nrf2. *Carcinogenesis.* (2008) 29:1235–43. doi: 10.1093/carcin/bgn095
72. Putzer D, Gabriel M, Kroiss A, Madleitner R, Eisterer W, Kendler D, et al. First experience with proteasome inhibitor treatment of radioiodine nonavid thyroid cancer using bortezomib. *Clin Nucl Med.* (2012) 37:539–44. doi: 10.1097/RLU.0b013e31824c5f24
73. McConkey DJ, Zhu K. Mechanisms of proteasome inhibitor action and resistance in cancer. *Drug Resist Updat.* (2008) 11:164–79. doi: 10.1016/j.drup.2008.08.002
74. Kim R, Emi M, Tanabe K, Murakami S. Role of the unfolded protein response in cell death. *Apoptosis.* (2006) 11:5–13. doi: 10.1007/s10495-005-3088-0
75. Wang HQ, Du ZX, Zhang HY, Gao DX. Different induction of GRP78 and CHOP as a predictor of sensitivity to proteasome inhibitors in thyroid cancer cells. *Endocrinology.* (2007) 148:3258–70. doi: 10.1210/en.2006-1564
76. Gao YY, Liu BQ, Du ZX, Zhang HY, Niu XF, Wang HQ. Implication of oxygen-regulated protein 150 (ORP150) in apoptosis induced by proteasome inhibitors in human thyroid cancer cells. *J Clin Endocrinol Metab.* (2010) 95:E319–26. doi: 10.1210/jc.2010-1043
77. Zong ZH, Du ZX, Li N, Li C, Zhang Q, Liu BQ, et al. Implication of Nrf2 and ATF4 in differential induction of CHOP by proteasome inhibition in thyroid cancer cells. *Biochim Biophys Acta.* (2012) 1823:1395–404. doi: 10.1016/j.bbamcr.2012.06.001
78. Zong ZH, Du ZX, Zhang HY, Li C, An MX, Li S, et al. Involvement of Nrf2 in proteasome inhibition-mediated induction of ORP150 in thyroid cancer cells. *Oncotarget.* (2016) 7:3416–26. doi: 10.18632/oncotarget.6636
79. Ling YH, Liebes L, Zou Y, Perez-Soler R. Reactive oxygen species generation and mitochondrial dysfunction in the apoptotic response to bortezomib, a novel proteasome inhibitor, in human H460 non-small cell lung cancer cells. *J Biol Chem.* (2003) 278:33714–23. doi: 10.1074/jbc.M302559200
80. Du ZX, Zhang HY, Meng X, Guan Y, Wang HQ. Role of oxidative stress and intracellular glutathione in the sensitivity to apoptosis induced by proteasome inhibitor in thyroid cancer cells. *BMC Cancer.* (2009) 9:56. doi: 10.1186/1471-2407-9-56
81. Du ZX, Yan Y, Zhang HY, Liu BQ, Gao YY, Niu XF, et al. Proteasome inhibition induces a p38 MAPK pathway-dependent antiapoptotic program via Nrf2 in thyroid cancer cells. *J Clin Endocrinol Metab.* (2011) 96:E763–71. doi: 10.1210/jc.2010-2642
82. Cha HY, Lee BS, Chang JW, Park JK, Han JH, Kim YS, et al. Downregulation of Nrf2 by the combination of TRAIL and Valproic acid induces apoptotic cell death of TRAIL-resistant papillary thyroid cancer cells via suppression of Bcl-xL. *Cancer Lett.* (2016) 372:65–74. doi: 10.1016/j.canlet.2015.12.016
83. Merino D, Lalaoui N, Morizot A, Solary E, Micheau O. TRAIL in cancer therapy: present and future challenges. *Expert Opin Ther Targets.* (2007) 11:1299–314. doi: 10.1517/14728222.11.10.1299
84. Palsamy P, Bidasee KR, Shinohara T. Valproic acid suppresses Nrf2/Keap1 dependent antioxidant protection through induction of endoplasmic reticulum stress and keap1 promoter DNA demethylation in human lens epithelial cells. *Exp Eye Res.* (2014) 121:26–34. doi: 10.1016/j.exer.2014.01.021
85. Ottilie S, Diaz JL, Horne W, Chang J, Wang Y, Wilson G, et al. Dimerization properties of human BAD. identification of a BH-3 domain and analysis of its binding to mutant BCL-2 and BCL-XL proteins. *J Biol Chem.* (1997) 272:30866–72. doi: 10.1074/jbc.272.49.30866
86. Tian H, Zhang B, Di J, Jiang G, Chen F, Li H, et al. Keap1: one stone kills three birds Nrf2, IKKbeta and Bcl-2/Bcl-xL. *Cancer Lett.* (2012) 325:26–34. doi: 10.1016/j.canlet.2012.06.007
87. Palsamy P, Ayaki M, Elanchezhian R, Shinohara T. Promoter demethylation of Keap1 gene in human diabetic cataractous lenses. *Biochem Biophys Res Commun.* (2012) 423:542–8. doi: 10.1016/j.bbrc.2012.05.164
88. Gao Y, Yan Y, Huang T. Human agerelated cataracts: epigenetic suppression of the nuclear factor erythroid 2related factor 2mediated antioxidant system. *Mol Med Rep.* (2015) 11:1442–7. doi: 10.3892/mmr.2014.2849
89. Yang PS, Hsu YC, Lee JJ, Chen MJ, Huang SY, Cheng SP. Heme oxygenase-1 inhibitors induce cell cycle arrest and suppress tumor growth in thyroid cancer cells. *Int J Mol Sci.* (2018) 19:E2502. doi: 10.3390/ijms19092502

Conflict of Interest Statement: The authors declare that the research was conducted in the absence of any commercial or financial relationships that could be construed as a potential conflict of interest.

frontiers in Endocrinology

ORIGINAL RESEARCH
published: 07 August 2019
doi: 10.3389/fendo.2019.00552

Differentiated Thyroid Carcinoma in Pediatric Age: Genetic and Clinical Scenario

Francesca Galuppini[1,2†], Federica Vianello[3†], Simona Censi[4], Susi Barollo[4], Loris Bertazza[4], Sofia Carducci[4], Chiara Colato[5], Jacopo Manso[4], Massimo Rugge[1], Maurizio Iacobone[6], Sara Watutantrige Fernando[7], Gianmaria Pennelli[1] and Caterina Mian[4]*

[1] Pathology Unit, Department of Medicine (DIMED), Padova University Hospital, Padova, Italy, [2] Department of Women's and Children's Health, Padova University Hospital, Padova, Italy, [3] Department of Radiotherapy, Istituto Oncologico del Veneto, IOV-IRCCS, Padova, Italy, [4] Endocrinology Unit, Department of Medicine (DIMED), Padova University Hospital, Padova, Italy, [5] Pathology Section, Department of Pathology and Diagnostics, University of Verona, Verona, Italy, [6] Endocrine Surgery Unit, Department of Surgical, Oncological and Gastroenterological Sciences (DiSCOG), Padova University Hospital, Padova, Italy, [7] Familial Cancer Clinic, Istituto Oncologico Veneto IOV-IRCCS, Padova, Italy

OPEN ACCESS

Edited by:
Vasyl Vasko,
Uniformed Services University of the Health Sciences, United States

Reviewed by:
Rocco Bruno,
Independent Researcher, Matera, Italy
Athanasios Bikas,
MedStar Georgetown University Hospital, United States

***Correspondence:**
Caterina Mian
caterina.mian@unipd.it

[†] These authors have contributed equally to this work

Specialty section:
This article was submitted to Thyroid Endocrinology, a section of the journal Frontiers in Endocrinology

Received: 19 April 2019
Accepted: 25 July 2019
Published: 07 August 2019

Citation:
Galuppini F, Vianello F, Censi S, Barollo S, Bertazza L, Carducci S, Colato C, Manso J, Rugge M, Iacobone M, Watutantrige Fernando S, Pennelli G and Mian C (2019) Differentiated Thyroid Carcinoma in Pediatric Age: Genetic and Clinical Scenario. Front. Endocrinol. 10:552. doi: 10.3389/fendo.2019.00552

Introduction: Follicular-derived differentiated thyroid carcinoma (DTC) is the most common endocrine and epithelial malignancy in children. The differences in the clinical and pathological features of pediatric vs. adult DTC could relate to a different genetic profile. Few studies are currently available in this issue, however, and most of them involved a limited number of patients and focused mainly on radiation-exposed populations.

Materials and Methods: We considered 59 pediatric patients who underwent surgery for DTC between 2000 and 2017. *RET/PTC* rearrangement was investigated with fluorescent *in situ* hybridization and real-time polymerase chain reaction. Sequencing was used to analyze mutations in the *BRAF*, *NRAS*, *PTEN*, *PIK3CA* genes, and the *TERT* promoter. The pediatric patients' clinical and molecular features were compared with those of 178 adult patients.

Results: In our pediatric sample, male gender and age <15 years coincided with more extensive disease and more frequent lymph node and distant metastases. Compared with adults, the pediatric patients were more likely to have lymph node and distant metastasis, and to need second treatments ($p < 0.01$). In all, 44% of the pediatric patients were found to carry molecular alterations. *RET/PTC* rearrangement was confirmed as the most frequent genetic alteration in childhood DTC (24.6%) and correlated with aggressive features. *BRAFV600E* was only identified in 16% of the pediatric DTCs, while NRASQ61R, NRASQ61K, and TERTC250T mutations were very rare.

Conclusions: Pediatric DTC is more aggressive at diagnosis and more likely to recur than its adult counterpart. Unlike the adult disease, point mutations have no key genetic role.

Keywords: childhood, thyroid cancer, BRAF, TERT, RAS

INTRODUCTION

Thyroid carcinoma is the most common malignant neoplasm of the endocrine system. Papillary (PTC) and follicular (FTC) carcinomas are the most frequently seen histological types (accounting for more than 90% of cases) and belong to the family of differentiated carcinomas (DTC) originating from follicular thyroid cells (1).

Though less frequent than the adult type, DTC can also develop in pediatric age. There are significant clinical, pathological, and molecular differences between pediatric and adult patients, however. DTC in the pediatric population must consequently be characterized as a distinct entity with a separate diagnostic pathway and different treatment (2).

At the time of diagnosis, children are more likely than adults to present with advanced disease (3, 4). The incidence of distant metastases is estimated to be 25% in children, with lymph node involvement ranging from 40 to 80% in various studies (3, 5, 6). Positive lymph nodes and distant metastases from thyroid cancers are amenable to surgical resection and radioactive iodine (RAI) therapy, and these interventions have produced favorable outcomes in the pediatric patient population (5).

Our study aimed to characterize pediatric DTC in a large monocentric series of patients, most of them not exposed to radiation, focusing on: (i) clinical features and outcomes; (ii) molecular profile, with particular reference to the study of point mutations of the *BRAF, RAS, TERT* genes, and *RET/PTC* translocations; (iii) correlations between clinical and molecular findings; and (iv) comparisons between the clinical and molecular profile of pediatric DTC and that of a large series of adult thyroid carcinoma cases coming from our center.

MATERIALS AND METHODS

Patients

Patients under 18 years of age with a histological diagnosis of DTC were retrospectively reviewed for this study, enrolling a series of 59 pediatric patients who underwent thyroid surgery between 2000 and 2017. Thirty of the Fifty-Nine patients (51%) also underwent neck dissection to remove the central/lateral lymph nodes.

All study samples were retrospectively selected from the electronic archives of the Surgical Pathology and Cytopathology Unit at Padua University. Clinical and histopathological data were obtained from electronic databases.

All patients underwent total thyroidectomy. Only information concerning their clinical presentation, pathological staging and histology was available for 8 patients; for the other 51, we had information concerning their clinical presentation, pathological staging and histology, local and systemic therapy, recurrences, subsequent treatments, and outcome. The follow-up was a mean 7 years (minimum 1, maximum 16), median 5.9 years.

After surgery, RAI ablation therapy was administered to 48/51 patients (94%), with a median dose of 100 mCi (range 30–200 mCi). Judging from their medical history, only 2 patients been exposed to radiation during childhood for the treatment of a previous tumor: one patient underwent fractioned total body irradiation (TBI) followed by allogenic bone marrow transplantation for acute lymphoblastic leukemia 11 years before the DTC development; the other patient underwent fractioned TBI plus chemotherapy followed by allogenic bone marrow transplantation for severe aplastic anemia 4 years before the DTC development.

The pediatric patients' clinical and molecular characteristics were compared with those of 178 consecutive adult patients who underwent surgery for PTC between 2007 and 2010, and were followed up at the Radiotherapy Unit and Endocrinology Unit in Padua. The TNM 7th edition (7) was applied to all patients to ensure a correct comparison of their pathological and clinical characteristics.

All studies were performed in accordance with the guidelines proposed in the Declaration of Helsinki: the local ethical committee (Ethical Committee for the Clinical Experimentation of the Hospital of Padua) approved our study protocol (Ref. 3388) and all patients (including the parent/guardian on behalf of the minor) gave their written informed consent.

Outcomes

Patients were classified as being in remission if, at the time of their latest follow-up, their suppressed thyroglobulin (Tg) was <1 ug/L, Tg antibodies were negative, neck US was free of suspicious signs, and there were no pathological findings on any other imaging studies performed for clinically indicated reasons [whole body scan (WBS), radiography, computed tomography, 18-fluorodeoxyglucose (18FDG) positron emission tomography, or any other modality] or in any biopsy specimen. Patients with persistent disease at the time of their latest follow-up were classified as having either biochemically or structurally persistent disease, i.e., those with suppressed and/or stimulated Tg levels >1 ug/L but no structural evidence of disease were classified as having biochemically persistent disease, while those with structural evidence of disease (with or without abnormal Tg levels) were classified as having structurally persistent disease. Clinical status at final follow-up reflected not only the initial response to total thyroidectomy and RAI ablation therapy, but also the potential effects of continued levothyroxine suppressant therapy, any additional surgery or radiation therapy, and the passage of time.

Molecular Analysis

BRAF, NRAS, PTEN, PIK3CA, and TERT Analysis

For all patients, DNA was extracted from formalin-fixed, paraffin-embedded (FFPE) tissues. The samples were deparaffinized as follows: 30 min in xylene; 15 min in 99% alcohol, 15 min in 95% alcohol; 15 min in 70% alcohol; 15 min in 50% alcohol; several washes in distilled water. DNA was extracted from the sample using the "DNeasy Blood and Tissue Handbook" extraction kit (Qiagen, Milano, Italy), according to the manufacturer's protocol. The *BRAF* gene (exon 5), *NRAS* (exon 3), *PTEN* (exons 5 and 8), *PIK3CA* (exons 9 and 20), and the *TERT* promoter were amplified using the polymerase chain reaction (PCR) technique. Mutation analyses were performed using direct sequencing ABI PRISM (Applied Biosystems, Foster City, California), as described elsewhere (8).

RET/PTC Rearrangement Analysis

RET/PTC translocations were investigated with both fluorescence *in situ* hybridization (FISH) and real-time polymerase chain reaction (RT-PCR).

To identify *RET/PTC* rearrangements (either 10q11.2 inversions or translocations), FISH was performed using the REPEAT-FREE POSEIDON RET (10q11) break-apart probe (Kreatech Diagnostics, Amsterdam, Netherlands) on FFPE samples. The FISH procedure was completed according to the Kreatech protocol with some modifications, as previously described (9). Slides were examined using an Olympus BIX-61 microscope (Olympus, Hamburg, Germany) with appropriate fluorescence excitation/emission filters. Signals were recorded by a CCD camera (Olympus Digital Camera). For microscopic examination, at least 100 intact and non-overlapping cell nuclei were scored for the presence of a split signal. Only cells with two overlapping signals, or one split and one overlapping signal, were counted to ensure that only complete cell nuclei had been scored. The signal pattern was interpreted as follows: interphase nuclei with two co-localized green/red fusion signals identified normal chromosomes 10, while separate red and green signals and green/red fusion signals indicated rearranged *RET*. To establish the cut-off for RET/PTC rearrangements, we performed a FISH analysis on ten samples of normal thyroid parenchyma and 100 nuclei were scored for the presence of a split signal. As previously reported, the cut-off was calculated as the mean +3 SD of *RET* rearranged cells (10).

For the RT-PCR analysis, tissue cores were deparaffinized with xylene at 50°C for 3 min. Total RNA extraction was done using the RecoverAll kit (Ambion, Austin, Texas, USA) according to the manufacturer's instructions. The nucleic acid extracted was analyzed with RT-PCR in an ABI-PRISM 7900HT Sequence Detector (Applied Biosystems, Milan, Italy) with the EntroGen Thyroid Cancer Mutation Analysis Panel Kit (EntroGen, Inc., Woodland Hills, California), which detects *RET/PTC1* (fusion between RET and CCDC6 genes), and *RET/PTC3* (fusion between RET and NCOA4 genes). Fusion detection reactions were performed with a 1-step procedure that combines complementary DNA synthesis and RT-PCR. The resulting RT-PCR amplification curves were visualized using Sequence Detection Software rel. 2.4 (Applied Biosystems).

Statistical Analysis

The personal, clinical, and histopathological data were summarized using rates and percentages. All statistical analyses were performed using the MedCalc software (rel. 11.6.0). The distributions of the continuous variables were examined and the data were consequently summarized. The Mann-Whitney test and the *t*-test for independent samples were used to assess the differences in continuous variables (age at diagnosis, tumor size, and follow-up) between the two groups (pediatric vs. adult patients). The χ^2-test was used to compare the variables within subgroups of the same series. Multivariate analysis was performed, using logistic regression, to confirm the independent role of different histopathological variables associated with final outcome. Differences were considered statistically significant when p was < 0.05.

RESULTS

Clinical Features of Pediatric DTC Cases

The main clinical features of each pediatric patient are shown in **Table 1**.

Average age at diagnosis was 14.4 ± 2.9 years (range 6.4–17.8 years): 29/59 patients (49%) were <15 years old (defined as "children"), and 30/59 (51%) were ≥15 (defined as "adolescents"). There were 16/59 males (27%), and 43/59 females (73%), with a male/female ratio of 1:2.7.

At histological analysis, 42/59 (71.2%) cases were the classic variant of PTC (cv-PTC), 7/59 (11.8%) were the follicular variant of PTC (fv-PTC), 4/59 (6.8%) were the sclerosing variant of PTC (sv-PTC), 1/59 (1.7%) was the tall cell variant of PTC (tcv-PTC), 3/59 (5.1%) were cases of follicular thyroid carcinoma (FTC), and 2/59 (3.4%) were poorly-differentiated thyroid carcinomas (PDTC).

Data on tumor size were available for 56/59 (95%) patients (no clear definition of tumor size was provided for 3 patients). The median size of the primary tumor was 20.0 mm (range 3–58 mm): 9/56 tumors (16.0%) were ≤10 mm (microcarcinomas), and 47/56 (84.0%) were >10 mm in size. As suggested by Nikita et al., the lesions' size was further classified as follows: 26/56 (46.4%) were <20 mm; 27/56 (48.2%) were 20–40 mm; and 3/56 (5.4%) were >40 mm (11).

Multifocality was detected in 25/59 patients (42.4%), extra-thyroid extension in 25/59 (42%), and vascular invasion in 48/59 (81.4%). There were lymph node metastases in the lateral compartment in 20/59 patients (33.9%). Distant metastases were identified on WBS in 10/48 patients who underwent RAI: the site involved was the lung in 9/10 and the mediastinum in 1/10.

No significant differences in tumor size emerged between the male and female patients (with a median tumor size of 24.6 mm and 20.1 mm, respectively; $p = 0.23$). The extent of the disease (T) was gender-related, however: 10/16 males (63%) had T3 or T4 disease, while the proportion among females was 22/43 (51%; $p < 0.01$). Gender was also significantly associated with the presence of distant metastases, and therefore with the most advanced stage: 6/16 (38%) males had metastatic disease, as opposed to only 4/43 (9%) females ($p = 0.03$). No significant associations came to light between histotype, multifocality, lymph node involvement, need for second treatment, or final disease status.

Table 2 shows the main pathological and clinical characteristics correlated with the presence/absence of metastases for all 59 patients. The 8 patients for which we had no information about their treatment and follow-up were included because they started with a low-risk disease. They were considered as M0-x.

The presence of distant metastases was found significantly associated with younger age ($p = 0.01$), larger and more extensive tumors ($p < 0.01$), and cervical lymph node metastases ($p = 0.02$).

On multivariate analysis, only T4 status was identified as an independent predictor of distant metastases (OR 43.75, CI: 4.04 to 474.27).

TABLE 1 | Clinic pathological features.

Patient	Age at the diagnosis (years)	Gender	Tumor size (Mm)	Histological variant	T	N	M	Second treatment	Disease status
1	17	F	8	cv-PTC	1a	X	X	0	BD
2	17	M	30	fv-PTC	2	0	0	0	Excellent
3	17	F	25	cv-PTC	2	1b	0	Surgery/RAI	Excellent
4	17	F	25	cv-PTC	3	0	0	n.a.	n.a.
5	17	M	10	cv-PTC	1a	1a	0	n.a.	n.a.
6	9	F	6	sv-PTC	1a	1a	0	0	Excellent
7	11	F	21	cv-PTC	3	1b	0	0	Excellent
8	17	F	22	cv-PTC	2	1a	0	Surgery	Excellent
9	18	F	13	cv-PTC	1b	X	0	n.a.	n.a.
10	18	F	12	cv-PTC	1b	1a	0	0	Excellent
11	16	F	24	cv-PTC	3	1b	0	RAI	BD
12	15	F	15	cv-PTC	3	1b	1	RAI	Excellent
13	17	F	25	cv-PTC	3	1b	0	0	Excellent
14	13	M	n.a.	PDTC	4a	1b	1	RAI/Surgery	BD
15	13	F	50	PDTC	3	1b	1	RAI	SD
16	8	M	20	cv-PTC	3	1b	1	RAI	SD
17	8	F	20	cv-PTC	3	0	0	n.a.	n.a.
18	16	F	12	cv-PTC	1b	1b	0	0	Excellent
19	17	F	3	cv-PTC	1a	X	0	n.a.	n.a.
20	14	M	12	cv-PTC	1b	1b	0	0	Excellent
21	15	M	35	FTC	2	X	1	0	Excellent
22	12	F	36	cv-PTC	3	1b	1	Surgery/RAI	SD
23	17	F	18	cv-PTC	3	1a	0	0	Excellent
24	17	F	13	cv-PTC	3	1b	0	0	Excellent
25	9	M	42	cv-PTC	4a	1	1	RAI	SD
26	14	F	40	cv-PTC	3	1a	0	Surgery	BD
27	13	F	11	cv-PTC	3	1a	0	Surgery	Excellent
28	14	F	20	cv-PTC	3	1b	0	RAI	SD (Neck)
29	9	F	35	cv-PTC	3	1b	0	0	Excellent
30	12	M	22	cv-PTC	4a	1a	1	Surgery/RAI	SD
31	14	F	3	cv-PTC	1a	1	0	0	Excellent
32	14	M	10	cv-PTC	3	0	0	Surgery/RAI	BD
33	17	F	11	cv-PTC	3	0	0	0	Excellent
34	17	F	35	fv-PTC	2	0	0	0	Excellent
35	11	F	20	cv-PTC	3	1a	0	0	Excellent
36	14	F	30	cv-PTC	3	1b	0	0	Excellent
37	15	F	12	cv-PTC	3	1a	0	Surgery	Indeterminate
38	17	F	25	fv-PTC	2	0	0	0	Excellent
39	15	F	15	cv_PTC	1b	0	0	0	Excellent
40	15	F	12	fv-PTC	1b	0	0	0	n.a.
41	17	M	20	FTC	4	1	1	RAI	Excellent
42	6	F	15	fv-PTC	1b	0	0	n.a.	n.a.
43	13	M	n.a.	sv-PTC	3	1b	0	0	Excellent
44	18	F	22	cv-PTC	3	1b	0	0	Excellent
45	16	M	38	cv-PTC	2	0	0	0	Excellent
46	17	F	7	fv-PTC	1a	0	0	n.a.	n.a.
47	13	F	25	fv-PTC	3	1a	0	0	Excellent
48	16	F	7	cv-PTC	1a	0	0	0	BD
49	16	F	15	cv-PTC	1b	0	0	0	Excellent
50	17	F	8	cv-PTC	1a	1a	0	Surgery	BD

(Continued)

TABLE 1 | Continued

Patient	Age at the diagnosis (years)	Gender	Tumor size (Mm)	Histological variant	T	N	M	Second treatment	Disease status
51	12	M	40	cv-PTC	4a	1b	0	0	BD
52	16	F	11	cv-PTC	1b	1a	0	0	Excellent
53	15	M	12	cv-PTC	1b	1a	0	0	Excellent
54	15	F	58	cv-PTC	3	1b	0	0	Excellent
55	17	M	35	cv-PTC	3	1b	0	0	SD (Neck)
56	11	F	n.a.	sv-PTC	4a	1b	1	RAI	SD
57	10	F	35	sv-PTC	3	1a	X	0	Excellent
58	17	M	19	tcv-PTC	1b	1a	0	0	Excellent
59	15	F	25	FTC	2	0	0	0	Excellent

M, male; F, female; n.a., not assessable/not available; cv-PTC, classical variant of papillary thyroid carcinoma; fv-PTC, follicular variant of PTC; sv-PTC, sclerosing diffuse variant of PTC; tcv-PTC, tall cell variant of PTC; FTC, follicular thyroid carcinoma; PDTC, poorly differentiated carcinoma; RAI, Radioactive Iodine; BD, biochemical disease; SD, structural disease.

TABLE 2 | Correlation with clinic-pathological features and presence of distant metastasis at the diagnosis.

	Total (59)	M1 (10)	M0-x (49)	*p*-value
Gender				**0.03**
M	16/59 (27%)	6/16 (37.5%)	10/16 (62.5%)	
F	43/59 (73%)	4/43 (9.3%)	39/43 (90.7%)	
Age (average)	14.40	12.50 ± 2.75	14.89 ± 2.44	**0.01**
Tumor size (median; mm)	20.0	30	21	0.08
T				**0.0007**
1	19/59 (21.7%)	0/19 (0%)	19/19 (100%)	
2	8/59 (13.6%)	1/8 (12.5%)	7/8 (87.5%)	
3	26/59 (44.1%)	4/26 (15.4%)	22/26 (84.6%)	
4	6/59 (10.2%)	5/6 (83.3%)	1/6 (16.7%)	
Extrathyroidal extension				0.10
Yes	25/59 (42.3%)	8/25 (32.0%)	17/25 (68%)	
No	34/59 (57.7%)	2/34 (5.9%)	32/34 (94.1%)	
Multifocality				0.13
Yes	25/59 (42.3%)	7/25 (28%)	18/25 (72%)	
No	34/59 (57.7%)	3/34 (8.8%)	31/34 (91.1%)	
Vascular invasion				0.28
Yes	48/59 (71.2%)	10/48 (20.8%)	38/48 (79.2%)	
No	11/59 (6.7%)	0/11 (0%)	11/11 (100%)	
Lymph nodal metastasis				**0.02**
N0 and N1a	30/59 (50.8%)	2/30 (6.7%)	28/30 (93.3%)	
N1b	20/59 (33.9%)	7/20 (35.0%)	13/20 (65%)	
Nx	9/59 (15.3%)	1/9 (11.1%)	8/9 (88.9%)	

F, female; M, male.
Bold values are the statistically significant associations.

During the follow-up, 18/51 (35.3%) patients received further treatments, including: second surgery in 5/18 (27.8%) patients; RAI in 8/18 (44.4%), and both in 5/18 (27.8%). Positive lymph nodes and distant metastases were associated with a higher likelihood of undergoing a second treatment ($p = 0.04$ and $p = 0.002$, respectively).

Among the 51 patients with follow-up data, the final state of the disease was remission in 34/51 (66.7%) cases, persistent disease in 16/51 (31.3%; 8 with biochemically evident disease, and 8 with structurally evident disease); and for one patient who recently had surgery for a recurrence in the lateral neck the final status was classified as undetermined (restaging is ongoing).

Of the 8 patients with a final status of structurally evident disease, 6 had distant metastases at: 5/6 had stable lung disease, and 1 had progression in the lung with lesions failing to uptake RAI or 18-FDG. The other 2 patients with structurally evident disease had a local progression and are currently being reassessed for further surgery.

Disease status at the end of the follow-up correlated with disease stage: 9/41 patients in stage I (22%) had

persistent/recurrent disease (biochemically evident in 7, and structurally evident in 2), while 7/10 (70%) patients in stage II had persistent/recurrent disease (biochemically evident in 1 and structurally evident in the lung in 6) ($p = 0.002$). There was also a significant association between disease status and the need for a second treatment: among patients who underwent a second treatment, 12/18 (66.7%) had persistent/recurrent disease (5 biochemically evident and 7 structurally evident); in the group of patients given no second treatments, 4/33 (12.1%) had persistent/recurrent disease (3 biochemically evident, 1 with a structurally evident neck progression being assessed for further surgery) ($p = 0.0001$). The final outcome also correlated significantly with tumor size, T stage, cervical lymph node and distant metastases ($p < 0.05$) (**Table 3**). Kaplan-Meier curves showed that patients with lymph node metastases in lateral neck compartments more frequently had persistent/recurrent disease ($p = 0.01$) (**Figure 1**).

One multivariate analysis, only the presence of distant metastases independently correlated with persistent disease (OR 13, 95% CI 2.19 to 77.03).

Molecular Characterization

In all, 26/59 patients (44%) of our series were carriers of molecular alterations.

Point Mutations

Mutually-exclusive point mutations were found in 13/50 (26%) tissue samples from which the genetic material could be amplified. No point mutations were documented in patients under 10 years old, while there was 1 among 13 (8%) 10- to 14-year-olds, and 12 among 13 (92%) 15- to 18-year-olds.

Among the samples that could be tested for the presence of *BRAF* mutations, the V600E mutation was found in 8/50 (16%) cases. All mutations belonged to samples of cv-PTC (7/8) and tcv-PTC (1/8). No other *BRAF* mutations were identified.

Among the samples that were examined for the presence of *NRAS* mutations, a total of 4/52 (8%) molecular events came to light. The Q61K mutation was found in 2 samples and the Q61R mutation in other 2. All mutations belonged to samples of fv-PTC. Among the samples tested for the presence of *TERT* promoter mutations, the C250T mutation was only found in one PTC sample (1/44).

Among the samples successfully amplified for PCR, no mutations were identified in exons 5 or 8 of PTEN, or in exons 9 or 20 of PIK3CA.

RET/PTC Rearrangements

Among the samples that could be tested for the presence of *RET/PTC* rearrangements, 14/57 (24.6%) cases were found to carry the translocation (**Figure 2**). RT-PCR data analysis confirmed the results obtained with the FISH method. Interestingly, 1 of these 14 patients had both the *RET/PTC* translocation and a *TERT* promoter mutation and was classified as a case of PDTC.

Correlation Between Clinical and Molecular Features

*BRAF*V600E was related to the need for a second treatment: 4/6 *BRAF*V600E-mutated patients (66.7%) underwent a second treatment, as opposed to only 8/35 (22.9%) in the group of patients without this mutation ($p = 0.04$). No information on any second treatment or follow-up were available for 2/8 *BRAF*V600E-mutated patients. Two of the 8 *BRAF*V600E-mutated patients (25%) were <15 years old, while 6/8 (75%) were ≥15–18 years old ($p = 0.11$) (**Table 4**). No significant association was found between *BRAF*V600E mutation status and sex, tumor size, histotype, multifocality, lymph node and distant metastasis, stage, or disease outcome.

NRAS mutations were associated with histology: 4/4 samples were fv-PTC. Significant associations were found between *NRAS*

TABLE 3 | Correlation with clinic-pathological features and outcome.

	Total (51)	Structural disease (8/51)	Biochemical disease (8/51)	Indeterminate (1/51)	Remission (34/51)	*P*-value
Tumor size (mm)	21.5	32.1	19.5	12	21.5	0.10
T						0.05
1	12 (23.5%)	0/12 (0%)	3/12 (25%)	0/12 (0%)	9/12 (75%)	
2	9 (17.6%)	0/9 (11.1%)	0/9 (0%)	0/9 (0%)	9/9 (100%)	
3	24 (47.1%)	5/24 (20.8%)	3/24 (12.5%)	1/24 (4.2%)	15/24 (62.5%)	
4	6 (11.8%)	3/6 (50%)	2/6 (33.3%)	0/6 (0%)	1/6 (16.7%)	
Lymph nodal metastasis						**0.01**
N0–N1a	30 (58.8%)	1/30 (3.3%)	4/30 (13.4%)	1/30 (3.3%)	24/30 (80%)	
N1b	19 (37.3%)	7/19 (36.8%)	3/18 (15.8%)	0/19 (0%)	9/19 (47.4%)	
Distant metastasis						**0.0008**
M1	10 (19.6%)	6/10 (60%)	1/10 (10%)	0/10 (0%)	3/10 (30%)	
TNM staging						
I	41 (80.4%)	2/41 (4.9%)	7/41 (17.1%)	1/41 (2.4%)	31/41 (75.6%)	**0.0003**
II	10 (19.6%)	6/10 (60%)	1/10 (10%)	0/10 (0%)	3/10 (30%)	
Second treatment	18 (35.3%)	7/18 (38.9)	5/18 (27.8%)	1/18 (5.6%)	5/18 (27.8%)	**0.0001**

Bold values are the statistically significant associations.

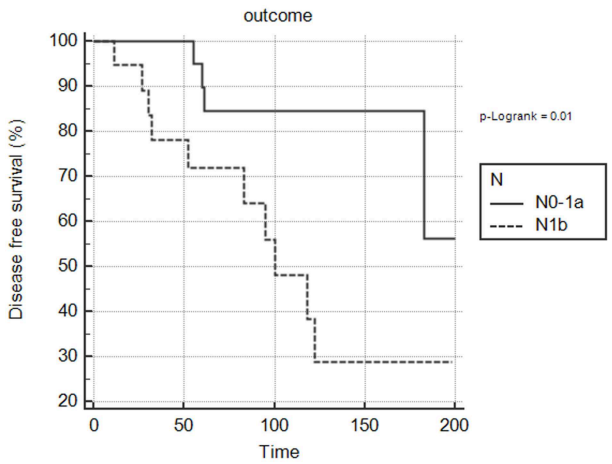

FIGURE 1 | Correlation between lateral cervical (N1b) lymph node metastases and disease status in pediatric population. The Kaplan-Meier curve shows N1b significantly associated with persistent/recurrent disease at the end of the follow-up ($p = 0.01$).

mutations and the absence of vascular invasion or lymph node metastases.

The only patient carrying the *TERT* promoter mutation (with a concomitant *RET/PTC* rearrangement, as mentioned above) had a locally advanced PDTC with cervical lymph node metastases (N1b) and distant metastases. At the end of the follow up (46 months) the patient had persistent disease.

As mentioned earlier, *RET/PTC* rearrangements were found in 14 patients: 5/14 were *RET/PTC* 3 (35.7%), and 9/14 (64.8%) were *RET/PTC* 1. The two patients with a history of exposure to radiation carried this translocation (1 with *RET/PTC* 1, the other with *RET/PTC* 3). As for histotype, 2 patients were cases of PDTC, 10 were cv-PTC, and 2 were sv-PTC. *RET/PTC* rearrangement was found significantly correlated with aggressive features such as lymph node metastases ($p = 0.01$), and *RET/PTC* 3, in particular, correlated with both cervical lymph node involvement (N1b) and distant metastases ($p = 0.02$ and $p = 0.03$, respectively). Moreover, 4/5 patients with *RET/PTC* 3 rearrangements needed a second treatment during their follow-up ($p = 0.03$). As for the 8 patients with a final status of structurally evident disease, 1 was a young female with lung progression whose lesions showed no uptake of RAI or 18-FDG, and she had the *RET/PTC 3* translocation.

The Clinical and Molecular Profile of Pediatric vs. Adult Thyroid Cancer

The main clinical, pathological and histopathological characteristics and outcomes of the samples of pediatric (children and adolescents) and adult patients are summarized in **Table 4**.

A more advanced disease at diagnosis was apparent in the younger patients: 22/29 patients <15 years old (75.8%) had T3 or T4 tumors, as opposed to 10/30 (33.3%) older pediatric patients ($p < 0.01$). Lymph node metastases were also more common in the former (24/28; 85.7%) than in the latter (14/27; 51.9%, $p = 0.007$). Of the 10 patients with distant metastases, 8 were <15 years old ($p = 0.01$). These two subgroups showed no significant differences in terms of primary tumor size, multifocality, histotype, need for second treatment, or disease status at the end of the follow-up, though only 56% of the younger group vs. 81% of the older one reached disease remission at the end of the follow-up.

In the adult population, 138/178 (77.5%) patients were female and 40/178 (22.5%) were male, with a male: female ratio of 1:3.5. The sex distribution was homogeneous between the pediatric and adult groups ($p = 0.46$). The average age of the adults was 48.6 ± 13.1 years (range 22–81 years).

The pediatric patients had larger lesions than the adults (median 23.6 vs. 19.3 mm); only 26/56 (46.4%) of the former, as opposed to 134/177 (75.7%) of the latter had a tumor <20 mm in diameter ($p = 0.0004$).

Lymph node metastases were found in 40/59 pediatric patients (67.8%) and 75/178 adults (42.1%) ($p < 0.001$). Distant metastases were more common in the pediatric patients too, involving 10/51 (19.6%) as opposed to 7/178 adults (3.9%) ($p < 0.001$). All distant metastases in both groups involved the lung, with the sole exception of a 17-year-old male with mediastinal disease.

The children and adolescents were significantly more likely to have a second treatment: 18/51 pediatric patients (35.3%) and 18/178 adults (10.1%) had further surgery or radiometabolic therapy ($p < 0.0001$). Age was found associated with final disease status: 34/51 pediatric patients (66.7%) and 157/176 adults (89.2%) were in remission ($p < 0.0001$). Among the adult patients, 4/176 (2.3%) died of their disease, while no pediatric patients died of cancer-related causes.

As regards the molecular profile, the rate of *BRAF*V600E mutations was significantly higher in adult PTC than in pediatric PTC, with 107/178 (60%) and 8/50 (16%), respectively ($p < 0.0001$). Although *NRAS* mutations emerged in 8% of the pediatric patients (4/52) as opposed to 2.2% (4/178) of the adults, this difference was not statistically significant.

DISCUSSION

DTC is rare in the pediatric population and its clinical, pathological and molecular characteristics differ from those of adult DTC (12). In children and adolescents, it has a more aggressive presentation at diagnosis, and a higher frequency of lymph node and distant metastases (13–18). There is also a greater risk of disease recurrence in the pediatric population. The prognosis is nonetheless excellent and the mortality rate is very low (2, 19).

Some Authors argue that the clinical and pathological differences between pediatric and adult DTC are due to a different genetic profile (20). The most common molecular event in children and adolescents (particularly after exposure to radiation) is represented by *RET/PTC* rearrangements, while point mutations in *BRAF*, *RAS* or *TERT* promoter genes are the main genetic drivers of tumorigenesis in adults (21). Somatic mutations (which are infrequent in pediatric age) are usually

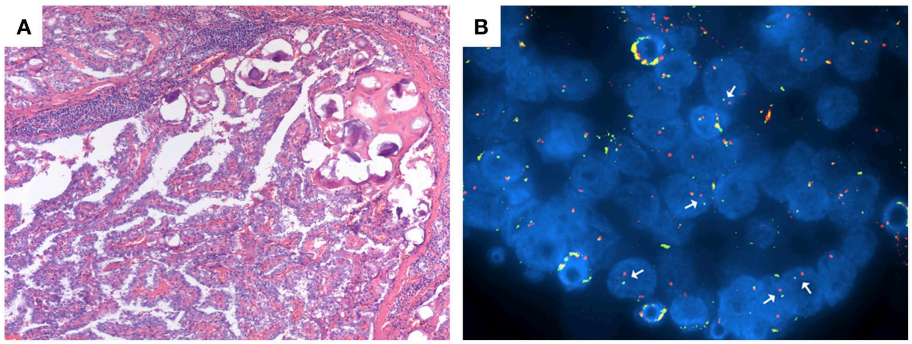

FIGURE 2 | (A,B) Patient n. 37: classical variant PTC at histological analysis with papillary structure and psammoma bodies (**A**; magnification 100x) and RET/PTC translocation at FISH analysis **(B)**.

TABLE 4 | Comparison of clinical and pathological features and outcomes between children and adolescents with DTC and between pediatric and adult patients.

	Children ($n = 29$)	Adolescents ($n = 30$)	p-Value	Pediatric patients ($n = 59$)	Adult patient ($n = 178$)	p- Value
Gender F/M	19/10 (1.9:1)	24/6 (4:1)	0.215	43/16 (2.7:1)	138/40 (3.5:1)	0.46
T			**0.009**			**0.01**
1	4/29 (13.8%)	14/30 (43%)		18/59 (30.4%)	68/177 (75.7%)	
2	3/29 (10.3%)	2/30 (20%)		9/59 (15.3%)	18/177 (10.2%)	
3	17/29 (58.6%)	9/30 (30%)		26/59 (44.1%)	88/177 (49.7%)	
4	5/29 (17.2%)	1/30 (3.3%)		6/59 (10.2%)	3/177 (1.7%)	
Lymph nodal metastasis	24/29 (82.6%)	16/30 (53.3%)	**0.03**	40/59 (67.8%)	75/178 (42.1%)	**0.0004**
Distant metastasis	9/29 (31%)	1/30 (3.3%)	**0.009**	10/59 (16.9%)	7/178 (3.9%)	**0.0003**
Second treatment	13/29 (44.8%)	5/25 (16.7%)	**0.03**	18/51 (35.3%)	18/178 (10.1%)	**<0.0001**
Disease Status			**0.02**			**<0.0001**
Remission	15/27 (55.6%)	19/24 (79.2%)		34/51 (66.7%)	157/176 (89.2%)	
Biochemical disease	4/27 (14.8%)	4/24 (16.7%)		16/51 (31.4%)*	14/176 (8%)*	
Structural disease	7/27 (25.9%)	1/24 (4.2%)				
Indeterminate	1/27 (3.7%)	0/24 (0%)		1/51 (8%)	1/176 (0.6%)	
Death	0/27 (0%)	0/24 (0%)		0/51 (1.9%)	4/176 (2.3%)	

F, female; M, male.

**In the comparison of final outcome between pediatric and adult population, biochemical and structural disease are considered together as persistence/recurrent disease.*

Bold values are the statistically significant associations.

associated with cellular dedifferentiation, genetic instability, and a reduced NIS iodine transporter expression. The paradox of pediatric DTC—with its worse presentation at diagnosis, but good outcome—could therefore be explained by a greater differentiation of the tumor cells and a consequently better response to radiometabolic treatments and TSH suppression therapy (22, 23) and also by a lower frequency of *BRAF* mutations (24) Regarding the potential effects of continued levothyroxine suppression, TSH contributes to the regulation of thyrocyte differentiation by modulating thyroid gene levels (25).

The clinical and histological features seen in our pediatric population are similar to those already described in other studies. The majority of our patients were female, with males and younger patients presenting with more advanced disease. Male gender coincides with more aggressive tumor features in terms of the extent of the primary tumor at diagnosis, dissemination outside the thyroid and to distant sites. On the other hand, males did not have significantly larger tumors, nor did they differ from females in terms of final outcome (26–28). Younger patients had a more aggressive tumor at diagnosis in terms of extent, lymph node involvement and distant metastases than older pediatric patients although, here again, age did not affect final outcome in our sample. In addition, the prevalence of DTC was higher among females in both subgroups, but the female/male ratio was higher for the older than for the younger pediatric patients, although the difference was not statistically significant (4:1 vs. 1.9:1). This trend is in line with findings in adult DTC, and could be influenced by hormonal aspects, and the impact of estrogens in particular. These data seem to suggest that DTC in childhood is locally more aggressive and should be considered as a distinct clinical entity from DTC in adolescence.

In the literature, the frequency of lymph node metastases in the pediatric population varies between 50 and 75%, while for distant metastases it ranges between 6 and 33% (5, 17, 19, 29, 30).

Our findings confirm this aggressiveness at diagnosis, with a prevalence of 67.7% for lymph node positivity and 19.6% for distant metastases. In our series, DTC dissemination outside the thyroid gland emerged as the main factor associated with the risk of distant metastases.

As expected, lymph node and distant metastases were significantly associated with a higher chance of undergoing further treatment during the follow-up.

The optimal management of neck disease depends on several factors, including the size and site of disease, previous treatments, disease progression rate, and the patient's age. Some patients in our sample known to have persistent disease were treated months or even years afterwards: 9 underwent second surgery, with or without further RAI, and all except one of them achieved at least a structurally evident remission.

Distant metastases in pediatric cases usually involve micronodular lung lesions with an excellent RAI uptake, characteristics that can explain why distant metastases in children are more amenable and responsive to RAI therapy than those in adults. There were 10 young patients with lung metastases in our sample and, after one or more RAI treatments, 3 obtained a complete remission, 1 had only biochemically evident disease, and 6 had persistent lung metastases, with only one patient in progression. Our multivariate analysis indicated that only the presence of distant metastases independently correlated with persistent disease (OR 13.95 % CI 2.19 to 77.03).

As emphasized by recent ATA guidelines (2), our data highlight the importance of a tailored assessment of children and adolescents with DTC. The aim should be to identify already at the initial diagnosis which pediatric patients would benefit from more aggressive surgical and radiometabolic approaches, and a closer follow-up. Clinical status at final follow-up reflects not only initial response to total thyroidectomy and RAI ablation, but also the potential effects of continued levothyroxine suppression and/or further surgery or RAI therapy over time.

Comparing our cohort of pediatric patients with an adult PTC population treated and followed up at the same center confirmed the greater aggressiveness at diagnosis of pediatric DTC. Tumor size was significantly larger in patients <18 years old, and there was a greater frequency of lymph node metastases (67.7 vs. 47.5%) and distant metastases (19.6 vs. 3.9%) than in adults. In terms of survival, however, the prognosis for pediatric DTC is excellent, and better than for the adult counterpart.

As for the molecular aspects, pediatric patients and adults clearly showed a different genetic profile. Even though almost all of the patients in our series had no history of exposure to radiation, *RET/PTC* rearrangements were confirmed as the most common genetic alteration in pediatric DTC (24.6%). *RET/PTC* rearrangements, and *RET/PTC* 3 in particular, were found to correlate with aggressive clinical and pathological features such as lymph node and distant metastases. Patients with the *RET/PTC* 3 translocation needed more second treatments ($p = 0.03$), suggesting [as reported in the literature (31)] that this molecular event results in a lower response to RAI and a consequent need for further treatments to achieve disease remission. In fact, the only patient with progressive lung disease in our series who became radio-refractory carries this translocation.

The *BRAFV600E* mutation is the most common in adult PTC (32–35), while in pediatric patients its prevalence varies between 0 and 37% (20). Our study is in line with previous reports: this mutation was found in 16% of our pediatric patients and 60.1% of our adult sample. Although the association was not statistically significant, we found that the frequency of *BRAF* mutations increased with age at diagnosis, even in the pediatric population, as seen in previous studies: it was 0% in patients under 10 years old, 14% among those between 11 and 14 years old, and 86% among the 15- to 18-yea-olds (21, 36). Several studies identified an association in adult DTC between *BRAF* mutations and more aggressive clinical, pathological and histopathological features, more recurrences and a higher mortality. This relationship has not been seen in pediatric populations (35, 36).

Our study also found no significant associations between *BRAF* mutations and gender, tumor size, histotype, multifocality, lymph node metastases, stage of disease or final outcome. The presence of a *BRAFV600E* mutation nonetheless correlated significantly with the need for a second treatment during the follow-up: among the *BRAFV600E*-positive patients, 4/6 (67%) received further treatment, as opposed to 11/42 (26%) in the group of patients without this mutation ($p = 0.04$). This finding prompts us to speculate that, as seen in adults, *BRAF* mutations may be associated with more aggressive clinical features and a higher risk of recurrence or persistence of disease in the pediatric population too.

Mutations in the *RAS* gene are rare in pediatric patients with DTC, the prevalence found in various studies to range between 0 and 7% (20). The rarity of this molecular event was confirmed in our study too: only 8% of pediatric patients had a *NRAS* mutation. In adults, *RAS* is more frequently mutated in cases of FTC (∼40%), and fv-PTC (∼15–20%) (37). The association between *RAS* gene alterations and the fv-PTC histology was confirmed in our pediatric series as well. In the adult control group, the frequency of *NRAS* gene mutations was 3%, i.e., lower than reported in the literature—a discrepancy probably due to the fact that only 6% of PTCs in our adult population were the follicular variant. In our pediatric population, some significant associations emerged between *NRAS* gene mutations and the clinical and pathological features of the DTC. *NRAS*-mutated DTC correlated with older age, no vascular invasion, and no lymph node or distant metastases. These data suggest that *NRAS* mutations do not have a key role in the pathogenesis of pediatric DTC, and might be a hallmark of a subset of less aggressive tumors, as seen in the albeit limited number of cases presenting this mutation in other studies (11, 18, 38).

TERT promoter, *PTEN*, and *PIK3CA* gene mutations are rare in adult DTC, while they have been found more frequently in poorly-differentiated carcinomas and anaplastic carcinoma (39–42). In pediatric age, though few studies have been conducted, the prevalence is even lower (1%) (38). This is consistent with the observation of a greater differentiation of tumor cells in pediatric DTC.

Interestingly, our one pediatric patient carrying a *TERT* mutation had advanced-stage disease at diagnosis, multifocality,

bilateral extra-thyroid extension, areas of poorly-differentiated carcinoma, and lymph node and distant metastases. He also had a concomitant *RET/PTC* translocation. The boy underwent second treatments involving both surgery and RAI, achieving a final disease status of biochemically persistent disease. This picture is consistent with previous reports in adult series: in thyroid carcinoma, *TERT* promoter mutations are associated with more aggressive histopathological features and a worse prognosis (40).

In conclusion, our study showed that DTC in pediatric age has different clinical, pathological and prognostic features from its counterpart in adults: it is more aggressive at diagnosis and carries a greater risk of persistence/recurrence. Within the pediatric group, special attention should be paid to male patients under 15 years old, as they are associated with a more advanced disease at diagnosis, although their final disease status does not seem to be affected by gender or age. As for the molecular profile, there are substantial differences between pediatric and adult DTC. *RET/PTC* translocations are the main molecular event in the pediatric population, while *BRAF*V600E mutations are significantly less common in pediatric DTC than in adults, and they are unassociated with the clinical and histopathological features of the disease. Finally, mutations in the *TERT* promoter and *NRAS*, *PTEN*, and *PIK3CA* genes are occasional molecular drivers of cancer in the pediatric population. Unlike the case in adults, point mutations do not have a key genetic role in children, even those not exposed to ionizing radiation.

DATA AVAILABILITY

The raw data supporting the conclusions of this manuscript will be made available by the authors, without undue reservation, to any qualified researcher.

ETHICS STATEMENT

This study was carried out in accordance with the recommendations of Padova Hospital Ethical Committee protocol No. 58403 with written informed consent from all subjects. All subjects gave written informed consent in accordance with the Declaration of Helsinki.

AUTHOR CONTRIBUTIONS

FG and FV: study concept and design, analysis and interpretation, drafting of the manuscript, and final approval of the version to be published. CM and GP: study concept and design, supervision, and final approval of the version to be published and agreement with all aspects of the work. SCe, SB, LB, SW, MR, MI, and SCa: substantial contributions to data acquisition and interpretation, critical revision of the manuscript, and final approval of the version to be published. JM: substantial contributions to data acquisition. CC: analysis and interpretation, critical revision of the manuscript, final approval of the version to be published, and agreement with all aspects of the work.

FUNDING

This research received a grant for a Ph.D. from Sanofi Genzyme Italy.

ACKNOWLEDGMENTS

This research was conducted using the resources of the Tissue Bank of the 1st Surgical Clinic, Padova University Hospital thanks to the technical support of Clara Benna. We thank Frances Coburn for text editing.

REFERENCES

1. Merino MJ. Thyroid cancer. In: Strayer DS, Rubin E, editors. *Rubin's Pathology*. 7th ed. Baltimore, MD; Philadelphia, PA: Wolters Kluwer (2015). p. 1192–6.
2. Francis GL, Waguespack SG, Bauer AJ, Angelos P, Benvenga S, Cerutti JM, et al. Management guidelines for children with thyroid nodules and differentiated thyroid cancer. *Thyroid.* (2015) 25:716–59. doi: 10.1089/thy.2014.0460
3. Dinauer CA, Breuer C, Rivkees SA. Differentiated thyroid cancer in children: diagnosis and management. *Curr Opin Oncol.* (2008) 20:59–65. doi: 10.1097/CCO.0b013e3282f30220
4. Halac I, Zimmerman D. Thyroid nodules and cancers in children. *Endocrinol Metab Clin North Am.* (2005) 34:725–44. doi: 10.1016/j.ecl.2005.04.007
5. Grigsby PW, Gal-or A, Michalski JM, Doherty GM. Childhood and adolescent thyroid carcinoma. *Cancer.* (2002) 95:724–9. doi: 10.1002/cncr.10725
6. Demidchik YE, Demidchik EP, Reiners C, Biko J, Mine M, Saenko VA, et al. Comprehensive clinical assessment of 740 cases of surgically treated thyroid cancer in children of Belarus. *Ann Surg.* (2006) 243:525–32. doi: 10.1097/01.sla.0000205977.74806.0b
7. UICC. Thyroid gland. In: Sobin LH, Gospodarowicz MK, Wittekind C, editors. *TNM Classification of Malignant Tumours.* 7th ed. Oxford: Wiley-Blackwell Publishers (2009). p. 58–62. doi: 10.1002/9780471420194.tnmc08.pub2
8. Pennelli G, Vianello F, Barollo S, Pezzani R, Merante Boschin I, Pelizzo MR, et al. BRAF(K601E) mutation in a patient with a follicular thyroid carcinoma. *Thyroid.* (2011) 21:1393. doi: 10.1089/thy.2011.0120
9. Colato C, Vicentini C, Cantara S, Pedron S, Brazzarola P, Marchetti I, et al. Break-apart interphase fluorescence *in situ* hybridization assay in papillary thyroid carcinoma: on the road to optimizing the cut-off level for RET/PTC rearrangements. *Eur J Endocrinol.* (2015) 172:571–82. doi: 10.1530/EJE-14-0930
10. Unger K, Zurnadzhy L, Walch A, Mall M, Bogdanova T, Braselmann H, et al. RET rearrangements in post-Chernobyl papillary thyroid carcinomas with a short latency analysed by interphase FISH. *Br J Cancer.* (2006) 94:1472–7. doi: 10.1038/sj.bjc.6603109
11. Nikita ME, Jiang W, Cheng SM, Hantash FM, McPhaul MJ, Newbury RO, et al. Mutational analysis in pediatric thyroid cancer and correlations with age, ethnicity, and clinical presentation. *Thyroid.* (2016) 26:227–34. doi: 10.1089/thy.2015.0401
12. Dermody S, Walls A, Harley EH Jr. Pediatric thyroid cancer: an update from the SEER database 2007-2012. *Int J Pediatr Otorhinolaryngol.* (2016) 89:121–6. doi: 10.1016/j.ijporl.2016.08.005
13. Chow SM, Law SC, Mendenhall WM, Au SK, Yau S, Mang O, et al. Differentiated thyroid carcinoma in childhood and adolescence - clinical course and role of radioiodine. *Pediatr Blood Cancer.* (2004) 42:176–83. doi: 10.1002/pbc.10410
14. Newman KD, Black T, Heller G, Azizkhan RG, Holcomb GW 3rd, Sklar C, et al. Differentiated thyroid cancer: determinants of disease progression in

patients <21 years of age at diagnosis: a report from the Surgical Discipline Committee of the Children's Cancer Group. *Ann Surg.* (1998) 227:533–41. doi: 10.1097/00000658-199804000-00014
15. Popovtzer A, Shpitzer T, Bahar G, Feinmesser R, Segal K. Thyroid cancer in children: management and outcome experience of a referral center. *Otolaryngol Head Neck Surg.* (2006) 135:581–4. doi: 10.1016/j.otohns.2006.04.004
16. Welch Dinauer CA, Tuttle RM, Robie DK, McClellan DR, Svec RL, Adair C, et al. Clinical features associated with metastasis and recurrence of differentiated thyroid cancer in children, adolescents and young adults. *Clin Endocrinol.* (1998) 45:619–28. doi: 10.1046/j.1365-2265.1998.00584.x
17. Agac Ay A, Kutun S, Cetin A. Are the characteristics of thyroid cancer different in young patients? *J Pediatr Endocrinol Metab.* (2014) 27:497–502. doi: 10.1515/jpem-2013-0192
18. Gertz RJ, Nikiforov Y, Rehrauer W, McDaniel L, Lloyd RV. Mutation in BRAF and other members of the MAPK pathway in papillary thyroid carcinoma in the pediatric population. *Arch Pathol Lab Med.* (2016) 140:134–9. doi: 10.5858/arpa.2014-0612-OA
19. Kiratli PO, Volkan-Salanci B, Gunay EC, Varan A, Akyuz C, Buyukpamukcu M. Thyroid cancer in pediatric age group: an institutional experience and review of the literature. *J Pediatr Hematol Oncol.* (2013) 35:93–7. doi: 10.1097/MPH.0b013e3182755d9e
20. Cordioli MI, Moraes L, Cury AN, Cerutti JM. Are we really at the dawn of understanding sporadic pediatric thyroid carcinoma? *Endocr Relat Cancer.* (2015) 22:R311–24. doi: 10.1530/ERC-15-0381
21. Cordioli MI, Moraes L, Bastos AU, Besson P, Alves MT, Delcelo R, et al. Fusion oncogenes are the main genetic events found in sporadic papillary thyroid carcinomas from children. *Thyroid.* (2017) 27:182–8. doi: 10.1089/thy.2016.0387
22. Faggiano A, Coulot J, Bellon N, Talbot M, Caillou B, Ricard M, et al. Age-dependent variation of follicular size and expression of iodine transporters in human thyroid tissue. *J Nucl Med.* (2004) 45:232–7.
23. Patel A, Jhiang S, Dogra S, Terrell R, Powers PA, Fenton C, et al. Differentiated thyroid carcinoma that express sodium-iodide symporter have a lower risk of recurrence for children and adolescents. *Pediatr Res.* (2002) 52:737–44. doi: 10.1203/00006450-200211000-00021
24. Durante C, Puxeddu E, Ferretti E, Morisi R, Moretti S, Bruno R, et al. BRAF mutations in papillary thyroid carcinomas inhibit genes involved in iodine metabolism. *J Clin Endocrinol Metab.* (2007) 92:2840–3. doi: 10.1210/jc.2006-2707
25. Bruno R, Ferretti E, Tosi E, Arturi F, Giannasio P, Mattei T, et al. Modulation of thyroid-specific gene expression in normal and nodular human thyroid tissues from adults: an *in vivo* effect of thyrotropin. *J Clin Endocrinol Metab.* (2005) 90:5692–7. doi: 10.1210/jc.2005-0800
26. Russo M, Malandrino P, Moleti M, Vermiglio F, D'Angelo A, La Rosa G, et al. Differentiated thyroid cancer in children: heterogeneity of predictive risk factors. *Pediatr Blood Cancer.* (2018) 65:e27226. doi: 10.1002/pbc.27226
27. Pires BP, Alves PA Jr, Bordallo MA, Bulzico DA, Lopes FP, Farias T, et al. Prognostic factors for early and long-term remission in pediatric differentiated thyroid carcinoma: the role of sex, age, clinical presentation, and the newly proposed American Thyroid Association Risk Stratification System. *Thyroid.* (2016) 26:1480–7. doi: 10.1089/thy.2016.0302
28. Balachandar S, La Quaglia M, Tuttle RM, Heller G, Ghossein RA, Sklar CA. Pediatric differentiated thyroid carcinoma of follicular cell origin: prognostic significance of histologic subtypes. *Thyroid.* (2016) 26:219–26. doi: 10.1089/thy.2015.0287
29. Wang JT, Huang R, Kuang AR. Comparison of presentation and clinical outcome between children and young adults with differentiated thyroid cancer. *Asian Pac J Cancer Prev.* (2014) 15:7271–5. doi: 10.7314/APJCP.2014.15.17.7271
30. Park S, Jeong JS, Ryu HR, Lee CR, Park JH, Kang SW, et al. Differentiated thyroid carcinoma of children and adolescents: 27-year experience in the Yonsei University Health System. *J Korean Med Sci.* (2013) 28:693–9. doi: 10.3346/jkms.2013.28.5.693
31. Prescott JD, Zeiger MA. The RET oncogene in papillary thyroid carcinoma. *Cancer.* (2015) 121:2137–46. doi: 10.1002/cncr.29044
32. Kimura ET, Nikiforova MN, Zhu Z, Knauf JA, Nikiforov YE, Fagin JA. High prevalence of BRAF mutations in thyroid cancer: genetic evidence for constitutive activation of the RET/PTC-RAS-BRAF signaling pathway in papillary thyroid carcinoma. *Cancer Res.* (2003) 63:1454–7.
33. Pelizzo MR, Dobrinja C, Casal Ide E, Zane M, Lora O, Toniato A, et al. The role of BRAF(V600E) mutation as poor prognostic factor for the outcome of patients with intrathyroid papillary thyroid carcinoma. *Biomed Pharmacother.* (2014) 68:413–7. doi: 10.1016/j.biopha.2014.03.008
34. Xing M. BRAF mutation in thyroid cancer. *Endocr Relat Cancer.* (2005) 12:245–62. doi: 10.1677/erc.1.0978
35. Frasca F, Nucera C, Pellegriti G, Gangemi P, Attard M, Stella M, et al. BRAF(V600E) mutation and the biology of papillary thyroid cancer. *Endocr Relat Cancer.* (2008) 15:191–205. doi: 10.1677/ERC-07-0212
36. Oishi N, Kondo T, Nakazawa T, Mochizuki K, Inoue T, Kasai K, et al. Frequent BRAF V600E and absence of TERT promoter mutations characterize sporadic pediatric papillary thyroid carcinomas in Japan. *Endocr Pathol.* (2017) 28:103–11. doi: 10.1007/s12022-017-9470-y
37. An JH, Song KH, Kim SK, Park KS, Yoo YB, Yang JH, et al. RAS mutations in indeterminate thyroid nodules are predictive of the follicular variant of papillary thyroid carcinoma. *Clin Endocrinol.* (2015) 82:760–6. doi: 10.1111/cen.12579
38. Alzahrani AS, Murugan AK, Qasem E, Alswailem M, Al-Hindi H, Shi Y. Single point mutations in pediatric differentiated thyroid cancer. *Thyroid.* (2017) 27:189–96. doi: 10.1089/thy.2016.0339
39. Xing M. Genetic alterations in the phosphatidylinositol-3 kinase/Akt pathway in thyroid cancer. *Thyroid.* (2010) 20:697–706. doi: 10.1089/thy.2010.1646
40. Penna GC, Vaisman F, Vaisman M, Sobrinho-Simoes M, Soares P. Molecular markers involved in tumorigenesis of thyroid carcinoma: focus on aggressive histotypes. *Cytogenet Genome Res.* (2016) 150:194–207. doi: 10.1159/000456576
41. Bamford S, Dawson E, Forbes S, Clements J, Pettett R, Dogan A, et al. The COSMIC (catalogue of somatic mutations in cancer) database and website. *Br J Cancer.* (2004) 91:355–8. doi: 10.1038/sj.bjc.6601894
42. Wu G, Mambo E, Guo Z, Hu S, Huang X, Gollin SM, et al. Uncommon mutation, but common amplifications, of the PIK3CA gene in thyroid tumors. *J Clin Endocrinol Metab.* (2005) 90:4688–93. doi: 10.1210/jc.2004-2281

Conflict of Interest Statement: The authors declare that the research was conducted in the absence of any commercial or financial relationships that could be construed as a potential conflict of interest.

frontiers in Endocrinology

ORIGINAL RESEARCH
published: 11 September 2019
doi: 10.3389/fendo.2019.00612

Analytical and Clinical Validation of Expressed Variants and Fusions From the Whole Transcriptome of Thyroid FNA Samples

Trevor E. Angell[1], Lori J. Wirth[2], Maria E. Cabanillas[3], Maisie L. Shindo[4], Edmund S. Cibas[5], Joshua E. Babiarz[6], Yangyang Hao[6], Su Yeon Kim[6], P. Sean Walsh[6], Jing Huang[6], Richard T. Kloos[7], Giulia C. Kennedy[8] and Steven G. Waguespack[3]*

[1] Division of Endocrinology, Diabetes and Metabolism, Keck School of Medicine, University of Southern California, Los Angeles, CA, United States, [2] Department of Medicine, Massachusetts General Hospital, Boston, MA, United States, [3] Department of Endocrine Neoplasia and Hormonal Disorders, The University of Texas MD Anderson Cancer Center, Houston, TX, United States, [4] Otolaryngology–Head & Neck Surgery, Oregon Health & Science University, Portland, OR, United States, [5] Department of Pathology, Brigham and Women's Hospital and Harvard Medical School, Boston, MA, United States, [6] Research and Development, Veracyte, South San Francisco, CA, United States, [7] Medical Affairs, Veracyte, South San Francisco, CA, United States, [8] Research and Development, Medical Affairs, and Clinical Affairs, Veracyte, South San Francisco, CA, United States

OPEN ACCESS

Edited by:
Vasyl Vasko, Uniformed Services University of the Health Sciences, United States

Reviewed by:
Joanna Klubo-Gwiezdzinska, National Institutes of Health (NIH), United States
Dorina Ylli, MedStar Health Research Institute (MHRI), United States

***Correspondence:**
Trevor E. Angell
trevor.angell@med.usc.edu

Specialty section:
This article was submitted to Thyroid Endocrinology, a section of the journal Frontiers in Endocrinology

Received: *01 May 2019*
Accepted: *22 August 2019*
Published: *11 September 2019*

Citation:
Angell TE, Wirth LJ, Cabanillas ME, Shindo ML, Cibas ES, Babiarz JE, Hao Y, Kim SY, Walsh PS, Huang J, Kloos RT, Kennedy GC and Waguespack SG (2019) Analytical and Clinical Validation of Expressed Variants and Fusions From the Whole Transcriptome of Thyroid FNA Samples. Front. Endocrinol. 10:612. doi: 10.3389/fendo.2019.00612

Introduction: The Afirma® Xpression Atlas (XA) detects gene variants and fusions in thyroid nodule FNA samples from a curated panel of 511 genes using whole-transcriptome RNA-sequencing. Its intended use is among cytologically indeterminate nodules that are Afirma GSC suspicious, Bethesda V/VI nodules, or known thyroid metastases. Here we report its analytical and clinical validation.

Methods: DNA and RNA were purified from the same sample across 943 blinded FNAs and compared by multiple methodologies, including whole-transcriptome RNA-seq, targeted RNA-seq, and targeted DNA-seq. An additional 695 blinded FNAs were used to define performance for fusions between whole-transcriptome RNA-seq and targeted RNA-seq. We quantified the reproducibility of the whole-transcriptome RNA-seq assay across laboratories and reagent lots. Finally, variants and fusions were compared to histopathology results.

Results: Of variants detected in DNA at 5 or 20% variant allele frequency, 74 and 88% were also detected by XA, respectively. XA variant detection was 89% when compared to an alternative RNA-based detection method. Low levels of expression of the DNA allele carrying the variant, compared with the wild-type allele, was found in some variants not detected by XA. 82% of gene fusions detected in a targeted RNA fusion assay were detected by XA. Conversely, nearly all variants or fusions detected by XA were confirmed by an alternative method. Analytical validation studies demonstrated high intra-plate reproducibility (89%-94%), inter-plate reproducibility (86–91%), and inter-lab accuracy (90%). Multiple variants and fusions previously described across the spectrum of thyroid cancers were identified by XA, including some with approved or investigational targeted therapies. Among 190 Bethesda III/IV nodules, the sensitivity of XA as a standalone test was 49%.

Conclusion: When the Afirma Genomic Sequencing Classifier (GSC) is used first among Bethesda III/IV nodules as a rule-out test, XA supplements genomic insight among those that are GSC suspicious. Our data clinically and analytically validate XA for use among GSC suspicious, or Bethesda V/VI nodules. Genomic information provided by XA may inform clinical decision-making with precision medicine insights across a broad range of FNA sample types encountered in the care of patients with thyroid nodules and thyroid cancer.

Keywords: molecular diagnostics, thyroid cancer, fine-needle aspiration, thyroid molecular assays, RNA-sequencing, transcriptome, atypia of undetermined significance, follicular neoplasm

INTRODUCTION

Genomic assessment for precision medicine is a story of incredible advancement. In the Nineteenth century, observations of dividing cancer cells suggested that they were abnormal clones caused by defects of hereditary material (1). The first isolation of a specific DNA variant responsible for cancer formation was in 1982, a G>T substitution in codon 12 of the *HRAS* gene (1). Since then there has been an explosion of cancer genome understanding, with the documentation of more than 350 cancer driving genes and 100,000 somatic mutations by the early Twenty-first century (1). Subsequently, a common theme that has emerged in oncology suggests that each cancer can be genomically subtyped and that the downstream gene expression profile predicts its cellular morphology, clinical presentation, prognosis, and that this presents an opportunity for the development of effective targeted therapies.

Investigation and understanding of benign and malignant thyroid nodules has followed a similar course as many insights have been gained from large genomic studies across a spectrum of histologic subtypes (2–14). Concomitantly, targeted therapies for advanced thyroid cancer have emerged, including FDA approved or investigational selective inhibitors of *AKT*[1], ALK (15, 16), *BRAF*[1] (16, 17), *cKIT*[1], *EGFR*[2], *HRAS*[3,4,5,6] (18), *KRAS*[2,4,5,6,7,8], *MET*[1], *mTOR* (16, 19), *NRAS*[1,4,5,6], *NTRK* (15, 16, 20), *PAX8/PPARG*[9], *PIK3CA* (PI3K) (21), *PTEN*[1], *RET* (16, 22, 23), *ROS1* (15, 16), and microsatellite instability-high or mismatch repair deficient solid tumors (24).

Currently, an important tool to avoid unnecessary diagnostic surgery among cytologically indeterminate thyroid nodules is the Afirma Genomic Sequencing Classifier (GSC) (25, 26). In this context, "cytologically indeterminate" refers to the two Bethesda categories Atypia of Undetermined Significance/ Follicular Lesion of Undetermined Significance ("Bethesda III") and Follicular Neoplasm/ Suspicious for a Follicular Neoplasm (Bethesda IV) (27) or their equivalents (28). The Afirma GSC is a cancer rule-out test that partners whole transcriptome RNA sequencing genomic information derived from a fine-needle aspiration (FNA) biopsy with machine learning to create algorithms that identify specific neoplasms, including MTC (see **Table 1** for histology subtype abbreviations), and ultimately classify the sample as GSC benign or suspicious. Nodules identified as GSC benign have a cancer risk of approximately 4% and can be considered for clinical observation *in lieu* of diagnostic surgery (29–31). Conversely, GSC suspicious nodules have an increased cancer risk of approximately 50%, which is roughly 2-fold higher than it was based on cytology alone. These nodules are typically considered for surgical resection (29–31). The GSC algorithms rely heavily on differential gene expression for sample classification. Several of the included modules make limited use of RNA-sequencing's ability to detect genomic variants and fusions in the transcribed RNA, including *BRAF* V600E variants, and *RET/PTC1* and *RET/PTC3* fusions, which are all highly predictive of malignancy. However, it was not until the introduction of the Afirma Xpression Atlas (XA) that variant and fusion identification by RNA-sequencing was more significantly harnessed. The use of whole transcriptome sequencing by both the Afirma GSC and Afirma XA allows the same sample collection and shipping method to be used for both tests, and both tests are run on the same FNA sample. Using one sample for both tests facilitates successful test results despite the small genomic sample obtained by FNA. XA findings may predict tissue cellular morphology, clinical syndromes, cancer behavior (including mode of metastasis), prognosis, and facilitate the selection of effective targeted therapy in the appropriate clinical setting.

Here we describe the analytical and clinical validation of XA to report nucleotide variants and gene fusions beyond *BRAF* V600E, *RET/PTC1,* and *RET/PTC3* fusions using whole transcriptome RNA-seq data derived from FNA samples. We compared the XA results to a targeted DNA panel for nucleotide variants and compared XA results to a targeted RNA fusion panel for gene/gene fusion detection. The data demonstrate a high level of agreement between methods and that these variant and fusion methods alone cannot serve as rule-out test to exclude cancer/noninvasive follicular thyroid neoplasm with papillary-like nuclear features (NIFTP). When used among Bethesda III/IV nodules that are GSC suspicious, Bethesda V/VI thyroid nodules, or by extension known thyroid cancer

[1]https://clinicaltrials.gov/ct2/show/NCT02465060
[2]https://clinicaltrials.gov/ct2/show/NCT03065387
[3]https://clinicaltrials.gov/ct2/show/NCT02383927
[4]https://clinicaltrials.gov/ct2/show/NCT03244956
[5]https://clinicaltrials.gov/ct2/show/NCT03181100
[6]https://clinicaltrials.gov/ct2/show/NCT00019331
[7]https://clinicaltrials.gov/ct2/show/NCT03600883
[8]https://clinicaltrials.gov/ct2/show/NCT03785249
[9]https://clinicaltrials.gov/ct2/show/NCT01655719

TABLE 1 | Histopathology subtypes.

Malignant subtypes	
FC	Follicular carcinoma. Variants include capsular invasion (FC-c) and vascular invasion (FC-v)
FVPTC	Follicular variant of papillary thyroid carcinoma. Variants include FVPTC micro carcinomas (mFVPTC)
HCC	Hürthle cell carcinoma. Variants include capsular invasion (HCC-c) and vascular invasion (HCC-v)
PTC	Papillary thyroid carcinoma. Variants include PTC micro carcinomas (mPTC), tall-cell variant (PTC-TCV), and tall-cell variant micro carcinomas (mPTC-TCV)
MTC	Medullary thyroid carcinoma
PDC	Poorly differentiated carcinoma
WDC-NOS	Well-differentiated carcinoma not otherwise specified
Benign subtypes	
BFN	Benign follicular nodule
CLT	Chronic lymphocytic thyroiditis (aka, Hashimoto's thyroiditis). Also known as LCT (lymphocytic thyroiditis)
FA	Follicular adenoma
HCA	Hürthle cell adenoma
HN	Hyperplastic nodule
HTA	Hyalinizing trabecular adenoma
FT-UMP	Follicular tumor with unknown malignant potential
WDT-UMP	Well-differentiated tumor with unknown malignant potential

metastases (data not shown), the genomic content provided by XA can provide additional information that may inform clinical decision-making.

MATERIALS AND METHODS

Nucleic Acid Extraction

RNA and DNA were extracted from thyroid FNAs or control tissues (described below under Cohorts and Controls, respectively) using the Qiagen AllPrep Micro Kit (Qiagen, Hilden, Germany) according to manufacturer's instructions. RNA was quantitated using Quantiflour (Promega, Madison, WI) and DNA was quantitated using PicoGreen (Promega, Madison, WI). Fluorescence was read on a Tecan Infinite M200 Pro (Tecan, Männedorf, Switzerland). RNA Integrity Number (RIN) was determined for RNA using RNA Pico Chips on the Bioanalyzer 2100 (Agilent, Santa Clara, CA).

Custom AmpliSeq Panels

The Ion AmpliSeq Designer (Thermo Fisher, Waltham, MA) was used to generate a custom DNA panel against 568 targets described in Pagan et al. (6). Nine Y chromosome SNPs were included to assign genomic gender, which was compared to clinical gender to ensure sample identity. A custom RNA AmpliSeq Variant Panel was designed against the same targets described for the DNA AmpliSeq panel. A custom AmpliSeq RNA Fusion Panel was also generated (Thermo Fisher, Waltham, MA), with 168 fusions plus 6 house-keeping genes for controls.

AmpliSeq Library Preparation

Ion Torrent Libraries were generated using the Ion AmpliSeq Library Kit 2.0 (Thermo Fisher, Waltham, MA) according to manufacturer's instructions using 10 ng input material. RNA was first reverse transcribed with SuperScript IV VILO (Thermo Fisher, Waltham, MA). Following cleanup, libraries were quantitated using qPCR on a QuantStudio 6 (Thermo Fisher, Waltham, MA), normalized to 100 pM, and loaded onto the IonChef (Thermo Fisher, Waltham, MA). Pooled libraries were loaded onto the Ion 540 Chip (Thermo Fisher, Waltham, MA) and sequenced on the Ion Torrent S5XL (Thermo Fisher, Waltham, MA).

Controls

Each DNA plate included the Horizon Quantitative Multiplex Reference Standard (HD701, Horizon, Cambridge, United Kingdom), NA12878 (Coriell, Camden, NJ), *BRAF* V600E positive thyroid tissue (Cooperative Human Tissue Network, National Cancer Institute, Bethesda, MD), and *TERT* C228T positive thyroid tissue (Asterand, Westbury, NY).

Targeted DNA/RNA Sequencing Data Analysis

The Ion Torrent Suite Software version 5.6.0 (Thermo Fisher, Waltham, MA) was used to demultiplex, map reads to the reference genome hg19, and call variants. Specifically, tmap version 5.6.8 was used for reads mapping, and Torrent Variant Caller version 5.6–10 was used to detect variants with parameter settings optimized for low frequency variant detection with minimal false negative calls on Ion AmpliSeq experiments.

Targeted RNA Sequencing for Fusion Data Analysis

The Ion Reporter version 5.6.0 was used to detect fusions. Key fusion detection parameters were set as follows: minimum 20,000 total valid mapped reads to qualify a sample for further analysis; minimum 20 reads required to call a fusion; medium sensitivity, which requires 70% overlap between reads and reference sequence with at-least 66.66% exact matches in the overlap.

qPCR Data

Taqman assays were obtained from Thermo Fisher or designed and synthesized by Integrated DNA Technologies (IDT, Coralville, IA). Ten nanogram of RNA was reverse transcribed with QuantiTect (Qiagen, Hilden, Germany). qPCR reactions were performed in duplicate using Fast Advanced Master Mix (Thermo Fisher, Waltham, MA), VIC-labeled primer-limited TBP (Hs00427620_m1, Thermo Fisher), and the FAM-labeled fusion-specific taqman assay (Thermo Fisher or IDT). qPCR assays were run on the QuantStudio 6 (Thermo Fisher, Waltham, MA) and Ct values were determined with the QuantStudio Real Time Software v1.3.

RNA-Seq Data

RNA-seq data was generated using the TruSeq RNA Exome kit (formerly RNA Access, Illumina, San Diego, CA) using 15 ng of total RNA as previously described (25). Libraries were sequenced on the NextSeq 500 platform (Illumina, San Diego, CA).

RNA-Seq Data Analysis

Fastq files were aligned to hg19 using STAR aligner, version 2.4.1b (32). Fusions were called using STAR-fusion version 0.5.4 (33). Variants were called using GATK version 3.3 (34), following the best practices for variant calling on RNA-seq (35, 36).

Fusion Nomenclature

All fusion partners are described in their 5′/3′ order. In the commercial Afirma XA report, all fusion partners are reported alphabetically except CCDC6/RET and NCOA4/RET, which are reported using their colloquial names of RET/PTC1 and RET/PTC3, respectively.

Cohorts

943 blinded FNA samples with sufficient DNA were utilized from the following sources: Afirma GSC Algorithm Training set (n = 32, 217, 75, 35, 36 from Bethesda categories II-VI, respectively) (25), the prospectively collected, and multicenter Afirma GSC clinical validation cohort (n = 152 Bethesda III/IV, n = 17 Bethesda II and n = 29 Bethesda V/VI) (25), samples with paired castPCR *BRAF* V600E truth Bethesda V (n = 52) and Bethesda VI (n = 51) (37), and Bethesda III/IV samples from Afirma GEC (n = 247).

An additional 695 blinded FNAs from the Veracyte CLIA laboratory with sufficient RNA were deidentified and examined for fusions, during which time the total rate of assay failure among all samples received was 3.85%. This blinded and consecutive cohort was chosen without bias to represent an XA intended use cohort (n = 634 Bethesda III/IV GSC suspicious and n = 61 Bethesda V/VI).

Statistics

To evaluate the agreement when comparing the whole transcriptome RNA-seq to targeted AmpliSeq panels, positive percent agreement (PPA), negative percent agreement (NPA) and confirmation were calculated following the FDA guideline[10]. Statistical analyses were performed using R statistical software version 3.2.3[11]. All confidence intervals are 2-sided 95% CIs and were computed using the exact binomial test. The chi-square test of independence was performed to examine if there is a relationship between two categorial variables.

RESULTS

A High Proportion of Variants Observed in DNA Are Expressed in RNA

To determine how many DNA variants could be detected in expressed RNA, RNA and DNA were first extracted from the same biological sample for direct comparison. Afirma GSC data was generated from the RNA, which utilizes whole-transcriptome RNA-seq data as an input to the machine learning algorithms. DNA was analyzed with a custom, targeted AmpliSeq panel that covers 761 variants that have been described in thyroid samples.

Nine hundred forty-three FNA samples were analyzed with the custom DNA AmpliSeq panel. Four hundred forty-two samples were used for parameter tuning to ensure accurate detection of variants, and after the analysis pipeline was locked, the remaining 501 samples were used to evaluate the performance of calling a variant from RNA-seq data relative to DNA-based detection. Using a DNA variant allele frequency (VAF) cutoff of 5%, 181 DNA variants were observed, and the same variants were observed in 134 RNA-seq samples (74%; **Table 2**). Using a 20% VAF threshold for a positive result in DNA, positive percent agreement (PPA) increases to 88%.

Low Levels of Variant Allele Expression May Account for Some Differences in Variant Detection Between RNA and DNA Methods

To further investigate the role of transcription in the detection of expressed variants, a targeted variant panel using RNA as the template was employed rather than DNA. From the 943 FNA samples, a representative set of 102 FNAs that were variant positive by DNA AmpliSeq were tested for expressed variants with an RNA AmpliSeq variant panel. The PPA of RNA-seq whole-transcriptome variants rose from 76.5% vs. DNA in this subset to 88.9% vs. RNA (**Table 2**). Next, RNA Variant AmpliSeq data was examined for 17 samples that had a DNA variant identified, but no variant identified in the whole-transcriptome RNA-seq. Six of these 17 samples had dramatically different VAFs when comparing the DNA and RNA (**Figure 1**), with VAFs observed in DNA >10% while RNA-based VAFs were <5%. These six samples had a DNA:RNA VAF ratio ranging from 5.7 to 38.1 (including 3 samples with a DNA:RNA VAF ratio >10). In these six samples, the wild type allele is predominantly expressed and that biological difference accounts for the lack of variant detection in the whole-transcriptome RNA-seq data. In the most striking sample, we observed a VAF of 32% in the DNA and <1% in RNA.

There Is High Agreement Between Fusion Detection by Whole-Transcriptome RNA-Seq and Targeted Fusion Seq

To determine the PPA of the fusion-calling capabilities of whole-transcriptome RNA-seq data, an in-house custom RNA fusion AmpliSeq assay was developed. A new series of 695 consecutive and blinded FNAs from the Veracyte CLIA stream that were either Afirma GSC Suspicious or Bethesda V/VI were tested for fusions with the RNA fusion AmpliSeq assay. Any sample that generated a discordant result between whole-transcriptome RNA-seq and the RNA fusion AmpliSeq assay were resolved with qPCR. A total of 61 fusions were observed in this series, and the fusions observed in greater than one FNA were: *PAX8/PPARG* (n = 16), *ETV6/NTRK3* (n = 13), *RET/PTC1* (n = 6), *STRN/ALK* (n = 6), *RET/PTC3* (n = 3), *AGK/BRAF* (n = 3), *SND1/BRAF* (n = 2), and *RBPMS/NTRK3* (n = 2) (**Supplementary Table 1**). This analysis revealed an 82.1% PPA between the RNA fusion AmpliSeq assay and whole-transcriptome RNA-seq data and demonstrated a 100% confirmation rate, as all 50 fusions

[10]https://www.fda.gov/RegulatoryInformation/Guidances/ucm071148.htm section 7.2

[11]https://www.r-project.org

TABLE 2 | Variant and Fusion Performance in whole transcriptome RNA-seq compared to targeted AmpliSeq panels.

Genomic alteration	Samples	PPA	NPA	Confirmation	RNA-seq only	AmpliSeq only	Both detected
DNA Variants	501	74% [67–80]	100% [100–100]	98.5% [95–100]	2	47	134
RNA Variants	102	88.9% [80–95]	100% [100–100]	94.7% [87–99]	4	9	72
Fusions	695	82% [70–91]	100% [100–100]	100% [93–100]	0	11	50

Positive Percent Agreement (PPA) is percentage of variants or fusions that are positive by RNA-seq compared to AmpliSeq. Negative Percent Agreement (NPA) is the percentage of variants or fusions that are negative by RNA-seq compared to AmpliSeq. Confirmation is the percentage of variants or fusions that were called positive by RNA-seq that are also positive by AmpliSeq.

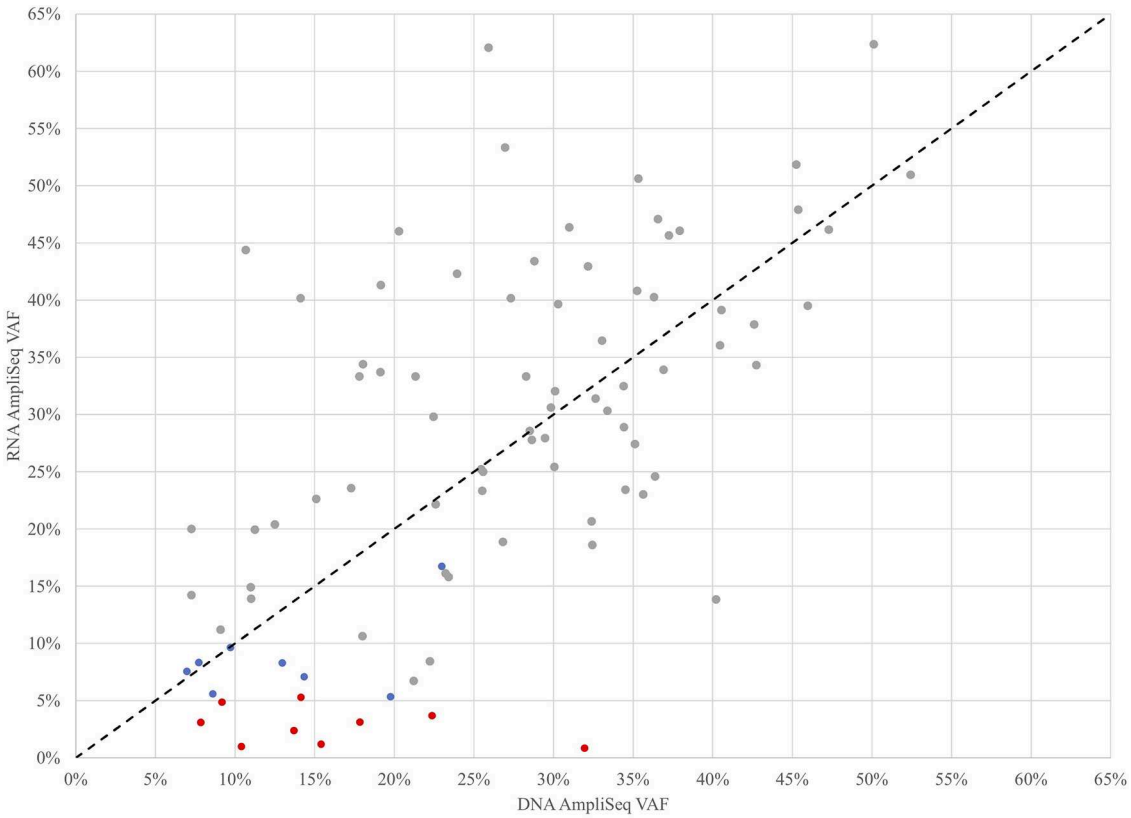

FIGURE 1 | Variant Allele Frequencies (VAF) determined by targeted DNA and RNA AmpliSeq methods for 102 FNAs that were variant positive by DNA AmpliSeq. Samples with low RNA AmpliSeq coverage of the variant were excluded. Gray points were detected by all 3 methods, blue points were detected by DNA AmpliSeq and RNA AmpliSeq, but not detected by XA, red points were detected by DNA AmpliSeq but not RNA AmpliSeq or XA. The black dotted line is x=y.

identified by RNA-seq were also identified by the AmpliSeq assay (**Table 2**).

Analytical Validation Shows the Variant and Fusion Calls Are Highly Reproducible Across Labs and Reagent Lots

To determine the reproducibility of the whole-transcriptome RNA-seq assay across laboratories and reagent lots, we examined the analytical validity of the assay. We compared the variant and fusion calls from RNA-seq data between two labs (R&D and CLIA) with the same lot of library prep reagents. Sixty-nine variant positive samples were used, and the between lab accuracy was 89.9% (**Supplementary Figure 1A**). For fusions, 36 positive samples were used, and the between lab accuracy was 94.4% (**Supplementary Figure 1B**). Next, we examined the reproducibility of the assay within one plate and across different reagent lots. Nine variant positive samples and 6 fusion positive samples were plated in triplicate across 3 plates. Each plate was run with different reagent lots and different operators. These experiments investigated intra-plate and inter-plate reproducibility. For variants, the intra-plate reproducibility

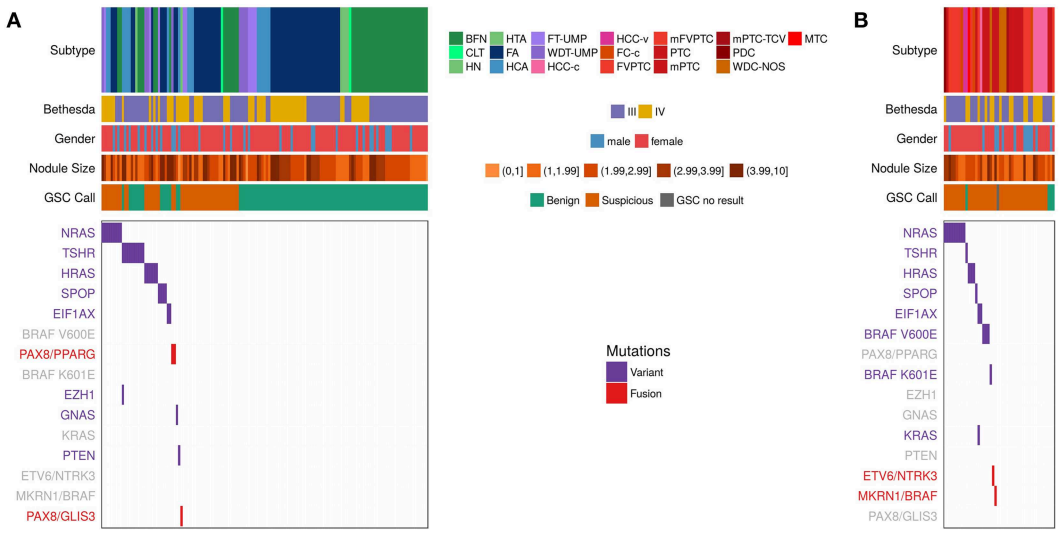

FIGURE 2 | Expressed Variants and fusions observed in RNA-seq data among the n = 191 Afirma GSC clinical validation study cohort, including the 1 sample classified as GSC no result due to inadequate follicular content (25), which is a subset of the 943. Each column represents a sample, while each row is either clinical information or a variant or fusion. Samples positive for a variant have a purple hash, while samples positive for a fusion have a red hash. Negative for a variant or fusion are white. Clinical information includes subtype, Bethesda category (III and IV only), Nodule size in cm, and GSC call. See **Table 1** for a list of subtype abbreviations. Variants/fusions are grayed out if no samples in a given cohort were positive for that alteration. **(A)** Histologically benign subtypes. **(B)** Histologically malignant subtypes.

was 88.9% and the inter-plate reproducibility was 86.4%. For fusions, the intra-plate reproducibility was 94.4% and the inter-plate reproducibility was 90.7%. These results passed pre-specified acceptance criteria for these studies.

Among Bethesda III/IV Nodules, 49% of Malignancies Harbor an RNA-Seq Detected Variant or Fusion

To understand the relationship between variants and fusions and histopathology diagnosis, we compared the variants/fusions observed in RNA-seq data from the primary test set of 190 Bethesda III/IV samples (**Figure 2** and **Table 3**) that were collected in a prospective, multicenter, and blinded protocol for the clinical validation of the Afirma GEC (38), and subsequently utilized to clinically validate the Afirma GSC (25). The histopathological diagnosis of these nodules was assigned by an expert panel of thyroid histopathologists who were masked to all clinical, molecular, and cytological data. In 145 histologically benign nodules, 76% had no variant or fusion observed (76% specificity). Of the 24% with a variant, *RAS* variants were the most common, followed by *TSHR*. In the 45 histologically malignant samples, 51% had no variant or fusion observed (49% sensitivity). Overall, the RNA-seq PPV and NPV were 38% and 83%, respectively, in this cohort with a 24% cancer prevalence. The 49% of samples with a positive variant or fusion mostly harbored *RAS* variants, *BRAF* variants, or fusions. Of the variants observed more than once, only *BRAF* V600E was confined to malignant nodules. Conversely, 10 of 11 *TSHR* variants and 4 of 5 *SPOP* variants occurred in histologically benign nodules. The only gene fusion observed more than once was *PAX8/PPARG* and both occurrences were in histologically benign nodules. *MKRN1/BRAF* and *ETV6/NTRK3* fusions were each identified once and were in malignant nodules (both PTC). *PAX8/GLIS3* was identified in the one hyalinizing trabecular adenoma, consistent with a recent report (39).

We next examined the combination of Afirma GSC classifier prediction and variant/fusion results (**Figure 2** and **Table 3**). In the 99 histologically benign nodules with GSC benign results (true negatives), 15% were variant positive and none contained a fusion. In the 46 benign nodules with GSC suspicious results (false positives), 39% harbored a variant and 6.5% contained a fusion (2 *PAX8/PPARG* and 1 *PAX8/GLIS3*). In the 41 histologically malignant nodules with GSC suspicious results (true positives), 46% had a variant, and 5% had a fusion (*MKRN1/BRAF* and *ETV6/NTRK3*). Finally, in the 4 GSC benign false negative nodules (2 PTC, 1 FVPTC, 1 HCC), only the HCC contained a variant (*TSHR*). Taken together, in the 190 thyroid nodules with definitive histology, malignant nodules were twice as likely to carry a variant or fusion relative to benign nodules (49 vs. 24%, $p = 0.003$ [$\chi 2$]). The most common genomic alteration identified among GSC suspicious nodules was a variant in a *RAS* family gene (present in 32% and conveying a PPV of 46%). Taken together, GSC suspicious nodules carried a variant or fusion in 48% compared with 16% of GSC benign nodules ($p < 0.0001$). The most common variants among GSC benign nodules were *TSHR*, and no variants or fusions known to be highly predictive of malignancy were identified among nodules with GSC benign results. In clinical use, variants and fusions are not reported among GSC benign nodules.

Among GSC suspicious nodules with a cancer prevalence of 47%, the sensitivity, specificity, and NPV of XA were 51,

TABLE 3 | Variants and fusions relative to their histopathologic and Afirma GSC outcomes (25). GSC Benign (B), GSC Suspicious (S).

			XA variant and fusions (*n*)	
Histopathological subtype	**Nodules, No. (%)**	**GSC B No./GSC S No.**	**GSC benign**	**GSC suspicious**
BENIGN				
Total	145 (100)	99/46		
BFN	49 (33.8)	38/11	EIF1AX:p.G8R(1)	HRAS:p.Q61R(2)
			TSHR:p.I486M(1)	NRAS:p.Q61K(1)
			TSHR:p.L512R(1)	NRAS:p.Q61R(1)
			TSHR:p.M453T(1)	
HN	5 (3.4)	5/0	TSHR:p.I568T(1)	NA
FA	54 (37.2)	37/17	GNAS:p.Q870H(1)	HRAS:p.Q61R(1)
			SPOP:p.P94R(3)	NRAS:p.Q61R(3)
			TSHR:p.D633Y(1)	PAX8/PPARG(1)
			TSHR:p.L629F(1)	
FT-UMP	9 (6.2)	4/5	NA	HRAS:p.Q61R(1)
				NRAS:p.Q61R(1)
				SPOP:p.P94R(1)
WDT-UMP	8 (5.5)	4/4	NA	HRAS:p.Q61R(2)
				NRAS:p.Q61R(1)
				PAX8/PPARG(1)
HCA	17 (11.7)	10/7	EIF1AX:p.G9D(1)	NRAS:p.Q61K(2)
			PTEN:p.G129R(1)	TSHR:p.M453T(1)
			TSHR:p.L629F, EZH1:p.Y642F(1)	TSHR:p.S281I(1)
			TSHR:p.S425I(1)	
CLT	2 (1.4)	1/1	NA	NA
HTA	1 (0.7)	0/1	NA	PAX8/GLIS3(1)
MALIGNANT				
Total	45 (100)	4/41		
PTC	15 (33.3)	2/13	NA	BRAF:p.V600E(3)
				NRAS:p.Q61R(1)
				SPOP:p.P94R(1)
				MKRN1/BRAF (1)
				ETV6/NTRK3(1)
PTC-TCV	1 (2.2)	0/1	NA	NA
FV-PTC	11 (24.4)	1/10	NA	HRAS:p.Q61R(1)
				KRAS:p.Q61R, EIF1AX:p.A113_splice(1)
				NRAS:p.Q61K(1)
				NRAS:p.Q61R(4)
HCC-c	9 (20)	1/8	TSHR:p.I568T(1)	EIF1AX:p.A113_splice(1)
				NRAS:p.Q61R(1)
FC	7 (15.6)	0/7	NA	BRAF:p.K601E(1)
				HRAS:p.G13R(1)
				NRAS:p.Q61R(1)
PDTC	1 (2.2)	0/1	NA	NRAS:p.Q61K(1)
MTC	1 (2.2)	0/1	NA	HRAS:p.Q61R(1)

54, and 56%, respectively. The overall PPV of an Afirma GSC suspicious nodule was 47%, regardless of variant/fusion status. The PPV was 50% among GSC suspicious nodules when a variant or fusions was identified, compared with 44% among GSC suspicious nodules when no variant or fusion was identified ($p = 0.77$ [$\chi 2$]).

Variants and Fusions Potentially Amenable to Targeted Therapy Were Identified Across Multiple Bethesda Categories

We determined the most common variants observed in thyroid FNAs from expressed variant data (**Figure 3** and **Supplementary Table 2**). Five genes showed variants in >1% of

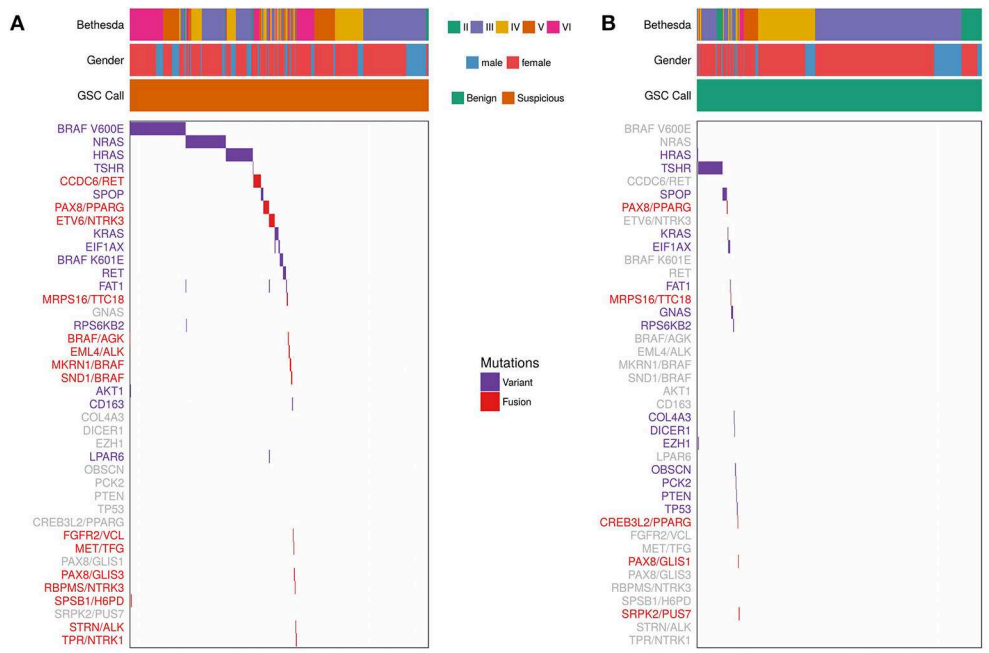

FIGURE 3 | Expressed Variants and Fusions from 943 FNAs (See Materials and Methods). Each column represents one sample and each row represents variants observed in one gene or fusion pair. Bethesda category, gender, and Afirma GSC call are represented for each sample. Purple indicates that a sample is positive for a variant. Red indicates that a sample is positive for a fusion. Variants/fusions are grayed out if no samples in a given cohort were positive for that alteration. **(A)** FNAs with a GSC Suspicious call. **(B)** FNAs with a GSC Benign call.

FNAs: *BRAF, NRAS, HRAS, TSHR,* and *SPOP*. For individual variants, *BRAF* V600E was most common, followed by *NRAS* Q61R, *HRAS* Q61R, *NRAS* Q61K, *TSHR* M453T, and *SPOP* P94R (**Supplementary Table 2**). *NRAS* and *HRAS* variants were primarily observed in Bethesda III/IV FNAs that were GSC Suspicious, while *BRAF* V600E was predominantly present in Bethesda V/VI FNAs. *TSHR* and *SPOP* variants were most frequently observed in GSC Benign FNAs (**Figure 3**), which is consistent with other observations (11, 40).

Fusions were also identified using whole-transcriptome RNA-seq. Fifty-two (5.5%) of the 943 samples harbored a fusion. The most common fusions were *CCDC6/RET* (aka *RET/PTC1*), *PAX8/PPARG,* and *ETV6/NTRK3* (**Figure 3** and **Supplementary Table 3**). *RET/PTC1* was primarily observed in Bethesda V/VI FNAs, while *PAX8/PPARG* was observed in Bethesda III/IV FNAs. *ETV6/NTRK3* was observed across Bethesda III-VI. A subset of 31 fusion-containing samples with sufficient RNA were selected for testing by qPCR (**Supplementary Table 4**). 100% of the RNA-seq detected fusions were also detected (i.e., confirmed) by qPCR. *ALK* fusions were also observed, although they were rare. *EML4/ALK* was observed twice in Bethesda VI samples and *STRN/ALK* was observed once in Bethesda III.

Overall, variants or fusions potentially amenable to targeted therapy involving *AKT, ALK, BRAF, HRAS, KRAS, MET, NRAS, NTRK, PPARG, PTEN*, and *RET* were identified across multiple Bethesda categories. Similarly, 4 *RET* point mutations suggestive of MTC were identified among Bethesda III-V samples (**Supplementary Table 2**). All 4 were identified as positive by the Afirma GSC MTC classifier (25, 41). Further, these variants may be somatic or germline and raise the possibility of multiple endocrine neoplasia type 2.

1% of Bethesda III/IV Nodules Harbor a TERT Promoter Variant, All Were in Combination With a RAS Variant and Were GSC Suspicious, and Most Were Histologically Benign

The DNA AmpliSeq panel included the *TERT* promoter. *TERT* promoter variants were observed in 15 samples of the 943 examined, across Bethesda categories (**Table 4**), and all were called Afirma GSC suspicious: 1 Bethesda II (1.89%), 0 Bethesda III (0%), 7 Bethesda IV (3.48%), 2 Bethesda V (1.90%), and 6 Bethesda VI (5.61%). The Bethesda II sample was *TERT* C228T plus *NRAS* Q61K. All 7 Bethesda IV FNAs were *TERT* C228T plus *RAS* positive. Seven of eight Bethesda V and VI FNAs were *TERT* C228T plus *BRAF* V600E, with the remaining Bethesda VI sample *TERT* C228T positive in isolation. Fourteen of fifteen *TERT* C228T positive FNAs had paired histopathology (**Table 4**). The Bethesda II sample was an FVPTC. In Bethesda IV, 5 FNAs were *TERT* C228T plus *NRAS* positive (4 Q61R and 1 Q61K) and 4/5 were histologically benign. Additionally, there were 2 FNAs that were positive for *TERT* C228T in combination with *KRAS* Q61R or *HRAS* Q61R, which were histologically malignant and benign, respectively. Finally, five Bethesda V and VI FNAs were *TERT* C228T in combination with *BRAF* V600E, and all 5 were histologically malignant. Three were PTC and two were PTC-TCV. The Bethesda VI sample with *TERT* C228T in isolation was an FC-v.

TABLE 4 | *TERT* Promoter variants observed in this study.

Bethesda	Histopathology	SubType	Afirma GSC	Variant	TERT Promoter Variant
Bethesda II	M	FVPTC	Suspicious	*NRAS*:p.Q61K	C228T
Bethesda IV	B	HCA	Suspicious	*HRAS*:p.Q61R	C228T
	B	HCA	Suspicious	*NRAS*:p.Q61K	C228T
	B	NHP	Suspicious	*NRAS*:p.Q61R	C228T
	B	FA	Suspicious	*NRAS*:p.Q61R	C228T
	B	WDT-UMP	Suspicious	*NRAS*:p.Q61R	C228T
	M	PTC	Suspicious	*KRAS*:p.Q61R	C228T
	M	FC-v	Suspicious	*NRAS*:p.Q61R	C228T
Bethesda V	M	PTC	Suspicious	*BRAF*:p.V600E	C228T
	M	PTC	Suspicious	*BRAF*:p.V600E	C228T
Bethesda VI	M	PTC	Suspicious	*BRAF*:p.V600E	C228T
	M	PTC-TCV	Suspicious	*BRAF*:p.V600E	C228T
	M	PTC-TCV	Suspicious	*BRAF*:p.V600E	C228T
	Unknown	Unknown	Suspicious	*BRAF*:p.V600E	C228T
	M	FC-v	Suspicious	None	C228T

Histopathology is shown as Malignant (M) or Benign (B). See ***Table 1*** *for a list of subtype abbreviations. Unknown subtype has no histopathology information available.*

DISCUSSION

This study demonstrates the analytical and clinical validation in thyroid nodule evaluation of the Afirma Xpression Atlas (XA), which detects gene variants and fusions from a curated panel of 511 genes via dedicated FNA samples using whole-transcriptome RNA-sequencing. More than 96% of consecutive real-world samples received has sufficient quantity and quality to receive an XA result. The data show that agreement is high between fusion detection by XA and an alternative fusion detection method, and that a high proportion of variants observed in DNA are also detected in the expressed RNA. As expected, agreement is even higher when comparing variant detection between two different RNA-based methods. Intriguingly, we found the wild type allele to be preferentially expressed compared with the variant allele in some samples (**Figure 1**), explaining some of the differences observed. Analytical studies show high reproducibility within plates and across reagent lots. Among Bethesda III/IV cytologically indeterminate nodules that were malignant, about half harbored a variant or fusion that was detected by XA. Detection of variants and fusions progressively increased along the Bethesda II to VI spectrum, and genomic findings potentially amenable to targeted therapeutics were identified across the Bethesda spectrum.

Afirma XA is not a cancer rule-out test. Among Bethesda III/IV nodules deemed suspicious by Afirma GSC and among Bethesda V/VI nodules, the impact of Afirma XA on nodule management extends beyond informing the risk of cancer when XA is negative or when XA is positive for a specific genomic alteration. Recent studies have begun to associate selected variant and fusions with *BRAF* V600E-like vs. *RAS*-like (or non-BRAF-non-RAS) pathway signaling, iodine metabolism, neoplasm histology, risk of lymph node metastasis, risk of recurrence, and risk of mortality (3, 9). How much these prognostic associations will remain significant independent predictors when traditional predictors are considered is presently unknown. For instance, *TERT* promoter mutations predict disease-free survival and disease-specific survival, but this effect is diminished or eliminated when the variant occurs in the absence of a *RAS* or *BRAF* variant, or among low and intermediate ATA risk patients and stage I-II TNM patients (42). Thus, for thyroid nodules seemingly confined to the thyroid gland and harboring Bethesda III-VI cytology, future studies may investigate how the preoperative identification of a presumed driver mutation may inform the pre-operative evaluation and surgical plan. For example, prospective randomized trials could investigate the roles of active surveillance or hemithyroidectomy for variants and fusions associated with a ∼50:50 chance of cancer, and/or those associated with less aggressive carcinomas. This may include nodules where a variant or fusion is not detected as some data suggests that such cancers may have less aggressive features when considering extrathyroidal extension, lymph node metastases, risk of recurrence, and risk of mortality (3, 9). Similarly, prospective randomized trials could investigate the role of total thyroidectomy vs. hemithyroidectomy (or whether or not adjuvant radioactive iodine ablation or TSH suppression would be used) for cancers with variants thought to predict more aggressive tumor behavior that are nevertheless clinically confined to the thyroid gland.

For patients presenting with locally advanced thyroid cancer, genomic findings on XA may suggest the possibility of neo-adjuvant therapy that may improve the outcome of a subsequent surgical resection (16, 43, 44).

For patients with thyroid carcinoma in the neck or in distant sites that is refractory to radioactive iodine and may warrant systemic therapy, use of XA from FNAs of known thyroid cancer deposits may inform treatment selection, although confirmation testing by an approved companion diagnostic test may still be required for patients to access certain pharmaceuticals.

Additionally, repeat testing from a site of disease progression during active treatment may provide additional genomic insights to potentially guide therapy (26).

Limitations of measuring variants in expressed RNA include that some variants and fusions identified by an alternative method were not identified by XA. The reason for these differences is not known, nor is it known which test should ideally be considered "correct." While imperfect test sensitivity is one possibility, it is also possible that some DNA variants may not be expressed due to gene silencing, or very low expression levels. Such phenomenon may explain some discrepancies among *BRAF* V600E variants detected by qPCR that are negative by immunohistochemistry (45). By employing a third variant detection methodology that used targeted sequencing of RNA templates, we have shown that some samples do have very low expression of the gene variants identified in DNA. The biological significance of such variants is unknown. The efficacy of targeted treatment aimed at non-expressed or poorly expressed genomic alterations may be diminished. Conversely, the vast majority of genomic abnormalities identified by XA were confirmed by the alternative method (**Table 2**). An additional limitation of RNA sequencing is that variants in non-coding regions, such as *TERT* promotor variants, are not detected by this method. However, our data demonstrate that these variants are uncommon among cytologically indeterminate nodules (<1%) and in the vast majority of cases, found in tandem with a *RAS* variant. Moreover, we show that *TERT* promoter variants in combination with *RAS* variants can occur in benign lesions in Bethesda IV FNAs. While current opinion is that nodules with a *RAS* variant (with or without *TERT* promoter variant) should be surgically removed given their potential malignant or pre-malignant status, it is unclear if cancers harboring a *TERT* promoter variant plus a *RAS* or *BRAF* variant should be treated differently based on this genomic information independent from traditional prognostic factors for risks of recurrence and death, especially among lower-risk patients (42). A DNA based detection method, or development of an RNA expression-based classifier, could be added to XA in the future should reporting of such non-expressed variants be desired.

In clinical practice, XA testing is offered for Bethesda III/IV Afirma GSC suspicious nodules, FNA Bethesda V/VI nodules, and for known thyroid cancer metastases. The Afirma Xpression Atlas became commercially available to most of the United States in 2018. Samples for Afirma GSC and/or XA are collected with two dedicated FNA needle passes that must be expressed into the provided FNAprotect tube, properly stored locally to avoid exposure to heat, and are shipped in the provided container with frozen foam bricks to ensure receipt of high-quality RNA material. These validated collection and shipping procedures are identical to those used to formerly collect and ship Afirma GEC samples (46). Detailed sample collection, packing, and shipping instructions are available on-line[12].

In summary, we have demonstrated clinical and analytical validation of the Afirma XA, which reports variants and fusions from a panel of 511 genes that have been associated with thyroid cancer. This added clinical information is intended to supplement clinical decision-making among patients with Bethesda III-VI nodules. Clinicians are to be reminded that most patients with thyroid cancer have an excellent prognosis, and the greatest impact of this added genomic information may be to facilitate treatment that is less aggressive, rather than more aggressive (47). The information obtained from variants and fusions assessment may offer new precision medicine insights from diagnostic FNA samples and the opportunity to advance individualized patient care.

[12] www.afirma.com/physicians/practice-resources

DATA AVAILABILITY

Restrictions apply to the datasets: The datasets for this manuscript are not publicly available because the dataset and the research methodologies are proprietary. Requests to access the datasets should be directed to GK, Ph.D.; Giulia@Veracyte.com.

ETHICS STATEMENT

This research was approved by the Copernicus Group Independent Review Board (Cary, North Carolina). A waiver of written informed consent was granted regarding de-identified biological materials from the CLIA laboratory. IRB approval and written Informed consent in accordance with the Declaration of Helsinki was provided by all patients whose samples were previously used for training and validation of the Afirma GSC as previously described (25, 38).

AUTHOR CONTRIBUTIONS

GK, JB, JH, PW, SK, and YH conceived and designed the study. JB, LW, PW, RK, SK, TA, and YH analyzed and interpreted the data. EC, GK, JB, LW, MC, MS, RK, SW, and TA drafted and critically revised the work for important intellectual content. SK and YH performed the bioinformatics and statistical analyses. All authors contributed to manuscript revision, read and approved the submitted version.

FUNDING

This research was funded by Veracyte, Inc.

ACKNOWLEDGMENTS

We would like to thank Ed Tom, Duncan Whitney, Zhanzhi Hu, Mei Wong, Grazyna Fedorowicz, Manqiu Cao, Huimin Jiang, Jessica Anderson, Tami Tu, Maggie Dorosz, Jennifer Huiras, and Jing Lu for their contributions to laboratory studies and data analysis.

SUPPLEMENTARY MATERIAL

The Supplementary Material for this article can be found online at: https://www.frontiersin.org/articles/10.3389/fendo.2019.00612/full#supplementary-material

REFERENCES

1. Stratton MR, Campbell PJ, Futreal PA. The cancer genome. *Nature*. (2009) 458:719–24. doi: 10.1038/nature07943
2. Agrawal N, Jiao Y, Sausen M, Leary R, Bettegowda C, Roberts NJ, et al. Exomic sequencing of medullary thyroid cancer reveals dominant and mutually exclusive oncogenic mutations in RET and RAS. *J Clin Endocrinol Metab*. (2013) 98:E364–369. doi: 10.1210/jc.2012-2703
3. Cancer Genome Atlas Research Network. Integrated genomic characterization of papillary thyroid carcinoma. *Cell*. (2014) 159:676–90. doi: 10.1016/j.cell.2014.09.050
4. Costa V, Esposito R, Ziviello C, Sepe R, Bim LV, Cacciola NA, et al. New somatic mutations and WNK1-B4GALNT3 gene fusion in papillary thyroid carcinoma. *Oncotarget*. (2015) 6:11242–51. doi: 10.18632/oncotarget.3593
5. Jung SH, Kim MS, Jung CK, Park HC, Kim SY, Liu J, et al. Mutational burdens and evolutionary ages of thyroid follicular adenoma are comparable to those of follicular carcinoma. *Oncotarget*. (2016) 7:69638–48. doi: 10.18632/oncotarget.11922
6. Pagan M, Kloos RT, Lin CF, Travers KJ, Matsuzaki H, Tom EY, et al. The diagnostic application of RNA sequencing in patients with thyroid cancer: an analysis of 851 variants and 133 fusions in 524 genes. *BMC Bioinform.* (2016) 17(Suppl. 1):6. doi: 10.1186/s12859-015-0849-9
7. Pan W, Zhou L, Ge M, Zhang B, Yang X, Xiong X, et al. Whole exome sequencing identifies lncRNA GAS8-AS1 and LPAR4 as novel papillary thyroid carcinoma driver alternations. *Hum Mol Genet*. (2016) 25:1875–84. doi: 10.1093/hmg/ddw056
8. Siraj AK, Masoodi T, Bu R, Beg S, Al-Sobhi SS, Al-Dayel F, et al. Genomic profiling of thyroid cancer reveals a role for thyroglobulin in metastasis. *Am J Hum Genet*. (2016) 98:1170–80. doi: 10.1016/j.ajhg.2016.04.014
9. Yoo SK, Lee S, Kim SJ, Jee HG, Kim BA, Cho H, et al. Comprehensive analysis of the transcriptional and mutational landscape of follicular and papillary thyroid cancers. *PLoS Genet*. (2016) 12:e1006239. doi: 10.1371/journal.pgen.1006239
10. Lu Z, Zhang Y, Feng D, Sheng J, Yang W, Liu B. Targeted next generation sequencing identifies somatic mutations and gene fusions in papillary thyroid carcinoma. *Oncotarget*. (2017) 8:45784–92. doi: 10.18632/oncotarget.17412
11. Ye L, Zhou X, Huang F, Wang W, Qi Y, Xu H, et al. The genetic landscape of benign thyroid nodules revealed by whole exome and transcriptome sequencing. *Nat Commun*. (2017) 8:15533. doi: 10.1038/ncomms15533
12. Ganly I, Makarov V, Deraje S, Dong Y, Reznik E, Seshan V, et al. Integrated genomic analysis of hurthle cell cancer reveals oncogenic drivers, recurrent mitochondrial mutations, and unique chromosomal landscapes. *Cancer Cell*. (2018) 34:256–70 e255. doi: 10.1016/j.ccell.2018.07.002
13. Gopal RK, Kubler K, Calvo SE, Polak P, Livitz D, Rosebrock D, et al. Widespread chromosomal losses and mitochondrial DNA alterations as genetic drivers in hurthle cell carcinoma. *Cancer Cell*. (2018) 34:242–55 e245. doi: 10.1016/j.ccell.2018.06.013
14. Pozdeyev N, Gay LM, Sokol ES, Hartmaier R, Deaver KE, Davis S, et al. Genetic analysis of 779 advanced differentiated and anaplastic thyroid cancers. *Clin Cancer Res*. (2018) 24:3059–68. doi: 10.1158/1078-0432.CCR-18-0373
15. Drilon A, Siena S, Ou SI, Patel M, Ahn MJ, Lee J, et al. Safety and antitumor activity of the multitargeted pan-TRK, ROS1, and ALK inhibitor entrectinib: combined results from two phase I trials (ALKA-372-001 and STARTRK-1). *Cancer Discov*. (2017) 7:400–9. doi: 10.1158/2159-8290.CD-16-1237
16. Rao SN, Cabanillas ME. Navigating systemic therapy in advanced thyroid carcinoma: from standard of care to personalized therapy and beyond. *J Endocr Soc*. (2018) 2:1109–30. doi: 10.1210/js.2018-00180
17. Subbiah V, Kreitman RJ, Wainberg ZA, Cho JY, Schellens JHM, Soria JC, et al. Dabrafenib and trametinib treatment in patients with locally advanced or metastatic BRAF V600-mutant anaplastic thyroid cancer. *J Clin Oncol*. (2018) 36:7–13. doi: 10.1200/JCO.2017.73.6785
18. Untch BR, Dos Anjos V, Garcia-Rendueles MER, Knauf JA, Krishnamoorthy GP, Saqcena M, et al. Tipifarnib inhibits HRAS-driven dedifferentiated thyroid cancers. *Cancer Res*. (2018) 78:4642–57. doi: 10.1158/0008-5472.CAN-17-1925
19. Tian T, Li X, Zhang J. mTOR signaling in cancer and mTOR inhibitors in solid tumor targeting therapy. *Int J Mol Sci*. (2019) 20:E755. doi: 10.3390/ijms20030755
20. Drilon A, Laetsch TW, Kummar S, DuBois SG, Lassen UN, Demetri GD, et al. Efficacy of larotrectinib in TRK fusion-positive cancers in adults and children. *N Engl J Med*. (2018) 378:731–9. doi: 10.1056/NEJMoa1714448
21. Thorpe LM, Yuzugullu H, Zhao JJ. PI3K in cancer: divergent roles of isoforms, modes of activation and therapeutic targeting. *Nat Rev Cancer*. (2015) 15:7–24. doi: 10.1038/nrc3860
22. Hu M, Taylor M, Wirth LJ, Zhu VW, Doebele RC, Lee D, et al. Clinical activity of selective RET inhibitor, BLU-667, in advanced RET-altered thyroid cancers: updated results from the phage 1 ARROW study (short call oral 5). *Thyroid*. (2018) 28, A-170.
23. Wirth LJ, Cabanillas ME, Sherman E, Solomon B, Leboulleux S, Robinson B, et al. Clinical activity of LOXO-292, a highly selective RET inhibitor, in patients with RET-altered thyroid cancers (short call oral 6). *Thyroid*. (2018) 28, A-171.
24. Marcus L, Lemery SJ, Keegan P, Pazdur R. FDA approval summary: pembrolizumab for the treatment of microsatellite instability-high solid tumors. *Clin Cancer Res*. (2019) 25:3753–8. doi: 10.1158/1078-0432.CCR-18-4070
25. Patel KN, Angell TE, Babiarz J, Barth NM, Blevins T, Duh QY, et al. Performance of a genomic sequencing classifier for the preoperative diagnosis of cytologically indeterminate thyroid nodules. *JAMA Surg*. (2018) 153:817–24. doi: 10.1001/jamasurg.2018.1153
26. Ali SZ, Siperstein A, Sadow PM, Golding AC, Kennedy GC, Kloos RT, et al. Extending expressed RNA genomics from surgical decision making for cytologically indeterminate thyroid nodules to targeting therapies for metastatic thyroid cancer. *Cancer Cytopathol*. (2019). doi: 10.1002/cncy.22132. [Epub ahead of print].
27. Cibas ES, Ali SZ. The 2017 bethesda system for reporting Thyroid Cytopathology. *Thyroid*. (2017) 27:1341–6. doi: 10.1089/thy.2017.0500
28. Parkinson D, Aziz S, Bentley R, Johnson SJ. Thyroid cytology-histology correlation using the RCPath terminology for thyroid cytology reporting. *J Clin Pathol*. (2017) 70:648–55. doi: 10.1136/jclinpath-2016-204022
29. Angell TE, Heller HT, Cibas ES, Barletta JA, Kim MI, Krane JF, et al. Independent comparison of the afirma genomic sequencing classifier and gene expression classifier for cytologically indeterminate Thyroid Nodules. *Thyroid*. (2019) 29:650–6. doi: 10.1089/thy.2018.0726
30. Endo M, Nabhan F, Porter K, Roll K, Shirley L, Azaryan I, et al. Afirma gene sequencing classifier compared to gene expression classifier in indeterminate Thyroid Nodules. *Thyroid*. (2019) 29:1115–24. doi: 10.1089/thy.2018.0733
31. Harrell RM, Eyerly-Webb SA, Golding AC, Edwards CM, Bimston DN. Statistical comparison of afirma gsc and afirma gec outcomes in a community endocrine surgical practice: early findings. *Endocr Pract*. (2019) 25:161–4. doi: 10.4158/EP-2018-0395
32. Dobin A, Davis CA, Schlesinger F, Drenkow J, Zaleski C, Jha S, et al. STAR: ultrafast universal RNA-seq aligner. *Bioinformatics*. (2013) 29:15–21. doi: 10.1093/bioinformatics/bts635
33. Haas B, Dobin A, Stransky N, Li B, Yang X, Tickle T, et al. STAR-Fusion: fast and accurate fusion transcript detection from RNA-Seq. *bioRxiv*. (2017). doi: 10.1101/120295
34. McKenna A, Hanna M, Banks E, Sivachenko A, Cibulskis K, Kernytsky A, et al. The Genome Analysis Toolkit: a MapReduce framework for analyzing next-generation DNA sequencing data. *Genome Res*. (2010) 20:1297–303. doi: 10.1101/gr.107524.110
35. DePristo MA, Banks E, Poplin R, Garimella KV, Maguire JR, Hartl C, et al. A framework for variation discovery and genotyping using next-generation DNA sequencing data. *Nat Genet*. (2011) 43:491–8. doi: 10.1038/ng.806
36. Van der Auwera GA, Carneiro MO, Hartl C, Poplin R, Del Angel G, Levy-Moonshine A, et al. From FastQ data to high confidence variant calls: the Genome Analysis Toolkit best practices pipeline. *Curr Protoc Bioinformatics*. (2013) 43, 11–33. doi: 10.1002/0471250953.bi1110s43
37. Diggans J, Kim SY, Hu Z, Pankratz D, Wong M, Reynolds J, et al. Machine learning from concept to clinic: reliable detection of BRAF V600E DNA mutations in thyroid nodules using high-dimensional RNA expression data. *Pac Symp Biocomput*. (2015) 371–82.
38. Alexander EK, Kennedy GC, Baloch ZW, Cibas ES, Chudova D, Diggans J, et al. Preoperative diagnosis of benign thyroid nodules with indeterminate cytology. *N Engl J Med*. (2012) 367:705–15. doi: 10.1056/NEJMoa1203208

39. Nikiforova MN, Nikitski AV, Panebianco F, Kaya C, Yip L, Williams M, et al. GLIS rearrangement is a genomic hallmark of hyalinizing trabecular tumor of the *Thyroid* Gland. *Thyroid*. (2019) 29:161–73. doi: 10.1089/thy.2018.0791
40. Guan H, Matonis D, Toraldo G, Lee SL. Clinical significance of thyroid-stimulating hormone receptor gene mutations and/or sodium-iodine symporter gene overexpression in indeterminate thyroid fine needle biopsies. *Front Endocrinol*. (2018) 9:566. doi: 10.3389/fendo.2018.00566
41. Randolph G, Angell TE, Babiarz J, Barth N, Blevins T, Duh Q, et al. Clinical validation of the afirma genomic sequencing classifier for medullary thyroid cancer (Clinical Oral Abstract 29). *Thyroid*. (2017) 27:A105.
42. Song YS, Lim JA, Choi H, Won JK, Moon JH, Cho SW, et al. Prognostic effects of TERT promoter mutations are enhanced by coexistence with BRAF or RAS mutations and strengthen the risk prediction by the ATA or TNM staging system in differentiated thyroid cancer patients. *Cancer*. (2016) 122:1370–9. doi: 10.1002/cncr.29934
43. Cabanillas ME, Busaidy NL, Zafereo M, Waguespack SG, Hu MI, Hofmann MC, et al. Neoadjuvant vemurafenib in patients with locally advanced papillary thyroid cancer (abstract). *Eur Thyroid J*. 6(supp 1):38. doi: 10.1159/000477987
44. Cabanillas ME, Ferrarotto R, Garden AS, Ahmed S, Busaidy NL, Dadu R, et al. Neoadjuvant BRAF- and immune-directed therapy for anaplastic *Thyroid* carcinoma. *Thyroid*. (2018) 28:945–51. doi: 10.1089/thy.2018.0060
45. Szymonek M, Kowalik A, Kopczynski J, Gasior-Perczak D, Palyga I, Walczyk A, et al. Immunohistochemistry cannot replace DNA analysis for evaluation of BRAF V600E mutations in papillary thyroid carcinoma. *Oncotarget*. (2017) 8:74897–909. doi: 10.18632/oncotarget.20451
46. Walsh PS, Wilde JI, Tom EY, Reynolds JD, Chen DC, Chudova DI, et al. Analytical performance verification of a molecular diagnostic for cytology-indeterminate thyroid nodules. *J Clin Endocrinol Metab*. (2012) 97:E2297–2306. doi: 10.1210/jc.2012-1923
47. Valderrabano P, Khazai L, Thompson ZJ, Leon ME, Otto KJ, Hallanger-Johnson JE, et al. Impact of oncogene panel results on surgical management of cytologically indeterminate thyroid nodules. *Head Neck*. (2018) 40:1812–23. doi: 10.1002/hed.25165

Conflict of Interest Statement: GK, JB, JH, PW, RK, SK and YH are Veracyte Inc. employees and equity owners.

The remaining authors declare that the research was conducted in the absence of any commercial or financial relationships that could be construed as a potential conflict of interest.

frontiers in Endocrinology

ORIGINAL RESEARCH
published: 29 October 2019
doi: 10.3389/fendo.2019.00734

Resveratrol Reverses Retinoic Acid Resistance of Anaplastic Thyroid Cancer Cells via Demethylating CRABP2 Gene

Xin Liu[1], Hong Li[1], Mo-Li Wu[1], Jiao Wu[1], Yuan Sun[1], Kai-Li Zhang[1] and Jia Liu[1,2]**

[1] *Liaoning Laboratory of Cancer Genetics and Epigenetics, Department of Cell Biology, College of Basic Medical Sciences, Dalian Medical University, Dalian, China,* [2] *Research Center, South China University School of Medicine, Guangzhou, China*

Background: Cellular retinoic acid binding protein 2 (CRABP2) mediates retinoic acid/RA anti-cancer pathways. Resveratrol effectively reverses RA tolerance and upregulates CRABP2 expression of anaplastic thyroid cancer cell line THJ-11T. As DNA methylation is responsible for CRABP2 silencing, the CRABP2 methylation status of THJ-11T cells and the demethylating effect of resveratrol on this gene are elucidated.

Materials and methods: The statuses of CRABP2 expression and methylation and the levels of DNA methyltransferases (DNMTs) DNMT1, DNMT3A, and DNMT3B of THJ-11T cells were examined before and after resveratrol treatment via multiple experimental methods. The human medulloblastoma UW228-2 cell line was cited as the control of CRABP2 methylation and gemcitabine as the demethylator control.

Results: RT-PCR, immunocytochemical staining and Western blotting showed that resveratrol significantly increased the CRABP2 expression and RA sensitivity of THJ-11T and UW228-2 cells. Bisulfite sequencing showed five CpG methylation sites at the CRABP2 promoter region of both cell lines, which were partially (3/5) demethylated by resveratrol and totally (5/5) by gemcitabine. DNMT1, DNMT3A, and DNMT3B were reduced in UW228-2 cells and DNMT1 and DNMT3A were reduced in THJ-11T cells after resveratrol treatment in a time-related fashion.

Conclusion: Resveratrol is able to erase CRABP2 methylation and can thereby increase the RA sensitivity of THJ-11T and UW228-2 cells. This study demonstrates the additional value of the natural polyphenolic compound resveratrol as a demethylator in cancer treatments.

Keywords: retinoic acid, resveratrol, DNA methylation, CRABP2, DNA methyltransferase

OPEN ACCESS

Edited by:
Terry Francis Davies, Icahn School of Medicine at Mount Sinai, United States

Reviewed by:
Cesidio Giuliani, Università degli Studi G. d'Annunzio Chieti e Pescara, Italy
Paul Webb, California Institute for Regenerative Medicine, United States

****Correspondence:***
Kai-Li Zhang
18940993315@163.com
Jia Liu
jialiudl@dmu.edu.cn

Specialty section:
This article was submitted to Thyroid Endocrinology, a section of the journal Frontiers in Endocrinology

Received: *25 April 2019*
Accepted: *10 October 2019*
Published: *29 October 2019*

Citation:
Liu X, Li H, Wu M-L, Wu J, Sun Y, Zhang K-L and Liu J (2019) Resveratrol Reverses Retinoic Acid Resistance of Anaplastic Thyroid Cancer Cells via Demethylating CRABP2 Gene. Front. Endocrinol. 10:734. doi: 10.3389/fendo.2019.00734

INTRODUCTION

All-trans retinoic acid (RA) has been commonly used in cancer chemotherapy (1, 2). Its biological effects are largely determined by two classical signaling pathways mediated by Cellular retinoic acid binding protein 2 (CRABP2) or Fatty acid-binding protein 5 (FABP5), which results in tumor suppression or tumor promotion (3). Anaplastic thyroid cancer (ATC) is the most lethal thyroid malignancy; post-diagnosis survival time is <1 year due to its strong

invasiveness and frequent metastasis (4, 5). Although ATCs are <2% of thyroid cancer cases, its mortality rate accounts for 33–50% of thyroid cancer-related death (6). RA has been used to enhance the radio-sensitivity of thyroid cancers via promoting thyroid cancer re-differentiation and, therefore, radioactive iodine uptake (7). However, the therapeutic effect of RA is controversial (8). Our recent data demonstrate that RA is ineffective or even promotes ATC cell growth, presumably due to low or absent CRABP2 expression (9), which is suggestive of the necessity to cautiously use RA in anti-ATC therapy. On the other hand, resveratrol effectively suppresses the growth of two RA-tolerant ATC cell lines (THJ-16T and THJ-21T); more interestingly, resveratrol fails to inhibit ATC THJ-11T cell growth by itself but causes extensive cell death when combined with RA (9). Further analysis revealed that resveratrol significantly upregulated CRABP2 expression and reversed the RA tolerance of THJ-11T by opening the RA tumor suppression pathway. These results demonstrate for the first time the therapeutic advantage of resveratrol for ATCs by itself or in combination with RA. Meanwhile, it would be worthwhile to shed light on the underlying mechanism of resveratrol-upregulated CRABP2 expression.

It has been recognized that RA anticancer signaling is activated when RA binds with CRABP2. CRABP2 transports lipophilic RA to the nucleus; RA then passes through heterodimers with its nuclear receptor (RARα/β/γ and RXRα/β/γ) to regulate its target gene expression, leading to differentiation, cell cycle arrest, and apoptosis of the treated cells (10). Therefore, the status of CRABP2 expression is considered a critical element in determining RA sensitivity in cancer cells, including those of medulloblastoma and pancreatic cancers (11, 12). We have found that DNA methylation is responsible for the low or silenced CRABP2 expression in medulloblastoma cells (12, 13). DNMT inhibitor 5-aza-2′-deoxycytidinecytidine (5-aza) is thus able to restore CRABP2 expression and reverse RA resistance of UW228-2 medulloblastoma cells (12). However, 5-aza causes several side effects including gene mutations and chromosomal rearrangements, and it may also affect embryonic development (14, 15), suggesting the necessity to explore lesser toxic demethylation agents such as resveratrol. The finding of recovered CRABP2 expression in resveratrol-treated anaplastic thyroid cancer cells has encouraged us to investigate the possible demethylating capacity of this polyphenol agent.

In order to shed light on the mechanism of resveratrol-upregulated CRABP2 expression and its relevance to RA sensitivities, the suitable cell model(s) would be required. Therefore, ATC THJ-11T and medulloblastoma UW228-2 cell lines were selected for this study because of their absence in CRABP2 expression and tolerance to RA treatment (12). Moreover, UW228-2 cells were found with CRABP2 methylation (12), and the recovery of CRABP2 expression increased their RA sensitivity. This study thus aims to check the methylation status of CRABP2 and the expression patterns of methylation enzymes (DNMT1, DNMT3A, and DNMT3B) in these two cell lines before and after resveratrol treatment and then compared the corresponding parameters obtain from gemcitabine-treated cells.

MATERIALS AND METHODS

Cell Lines and Cell Culture

Anaplastic thyroid cancer ATC (THJ-11T) cell lines were provided by Quentin Liu, Institute of Cancer Stem Cell, Dalian Medical University (16). The medulloblastoma cell lines (UW228-2) were kindly provided by the Department of Neurological Surgery, University of Washington at Seattle (12). The THJ-11T cell line was maintained in RPMI 1640 (GE Healthcare Life Sciences, HyClone Laboratories, Utah, USA) supplemented with 10% fetal bovine serum (FBS, Gibco, Grand Island, NY, USA). The UW228-2 cell line was cultured in DMEM (Invitrogen, Grand Island, NY, USA) containing 10% fetal bovine serum (FBS, Gibco, Grand Island, NY, USA), penicillin (100 U/ml), and streptomycin (100 mg/ml) and was maintained in a humidified incubator at 37°C with 5% CO_2.

Cell Treatments

Resveratrol (Res), all-trans retinoic acid (RA; Sigma-Aldrich, St. Louis, MO, USA), and Gemcitabine (GEM; Sigma-Aldrich, St. Louis, MO, USA) were dissolved in dimethylsulfoxide (DMSO, Sigma-Aldrich) to 100, 80, and 50 mM stock concentrations, respectively, and diluted with a culture medium to an optimal working concentration of 100 (16), 10 (12), and 10 μM (17) just before use. THJ-11T and UW228-2 cells were treated with 100 μM resveratrol and 10 μM gemcitabine for 12, 24, 48 h. A total of 5×10^4/ml of the cells were plated to culture dishes (Nunc A/S, Roskilde, Denmark) and incubated for 24 h before further experiments. Dozens of cell-bearing coverslips were concurrently prepared under the same experimental condition using the high throughput coverslip-preparation dishes (Jet Biofile Tech. Inc., Guangzhou, China; China invention patent No. ZL200610047607.8), which were collected during drug treatments, fixed with cold acetone, and used for haematoxylin and eosin (H/E) staining, immunocytochemical labeling (ICC), and TUNEL apoptosis assay. The experimental groups were set in triplicate, and the experiments were repeated three times to establish a definite conclusion.

Cell Proliferation and Apoptotic Death Assays

Hematoxylin-Eosin (H/E) staining was used to observe the morphological changes of THJ-11T cells treated with resveratrol alone, retinoic acid alone, resveratrol, and retinoic acid. A terminal deoxynucleotide transferase (TdT)–mediated dUTP-biotin nick-end labeling (TUNEL) assay was employed to detect apoptotic cells according to producer's instructions (Promega Corporation, USA). The effect of drug treatment on cell proliferation was determined by 3-[4,5-dimethylthiazol-2-yl]-2,5-diphenyl-tetrazolium bromide (MTT) assay. Cells (1×10^4/well) were plated in 96-well flat-bottomed culture plates (Falcon, Becton–Dickinson Labware, Franklin Lakes, NJ, USA) and routinely cultured in 100 μl RPMI1640 medium for 24 h, followed by 48 h of 100 μM Res, 10 μM RA, or their combination (Res/RA) treatment. By the end of the treatments, MTT reagent was added to each well and the plate was incubated for 4 h at

37°C. DMSO was added and the optical density (OD) of the sample plate was measured at 492 nm in a microplate reader.

Genomic DNA Extraction and Bisulfite Sequencing PCR

By the method described elsewhere (12), DNA samples were extracted from THJ-11T and UW228-2 cells, placed in a 1.5-ml Eppendorf tube containing 10–30 μl of a 1% sodium dodecyl sulfate-containing TE buffer (Tris.Cl + EDTA, pH8.0). Bisulfite treatment of the isolated DNA was carried out using a BisulFlash DNA Modification Kit (EPIGENTEK, USA), according to manufacturer's protocol. A pair of PCR primers in the sequences of CRABP2-F, 5′-GGGTTTTTGTTTAATTTTTTAATGTT-3′ and CRABP2-R, 5′-CCTCACCAAAATAACCTAAATCAA-3′ was used for sequencing critical CpG sites within an intron of the CRABP2 gene (12). According to the protocol provided with the TaKaRa EpiTaq HS (R110Q, TaKaRa), the DNA samples were converted for bisulfite sequencing PCR (BSP) and the selected promoter regions were amplified thereafter.

Methylation Sequencing and Analysis

The modified DNA samples were amplified using a TaKaRa PCR amplification Kit (TaKaRa Biotech. Inc., Dalian, China) and the products were sequenced in reverse direction by TaKaRa Biotech Inc. using an ABI PRISM^{TM} (Applied Biosystems Inc., Foster City, CA, USA) 3730XL DNA Analyzer and ABI PRISM^{TM} 377XL DNA sequencer. Simultaneously, the sample DNA isolated from UW228-2 cells expressing CRABP2 was used as positive control for promoter methylation. The BSP-generated sequences were compared with the sequence of the corresponding region in the normal human genome (https://www.ncbi.nlm.nih.gov/nuccore/NC_000001.11?from=156699606&to=156706251&report=genbank&strand=true).

RNA Isolation and RT-PCR

After resveratrol and gemcitabine treatments for 12, 24, and 48 h, total RNA samples were isolated from the cells using Trizol solution (Life Tech, Texas, USA) and subjected to RT-PCR, using the primers specific for CRABP2, DNMT1, DNMT3A, and DNMT3B (**Table 1**), according to the producer's protocols of Takara RNA PCR kit (AMV) version 3.1 (Takara, Dalian Branch, Dalian, China). The PCR products were separated on 1.2% agarose gel containing ethidium bromide (0.5 mg/ml), visualized, and photographed using the UVP Biospectrum Imaging System (UVP Inc., Upland, CA). mRNA levels were normalized to levels of β-actin.

Protein Preparation and Western Blotting

Proteins were extracted from the drug-treated cells under different experimental conditions. Equivalent amounts of sample proteins were separated by 8–12% SDS-PAGE electrophoresis and transferred to a polyvinylidene difluoride membrane (Amersham, Buckinghamshire, UK). The membrane was blocked with 5% non-fat dry milk (Sigma-Aldrich) in TBS-T (10 mM Tris-HCl, PH8.0, 150 mM NaCl, and 0.5% Tween 20) for 2 h at room temperature and incubated with anti-caspases-3 (Abcam Inc., Cambridge, UK;1:500), anti-CRABP2 (Proteintech, Chicago, IL, USA; 1:200), anti-DNMT1 (Bioss. Inc., Beijing, China; 1:300), anti-DNMT3A (Bioss. Inc., Beijing, China; 1:1,000), and anti-DNMT3B (Bioss. Inc., Beijing, China; 1:300) primary antibodies overnight at 4°C. After three washes with TBS-T, the membrane was incubated for 1.5 h with HRP-conjugated anti-mouse or anti-rabbit IgG (Zymed Lab, Inc.). Protein expression was detected using chemiluminescent ECL reagents (Roche GmbH, Mannheim, Germany). A Gel-Pro analyzer was used to measure the density of bands. Simultaneously, the expression of a target protein was normalized to that of β-Actin.

TABLE 1 | Primer sequences for conventional RT-PCR and methylation specific PCR.

Gene	Primers	Amplicon size	Annealing
CRABP2	F:5′-ATGCCCAACTTCTCTGGCAA-3′ R:5′-CGTCATGGTCAGGATCAGTT-3′	375 bp	59°C
DNMT1	F: 5′-ACC GCT TCT ACTTCCTCGAGG CCTA-3′ R:5′-GTTGCAGTCCTCTGTGAACACT GTGG-3′	335 bp	55°C
DNMT3A	F:5′-GGGGACGTCCGcAGcGTC ACAC-3′, R:5′-CAGGGTTGGACTCGAGAAA TCGC-3′;	280 bp	65°C
DNMT3B	F:5′ -CCT GCT GAATTACTCACGCCCC-3′, R:5′-GTCTGTGTAGTGCACAGGAA AGCC-3′;	421 bp	65°C
ß-actin	F:5′-GCATGGAGTCCTGTGGCAT-3′, R:5′-CATGAAGCATTTGCGGTGG-3′	326 bp	58°C
Primers for bisulfite sequencing PCR			
CRABP2	F:5′-GGGTTTTTGTTTAATTTTTTAA TGTT-3′, R:5′-CCTCACCAAAATAACCTAAA TCAA-3′	215 bp	58°C

Immunocytochemical Staining

Immunocytochemical staining (ICC) was performed on the cell-bearing coverslips obtained from each of the experimental groups by the method described elsewhere (18). The antibodies used were: DNMT1 (Bioss Inc., Beijing, China; 1:400), DNMT3A (Bioss. Inc., Beijing, China; 1:400), DNMT3B (Bioss. Inc., Beijing, China; 1:400), and CRABP2 (Proteintech, Chicago, IL, USA; 1:150). The color reaction was performed by using 3,30-diaminobenzidine tetrahydrochloride (DAB). According to the labeling intensity, the staining results were evaluated by two independent researchers and scored as negative (–) if no immunolabeling was observed in target cells, weakly positive (+) if the labeling was faint, moderately positive (++), and strongly positive (> ++) when the labeling was stronger or distinctly stronger than (++).

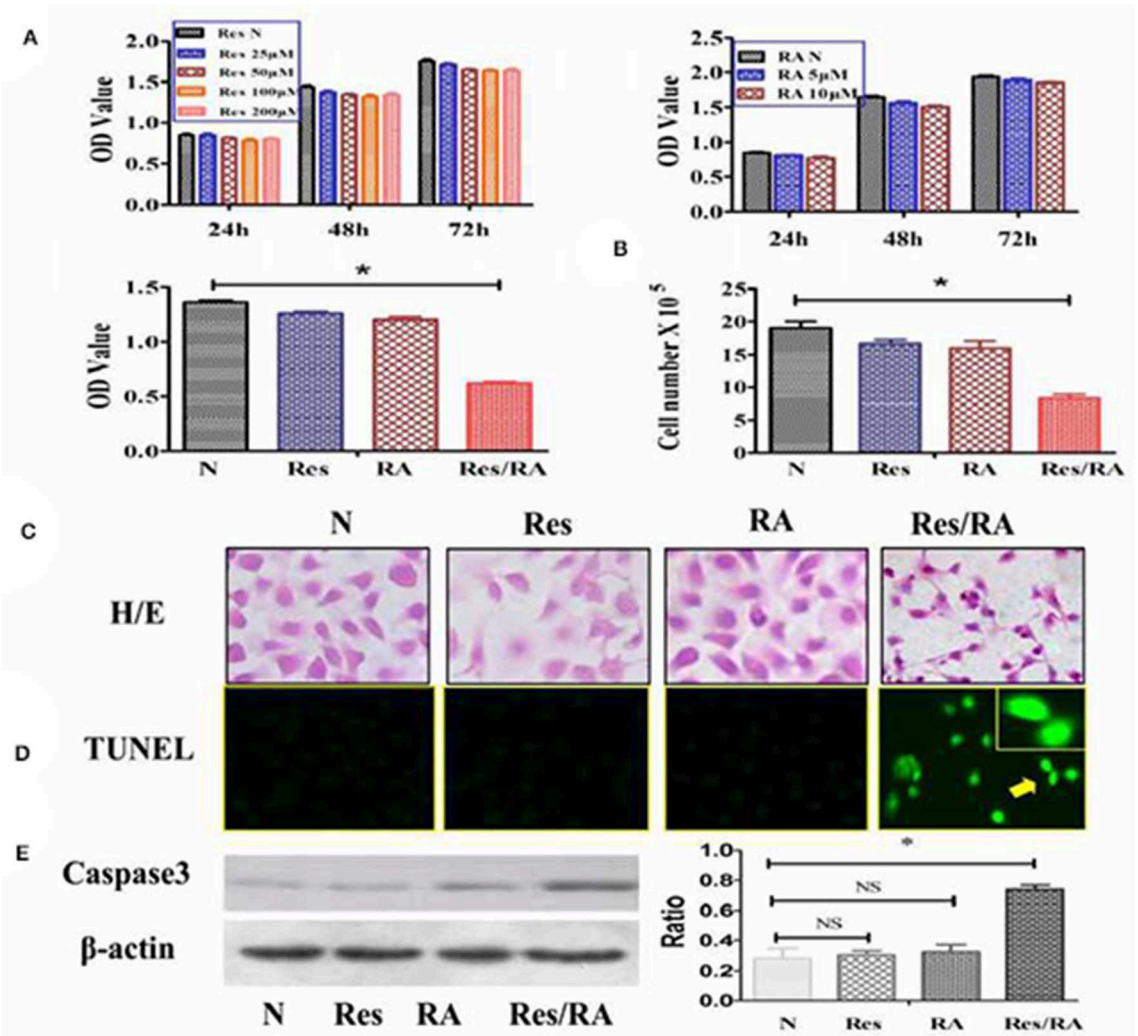

FIGURE 1 | Resveratrol improved RA sensitivity of anaplastic thyroid cancer THJ-11T cells. **(A)** 3-[4,5-Dimethylthiazol-2-yl]-2,5-diphenyl-tetrazolium bromide (MTT) cell proliferation assay; **(B)** viable cell counting after drug treatment for 48 h; **(C)** H&E morphological staining(×40); **(D)** deoxynucleotidyl transferase-mediated dUTP-biotin nick and labeling assay (TUNEL) for apoptotic cell labeling (Green in color; ×40); **(E)** Western Blotting; N, cultured in 0.2% dimethylsulfoxide (DMSO)-containing medium; Res, 100 μM resveratrol treatment; RA, 10 μM retinoic acid treatment; Res/RA, treated with a combination of 100 μM resveratrol and 10 μM retinoic acid for 48 h. Ratio, the ratio between the levels of the target molecules and that of β-actin; NS, no statistical significance ($p > 0.05$); *$p < 0.01$; the error bars, the mean ± standard deviation. Arrows indicate the region with higher magnification (×80) in the insets.

Statistical Analyses

Each experiment was conducted three times, and the data obtained were analyzed together. The results of the MTT cell proliferation assay and cell counting were evaluated with ANOVA and the independent-samples *t*-test. The bar graphs present the mean ± standard deviation (SD) of separate experiments. When required, *p*-values are provided in the figures and their legends.

RESULTS

Resveratrol Reversed RA Tolerance

The MTT cell proliferation assay was conducted on THJ-11T cells treated with Res in the concentrations of 25, 50, 100, or 200 μM and with RA in the concentrations of 5 or 10 μM for 24, 48, and 72 h respectively. As shown in **Figure 1A**, all of the experimental groups had similar OD values in comparison with that of the 0.2% dimethyl sulfoxide (DMSO)-treated cells (N) ($p > 0.05$). In contrast, the OD value of the 100 μM Res/10 μM RA-treated THJ-11T cells was significantly reduced in comparison with those of other groups ($P < 0.01$). The total number of THJ-11T cells was remarkably decreased (**Figure 1B**) after 48 h 100 μM resveratrol/10 μM RA treatment ($p < 0.05$). No significant phenotypic change was observed either in the 100 μM Res or in the 10 μM RA treated population, whereas the size of Res/RA-treated cells became smaller with elongated protrusion (**Figure 1C**). TUNEL assay showed distinct cell death only in the THJ-11T cell population treated by Res/RA

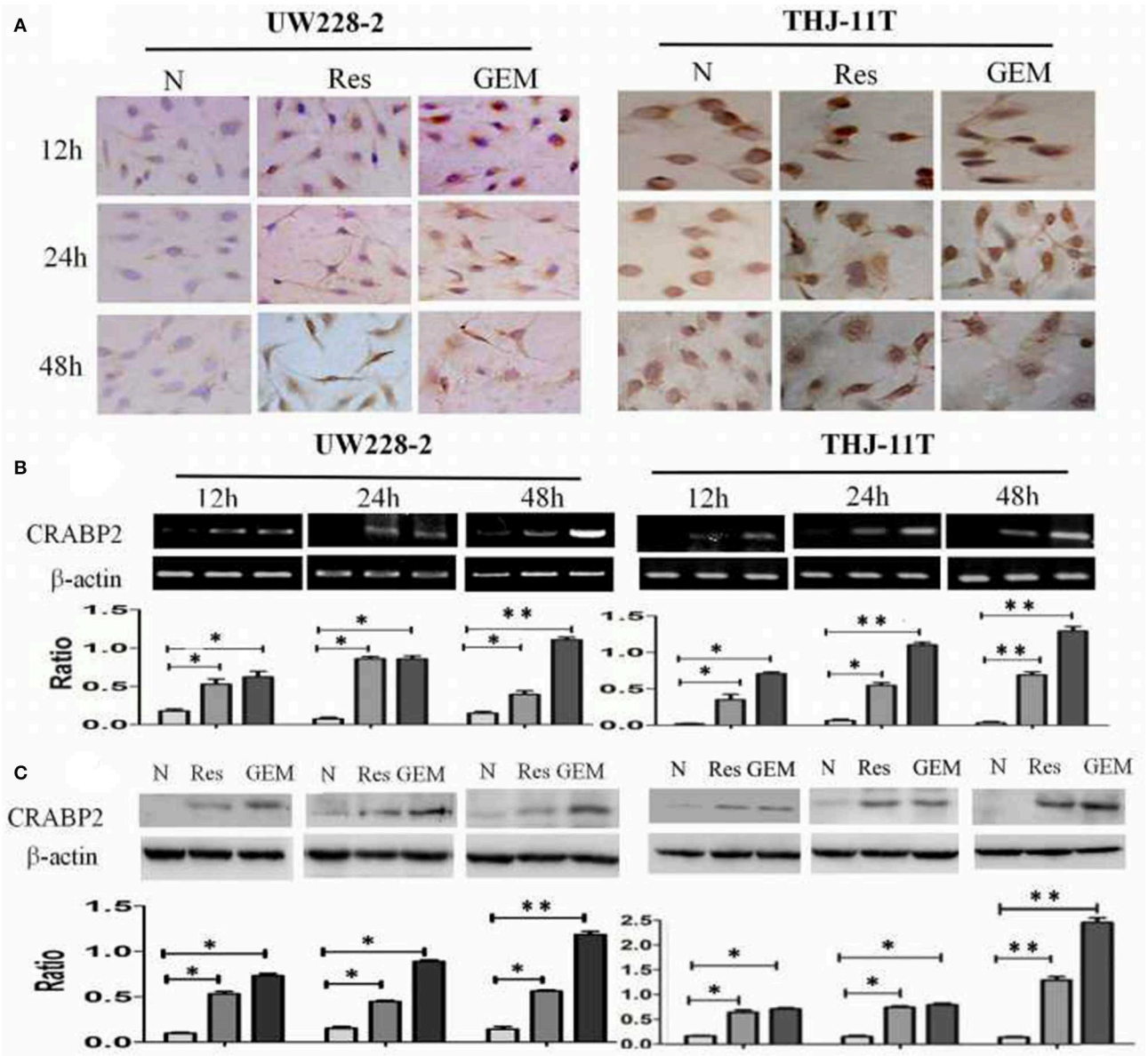

FIGURE 2 | Demonstration of upregulated CRABP2 expression in 100 μM resveratrol (Res) or 10 μM gemcitabine (GEM)-treated THJ-11T and UW228-2 cells. **(A)** Immunocytochemical staining (×40); **(B)** RT-PCR; **(C)** Western blotting. β-actin was used as qualitative and quantitative control. N, cultured in 0.2% dimethylsulfoxide (DMSO)-containing medium; Res, 100 μM resveratrol; GEM, 10 μM gemcitabine. Ratio, the ratio between the levels of the target molecules and that of β-actin; NS, no statistical significance ($p > 0.05$); *with statistical significance ($p < 0.01$; **$p < 0.001$) the error bars, the mean ± standard deviation.

combination for 48 h (**Figure 1D**). The gray density analyses of the Western blotting results showed a 2.6-fold increase of caspase 3 production in Res/RA-treated cells but not in ones treated by Res or RA alone (**Figure 1E**).

Resveratrol Upregulated CRABP2 Expression

THJ-11T and UW228-2 cells were treated with resveratrol and gemcitabine for 12, 24, and 48 h, respectively to evaluate the levels of CRABP2 expression. Accompanied by morphological changes, both cell lines showed CRABP2 upregulation by either resveratrol or gemcitabin in a time-related fashion (**Figures 2A–C**; **Table 2**). It was also found that CRABP2 levels in gemcitabine-treated THJ-11T and UW228-2 cells

TABLE 2 | CRABP2 immunocytochemical staining patterns in UW228-2 and THJ-11T cells under different experimental conditions.

	12 h			24 h			48 h		
	N	Res	GEM	N	Res	GEM	N	Res	GEM
UW228-2	-	+	+	-	+	+	-	++	+++
THJ-11T	-	+	+	-	+	+	-	+	++

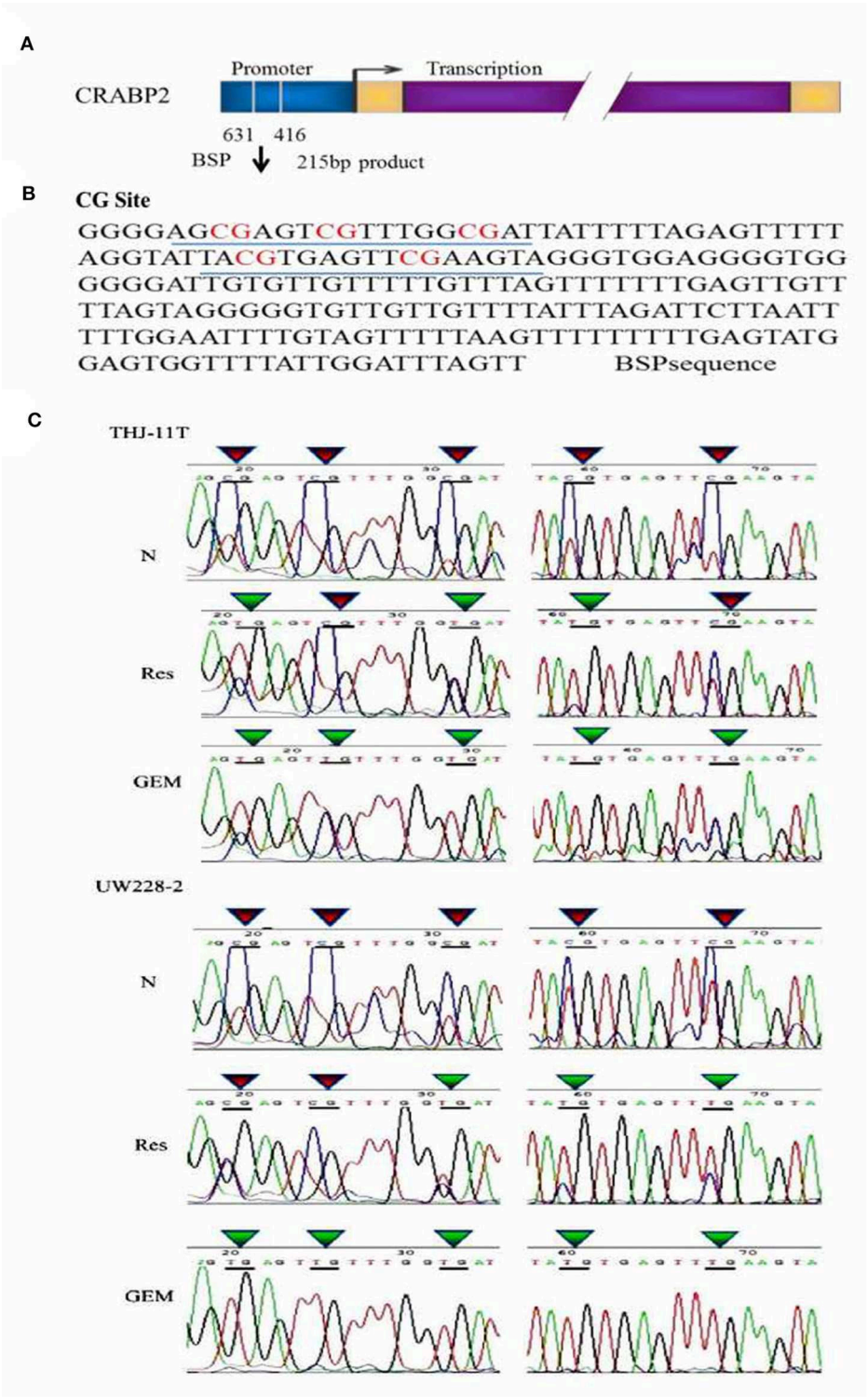

FIGURE 3 | BSP sequencing demonstration of 5 CG site methylation of −631 to −416 CRABP2 promoter region and differential demethylation effects of resveratrol and gemcitabine **(A)** Scheme of CRABP2 gene and the location of BSP amplified promoter region; **(B)** the nucleotide sequence of BSP product and the locations of 5 CG sites; **(C)** demonstration of the sequencing result of the underlined region **(B)** of CRABP2 BSP product generated from UW228-2 and THJ-11T sample DNAs without (N) and with 48 h 100 μM resveratrol (Res) or 10 μM gemcitabine (GEM) treatment. In bisulfite sequencing PCR (BSP), the unmethylated C-bases become U-base in sulfite-treated DNA and are replaced by T-base after PCR; the methylated C-base cannot be converted by sulfite and remain as a C-base in the BSP product. Our sequencing results revealed five CpG methylation sites in the CRABP2 promoter region which were partially (3/5) erased (CpG to TpG) by resveratrol and completely (5/5) erased by gemcitabine.

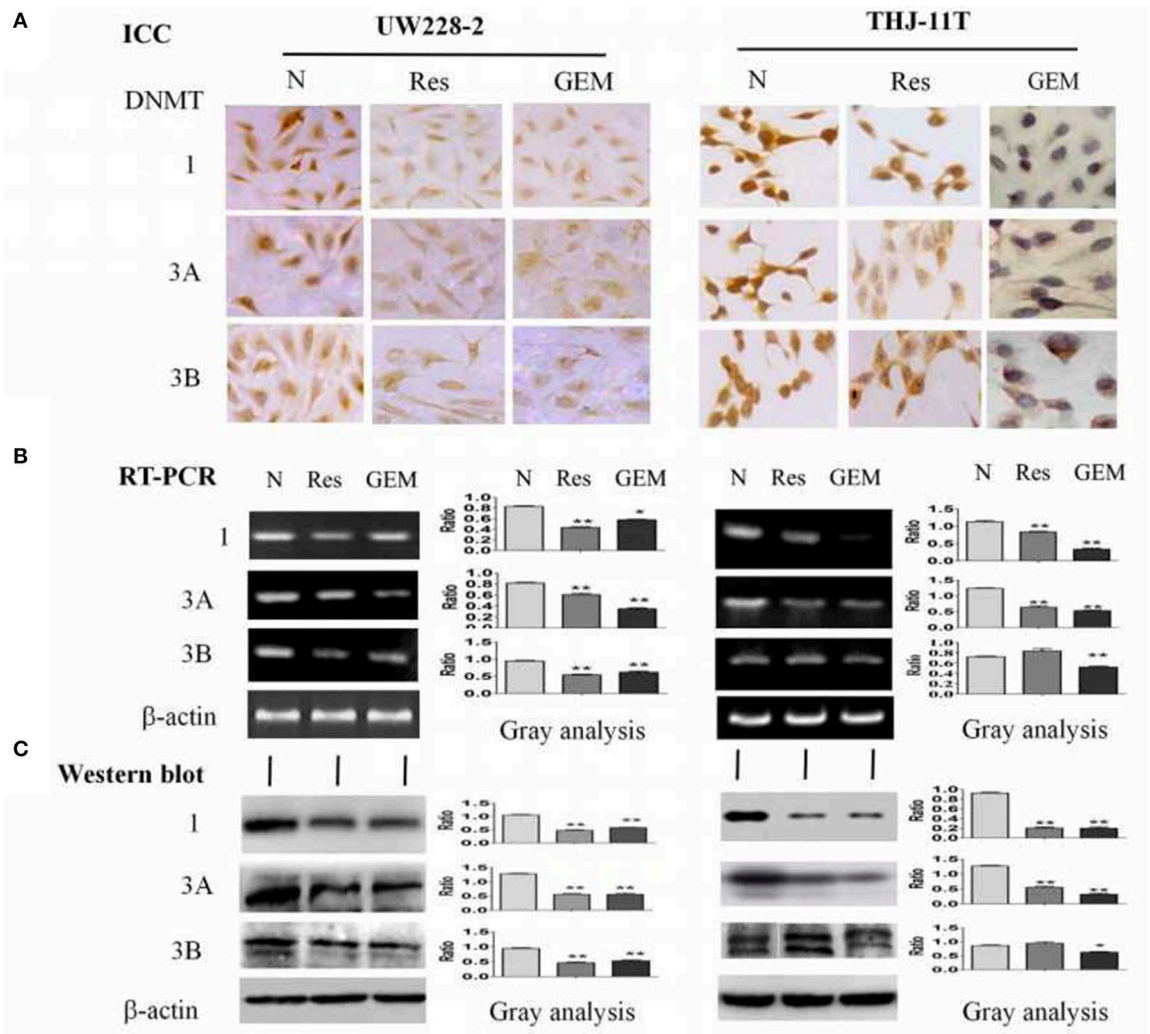

FIGURE 4 | Demonstration of suppressed DNMT1, DNMT3A, and DNMT3B expression in 100 μM resveratrol (Res) or 10 μM gemcitabine (GEM) treated THJ-11T and UW228-2 cells for 48 h. **(A)** Immunocytochemical staining (×40); **(B)** RT-PCR; **(C)** Western blotting. β-actin was used as qualitative and quantitative control. N, cultured in 0.2% dimethylsulfoxide (DMSO)-containing medium; Res, 100 μM resveratrol; GEM, 10 μM gemcitabine. Ratio, the ratio between the levels of the target molecules and that of β-actin; NS, no statistical significance ($p > 0.05$); *with statistical significance ($p < 0.05$); **$p < 0.01$; ***$p < 0.001$; the error bars, the mean ± standard deviation.

were 36 and 33% higher than that of their resveratrol-treated counterparts.

CRABP2 Promoter Methylation in UW228-2 and THJ-11T Cells

In accordance with our previous finding (12), the methylation of the CRABP2 promoter region in UW228-2 cells was re-evidenced and therefore cited as the positive control in the sequencing analysis of the CRABP2 PCR product of THJ-11T sample DNA. As shown in **Figure 3**, five CpG islands in the CRABP2 promoter region of ATC THJ-11T cells and medulloblastoma UW228-2 cells were methylated.

Partial Demethylation of CRABP2 by Resveratrol in Bisulfite Sequencing

To investigate the effect of resveratrol on methylation of the CRABP2 promoter region, THJ-11T and UW228-2 cells were treated with resveratrol and gemcitabine for 48 h and their CRABP2 PCR products were sequenced. As shown in **Figure 3C**, the five methylation sites of THJ-11T and UW228-2 were partly (3/5) erased after resveratrol and totally (5/5) after gemcitabine treatment.

Resveratrol Inhibited DNA Methyltransferase Expression

To disclose the underlying mechanism of resveratrol-mediated demethylation, THJ-11T and UW228-2 cells were treated by resveratrol or gemcitabine for 48 h, followed by RT-PCR, ICC and Western blot examinations for DNA methyltransferase DNMT1, DNMT3A, and DNMT3B, respectively. As shown in **Figure 4** and **Table 3**, the three enzymes in resveratrol-treated UW228-2 cells were obviously downregulated in both RNA and protein levels. DNMT1 and DNMT3A were downregulated in resveratrol-treated THJ-11T cells, while DNMT3B did not

TABLE 3 | DNMT1, DNMT3A, and DNMT3B immunocytochemical staining patterns of UW228-2 and THJ-11T cells cultured for 48 h under different experimental conditions.

	UW228-2			THJ-11T		
	N	Res	GEM	N	Res	GEM
DNMT1	++	+	+	+++	++	-
DNMT3A	++	+	-	+++	+	-
DNMT3B	++	+	-	+	++	-

change significantly. The expression of three methyltransferases was downregulated in both cell lines after gemcitabine treatment, and their overall reductions were more distinct in comparison with that of resveratrol-treated UW228-2 and, especially, THJ-11T cells.

DISCUSSION

CRABP2 has been known to be a central player in RA anticancer signal transduction (19, 20). However, this gene is often down-regulated or silenced by methylation and, therefore, results in RA tolerance in a variety of cancer cells (11–13, 21, 22). For instance, CRABP2 is silenced in the RA-resistant medulloblastoma UW228-2 cells due to CpG island methylation in the promoter region (12). When CRABP2 expression was restored by 5-aza-2′-deoxycytidine, UW228-2 cells showed increased RA sensitivity in terms of growth suppression and apoptosis (10), suggesting that the methylation-silenced CRABP2 expression is responsible for RA tolerance of UW228-2 cells. Our recent data demonstrated that resveratrol could effectively overcome RA resistance of THJ-11T cells in which CRABP2 expression was downregulated (9). Considering the important role of CRABP2 in the RA anticancer pathway, we speculated that resveratrol might enhance the RA sensitivity of THJ-11T via altering the methylation status of CRABP2.

Bisulfite sequencing PCR (BSP) product sequencing has been commonly used to identify gene methylation, because the unmethylated C bases—rather than the methylated C—are changed to U in the sulfite-treated DNA, and only the unmethylated C base is replaced by T after PCR amplification, which can be detected by BSP sequencing (23–25). To ascertain the relevance of resveratrol-upregulated CRABP2 expression with DNA demethylation, the sample DNAs were isolated from medulloblastoma UW228-2 and anaplastic thyroid cancer THJ-11T cells before and after resveratrol treatment and subjected to BSP PCR and the sequencing of BSP products. The results showed that, in a similar fashion to the situation of UW228-2 cells, five methylated CpG sites at the CRABP2 promoter region of THJ-11T cells were methylated. In the case of DNA samples isolated from UW228-2 and THJ-11T cells treated by resveratrol and gemcitabine, CpG island methylation in the CRABP2 promoter region was partly erased (3/5) by resveratrol and totally (5/5) by gemcitabine, indicating that gemcitabine posed a more powerful demethylation effect than resveratrol. Despite this, the results of the current study once again demonstrate the demethylation activity of resveratrol in cancer cells (26). Because DNA methylation is the major cause of drug tolerance in many cancer cells (27–30), gemcitabine and other demethylators are increasingly used in clinical cancer treatments in a single dose or a more comprehensive manner (31–33). Nevertheless, these agents cause some toxic effects, such as gene mutation, chromosomal rearrangement, and embryonic development defects (15). Unlike conventional demethylating agents, resveratrol exerts little adverse effects on normal tissues/cells in anticancer doses (34). Taking CRABP2 as an example, although the demethylation efficacy of resveratrol is not as strong as gemcitabine, it is still sufficient to upregulate CRABP2 expression and consequently reverse RA resistance of UW228-2 and THJ-11T cells. These findings thus provide an alternative approach to treat cancers using resveratrol as an epigenetic regulator.

It has been recognized that DNA methylation is mediated by the DNA methyltransferase (DNMT) enzyme family, of which DNMT1, DNMT3A, and DNMT3B play active roles (35, 36). The DNMTs can catalyze the transfer of methyl group from S-adenosylmethionine to C in CpG dinucleotide and methylation to 5-methylcytosine (5mC) (37). Therefore, the levels of DNA methyltransferase expression are positively correlated with the extent of CpG island methylation (38). In the stepwise carcinogenesis, over-expressed DNMTs lead to methylation silencing of some tumor suppressor genes (39), and downregulation of DNMT expression can reverse the silencing of those genes by weakening their promoter methylation (40–42). Therefore, demethylation of tumor suppressor genes has become an anticancer strategy and suppression of DNA methyltransferase activity with DNMT inhibitors such as gemcitabine is proved as an efficient way (43, 44). To investigate the underlying mechanism of resveratrol-caused demethylation, the patterns of DNMT1, DNMT3A, and DNMT3B expression in UW228-2 and THJ-11T cells before and after resveratrol treatment were analyzed. The results revealed the downregulated DNMT1, DNMT3A, and DNMT3B expression in resveratrol-treated UW228-2 cells and downregulated DNMT1 and DNMT3A in THJ-11T cells. In a similar vein as with the different demethylation efficacies of resveratrol and gemcitabine on CRABP2, gemcitabine shows better suppressive effects on the three DNMTs. Given the above evidence, it would be possible that suppression of DNMT expression may be responsible for resveratrol-caused CRABP2 demethylation, although the causality of these two molecular events remains to be confirmed. Alternatively, this correlative analysis indicates that resveratrol may exert demethylation in the same way as gemcitabine. Given the evidence of the non-toxic and multiple targeting properties of resveratrol, this polyphenol compound may have distinct advantages over gemcitabine and would be an alternative demethylating drug for cancer prevention and treatment. As our *in vitro* results are obtained from the cancer cells treated by a high

concentration (100 μM) of resveratrol, the practical anti-ATC values of resveratrol should be further investigated in the animal cancer models by optimizing the dose and the way of resveratrol administration.

Taken together, CpG island methylation in the CRABP2 promoter region is evidenced in RA-resistant human ATC THJ-11T and medulloblastoma UW228-2 cells, which can be largely erased by resveratrol in the same manner as gemcitabine, demonstrating the ability of resveratrol in DNA demethylation. Reduction of DNMT1, DNMT3A, and DNMT3B expression is found in both resveratrol- and gemcitabine-treated cells, which is correlated to the recovered levels of CRABP2 expression. Although the efficacy of the epigenetic regulation of resveratrol is not as powerful as that of gemcitabine, it is still able to resume CRABP2 expression and reverses RA-resistance of the two checked cell lines. In this context, resveratrol can be regarded as either a DNA demethylator or multiple targeting agent in cancer management (45–48). The preventive potential of oral and intraperitoneal administered resveratrol in DEN/MNU/DHPN-induced rat thyroid tumorigenesis may further support this notion (49).

DATA AVAILABILITY STATEMENT

The raw data supporting the conclusions of this manuscript will be made available by the authors, without undue reservation, to any qualified researcher.

AUTHOR CONTRIBUTIONS

K-LZ and JL contributed conception and design of the study. HL organized the database. XL, HL, JW, and M-LW performed the statistical analysis. XL and HL wrote the first draft of the manuscript. XL, HL, and YS wrote sections of the manuscript. All authors contributed to manuscript revision, read, and approved the submitted version.

FUNDING

This work was supported by the grants from the National Natural Science Foundation of China (No. 81272786 and 81450016), the Program Fund for Liaoning Provincial Department of Education Key Laboratory (LF2017002), the Liaoning Provincial Program for Top Discipline of Basic Medical Sciences, and the special grant to the creative research team from South China University of Technology.

ACKNOWLEDGMENTS

The authors express gratitude to Dr. Quentin Liu at the Institute of Cancer Stem Cell, Dalian Medical University, for providing anaplastic thyroid cancer THJ-11T cell lines and the doctors in the Department of Neurological Surgery, University of Washington, Seattle, for providing the UW228-2 medulloblastoma cell lines.

REFERENCES

1. Simon D, Kohrle J, Schmutzler C, Mainz K, Reiners C, Roher HD. Redifferentiation therapy of differentiated thyroid carcinoma with retinoic acid: basics and first clinical results. *Exp Clin Endocrinol Diab*. (1996) 104(Suppl 4):13–5. doi: 10.1055/s-0029-1211692
2. Schmutzler C, Kohrle J. Retinoic acid redifferentiation therapy for thyroid cancer. *Thyroid*. (2000) 10:393–406. doi: 10.1089/thy.2000.10.393
3. Schug TT, Berry DC, Shaw NS, Travis SN, Noy N. Opposing effects of retinoic acid on cell growth result from alternate activation of two different nuclear receptors. *Cell*. (2007) 129:723–33. doi: 10.1016/j.cell.2007.02.050
4. Are C, Shaha AR. Anaplastic thyroid carcinoma: biology, pathogenesis, prognostic factors, and treatment approaches. *Ann Surg Oncol*. (2006) 13:453–64. doi: 10.1245/ASO.2006.05.042
5. Wu H, Sun Y, Ye H, Yang S, Lee SL, de las Morenas A. Anaplastic thyroid cancer: outcome and the mutation/expression profiles of potential targets. *Pathol Oncol Res*. (2015) 21:695–701. doi: 10.1007/s12253-014-9876-5
6. Molinaro E, Romei C, Biagini A, Sabini E, Agate L, Mazzeo S, et al. Anaplastic thyroid carcinoma: from clinicopathology to genetics and advanced therapies. *Nat Rev Endocrinol*. (2017) 13:644–60. doi: 10.1038/nrendo.2017.76
7. Malehmir M, Haghpanah V, Larijani B, Ahmadian S, Alimoghaddam K, Heshmat R, et al. Multifaceted suppression of aggressive behavior of thyroid carcinoma by all-trans retinoic acid induced re-differentiation. *Mol Cell Endocrinol*. (2012) 348:260–9. doi: 10.1016/j.mce.2011.09.002
8. Courbon F, Zerdoud S, Bastie D, Archambaud F, Hoff M, Eche N, et al. Defective efficacy of retinoic acid treatment in patients with metastatic thyroid carcinoma. *Thyroid*. (2006) 16:1025–31. doi: 10.1089/thy.2006.16.1025
9. Li YT, Tian XT, Wu ML, Zheng X, Kong QY, Cheng XX, et al. Resveratrol suppresses the growth and enhances retinoic acid sensitivity of anaplastic thyroid cancer cells. *Int J Mol Sci*. (2018) 19:E1030. doi: 10.3390/ijms19041030.
10. Chen NN, Li Y, Wu ML, Liu ZL, Fu YS, Kong QY, et al. CRABP-II- and FABP5-independent all-trans retinoic acid resistance in COLO 16 human cutaneous squamous cancer cells. *Exp Dermatol*. (2012) 21:13–8. doi: 10.1111/j.1600-0625.2011.01392.x
11. Gupta S, Pramanik D, Mukherjee R, Campbell NR, Elumalai S, de Wilde RF, et al. Molecular determinants of retinoic acid sensitivity in pancreatic cancer. *Clin Cancer Res*. (2012) 18:280–9. doi: 10.1158/1078-0432.CCR-11-2165
12. Fu YS, Wang Q, Ma JX, Yang XH, Wu ML, Zhang KL, et al. CRABP-II methylation: a critical determinant of retinoic acid resistance of medulloblastoma cells. *Mol Oncol*. (2012) 6:48–61. doi: 10.1016/j.molonc.2011.11.004
13. Zhang GM, Song CC, Li LJ, He H, Shi SY, Lei CZ, et al. DNA methylation status of CRABP2 promoter down-regulates its expression. *Gene*. (2018) 676:243–8. doi: 10.1016/j.gene.2018.07.049
14. Unnikrishnan A, Papaemmanuil E, Beck D, Deshpande NP, Verma A, Kumari A, et al. Integrative genomics identifies the molecular basis of resistance to azacitidine therapy in myelodysplastic syndromes. *Cell Rep*. (2017) 20:572–85. doi: 10.1016/j.celrep.2017.06.067
15. Gravina GL, Festuccia C, Marampon F, Popov VM, Pestell RG, Zani BM, et al. Biological rationale for the use of DNA methyltransferase inhibitors as new strategy for modulation of tumor response to chemotherapy and radiation. *Mol Cancer*. (2010) 9:305. doi: 10.1186/1476-4598-9-305
16. Zheng X, Jia B, Tian XT, Song X, Wu ML, Kong QY, et al.. Correlation of reactive oxygen species levels with resveratrol sensitivities of anaplastic thyroid cancer cells. *Oxid Med Cell Longev*. (2018) 2018:6235417. doi: 10.1155/2018/6235417
17. Koh V, Kwan HY, Tan WL, Mah TL, Yong WP. Knockdown of POLA2 increases gemcitabine resistance in lung cancer cells. *BMC Genomics*. (2016) 17(Suppl 13):1029. doi: 10.1186/s12864-016-3322-x
18. Yu LJ, Wu ML, Li H, Chen XY, Wang Q, Sun Y, et al. Inhibition of STAT3 expression and signaling in resveratrol-differentiated medulloblastoma cells. *Neoplasia*. (2008) 10:736–44. doi: 10.1593/neo.08304

19. Liu RZ, Li S, Garcia E, Glubrecht DD, Poon HY, Easaw JC, et al. Association between cytoplasmic CRABP2, altered retinoic acid signaling, and poor prognosis in glioblastoma. *Glia*. (2016) 64:963–76. doi: 10.1002/glia.22976
20. Favorskaya I, Kainov Y, Chemeris G, Komelkov A, Zborovskaya I, Tchevkina E. Expression and clinical significance of CRABP1 and CRABP2 in non-small cell lung cancer. *Tumour Biol*. (2014) 35:10295–300. doi: 10.1007/s13277-014-2348-4
21. Campos B, Warta R, Chaisaingmongkol J, Geiselhart L, Popanda O, Hartmann C, et al. Epigenetically mediated downregulation of the differentiation-promoting chaperon protein CRABP2 in astrocytic gliomas. *Int J Cancer*. (2012) 131:1963–8. doi: 10.1002/ijc.27446
22. Calmon MF, Rodrigues RV, Kaneto CM, Moura RP, Silva SD, Mota LD, et al. Epigenetic silencing of CRABP2 and MX1 in head and neck tumors. *Neoplasia*. (2009) 11:1329–39. doi: 10.1593/neo.91110
23. Herrmann A, Haake A, Ammerpohl O, Martin-Guerrero I, Szafranski K, Stemshorn K, et al. Pipeline for large-scale microdroplet bisulfite PCR-based sequencing allows the tracking of hepitype evolution in tumors. *PLoS ONE*. (2011) 6:e21332. doi: 10.1371/journal.pone.0021332
24. Eckhardt F, Lewin J, Cortese R, Rakyan V. K, Attwood J, Burger M, et al. DNA methylation profiling of human chromosomes 6, 20 and 22. *Nat Genet*. (2006) 38:1378–85. doi: 10.1038/ng1909
25. Zeschnigk M, Martin M, Betzl G, Kalbe A, Sirsch C, Buiting K, et al. Massive parallel bisulfite sequencing of CG-rich DNA fragments reveals that methylation of many X-chromosomal CpG islands in female blood DNA is incomplete. *Hum Mol Genet*. (2009) 18:1439–48. doi: 10.1093/hmg/ddp054
26. Kang S, Wang Z, Li B, Gao X, He W, Cao S, et al. Anti-tumor effects of resveratrol on malignant melanoma is associated with promoter demethylation of RUNX3 gene. *Pharmazie*. (2019) 74:163–7. doi: 10.1691/ph.2019.8838
27. Da Costa EM, McInnes G, Beaudry A, Raynal NJ. DNA methylation-targeted drugs. *Cancer J*. (2017) 23:270–6. doi: 10.1097/PPO.0000000000000278
28. Hsieh TH, Liu YR, Chang TY, Liang ML, Chen HH, Wang HW, et al. Global DNA methylation analysis reveals miR-214-3p contributes to cisplatin resistance in pediatric intracranial nongerminomatous malignant germ cell tumors. *Neuro Oncol*. (2018) 20:519–30. doi: 10.1093/neuonc/nox186
29. Abdel-Hafiz HA. Epigenetic mechanisms of tamoxifen resistance in luminal breast cancer. *Diseases*. (2017) 5:E16. doi: 10.3390/diseases5030016.
30. Zhang Y, Xiang C, Wang Y, Duan Y, Liu C, Zhang Y. PD-L1 promoter methylation mediates the resistance response to anti-PD-1 therapy in NSCLC patients with EGFR-TKI resistance. *Oncotarget*. (2017) 8:101535–44. doi: 10.18632/oncotarget.21328
31. Linnekamp JF, Butter R, Spijker R, Medema JP, van Laarhoven HWM. Clinical and biological effects of demethylating agents on solid tumours–a systematic review. *Cancer Treat Rev*. (2017) 54:10–23. doi: 10.1016/j.ctrv.2017.01.004
32. Sato T, Issa JJ, Kropf P. DNA hypomethylating drugs in cancer therapy. *Cold Spring Harb Perspect Med*. (2017) 7:a026948. doi: 10.1101/cshperspect.a026948
33. Azad NS, El-Khoueiry A, Yin J, Oberg AL, Flynn P, Adkins D, et al. Combination epigenetic therapy in metastatic colorectal cancer (mCRC) with subcutaneous 5-azacitidine and entinostat: a phase 2 consortium/stand up 2 cancer study. *Oncotarget*. (2017) 8:35326–38. doi: 10.18632/oncotarget.15108
34. Zhong LX, Zhang Y, Wu ML, Liu YN, Zhang P, Chen XY, et al. Resveratrol and STAT inhibitor enhance autophagy in ovarian cancer cells. *Cell Death Discov*. (2016) 2:15071. doi: 10.1038/cddiscovery.2015.71
35. Jin B, Robertson KD. DNA methyltransferases, DNA damage repair, and cancer. *Adv Exp Med Biol*. (2013) 754:3–29. doi: 10.1007/978-1-4419-9967-2_1
36. Robertson KD, Uzvolgyi E, Liang G, Talmadge C, Sumegi J, Gonzales FA, et al. The human DNA methyltransferases (DNMTs) 1, 3a and 3b: coordinate mRNA expression in normal tissues and overexpression in tumors. *Nucleic Acids Res*. (1999) 27:2291–8. doi: 10.1093/nar/27.11.2291
37. Bird A. DNA methylation patterns and epigenetic memory. *Genes Dev*. (2002) 16:6–21. doi: 10.1101/gad.947102
38. Yang J, Wei X, Wu Q, Xu Z, Gu D, Jin Y, et al. Clinical significance of the expression of DNA methyltransferase proteins in gastric cancer. *Mol Med Rep*. (2011) 4:1139–43. doi: 10.3892/mmr.2011.578
39. Toyota M, Yamamoto E. DNA methylation changes in cancer. *Prog Mol Biol Transl Sci*, (2011) 101:447–57. doi: 10.1016/B978-0-12-387685-0.00014-7
40. Damiani LA, Yingling CM, Leng S, Romo PE, Nakamura J, Belinsky SA. Carcinogen-induced gene promoter hypermethylation is mediated by DNMT1 and causal for transformation of immortalized bronchial epithelial cells. *Cancer Res*. (2008) 68:9005–4. doi: 10.1158/0008-5472.CAN-08-1276
41. Zhou D, Wan Y, Xie D, Wang Y, Wei J, Yan Q, et al. DNMT1 mediates chemosensitivity by reducing methylation of miRNA-20a promoter in glioma cells. *Exp Mol Med*. (2015) 47:e182. doi: 10.1038/emm.2015.57
42. Suzuki M, Sunaga N, Shames DS, Toyooka S, Gazdar AF, Minna JD. RNA interference-mediated knockdown of DNA methyltransferase 1 leads to promoter demethylation and gene re-expression in human lung and breast cancer cells. *Cancer Res*. (2004) 64:3137–43. doi: 10.1158/0008-5472.CAN-03-3046
43. Gray SG, Baird AM, O'Kelly F, Nikolaidis G, Almgren M, Meunier A, et al. Gemcitabine reactivates epigenetically silenced genes and functions as a DNA methyltransferase inhibitor. *Int J Mol Med*. (2012) 30:1505–11. doi: 10.3892/ijmm.2012.1138
44. Levenson VV. DNA methylation as a universal biomarker. *Expert Rev Mol Diagn*. (2010) 10:481–8. doi: 10.1586/erm.10.17
45. Wu ML, Li H, Yu LJ, Chen XY, Kong QY, Song X, et al. Short-term resveratrol exposure causes *in vitro* and *in vivo* growth inhibition and apoptosis of bladder cancer cells. *PLoS ONE*. (2014) 9:e89806. doi: 10.1371/journal.pone.0089806
46. Shu XH, Wang LL, Li H, Song X, Shi S, Gu JY, et al. Diffusion Efficiency and Bioavailability of Resveratrol Administered to Rat Brain by Different Routes: Therapeutic Implications. *Neurotherapeutics*. (2015) 12:491–501. doi: 10.1007/s13311-014-0334-6
47. Song X, Shu XH, Wu ML, Zheng X, Jia B, Kong QY, et al. Postoperative resveratrol administration improves prognosis of rat orthotopic glioblastomas. *BMC Cancer*. (2018) 18:871. doi: 10.1186/s12885-018-4771-1
48. Zhong LX, Wu ML, Li H, Liu J, Lin LZ. Efficacy and safety of intraperitoneally administered resveratrol against rat orthotopic ovarian cancers. *Cancer Manag Res*. (2019) 11:6113–24. doi: 10.2147/CMAR.S206301
49. Zheng X, Jia B, Song X, Kong QY, Wu ML, Qiu ZW, et al. Preventive potential of resveratrol in carcinogen-induced rat thyroid tumorigenesis. *Nutrients*. (2018) 10:E279. doi: 10.3390/nu10030279

Conflict of Interest: The authors declare that the research was conducted in the absence of any commercial or financial relationships that could be construed as a potential conflict of interest.

frontiers in Endocrinology

ORIGINAL RESEARCH
published: 08 November 2019
doi: 10.3389/fendo.2019.00769

PKA Activates AMPK Through LKB1 Signaling in Follicular Thyroid Cancer

Suresh Kari[1†], *Vasyl V. Vasko*[2], *Shivam Priya*[1] *and Lawrence S. Kirschner*[1,3*]

[1] Department of Cancer Biology and Genetics, The Ohio State University, Columbus, OH, United States, [2] Uniformed Services University of Health Sciences, Bethesda, MD, United States, [3] Division of Endocrinology, Diabetes, and Metabolism, Department of Internal Medicine, The Ohio State University, Columbus, OH, United States

Thyroid cancer affects about one percent of the population, and has seen rising incidence in recent years. Follicular thyroid cancer (FTC) comprises 10–15% of all thyroid cancers. Although FTC is often localized, it can behave aggressively with hematogenous metastasis, leading to an increased risk of cancer death. We previously described a mouse model for FTC caused by tissue-specific ablation of the Protein Kinase A (PKA) regulatory subunit *Prkar1a*, either by itself or in combination with knockout of *Pten.* Loss of *Prkar1a* causes enhanced activity of PKA, whereas ablation of *Pten* causes activation of Akt signaling. At the molecular level, these genetic manipulations caused activation of mTOR signaling, which was also observed in human FTC cases. To understand the mechanism by which PKA activates mTOR, we began by studying intracellular kinases known to modulate mTOR function. Although AMP-activated kinase (AMPK) has been characterized as a negative regulator of mTOR activity, our tumor model exhibited activation of both AMPK and mTOR. To understand the mechanism by which AMPK was turned on, we next studied kinases known to cause its phosphorylation. In this paper, we report that PKA leads to AMPK activation through the LKB1 kinase. Although LKB1 has traditionally been considered a tumor suppressor, our data indicates that it may have a complex role in the thyroid gland, where its activation appears to be frequently associated with follicular thyroid carcinoma in both mice and humans.

Keywords: mouse models, thyroid cancer, AMPK, LKB1, PKA

OPEN ACCESS

Edited by:
Yuji Nagayama,
Nagasaki University, Japan

Reviewed by:
Wei Zhou,
Emory University School of Medicine, United States
Misa Imaizumi,
Radiation Effects Research Foundation, Japan

***Correspondence:**
Lawrence S. Kirschner
lawrence.kirschner@osumc.edu

†Present address:
Suresh Kari,
University of Texas Health Science Center, San Antonio, TX, United States

Specialty section:
This article was submitted to Thyroid Endocrinology, a section of the journal Frontiers in Endocrinology

Received: *07 June 2019*
Accepted: *23 October 2019*
Published: *08 November 2019*

Citation:
Kari S, Vasko VV, Priya S and Kirschner LS (2019) PKA Activates AMPK Through LKB1 Signaling in Follicular Thyroid Cancer. Front. Endocrinol. 10:769. doi: 10.3389/fendo.2019.00769

INTRODUCTION

Thyroid cancer is the most common endocrine malignancy, affecting about one percent of the population. It is also the cancer that is rising at the fastest rate. Although there appears to be an ascertainment bias, recent data suggests that the increased incidence is also driven by other factors as well (1–3). Of the thyroid cancers, the majority are designated as papillary thyroid cancer (PTC), whereas the next most common type is follicular thyroid cancer (FTC) (4). Although the behavior of FTCs varies widely, this type of cancer has a stronger predilection for hematogenous dissemination (5); once metastatic, there exist no curative therapies for this type of cancer. An enhanced incidence of FTC relative to PTC is associated with Carney complex (CNC) and Cowden syndrome (CS), two tumor predisposition syndromes (6, 7). CNC is caused by inactivating mutations in *PRKAR1A*, encoding for the type 1a regulatory subunit of cAMP (cyclic adenosine monophosphate) dependent protein kinase, or PKA (6); loss of this regulatory subunit causes an increase in PKA activity. CS, on the other hand, is most commonly caused by inactivating mutations of *PTEN*, leading to increased signaling through the PI3K/AKT pathway (7). In order to probe the role of these genes in thyroid

cancer, our lab generated mice carrying a thyroid-specific knockout of *Prkar1a* and *Pten*, both singly and in combination (8, 9). *Pten-KO* mice develop thyroid adenomas, whereas *Prkar1a-KO* mice develop locally invasive FTC by 1 year of age in around 45% cases (9). In the double KO mice, thyroid cancers were observed in 100% of mice by 2 months of age, and about 1/3 of the mice developed well-differentiated lung metastasis, mimicking the human disease (8).

Of the many alterations that occur in a cancer cell leading to uncontrolled growth, metabolic changes are important ones. Recent work has started to characterize many of these metabolic changes (10–13). We have previously shown that *Prkar1a-KO* and the double KO mice exhibit activation of the mechanistic Target of Rapamycin (mTOR), with higher levels in the double KO animals (8). Similar findings were made in human FTC (8), and have been previously reported in PTC, particularly associated with *BRAF* mutations (14). mTOR is an important regulator of cellular metabolism, cellular growth and proliferation (15), and is an important player in promoting the metabolic changes that occur during tumorigenesis. mTOR is regulated by the AMP-dependent protein kinase (AMPK), which is activated in conditions of nutrition restriction or increased AMP/ATP ratio to enhance energy production (16). Activation of AMPK typically leads to suppression of mTOR activity through phosphorylation of the TSC complex as well as Raptor (17, 18).

There is, however, emerging evidence that AMPK activation can be decoupled from the mTOR pathway (19). These observations suggest that under certain conditions, AMPK may act as a tumor promoter rather than a tumor suppressor (20, 21). Thus, AMPK may serve a context-dependent function, in which the outcome from increased/diminished signaling may depend on tissue type and the presence of other intracellular signals. Although AMPK has been reported as elevated in PTC (22), its role in mediating cell growth *in vitro* is unclear, as studies in rat or human thyroid cell lines have yielded contradictory results (23, 24). Analysis of FTC tumors has not been described.

In this manuscript, we report that AMPK is activated in both mouse and human FTCs, which have concurrent activation of the mTOR pathway. Using mouse models and *in vitro* studies, we determined that LKB1, the tumor suppressor which causes Peutz-Jeghers syndrome (25, 26), mediates signaling from PKA to AMPK. These data suggest that not only does AMPK have context-specific function in modulating the behavior of thyroid tumors, but that LKB1 shares this complex role in the thyroid.

MATERIALS AND METHODS

Mice and Tumor Cell Lines

Mice were housed in University Laboratory Animal Resources maintained vivarium at the Ohio State University. *Prkar1a*$^{loxP/loxP}$, *Pten*$^{loxP/loxP}$, and *Thyroid Peroxidase-cre* (*TPO-cre*) mice have been previously described (27–29). All mice were of mixed background, with predominant contributions of 129/SvJ and FVB/N. All animal studies were carried out with approval of the Ohio State University Institutional Animal Care and Use Committee under animal research protocol 2009A0084.

Immunohistochemistry

Tumors sections were processed and stained as described previously (30) with the following antibodies: p-ACC (#3661-Cell signaling), p-P70S6K1 (#ab129230 Abcam), p-LKB1 (S-428) (#ab138386-Abcam), LKB1 (#ab185734 Abcam), STRAD-α (#ab192789 Abcam) p-CAMKII (#ab32678 Abcam), HADHA (#PA5-27348 Thermo Scientific), HSD17β4 (#OAGA1102-Aviva systems biology). For mouse analyses, thyroid sections from 3-5 independent mouse tumors from each genotype were analyzed, with consistent findings observed within each group.

Maintenance of Cell Lines

The FTC-133 cell line was maintained in high glucose DMEM-10% FCS, supplemented with 25 mM Hepes buffer, 100 U/ml penicillin, 100 μg/ml streptomycin, 2 mM L-glutamine.

Western Blot Analysis and Immunoprecipitations

Cell lysis and Immunoblotting was performed as described previously (8). 30 μg of protein was loaded per lane in 8–10% SDS gels. The following antibodies were used to probe the membranes: p-ACC (S-79) (#11818 Cell signaling), p-mTOR (S-2448) (#ab109268 Abcam), mTOR (#ab2732 Abcam), p-LKB1 (S-428) (#3482 Cell signaling), LKB1 (#3050 Cell signaling), p-AMPK (T-172) (#2535 Cell signaling), p-AMPK (S-173) (#ab55886 Abcam), GAPDH (#2118 Cell signaling), Vinculin (sc-5573, Santa Cruz Biotechnologies), p-TAK1 (#4508 Cell signaling), TAK1 (#5206 Cell signaling), p-CAMKII (#12716 Cell Signaling). For **Figures 1**, **5**, Western blots were developed using near-IR-labeled secondary antibodies and quantitated on a Li-COR Odyssey CLx and analyzed using ImageStudio v5.2. Other blots were developed on film and analyzed semi-quantitatively. All *in vitro* experiments were repeated 2–4 times with consistent results observed.

Statistical Analysis

Quantitative western blots (**Figures 1**, **5**) were analyzed by one-way ANOVA, followed by *post-hoc* Holm-Sidak multiple comparison test using GraphPad Prism software.

SiRNA Knockdown

For LKB1 knockdown, smartpool siRNA (On-target plus smartpool, Dharmacon) was used following the manufacturer's recommendations. Briefly, cells were transfected with a 5 μM solution of LKB1 siRNA using Lipofectamine in Optimem (Thermo-Fisher). The cells were treated for 48 h, following which the solution was replaced with DMEM with 10% FBS and treated with PKA activator and/or inhibitor for either 1 or 48 h. Total protein lysate was collected and analyzed by western blotting as above.

Analysis of Human Thyroid Samples

Paraffin-embedded thyroid tissue samples from patients with thyroid were selected from the thyroid tumor bank maintained under an IRB-approved protocol at the Uniformed Services University of the Health Sciences (USUHS, Bethesda, MD). The tumor bank specimens were obtained as extra

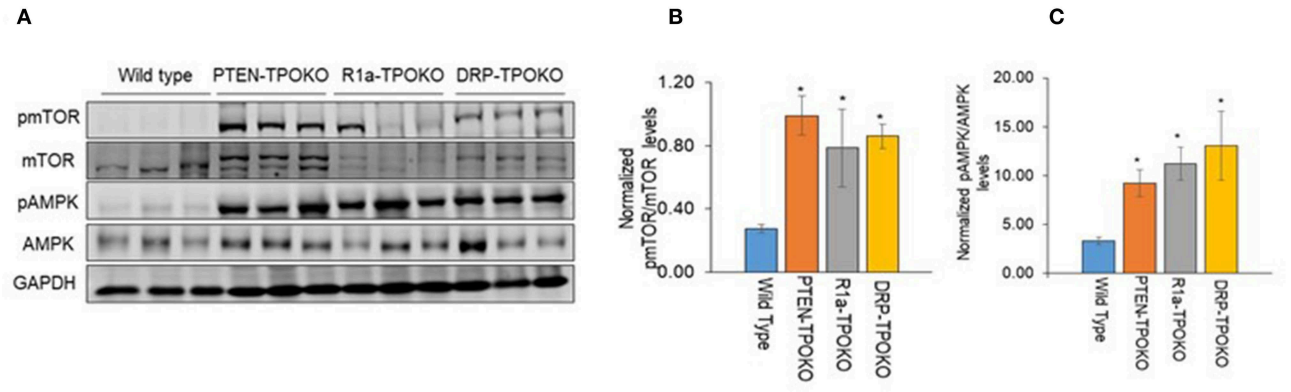

FIGURE 1 | *DRP-TPOKO* and *R1a-TPOKO* tumors show mTOR and AMPK activation. **(A)** Total protein lysates of wild type, *PTEN-TPOKO*, *R1a-TPOKO*, and *DRP-TPOKO* were run on an SDS gel and immunoblotted for the indicated proteins. GAPDH is used as a loading control. **(B,C)** Western blot analysis of phospho and total mTOR and AMPK was done, which was further normalized to GAPDH. Data is represented as mean± S.E. $^*p < 0.05$.

material from clinical thyroidectomies and were stripped of identifying information prior to banking; the research therefore is considered exempt and the USUHS IRB waived the requirement for written informed consent for this study.

Histological typing was performed by an experienced pathology (VV) based on World Health Organization criteria. Genetic data for these samples was not considered in choosing thyroid specimens Human tissues for analysis were fixed in neutral buffered formalin and then embedded in paraffin. Sections (4 mm) were dewaxed, rehydrated through graded ethanol, and antigen retrieval was performed in 10 mmol/L citrate buffer, pH 6.0, for 10 min. The sections were cooled and incubated with 3% hydrogen peroxide for 15 min. Sections were next incubated with blocking solution (Vector Labs) for 10 min, followed by incubation with primary antibodies overnight at 4°C. Primary antibody binding was detected with a biotinylated secondary antibody (Vector Labs) followed by a streptavidin-horseradish peroxidase conjugate. Immunoreactivity was revealed with 3,3-diaminobenzidine (Vector Labs). Sections were counterstained with hematoxylin. Every tumor was given a score according to the intensity of the staining and the extent of stained tumor areas (0% score 0; 1–10% score 1; 11–50% score 2; and 51–100% score 3.

RESULTS

AMPK and mTOR Activation in Mouse FTC Tumors

We have previously reported that mice with thyroid-specific KO of *Prkar1a* alone *(R1a*-TpoKO) or in combination with *Pten* KO (Double *R1a-Pten KO*, or DRP-TpoKO) exhibit activation of mTOR (8). First, we confirmed this observation in a set of new tumor samples (**Figure 1A**). To begin understanding the implications of mTOR activation, we next turned to AMPK, which is considered to be a negative regulator of mTOR under most circumstances (31). Surprisingly, when we analyzed thyroid lysates from our mouse models, we found a significant increase in phospho-T172 AMPK, a post-translational modification which leads to protein activation. Activation of AMPK correlated with tumorigenic potential, with minimal increases in WT or non-carcinogenic *Pten* KO, and much higher levels in the carcinogenic R1a- KO and the double KO (**Figures 1B,C**).

To confirm dual activation of mTOR and AMPK in the tumors, we studied mouse thyroids sections from 3 to 5 independent mouse tumors from each genotype by immunohistochemistry. We first checked phospho-p70S6K as a marker of mTOR activation, which revealed strong staining in the cancers (**Figure 2**, top row), as we have previously described (8). To verify AMPK activation, we assessed staining for activated Acyl-coA-Carboxylase (ACC), a downstream target for activated AMPK. This experiment demonstrated diffuse cytoplasmic expression of p-ACC in all tumor mice (**Figure 2**, second row), with most intense staining intensity observed in more aggressive, invasive and metastatic DKO mice. From a metabolic viewpoint, it has been reported that AMPK activation enhances fatty acid oxidation (FAO) which helps expand energy metabolites for growing tumor and promotes tumor growth. To examine the activation of FAO pathway in mouse tumors, we examined the expression of two enzymes involved in FAO pathway: the mitochondrial protein HADHA (Hydroxyacyl-CoA Dehydrogenase/3-Ketoacyl-CoA Thiolase/Enoyl-CoA Hydratase, Alpha subunit, also known as mitochondrial trifunctional protein), and the peroxisomal protein HSD17B4 (hydroxysteroid 17-beta dehydrogenase 4) (**Figure 2**, bottom rows). We found overexpression of both of these enzymes in R1a-KO and DKO mice but not in Pten-KO or wild type mice, supporting a functional role for AMPK in altering tumor metabolism. These data indicate that these mouse models of FTC in which PKA is activated exhibit activation of both AMPK and mTOR.

AMPK Activation Is Mediated by LKB1

To understand the mechanism by which AMPK is activated in thyroid cancer, we turned our attention to kinases known to phosphorylate (activate) AMPK downstream of PKA. There

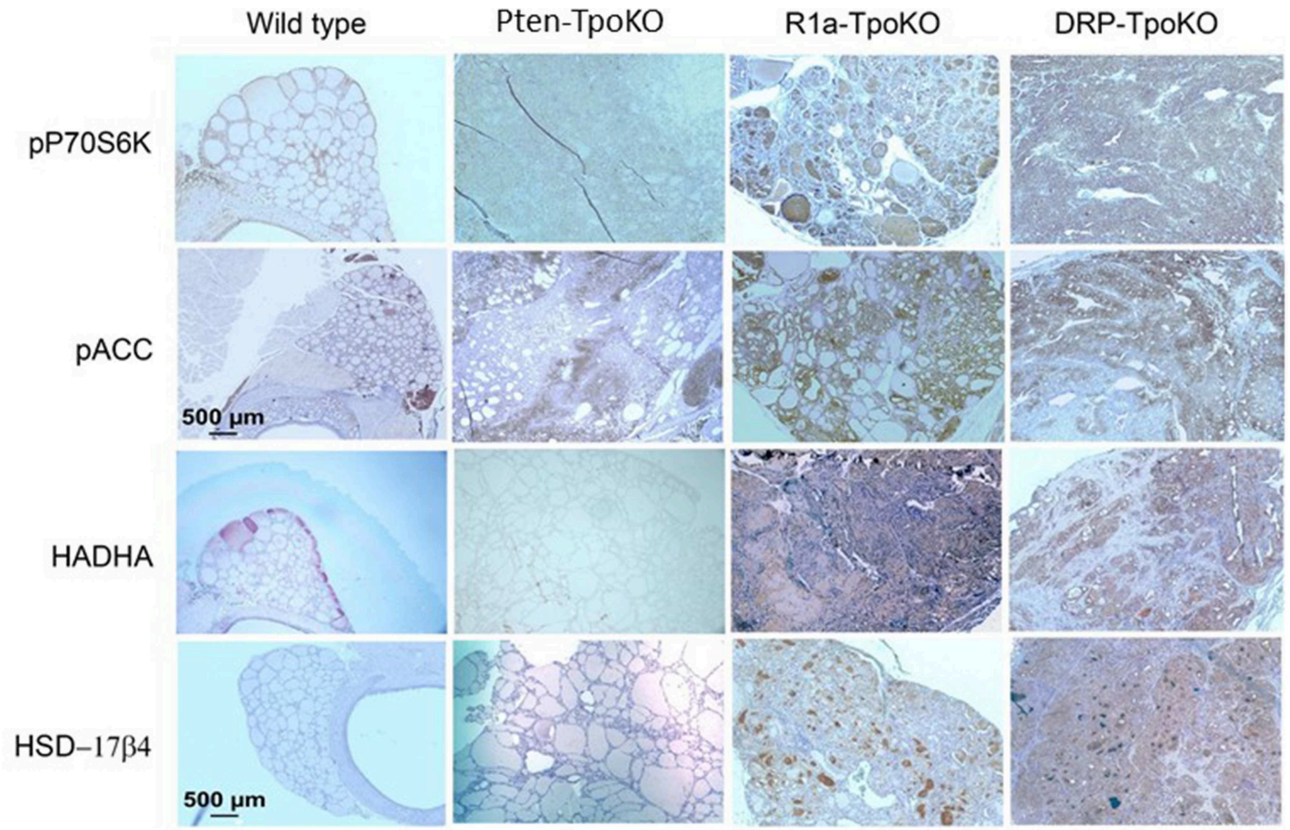

FIGURE 2 | Mouse tumors shown activation of mTOR and AMPK pathways. Representative mouse tumors from the genotypes shown at the top were analyzed by immunohistochemistry for the proteins shown at left. WT, Pten-TpoKO, and R1a-TpoKO mice were 1 year of age, whereas DRP-TpoKO mice were 6 months of age. All photos were taken at the same magnification, with scale bars shown in two panels in the left column.

are three major kinases responsible for AMPK phosphorylation: LKB1, CamKII, and TAK1 (19). Mining of our microarray data demonstrated that expression of these kinases was not altered in the tumors, although there were some shifts in isoform expression for CAMKII, with decreases in Camk2a and b, and increases in Camk2d (data not shown). To address alterations in signaling, we used the human FTC cell line FTC-133 to probe the activation of these kinases at baseline and in response to PKA activation.

We first examined LKB1, which has been shown to function as a tumor suppressor, as inactivating mutations in the gene cause the inherited tumor predisposition Peutz-Jeghers syndrome (25, 26). Although there are rare cases of *LKB1* mutations in thyroid cancer (32), thyroid cancer's association with this syndrome remains unclear (33, 34). Loss of the gene is also a common somatic event in a subset of patients with non-small cell lung cancer, melanoma, and cervical cancer (35), but activating mutations have not been described. LKB1 is also known to be a substrate for PKA phosphorylation, with this phosphorylation promoting LKB1 activity (36). To explore the role of LKB1 in activating AMP, we measured both LKB1 and AMPK phosphorylation in FTC-133 cells after manipulation of PKA activity (**Figure 3A**). Treatment of cells with the specific PKA activator 6-Bnz-cAMP led to an increase in both pLKB1 and pAMPK. Treatment of cells with the peptide inhibitor of PKA (PKI) blocked this effect. Despite the activation of AMPK there was no change to p-mTOR phosphorylation levels in response to these manipulations, confirming our underlying observation that AMPK and mTOR activation are decoupled in this system.

We also examined the activation of CAMKII and TAK1 using this same system, as both of these kinases may also be activated by PKA (37, 38). Although we observed CAMKII and p-CAMKII in the cells, levels were not enhanced in response to PKA activation (**Figure 3B**). Levels of TAK1 were very low in the FTC cells, and there was also no increase in p-TAK1 after activation of PKA. (**Figure 3B**) These data suggested that PKA activates AMPK through LKB1.

To further confirm the ability of PKA to activate AMPK through LKB1, we used siRNA to generate transient knockdown (KD) of LKB1 in FTC-133 cells. The siRNA was consistently able to achieve >80% of the target protein (**Figure 4A**). After LKB1 KD, the cells were treated with PKA activator and inhibitor to examine AMPK activation. LKB1 knockdown at both 1 and 48 h led to a significant reduction of AMPK activation (**Figure 4B**) suggesting that LKB1 is the major kinase responsible for AMPK activation downstream of PKA. Note that

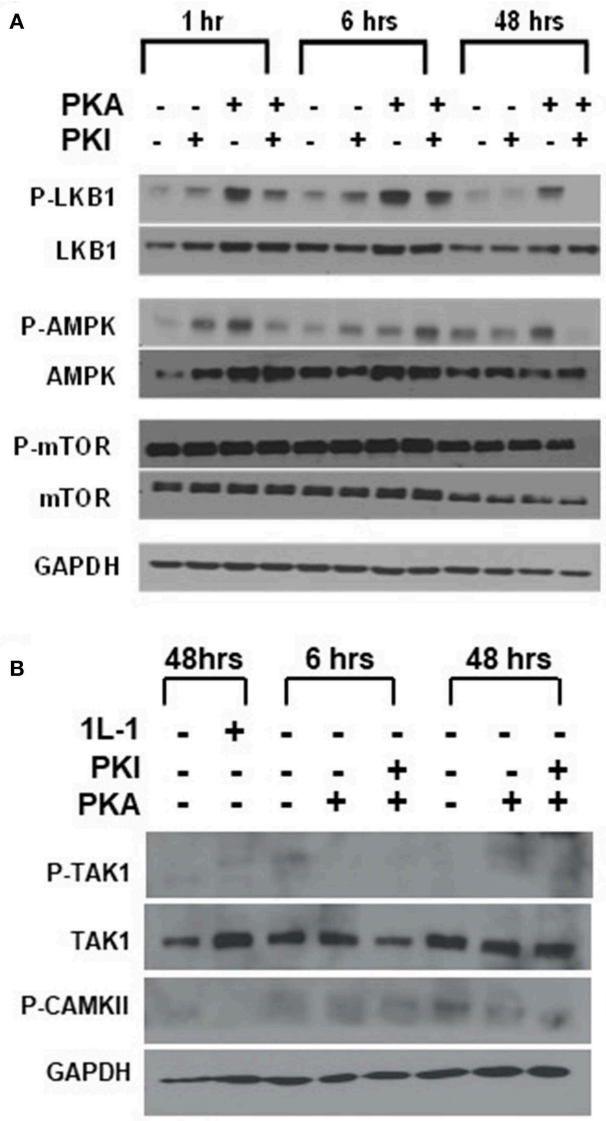

FIGURE 3 | LKB1 is responsible for PKA-mediated stimulation of AMPK. **(A)** FTC-133 cells were treated with PKA activator (PKA) and/ or inhibitor (PKI) for the times shown, and immunoblotted for total and phospho- isoforms of LKB1, AMPK, and mTOR. Note that pLKB1 and pAMPK increase after PKA activator and this is blocked by PKI. **(B)** FTC-133 were treated as above and probed for total or phospho-TAK1 and for pCAMKII. IL-1 treatment is used as a positive control for pTAK1 induction, although induction is very modest in these cells. Note that neither protein is activated in response to PKA. GAPDH is shown as a loading control.

AMPK phosphorylation was not completely abrogated by LKB1 knockdown, suggesting that either residual LKB1 may suffice to partly activate AMPK, or that other kinases may also play a role in this process. AMPK may also be phosphorylated on S173, which is an inactivating modification of AMPK (39). Although PKA activation has been proposed to cause phosphorylation at this site in hepatocytes (39, 40), we did not observe a band corresponding to AMPK-pS173 under any of our treatment conditions (data not shown).

LKB1 Activation in Mouse Models of FTC Tumors

In order to make sure that these observations were relevant *in vivo,* we next sought to assess LKB1 activation in mouse tumors (**Figure 5A**). In WT thyroids, there was little staining of either total or pLKB1 in the tissue. For the tumor models, total and pLKB1 were increased in *Pten* and *R1a* knockouts, and further increased in the double KO. These observations were confirmed by western blot for pLKB1 from tumor lysates (**Figure 5B**). As LKB1 function is partly dependent on nuclear-cytoplasmic shuttling mediated by the pseudosubstrate Strad-α (41), we also performed IHC for this protein. Our results demonstrate that Strad-α is not expressed in WT thyroids or *Pten* tumors, but exhibits strong staining in the *R1a*-KO and DKO tumors. Taken together, our results suggest that PKA activates the LKB1-AMPK pathway in PKA-driven mouse models of FTC, including both locally aggressive and metastatic disease.

Since activation of CAMKII was also observed *in vitro* (**Figure 3B**), we assessed its expression in our mouse tumors. We found increased expression of p-CAMKII in *R1a-KO* and DKO tumors compared to that from *Pten*-KO and wild type thyroids (**Figure 5A**, bottom row). Interestingly, although p-CAMKII expression was uniform in the R1a KO tumors, expression in the DKO tumors showed regional differences, with much darker staining in the outer edges of the tumor compared to its central region. This expression pattern in the DKO tumors did not correlate with the patterns of AMPK or mTOR activation (**Figure 2**).

Lack of Inhibition of CREB Pathway by LKB1 and Activation of AMPK Related Kinases

LKB1 not only activates AMPK but 13 other AMPK-like kinases. To assess the expression levels of these AMPK-like kinases, we mined data from our previous microarray analysis of tumors (8). We found no loss of expression of any of the 8 AMPK-related kinases or LKB1 binding partners including CAB39 (MO25) or Strad-α (**Figure 6**) (42). Our data does show preferential upregulation of the expression of NUAK2 and SIK1 in *R1a* and DKO tumors, although we did not perform measurements of the activity of these kinases. In lung cancer, the functional significance of LKB1 loss has been assessed, and it was demonstrated that LKB1 activation inhibits a set of 200 genes which were defined as a CREB-dependent cluster (43). Examination of this gene set demonstrated no significant change in the *R1a* and DKO mice, suggesting that LKB1 does not inhibit the CREB-mTOR pathway in our mouse model of FTC (data not shown).

LKB1-AMPK Pathway in Human Thyroid Cancer

So far, our data suggests that PKA activates the LKB1-AMPK pathway in our mouse models of FTC. However, we wanted to assess the activation of this pathway in human follicular thyroid lesions. Phospho-AMPK staining (**Figure 7**, **Table 1**) was detected in thyrocytes in 15% (3/20) of benign follicular

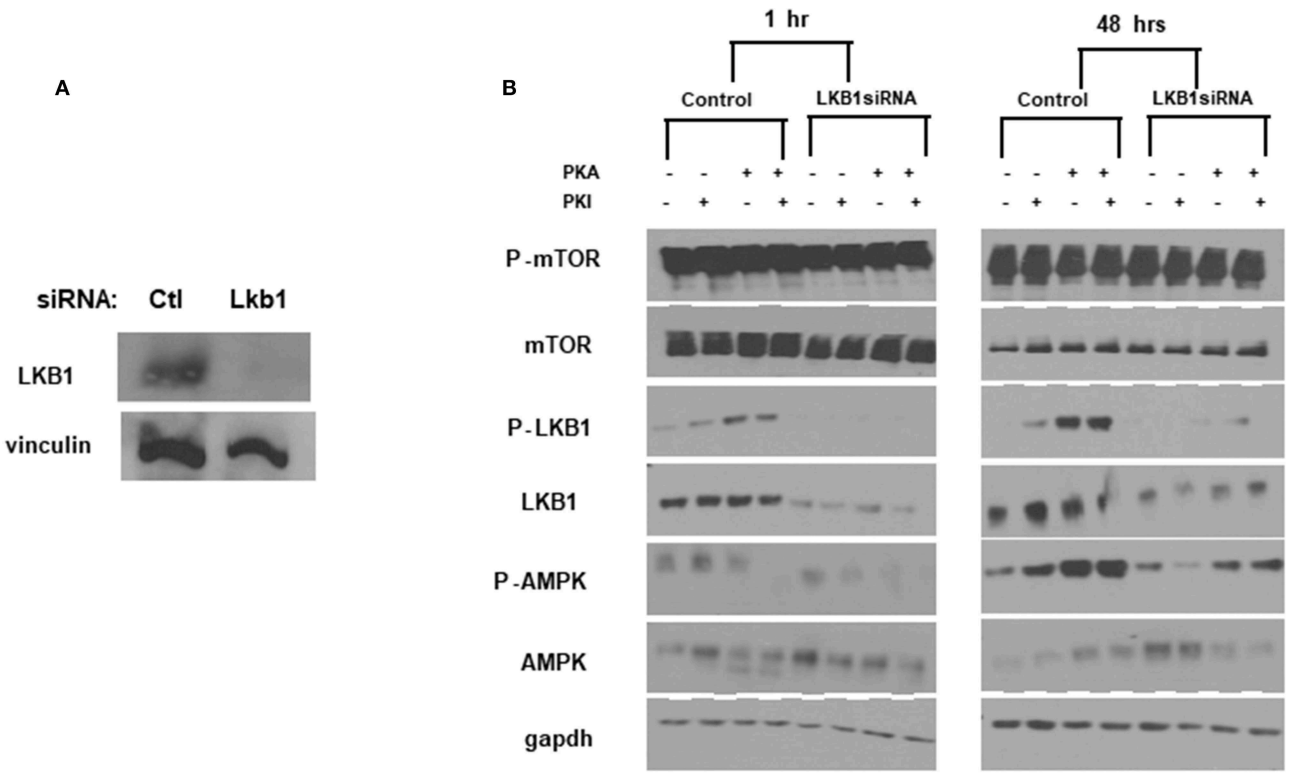

FIGURE 4 | *LKB1* knockdown suppresses PKA-mediated AMPK activation. **(A)** *LKB1*-specific siRNA pool causes knockdown of LKB1 in FTC−133 cells. Non-targeting siRNA was used as a control. Proteins were analyzed 48 h after transfection. Vinculin is shown as a loading control. **(B)** Cells treated with control- or *LKB1*-specific siRNAs were treated with PKA activator (PKA) and/or inhibitor (PKI) for the indicated times and probed for activation (phosphorylation) of mTOR, LKB1, and AMPK. GAPDH was used as a loading control.

adenomas with rates that were slightly higher for FV-PTC (20%) and FTC (30%), although these numbers are not large enough to say if these modest differences are significant. The overall intensity of staining assessed on a graded scale was highest in FTCs, but again small numbers preclude any type of statistical conclusion. We did note that less-differentiated and widely invasive FTCs did not stain for p-AMPK. As in the mouse models, p-AMPK staining in human tumors generally correlated with activation of its downstream target p-ACC (**Table 2**), although p-ACC staining was much more common, including ready detection in the normal thyroid gland.

Using a different cohort of human samples, we also assessed total and phospho-LKB1 staining in the thyroid (**Figure 7** right, **Table 3**). In the wild type gland, LKB1 was detected in half the cases (5/10), but was rarely phosphorylated (1/10 cases). Follicular adenomas exhibited light staining for total and p-LKB in about half the cases (4/8), with another 25% lacking staining. In contrast, there was much more prominent activation of this kinase in malignant lesions, with 6/12 PTCs showing heavy staining for both protein forms (total and phosphorylated). Further, all FTCs stained for total LKB1, with 9/13 (69%) showing intense staining for the total protein and the large majority of tumors (10/13, 77%) showing high level phosphorylation of LKB1. Of note, immunoactive LKB1 was greatest in regions of capsular invasion; and was localized to the nucleus in follicular as well as in papillary cancer cells. The highest intensity staining was observed in tumors characterized as Hurthle cell cancers (data not shown). We have previously reported that human FTCs exhibit strong nuclear staining for phospho-CREB as a marker of PKA activation (8). These observations suggest that the PKA-LKB1 axis is active in human FTCs as well as those from our mouse model.

DISCUSSION

Carney complex (CNC) is a tumor predisposition syndrome which includes thyroid neoplasia in about 25% of patients, including 2.5% of patients who develop frank thyroid carcinoma (44), including a predominance of the FTC subtype. It has been demonstrated that CNC is caused by inactivating mutations in *PRKAR1A* gene, which is a regulatory subunit of PKA (6), suggesting that dysregulation of PKA signaling can cause tumor formation in the thyroid gland, and in other affected tissues. We have previously demonstrated that activation of PKA is the main driver of tumorigenesis and other phenotypes related to KO of *Prkar1a*, as genetic reduction of PKA catalytic subunits suppresses these phenotypes (45). However, the exact signaling

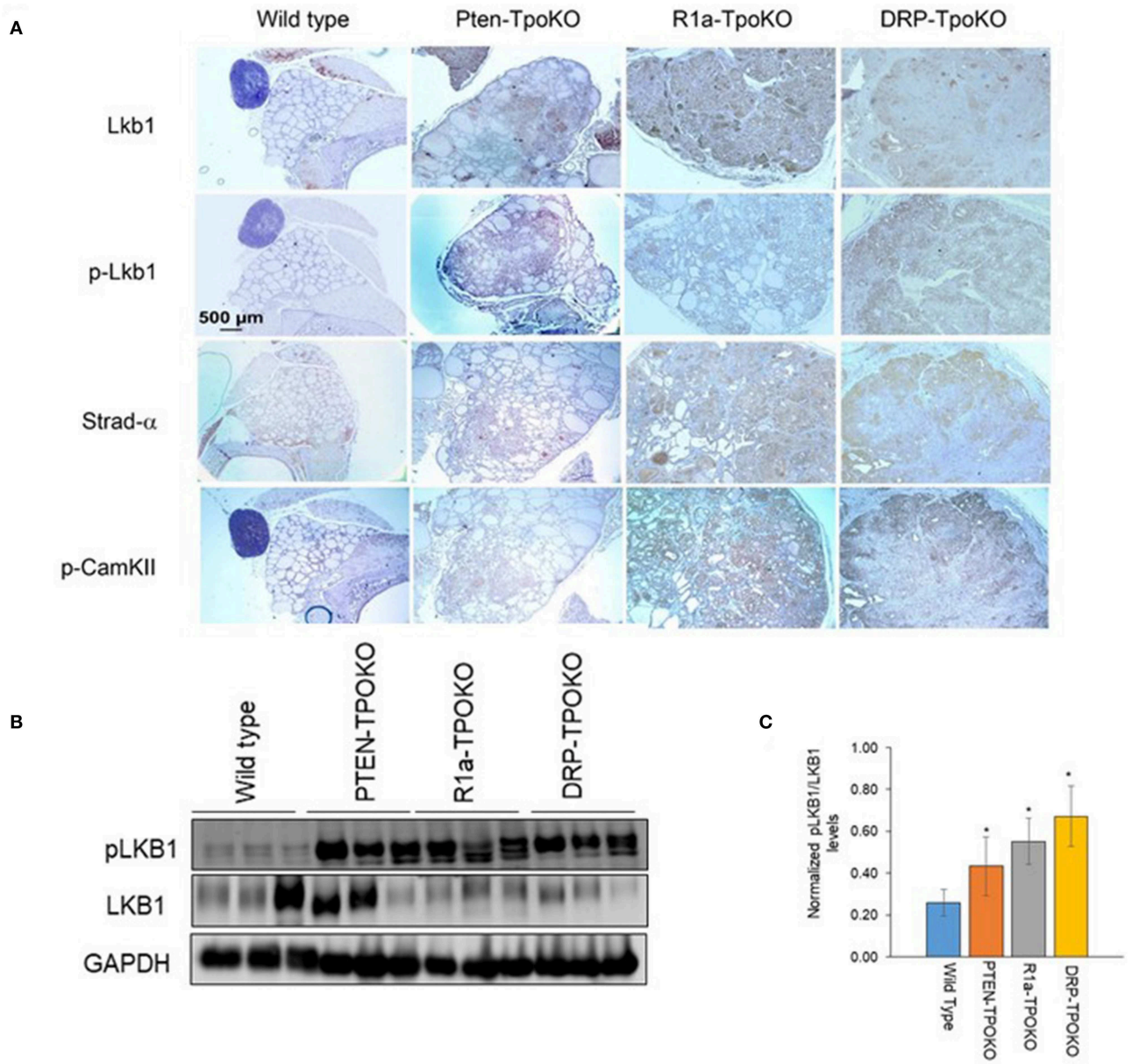

FIGURE 5 | LKB1 is activated in mouse thyroid tumors. **(A)**. Representative immunohistochemical images of wild type, *Pten-*, *R1a-*, and *DRP-TpoKO* tumors stained for the proteins shown at left. All images were taken at the same magnification corresponding to the scale bar shown in the left column. **(B)** Western blotting of tumor lysates for pLKB1 and total LKB1. GAPDH is shown as a loading control. **(C)** Quantitation of data in panel B. Data is represented as mean± S.E. $^{*}p < 0.05$.

pathways activated by PKA which cause tumor formation have not been elucidated in detail. Furthermore, our previous publication demonstrated that PKA-mediated tumors do not involve typical signaling pathways such as AKT and ERK activation (9). Therefore, our present endeavor was to understand the PKA signaling and understand the molecular signaling pathways involved in PKA-mediated FTC tumors.

The role of AMPK in cancer development is controversial with conventional wisdom terming it a tumor suppressor (17). However, evidence in the recent literature points to a more nuanced context-dependent role, which may include activity as either a tumor promoter or a suppressor (46). In many cancers, AMPK has been shown to negatively regulate the mTOR pathway through TSC-2 and Raptor and dephosphorylation of PRAS40 (47, 48). However, our mouse tumors and also *in vitro* data from FTC-133 cells show an absence of negative regulation of mTOR pathway despite AMPK activation. Some authors have also concluded that activated AMPK and mTOR can coexist together without affecting each other (19). Other research has shown that AMPK may not be completely sufficient to inhibit

the mTOR pathway, and AMPK inactivation does not necessarily activate mTOR pathway (19). Of particular interest to us was the observation that AMPK was activated in R1a-KO and DKO mice suggesting that this pathway must involve PKA signaling. Of the major AMPK kinases responsible for activation of AMPK, LKB1 and CAMKII both have been shown in the literature to be activated by PKA (37, 49). Therefore, we decided to explore whether PKA could be signaling through either of these kinases to activate AMPK.

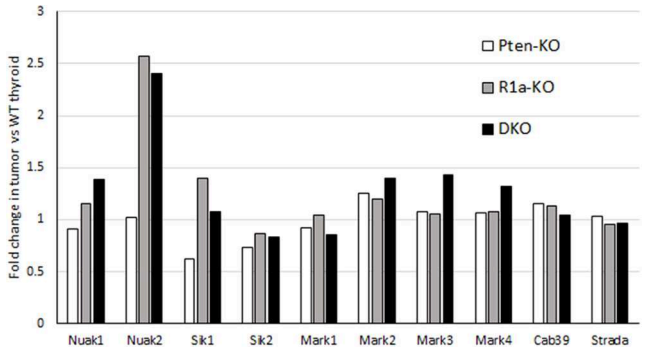

FIGURE 6 | mRNA expression of LKB1 binding partners and AMPK-like kinases in mouse models of FTC. For each model, mRNA expression is expressed as fold-change compared to WT littermates. Data is collected from Pringle et al. (8).

The serine-threonine kinase LKB1 (STK11) is mutated in the tumor predisposition Peutz-Jeghers syndrome (PJS), an inherited human disorder characterized by skin pigmentation and hamartomatous polyps of the GI tract (50). Because PJS mutations are inactivating, *LKB1* has been termed as a tumor suppressor gene, and its loss is associated with lung cancer, melanoma, and cervical cancer (35). It has been suggested that PJS patients may be associated with an enhanced risk for thyroid cancer (51), but larger studies of this patient population have failed to confirm a clear predisposition (33, 34). In sporadic thyroid cancers, LKB1 has not been well studied, although two recent publications have reported a total of 3 *LKB1* mutants in thyroid cancer, including a frameshift, a splice site mutation, and a missense mutation (32, 52). The functional significance of these mutants needs to be characterized, but this data points to that fact that *LKB1* mutations are rare in thyroid cancer.

LKB1 is known to inhibit the mTOR pathway through activation of AMPK, which may inhibit tumor cell proliferation, inhibit tumor cell polarization, and inhibit tumor metastasis

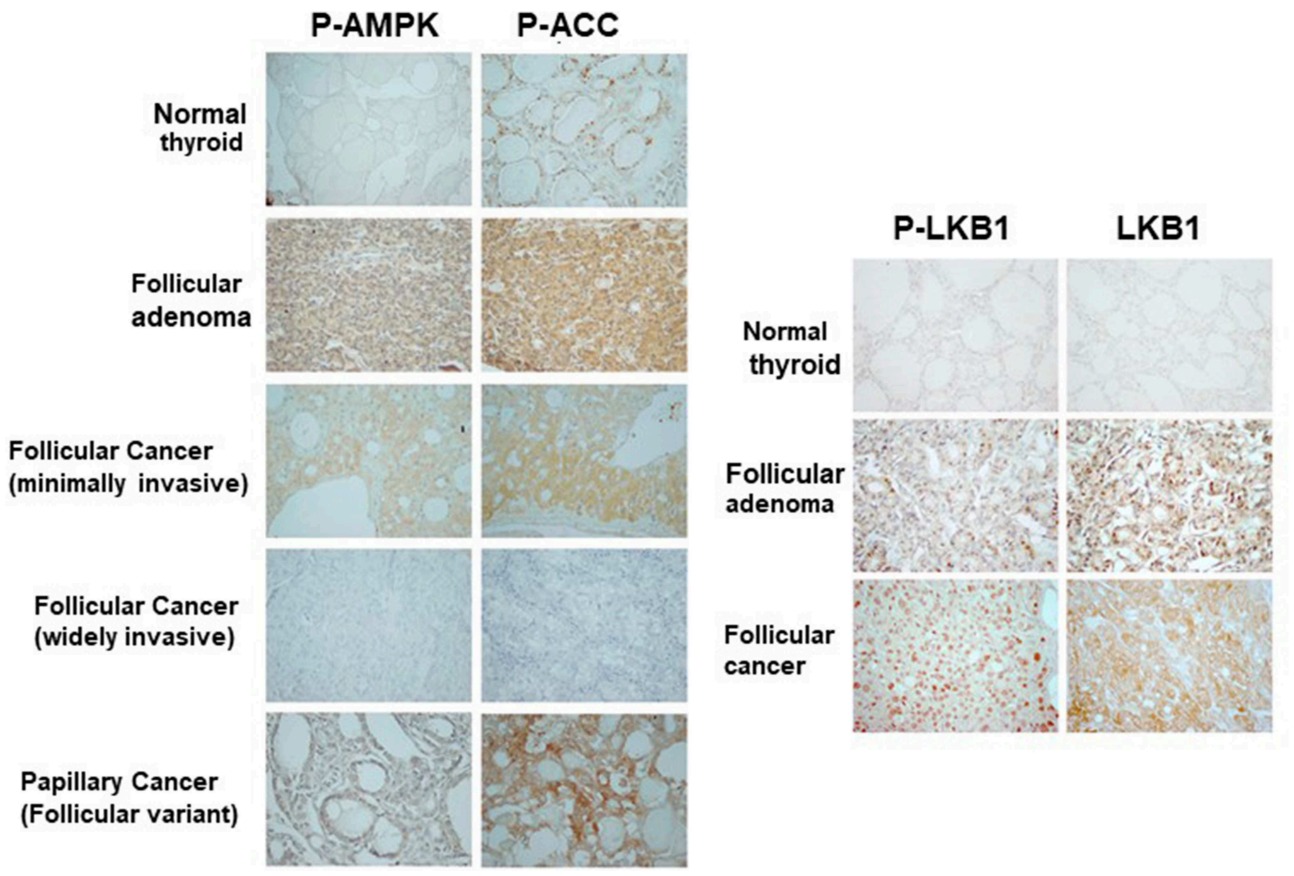

FIGURE 7 | Activation of AMPK and LKB1 in human thyroid neoplasias. Representative immunohistochemical images of tissue sections from patients with benign and malignant follicular thyroid lesions stained for p-AMPK, p-ACC, and pLKB1. These data are quantitated in **Tables 1**–**3**.

TABLE 1 | p-AMPK expression in human follicular thyroid lesions.

Histology	# of cases	pAMPK IHC score			% Low staining (1)	% High staining (2)
		0	1	2		
Normal thyroid	20	18	2	0	10	0
Follicular adenoma	20	17	2	1	10	5
Follicular cancer	20	14	4	2	20	10
Follilcular variant of papillary thyroid cancer	20	16	4	0	20	20

TABLE 2 | p-ACC expression in human follicular thyroid lesions.

Histology	# of cases	pAMPK IHC score			% Low staining (1)	% High staining (2)
		0	1	2		
Normal thyroid	20	10	9	1	45	5
Follicular adenoma	20	8	8	4	40	20
Follicular cancer	20	12	4	4	20	20
Follilcular variant of papillary thyroid cancer	20	8	8	4	40	20

TABLE 3 | LKB expression in human thyroid tumors.

Histology	# of cases	LKB IHC score			% High staining (2)	pLKB IHC score			% High staining (2)
		0	1	2		0	1	2	
Normal thyroid	10	5	4	1	10	7	2	1	10
Follicular adenoma	8	2	4	2	25	2	4	2	25
Follicular cancer	13	0	4	9	69	1	2	10	77
Papillary thyroid cancer	12	3	3	6	50	2	4	3	25

(42). In many tumors therefore, LKB1 expression has been negatively associated with increased aggressiveness of the tumor (42), observations which have also been confirmed in mouse models and using *in vitro* systems (53, 54). In *LKB1* heterozygous mice, there was no loss of LKB1 expression observed from the gastrointestinal polyps, suggesting initiation of polyp formation may not be due to LKB1 loss (54). These observations have led authors to suggest a context-dependent function of LKB1, where loss in early tumorigenesis leads to the formation of benign tumors whereas its loss in late tumorigenesis induces the formation of malignant tumors (53).

Our interest in examining the role of LKB1 arose from the fact that LKB1 is known to be a direct substrate of PKA (36). Our tumors demonstrated robust total LKB1 expression which was diffuse and cytoplasmic or membranous. A recent article examining LKB1 expression in breast cancer has suggested that the cytoplasmic localization of LKB1 was associated with worse prognosis (55). Of particular interest was the role of phosphorylation of LKB1 at Serine 428 (Ser428). This particular site has been known to be a target of p90RSK and PKA (36, 49). Ser428 has been reported to inhibit the basal phosphorylation of AMPK but seems to be required for inducible phosphorylation (49). Data in this manuscript indicates, at least in the thyroid, that AMPK is activated in response to LKB1 Ser428 phosphorylation by PKA. Further, activation of AMPK by this signaling cascade does not inhibit mTOR activation in our mouse tumors, an FTC cell line, and a subset of human thyroid tumors (which show high AMPK pathway activation). This observation also suggests the presence of additional regulatory proteins which prevent AMPK from inhibiting mTOR pathway. Recently there is increasing evidence suggesting that LKB1 subcellular location is regulated by various proteins and nuclear receptors, such as PKC-zeta (56), ROR-alpha, estrogen receptor, Farnesoid X receptor, and Nur77 orphan nuclear receptor (57). Nur77, another well-known PKA target (58, 59), has been shown to directly bind to LKB1 and shuttle it to nucleus and thus modulate AMPK activation levels in tissues (57). However, in our tumors we did not find any evidence of nuclear localization of Nur77, suggesting that this protein might not be responsible for nuclear localization of p-LKB1 in our tumor models (data not shown).

LKB1 in recent years has been linked to activation and phosphorylation of 13 AMPK- related kinases, such as the MARK, SIK, and NUAK family of proteins (42). In general, these kinases have been termed as tumor promoters/suppressors, depending on the tumor type and context. For instance, NUAK2 has been shown as a tumor promoter in different tumor models (60–63). SIK-1, -2, and -3 have been demonstrated to be acting as tumor suppressors and also tumor promoters; the latest example being of SIK2 which was shown to be acting

as a metastasis promoter in ovarian cancer (64). Similarly, the MARK family of proteins have also been implicated to aid in invasion and aggressiveness of tumor growth (46, 65). Although there are various pathways implicated in overexpression of these proteins, they all seem to require active LKB1 (42). Indeed, the fact that human FTCs exhibited frequent LKB1 activation, even when AMPK was not present, suggests that LKB1 may signal through multiple pathways to promote tumor formation and/or progression. These observations suggest that LKB1 can act as tumor promoter/suppressor through various pathways promoting/suppressing metabolism, aggressiveness, invasion and metastasis.

In summary, our combined *in vitro-in vivo* study clearly demonstrates that FTCs can have concomitant activation of both the mTOR and AMPK pathways. In PKA-driven tumors, PKA activates AMPK through the LKB1 kinase. Although LKB1 has generally been considered to be a tumor suppressor, our data indicates that its role in the thyroid can be more complex, with the protein serving as mediator downstream of PKA activation in driving tumorigenesis. Like AMPK, LKB1 appears to serve as a context-dependent tumor promoter, and activation of this signaling pathway can be decoupled from regulation of mTOR signaling. Our ongoing studies continue to be focused around elucidating the details of these steps in the process of tumor formation and tumor growth.

DATA AVAILABILITY STATEMENT

All datasets generated for this study are included in the article/supplementary material.

ETHICS STATEMENT

Ethical review and approval was not required for the study on human participants in accordance with the local legislation and institutional requirements. Written informed consent for participation was not required for this study in accordance with the national legislation and the institutional requirements. The animal study was reviewed and approved by The Ohio State University Institutional Animal Care and Use Committee.

AUTHOR CONTRIBUTIONS

SK performed and analyzed experiments for this study, and wrote and edited the manuscript. VV performed all analysis of human pathology specimens and reviewed the manuscript. SP performed and analyzed additional experiments for the study, and edited the manuscript. LK designed, supervised, and analyzed the work, and wrote and edited the manuscript.

FUNDING

This work was supported by the National Institutes of Health grant 1 R01 CA170249 (to LK) and by P30 CA016058 (to the OSU Comprehensive Cancer Center).

ACKNOWLEDGMENTS

The authors wish to thank Drs. Danielle Huk, Amruta Ashtekar, and Karthik Chakravarthy for helpful discussions during the performance and analysis of these studies.

REFERENCES

1. Jemal A, Siegel R, Ward E, Hao Y, Xu J, Murray T, et al. Cancer statistics, 2008. *CA Cancer J Clin*. (2008) 58:71–96. doi: 10.3322/CA.2007.0010
2. Lim H, Devesa SS, Sosa JA, Check D, Kitahara CM. Trends in thyroid cancer incidence and mortality in the United States, 1974-2013. *JAMA*. (2017) 317:1338–48. doi: 10.1001/jama.2017.2719
3. Nikiforova MN, Nikiforov YE. Molecular genetics of thyroid cancer: implications for diagnosis, treatment and prognosis. *Expert Rev Mol Diagn*. (2008) 8:83–95. doi: 10.1586/14737159.8.1.83
4. Kitahara CM, Sosa JA. The changing incidence of thyroid cancer. *Nat Rev Endocrinol*. (2016) 12:646–53. doi: 10.1038/nrendo.2016.110
5. Nguyen XV, Roy Choudhury K, Tessler FN, Hoang JK. Effect of tumor size on risk of metastatic disease and survival for thyroid cancer: implications for biopsy guidelines. *Thyroid*. (2018) 28:295–300. doi: 10.1089/thy.2017.0526
6. Kirschner LS, Carney JA, Pack SD, Taymans SE, Giatzakis C, Cho YS, et al. Mutations of the gene encoding the protein kinase A type I-alpha regulatory subunit in patients with the Carney complex. *Nat Genet*. (2000) 26:89–92. doi: 10.1038/79238
7. Nagy R, Ganapathi S, Comeras I, Peterson C, Orloff M, Porter K, et al. Frequency of germline PTEN mutations in differentiated thyroid cancer. *Thyroid*. (2011) 21:505–10. doi: 10.1089/thy.2010.0365
8. Pringle DR, Vasko VV, Yu L, Manchanda PK, Lee AA, Zhang X, et al. Follicular thyroid cancers demonstrate dual activation of PKA and mTOR as modeled by thyroid specific deletion of Prkar1a and Pten in mice. *J Clin Endocrinol Metab*. (2014) 99:E804–12. doi: 10.1210/jc.2013-3101
9. Pringle DR, Yin Z, Lee AA, Manchanda PK, Yu L, Parlow AF, et al. Thyroid-specific ablation of the Carney complex gene, PRKAR1A, results in hyperthyroidism and follicular thyroid cancer. *Endocr Relat Cancer*. (2012) 19:435–46. doi: 10.1530/ERC-11-0306
10. Currie E, Schulze A, Zechner R, Walther TC, Farese RV Jr. Cellular fatty acid metabolism and cancer. *Cell Metab*. (2013) 18:153–61. doi: 10.1016/j.cmet.2013.05.017
11. Hsu PP, Sabatini DM. Cancer cell metabolism: warburg and beyond. *Cell*. (2008) 134:703–7. doi: 10.1016/j.cell.2008.08.021
12. Shaw RJ. Glucose metabolism and cancer. *Curr Opin Cell Biol*. (2006) 18:598–608. doi: 10.1016/j.ceb.2006.10.005
13. Svensson RU, Shaw RJ. Cancer metabolism: tumour friend or foe. *Nature*. (2012) 485:590–1. doi: 10.1038/485590a
14. Faustino A, Couto JP, Populo H, Rocha AS, Pardal F, Cameselle-Teijeiro JM, et al. mTOR pathway overactivation in BRAF mutated papillary thyroid carcinoma. *J Clin Endocrinol Metab*. (2012) 97:E1139–49. doi: 10.1210/jc.2011-2748
15. Zoncu R, Efeyan A, Sabatini DM. mTOR: from growth signal integration to cancer, diabetes and ageing. *Nat Rev Mol Cell Biol*. (2011) 12:21–35. doi: 10.1038/nrm3025
16. Lin SC, Hardie DG. AMPK: sensing glucose as well as cellular energy status. *Cell Metab*. (2018) 27:299–313. doi: 10.1016/j.cmet.2017.10.009
17. Brunton J, Steele S, Ziehr B, Moorman N, Kawula T. Feeding uninvited guests: mTOR and AMPK set the table for intracellular pathogens. *PLoS Pathog*. (2013) 9:e1003552. doi: 10.1371/journal.ppat.1003552
18. Luo Z, Zang M, Guo W. AMPK as a metabolic tumor suppressor: control of metabolism and cell growth. *Fut Oncol*. (2010) 6:457–70. doi: 10.2217/fon.09.174
19. Dasgupta B, Chhipa RR. Evolving lessons on the complex role of AMPK in normal physiology and cancer. *Trends Pharmacol Sci*. (2016) 37:192–206. doi: 10.1016/j.tips.2015.11.007

20. Jeon SM, Chandel NS, Hay N. AMPK regulates NADPH homeostasis to promote tumour cell survival during energy stress. *Nature*. (2012) 485:661–5. doi: 10.1038/nature11066
21. Jeon SM, Hay N. The dark face of AMPK as an essential tumor promoter. *Cell Logist.* (2012) 2:197–202. doi: 10.4161/cl.22651
22. Vidal AP, Andrade BM, Vaisman F, Cazarin J, Pinto LF, Breitenbach MM, et al. AMP-activated protein kinase signaling is upregulated in papillary thyroid cancer. *Eur J Endocrinol*. (2013) 169:521–8. doi: 10.1530/EJE-13-0284
23. Andrade BM, Araujo RL, Perry RL, Souza EC, Cazarin JM, Carvalho DP, et al. A novel role for AMP-kinase in the regulation of the Na+/I–symporter and iodide uptake in the rat thyroid gland. *Am J Physiol Cell Physiol*. (2011) 300:C1291–7. doi: 10.1152/ajpcell.00136.2010
24. Malaguarnera R, Chen KY, Kim TY, Dominguez JM, Voza F, Ouyang B, et al. Switch in signaling control of mTORC1 activity after oncoprotein expression in thyroid cancer cell lines. *J Clin Endocrinol Metab*. (2014) 99:E1976–87. doi: 10.1210/jc.2013-3976
25. Hemminki A, Markie D, Tomlinson I, Avizienyte E, Roth S, Loukola A, et al. A serine/threonine kinase gene defective in Peutz-Jeghers syndrome. *Nature*. (1998) 391:184–7. doi: 10.1038/34432
26. Jenne DE, Reimann H, Nezu J, Friedel W, Loff S, Jeschke R, et al. Peutz-Jeghers syndrome is caused by mutations in a novel serine threonine kinase. *Nat Genet*. (1998) 18:38–43. doi: 10.1038/ng0198-38
27. Kirschner LS, Kusewitt DF, Matyakhina L, Towns WH II, Carney JA, Westphal H, et al. A mouse model for the Carney complex tumor syndrome develops neoplasia in cyclic AMP-responsive tissues. *Cancer Res.* (2005) 65:4506–14. doi: 10.1158/0008-5472.CAN-05-0580
28. Kusakabe T, Kawaguchi A, Kawaguchi R, Feigenbaum L, Kimura S. Thyrocyte-specific expression of Cre recombinase in transgenic mice. *Genesis*. (2004) 39:212–6. doi: 10.1002/gene.20043
29. Trimboli AJ, Cantemir-Stone CZ, Li F, Wallace JA, Merchant A, Creasap N, et al. Pten in stromal fibroblasts suppresses mammary epithelial tumours. *Nature*. (2009) 461:1084–91. doi: 10.1038/nature08486
30. Jones GN, Tep C, Towns WH II, Mihai G, Tonks ID, Kay GF, et al. Tissue-specific ablation of Prkar1a causes schwannomas by suppressing neurofibromatosis protein production. *Neoplasia*. (2008) 10:1213–21. doi: 10.1593/neo.08652
31. Hindupur SK, Gonzalez A, Hall MN. The opposing actions of target of rapamycin and AMP-activated protein kinase in cell growth control. *Cold Spring Harb Perspect Biol*. (2015) 7:a019141. doi: 10.1101/cshperspect.a019141
32. Wei S, LiVolsi VA, Brose MS, Montone KT, Morrissette JJ, Baloch ZW. STK11 mutation identified in thyroid carcinoma. *Endocr Pathol.* (2016) 27:65–9. doi: 10.1007/s12022-015-9411-6
33. Son EJ, Nose V. Familial follicular cell-derived thyroid carcinoma. *Front Endocrinol*. (2012) 3:61. doi: 10.3389/fendo.2012.00061
34. Triggiani V, Guastamacchia E, Renzulli G, Giagulli VA, Tafaro E, Licchelli B, et al. Papillary thyroid carcinoma in Peutz-Jeghers syndrome. *Thyroid.* (2011) 21:1273–7. doi: 10.1089/thy.2011.0063
35. Zhou W, Zhang J, Marcus AI. LKB1 tumor suppressor: therapeutic opportunities knock when LKB1 is inactivated. *Genes Dis.* (2014) 1:64–74. doi: 10.1016/j.gendis.2014.06.002
36. Collins SP, Reoma JL, Gamm DM, Uhler MD. LKB1, a novel serine/threonine protein kinase and potential tumour suppressor, is phosphorylated by cAMP-dependent protein kinase (PKA) and prenylated *in vivo*. *Biochem J*. (2000) 345(Pt 3):673–80. doi: 10.1042/bj3450673
37. Cabrera-Pastor A, Llansola M, Felipo V. Extracellular protein kinase a modulates intracellular calcium/calmodulin-dependent protein kinase II, nitric oxide synthase, and the glutamate-nitric oxide-cGMP pathway in cerebellum. Differential effects in hyperammonemia. *ACS Chem Neurosci.* (2016) 7:1753–1759. doi: 10.1021/acschemneuro.6b00263
38. Ouyang C, Nie L, Gu M, Wu A, Han X, Wang X, et al. Transforming growth factor (TGF)-beta-activated kinase 1 (TAK1) activation requires phosphorylation of serine 412 by protein kinase A catalytic subunit alpha (PKACalpha) and X-linked protein kinase (PRKX). *J Biol Chem*. (2014) 289:24226–37. doi: 10.1074/jbc.M114.559963
39. Aw DK, Sinha RA, Xie SY, Yen PM. Differential AMPK phosphorylation by glucagon and metformin regulates insulin signaling in human hepatic cells. *Biochem Biophys Res Commun.* (2014) 447:569–73. doi: 10.1016/j.bbrc.2014.04.031
40. Ferretti AC, Tonucci FM, Hidalgo F, Almada E, Larocca MC, Favre C. AMPK and PKA interaction in the regulation of survival of liver cancer cells subjected to glucose starvation. *Oncotarget*. (2016) 7:17815–28. doi: 10.18632/oncotarget.7404
41. Dorfman J, Macara IG. STRADalpha regulates LKB1 localization by blocking access to importin-alpha, and by association with Crm1 and exportin-7. *Mol Biol Cell.* (2008) 19:1614–26. doi: 10.1091/mbc.e07-05-0454
42. Lizcano JM, Goransson O, Toth R, Deak M, Morrice NA, Boudeau J, et al. LKB1 is a master kinase that activates 13 kinases of the AMPK subfamily, including MARK/PAR-1. *EMBO J.* (2004) 23:833–43. doi: 10.1038/sj.emboj.7600110
43. Kaufman JM, Amann JM, Park K, Arasada RR, Li H, Shyr Y, et al. LKB1 Loss induces characteristic patterns of gene expression in human tumors associated with NRF2 activation and attenuation of PI3K-AKT. *J Thorac Oncol.* (2014) 9:794–804. doi: 10.1097/JTO.0000000000000173
44. Bertherat J, Horvath A, Groussin L, Grabar S, Boikos S, Cazabat L, et al. Mutations in regulatory subunit type 1A of cyclic adenosine 5'-monophosphate-dependent protein kinase (PRKAR1A): phenotype analysis in 353 patients and 80 different genotypes. *J Clin Endocrinol Metab*. (2009) 94:2085–91. doi: 10.1210/jc.2008-2333
45. Yin Z, Pringle DR, Jones GN, Kelly KM, Kirschner LS. Differential role of PKA catalytic subunits in mediating phenotypes caused by knockout of the Carney complex gene Prkar1a. *Mol Endocrinol*. (2011) 25:1786–93. doi: 10.1210/me.2011-1008
46. Monteverde T, Muthalagu N, Port J, Murphy DJ. Evidence of cancer-promoting roles for AMPK and related kinases. *FEBS J.* (2015) 282:4658–71. doi: 10.1111/febs.13534
47. Bian S, Sun X, Bai A, Zhang C, Li L, Enjyoji K, et al. P2X7 integrates PI3K/AKT and AMPK-PRAS40-mTOR signaling pathways to mediate tumor cell death. *PLoS ONE.* (2013) 8:e60184. doi: 10.1371/journal.pone.0060184
48. Gwinn DM, Shackelford DB, Egan DF, Mihaylova MM, Mery A, Vasquez DS, et al. AMPK phosphorylation of raptor mediates a metabolic checkpoint. *Mol Cell.* (2008) 30:214–26. doi: 10.1016/j.molcel.2008.03.003
49. Zheng B, Jeong JH, Asara JM, Yuan YY, Granter SR, Chin L, et al. Oncogenic B-RAF negatively regulates the tumor suppressor LKB1 to promote melanoma cell proliferation. *Mol Cell.* (2009) 33:237–47. doi: 10.1016/j.molcel.2008.12.026
50. McGarrity TJ, Amos C. Peutz-Jeghers syndrome: clinicopathology and molecular alterations. *Cell Mol Life Sci.* (2006) 63:2135–44. doi: 10.1007/s00018-006-6080-0
51. Francis GL, Waguespack SG, Bauer AJ, Angelos P, Benvenga S, Cerutti JM, et al. Management Guidelines for Children with Thyroid Nodules and Differentiated Thyroid Cancer. *Thyroid*. (2015) 25:716–59. doi: 10.1089/thy.2014.0460
52. Yoo SK, Lee S, Kim SJ, Jee HG, Kim BA, Cho H, et al. Comprehensive analysis of the transcriptional and mutational landscape of follicular and papillary thyroid cancers. *PLoS Genet.* (2016) 12:e1006239. doi: 10.1371/journal.pgen.1006239
53. Bardeesy N, Sinha M, Hezel AF, Signoretti S, Hathaway NA, Sharpless NE, et al. Loss of the Lkb1 tumour suppressor provokes intestinal polyposis but resistance to transformation. *Nature*. (2002) 419:162–7. doi: 10.1038/nature01045
54. Miyoshi H, Nakau M, Ishikawa TO, Seldin MF, Oshima M, Taketo MM. Gastrointestinal hamartomatous polyposis in Lkb1 heterozygous knockout mice. *Cancer Res*. (2002) 62:2261–6. Available online at: https://cancerres.aacrjournals.org/content/canres/62/8/2261.full.pdf
55. Bouchekioua-Bouzaghou K, Poulard C, Rambaud J, Lavergne E, Hussein N, Billaud M, et al. LKB1 when associated with methylatedERalpha is a marker of bad prognosis in breast cancer. *Int J Cancer.* (2014) 135:1307–18. doi: 10.1002/ijc.28781
56. Xie Z, Dong Y, Zhang J, Scholz R, Neumann D, Zou MH. Identification of the serine 307 of LKB1 as a novel phosphorylation site essential for its nucleocytoplasmic transport and endothelial cell angiogenesis. *Mol Cell Biol.* (2009) 29:3582–96. doi: 10.1128/MCB.01417-08
57. Zhan YY, Chen Y, Zhang Q, Zhuang JJ, Tian M, Chen HZ, et al. The orphan nuclear receptor Nur77 regulates LKB1 localization and activates AMPK. *Nat Chem Biol.* (2012) 8:897–904. doi: 10.1038/nchembio.1069
58. Kovalovsky D, Refojo D, Liberman AC, Hochbaum D, Pereda MP, Coso OA, et al. Activation and induction of NUR77/NURR1 in corticotrophs by

CRH/cAMP: involvement of calcium, protein kinase A, and MAPK pathways. *Mol Endocrinol.* (2002) 16:1638–51. doi: 10.1210/mend.16.7.0863
59. Maira M, Martens C, Batsche E, Gauthier Y, Drouin J. Dimer-specific potentiation of NGFI-B (Nur77) transcriptional activity by the protein kinase A pathway and AF-1-dependent coactivator recruitment. *Mol Cell Biol.* (2003) 23:763–76. doi: 10.1128/MCB.23.3.763-776.2003
60. Fu TG, Wang L, Li W, Li JZ, Li J. miR-143 inhibits oncogenic traits by degrading NUAK2 in glioblastoma. *Int J Mol Med.* (2016) 37:1627–35. doi: 10.3892/ijmm.2016.2562
61. Namiki T, Tanemura A, Valencia JC, Coelho SG, Passeron T, Kawaguchi M, et al. AMP kinase-related kinase NUAK2 affects tumor growth, migration, and clinical outcome of human melanoma. *Proc Natl Acad Sci USA.* (2011) 108:6597–602. doi: 10.1073/pnas.1007694108
62. Namiki T, Yaguchi T, Nakamura K, Valencia JC, Coelho SG, Yin L, et al. NUAK2 amplification coupled with PTEN deficiency promotes melanoma development via CDK activation. *Cancer Res.* (2015) 75:2708–15. doi: 10.1158/0008-5472.CAN-13-3209
63. Tang L, Tong SJ, Zhan Z, Wang Q, Tian Y, Chen F. Expression of NUAK2 in gastric cancer tissue and its effects on the proliferation of gastric cancer cells. *Exp Ther Med.* (2017) 13:676–680. doi: 10.3892/etm.2016.3983
64. Miranda F, Mannion D, Liu S, Zheng Y, Mangala LS, Redondo C, et al. Salt-inducible kinase 2 couples ovarian cancer cell metabolism with survival at the adipocyte-rich metastatic niche. *Cancer Cell.* (2016) 30:273–89. doi: 10.1016/j.ccell.2016.06.020
65. Hubaux R, Thu KL, Vucic EA, Pikor LA, Kung SH, Martinez VD, et al. Microtubule affinity-regulating kinase 2 is associated with DNA damage response and cisplatin resistance in non-small cell lung cancer. *Int J Cancer.* (2015) 137:2072–82. doi: 10.1002/ijc.29577

Conflict of Interest: The authors declare that the research was conducted in the absence of any commercial or financial relationships that could be construed as a potential conflict of interest.

Advantages of publishing in Frontiers

OPEN ACCESS
Articles are free to read for greatest visibility and readership

FAST PUBLICATION
Around 90 days from submission to decision

HIGH QUALITY PEER-REVIEW
Rigorous, collaborative, and constructive peer-review

TRANSPARENT PEER-REVIEW
Editors and reviewers acknowledged by name on published articles

Frontiers
Avenue du Tribunal-Fédéral 34
1005 Lausanne | Switzerland

Visit us: www.frontiersin.org
Contact us: info@frontiersin.org | +41 21 510 17 00

REPRODUCIBILITY OF RESEARCH
Support open data and methods to enhance research reproducibility

DIGITAL PUBLISHING
Articles designed for optimal readership across devices

FOLLOW US
@frontiersin

IMPACT METRICS
Advanced article metrics track visibility across digital media

EXTENSIVE PROMOTION
Marketing and promotion of impactful research

LOOP RESEARCH NETWORK
Our network increases your article's readership